



The
University
Of
Sheffield.

Exploring a role for Tribbles homologue 3 (TRIB3) in platelet function

By:

Ahmed Gassim Bukhari

A thesis submitted in partial fulfilment of the requirements for the degree of
Doctor of Philosophy

The University of Sheffield
Faculty of Medicine, Dentistry and Health
Department of Infection, Immunity & Cardiovascular Disease

Submission Date

December 2020

Abstract

Maintaining physiological haemostasis in the vasculature demands optimal platelet function. The pseudokinase TRIB3 has previously been implicated in the regulation of platelet production, but no published studies have addressed the role of this protein in platelet function. The work presented here aimed to fill this knowledge gap. We identified five rare non-synonymous variants in *TRIB3* (predicting p.V107M, p.S146N, p.R149G, p.R153H and p.R181C amino acid substitutions) following analysis of whole exome sequence from 34 patients with unexplained platelet bleeding disorders, who were recruited to the UK Genotyping and Phenotyping of Platelets study. Bioinformatic analysis predicted all five variants to be deleterious, and structural studies using a 3D model of TRIB3 revealed that the amino acid substitutions affected residues that were likely to be located on the protein surface, and thus expected to affect interactions with other proteins. The mass spectrometric analysis showed that all variants caused a gain and loss of interactions with other proteins, including mitochondrial peptides and proteins that have been implicated in platelet activation. *In vitro* expression showed that whilst wild-type TRIB3 and all five TRIB3 variants localised to the nucleus, the p.V107M, p.R149G and p.R181C variants showed a diffuse expression pattern in contrast to the punctate expression pattern observed for wild-type TRIB3 and the p.S146N and p.R153H variants. Visualisation of the TRIB3/AKT1 protein complex, using a YFP protein complementation assay, revealed four expression patterns, two of which showed subcellular localisation to the cytoplasm, with the cytoplasmic punctate expression pattern of the TRIB3/AKT1 complex co-localising with mitochondria. The R149G, R153H and R181C variants exerted a gain-of-function effect on the interaction with AKT1, but not AKT2. Quantification of a platelet activation marker CD62p showed a gender-specific effect, affecting activation only in platelets from female *Trib3*^{-/-} mice, and a similar observation was noted for platelet ATP secretion. In summary, our data provide preliminary evidence for the role of TRIB3 in platelet activation and degranulation, and further studies will be necessary to confirm the involvement of TRIB3 in regulating platelet functions, and to correlate the identified rare TRIB3 variants with the observed bleeding phenotypes.

Acknowledgements

Nothing of the work described in this thesis would have been accomplished without the guidance, support, care, encouragement I received from my supervisors, Professor Martina Daly and Professor Endre Kiss-Toth. They dedicated their time and spared no effort to provide the best experience any PhD student can ever expect. Additionally, I would like to thank members of the Haemostasis group for their unconditional support and help including; Prof Ian Peake, Prof Anne Goodeve, Dr Daniel Hampshire, Dr Vin Leo, Dr Simon Webster, and Dr Joanne Lacy, and Dr Maryam Aldossary. Also, I would like to thank members of the Inflammation and Metabolism group including; Dr Heather Wilson, Dr Jessica Johnston, Dr Li Yang, Dr Kajus Baidzajevs, Dr Taewoo Kim, Dr Chiara Niespolo, and Laura Martinez Campesino. I feel that I was privileged and honoured to have such wonderful scientists surrounding me, and hope the friendship and the collaboration remain indefinitely.

During my studies, I received a lot of support from colleagues outside the University of Sheffield, and I would like to thank them for their valuable inputs. The UK-GAPP study group who permitted the use of the whole-exome-sequencing data. Miguel Hernández-Quiles (Centre for Molecular Medicine, UMC Utrecht, Utrecht, Netherlands) who performed the Mass Spectrometry and guided me through analysing and interpreting the data. Juan Salamanca Vilorio (Barcelona, Spain) who generated the 3D structure of TRIB3 and provided further predictions about the protein-protein interactions.

Within the University of Sheffield, I received the greatest support and guidance, and I would like to acknowledge them. The Medical School administrative staff, the Medical School PGR team, the medical IT team, the Western Bank and the Hallamshire Biological Services Unit team, the microscopy core facility team, the flow cytometry core facility team, the core genomic facility team, and all staff and members of the Infection, Immunity and Cardiovascular Disease Department.

I would also like to acknowledge my sponsor King Abdulaziz University (Jeddah, KSA), and thank my colleagues at the Faculty of Applied Medical Sciences, and the Medical Laboratory Technology Department. Also, I would like to thank the Saudi Arabian Cultural Bureau and the Saudi Arabian Embassy in London, UK.

Dedication

This is dedicated...

To my beloved mother, Fakhriah, I remember the day you enquired my high school grades and found that they were not enough for medical school, you looked at me in the eyes and sadly said: "I was hoping that one day I would call my only son (doctor)". That moment has always been in my mind whenever I struggled and it has always been the thrust I needed to overcome whatever I am facing. I can never forget the sorrow and the disappointment I saw in your eyes. Since then, I vowed to do whatever I can do to replace that look from my memory with your joy and your magical smile when I say to you "my sweetheart mom, you can now officially call your son a DOCTOR". Now, and after 17 years from that day, I am close to achieving this, and cannot wait to tell you how your wishes encouraged me to be a better person and guided me for a brighter future. There are absolutely no words in all languages that can describe how much I love you, but I would like to say it anyways, I love you.

To my father, Gassim, who taught me how to be reliable, wise and realistic in dealing with different life situations and shielded me with his love and prayers. To my lovely sisters Maram, Rana, Roaa, Afnan and Shahad who overwhelmed my life with absolute love and care. To my life-long love, my wife, Alyaa, who loved me, believed in me and unconditionally supported me by all possible and impossible means. To my In-laws, who were a family in everything but blood, and were a pillar to be relied upon. To my nieces and nephews, the life of the family who were always there to give me the laughs I needed when stress took control.

I feel that I am the luckiest person the world to have you surrounding me, and will do my best to repay you the love, the care, the kindness and the support you all offered me.

I love you all and love having you in my life,,,

*Yours,
Ahmed Bukhari*

Table of Contents

| | |
|--|------------|
| Abstract | II |
| Acknowledgements | III |
| Dedication | IV |
| Table of Contents | V |
| List for Figures | IX |
| List of Tables | XI |
| List of Abbreviations | XII |
| Chapter 1: General introduction | 15 |
| 1.1 Platelets..... | 16 |
| 1.1.1 Normal physiological function of platelets..... | 20 |
| 1.1.2 Intracellular signalling in platelets..... | 20 |
| 1.3 Platelet bleeding disorders..... | 24 |
| 1.1.3.1 Phenotypic characterisation of platelets in bleeding disorders..... | 26 |
| 1.1.3.2 Genetic investigations in patients with platelet bleeding disorders | 26 |
| 1.1.3.2.1 The UK-GAPP study..... | 27 |
| 1.2 Mammalian Tribbles homologues..... | 28 |
| 1.2.1 Tribbles homologue 3 (TRIB3)..... | 30 |
| 1.2.2 TRIB3 in pathological situations and altered expression of TRIB3..... | 32 |
| 1.3 Background, hypothesis and aims of the study..... | 34 |
| 1.3.1 Background of this study..... | 34 |
| 1.3.2 Hypothesis..... | 35 |
| 1.3.3 Aims..... | 35 |
| Chapter 2: Materials and Methods | 36 |
| 2.1 Materials..... | 37 |
| 2.1.1 Animals..... | 37 |
| 2.1.2 Platelet collection and activation reagents..... | 37 |
| 2.1.3 Plasmids..... | 38 |
| 2.1.4 Oligonucleotide Primers..... | 38 |
| 2.1.5 Mutagenesis, cloning, and DNA extraction kits..... | 40 |
| 2.1.6 Electrophoresis reagents..... | 40 |
| 2.1.7 Bacterial cultures..... | 40 |
| 2.1.8 Cell lines, Tissue culture, and transfection reagents..... | 40 |
| 2.1.9 Protein extraction and blotting..... | 41 |
| 2.1.10 Laboratory equipment..... | 42 |

| | |
|---|----|
| 2.1.11 Laboratory plastics..... | 42 |
| 2.2 Methods..... | 43 |
| 2.2.1 Site-directed mutagenesis of the TRIB3 Entry clones | 43 |
| 2.2.1.1 Designing mutagenic oligonucleotide primers | 43 |
| 2.2.1.2 Plasmid preparation..... | 44 |
| 2.2.1.3 Mutant strand synthesis..... | 44 |
| 2.2.1.4 Digestion of parental strands..... | 44 |
| 2.2.1.5 Transformation of ultracompetent cells | 44 |
| 2.2.2 Entry clones DNA extraction and purification | 45 |
| 2.2.2.1 DNA purification using QIAprep® Spin Miniprep kit | 45 |
| 2.2.2.2 DNA purification using GenElute™ HP Plasmid Midiprep kit | 45 |
| 2.2.2.3 DNA purification using EndoFree® Plasmid Maxi kit | 45 |
| 2.2.2.4 Assessment of purified mutated plasmids | 46 |
| 2.2.3 Cloning mutated TRIB3 cDNA into expression vectors | 46 |
| 2.2.3.1 Gateway cloning | 46 |
| 2.2.3.2 Assessment of purified recombinant plasmids | 47 |
| 2.2.4 Cell line maintenance | 48 |
| 2.2.4.1 Thawing cells..... | 48 |
| 2.2.4.2 Passaging cells..... | 48 |
| 2.2.4.3 Freezing cells | 48 |
| 2.2.5 Expression and localisation of TRIB3 in HeLa cells | 49 |
| 2.2.5.1 Seeding and transfecting HeLa cells | 49 |
| 2.2.5.2 Imaging transfected live cells | 49 |
| 2.2.5.3 Quantification of fluorescence in transfected live cells and statistical analysis..... | 49 |
| 2.2.6 Assessment of interaction strength of TRIB3/AKT1 complex in HEK293T using Protein complementation assay..... | 50 |
| 2.2.7 Electrophoresis and immunoblotting of phosphorylated AKT | 50 |
| 2.2.7.1 Preparation of cell lysates | 50 |
| 2.2.7.2 Measurement of total protein concentrations in cell lysates | 51 |
| 2.2.7.3 Denaturing gel electrophoresis..... | 51 |
| 2.2.7.4 Protein blotting and detection | 51 |
| 2.2.8 Assessment of murine platelet activation and ATP secretion..... | 52 |
| 2.2.8.1 Quantifying platelet activation using activation markers..... | 52 |
| 2.2.8.2 Assessment of ATP secretion from murine platelets..... | 52 |

| | |
|---|------------|
| Chapter 3: In-silico predictions of the effects of non-synonymous TRIB3 variants on TRIB3 structure and function | 54 |
| 3.1 Introduction..... | 55 |
| 3.2 Methods..... | 57 |
| 3.2.1 Patients..... | 57 |
| 3.2.2 In-silico predictions of the effects of TRIB3 variants..... | 57 |
| 3.2.3 Mass spectrometry of peptides interacting with wild-type and variant forms of TRIB3..... | 58 |
| 3.3 Results | 62 |
| 3.3.1 Identification of TRIB3 variants and in-silico predictions | 62 |
| 3.3.3 TRIB3 interactors affected by TRIB3 variants | 68 |
| 3.4 Discussion | 77 |
| Chapter 4: Gateway cloning of TRIB3 variants and optimisation of protein complementation assays to investigate the interaction between TRIB3 and AKT | 81 |
| 4.1 Introduction..... | 82 |
| 4.1.1 Gateway™ cloning technology..... | 83 |
| 4.1.2 Protein fragment complementation assays..... | 85 |
| 4.1.2.1 Investigation of the interaction between TRIB3 and either AKT1 or AKT2 using a Split-NanoLuc luciferase complementation assay | 85 |
| 4.1.2.2 Localisation of TRIB3/AKT1 interactions using a Split-YFP fragment complementation assay..... | 87 |
| 4.2 Methods..... | 89 |
| 4.3 Results | 90 |
| 4.3.1 Generation of Gateway entry plasmids and expression vectors encoding wild-type and variant forms of TRIB3..... | 90 |
| 4.3.2 Optimisation of the split-NanoLuc complementation assay of the TRIB3/AKT interaction..... | 93 |
| 4.3.3 Optimisation of the split-YFP complementation assay for localisation of TRIB3/AKT1 interactions | 96 |
| 4.4 Discussion | 98 |
| Chapter 5: TRIB3 is an intracellular signalling regulator for platelet activation and secretion | 100 |
| 5.1 Introduction..... | 101 |
| 5.2 Methods..... | 102 |

| | |
|--|------------|
| 5.2.1 Mice | 102 |
| 5.2.2 Localisation of TRIB3 variants using TRIB3/YFP fusion proteins and TRIB3/AKT1 complexes using the split-YFP PCA system | 102 |
| 5.2.3 Assessment of the interaction between TRIB3 variants and either AKT1 or AKT2 using the Nano-Luc PCA system..... | 103 |
| 5.2.4 Assessment of murine platelet function | 103 |
| 5.3 Results | 104 |
| 5.3.1 Variants of TRIB3 show altered expression patterns | 104 |
| 5.3.2 The TRIB3/AKT1 complex shows four different patterns of expression | 104 |
| 5.3.3 Interaction of TRIB3 variants with AKT1 and AKT2..... | 107 |
| 5.3.4 Altered platelet activation in female Trib3 knockout mice..... | 110 |
| 5.4 Discussion | 112 |
| Chapter 6: Mitochondrial localisation of the TRIB3/AKT1 complex..... | 116 |
| 6.1 Introduction..... | 117 |
| 6.1.1 Hypothesis and Aims | 119 |
| 6.2 Methods..... | 120 |
| 6.2.1 Staining subcellular compartments..... | 120 |
| 6.2.2 Staining of Mitochondria in transfected HeLa cells..... | 121 |
| 6.2.3 Confocal imaging of mitochondria in live cells | 121 |
| 6.2.4 Quantification of YFP fluorescence localised to mitochondria using Pixel analysis..... | 121 |
| 6.3 Results | 122 |
| 6.3.1 Optimising mitochondrial, ER, and lysosomal stains | 122 |
| 6.3.2 TRIB3/AKT1 complex localised to mitochondria only when expressed in a cytoplasmic punctate pattern | 123 |
| 6.3.2 The R149G variant did not affect the translocation of the TRIB3/AKT1 complex to mitochondria | 125 |
| 6.4 Discussion | 126 |
| Chapter 7: General Discussion, Final Summary, and Future Work..... | 128 |
| Appendices | 134 |
| Appendix 1. Schematic representation of TRIB3/YFP fusion construct | 135 |
| Appendix 2. Schematic representation of TRIB3/V2 plasmid | 136 |
| Appendix 3. Schematic representation of TRIB3/LgBiT 1.1C plasmid | 137 |
| Appendix 4. Schematic representation of TRIB3/SmBiT 2.1N plasmid..... | 138 |
| Bibliography | 179 |

List for Figures

| | |
|---|-----------|
| Figure 1.1: Platelet Ultrastructure | 19 |
| Figure 1.2: Platelet membrane receptors, agonists, and intracellular signalling pathways..... | 23 |
| Figure 1.3: Platelet bleeding disorder data from 2011 to 2019..... | 25 |
| Figure 1.4: The three domains of TRIBBLES proteins and their functions..... | 29 |
| Figure 1.5: TRIB3 gene and protein domains..... | 31 |
| Figure 3.1: Pipelines for sample preparation and analysis of mass spectrometry data generated to identify peptides that interact differentially with variant forms of TRIB3..... | 61 |
| Figure 3.2: Multiple sequence alignment of TRIB3 from different species..... | 65 |
| Figure 3.3: Predicted 3D structure of the pseudokinase domain of TRIB3..... | 66 |
| Figure 3.4: Amino acid substitutions on the surface of the pseudokinase domain of TRIB3..... | 67 |
| Figure 3.5: Scatter plots of peptides that interacted with wild-type and variant TRIB3 molecules quantified using mass spectrometry..... | 69 |
| Figure 3.6: Gene ontology analysis to identify processes that may be affected by TRIB3 variants..... | 73 |
| Figure 4.1: LR Gateway™ cloning strategy..... | 84 |
| Figure 4.2: Optimisation of the Split-NanoLuc fragment complementation assay..... | 86 |
| Figure 4.3: The Split-YFP fragment complementation assay..... | 88 |
| Figure 4.4: Analysis of variant TRIB3 entry plasmids..... | 91 |
| Figure 4.5: Restriction analysis of TRIB3 expression plasmids..... | 92 |
| Figure 4.6: Nano-Luciferase activity in HEK293 cells transfected with plasmids encoding TRIB3 and AKT1 tagged with LB or SB luciferase fragments... | 94 |

| | |
|---|------------|
| Figure 4.7: Nano-Luciferase activity in cells transfected with TRIB3 and AKT2 plasmids tagged with LB or SB luciferase fragments..... | 95 |
| Figure 4.8 Split-YFP fluorescence in cells co-transfected with TRIB3 and AKT1 plasmids tagged with V1 or V2 YFP fragments..... | 97 |
| Figure 5.1: Expression patterns of wild-type and variant forms of TRIB3 fused to YFP in HeLa cells..... | 105 |
| Figure 5.2: Distribution of the TRIB3/AKT1 complex..... | 106 |
| Figure 5.3: Luciferase activity in cells co-expressing wild-type or variant forms of TRIB3 and AKT1 (A) or AKT2 (B)..... | 108 |
| Figure 5.4: Detection and quantification of phosphorylated AKT in cells co-expressing AKT1 and wild-type or variant forms of TRIB3 | 109 |
| Figure 5.5: Gender-specific activation defect in platelets from Trib3 ^{-/-} and Trib3 ^{+/-} mice | 111 |
| Figure 6.1: Protein import into mitochondria | 118 |
| Figure 6.2: Staining of subcellular compartments | 122 |
| Figure 6.3: Localisation of TRIB3/AKT1 complex to mitochondria in cytoplasmic punctate expression pattern..... | 124 |
| Figure 6.4: Violin plots comparing mitochondrial localisation of the wild-type TRIB3/AKT1 and the R149G TRIB3/AKT1 complexes..... | 125 |
| Figure 7.1: Proposed mechanism of the role of estrogen in regulating platelet activation through TRIB3..... | 131 |

List of Tables

| | |
|---|------------|
| Table 2.1: Oligonucleotide primer sequences. | 39 |
| Table 3.1: TRIB3 variants identified in patients recruited to the UK-GAPP study .. | 633 |
| Table 3.2: Single Nucleotide Variations identified by WES analysis of patients recruited to the GAPP study | 644 |
| Table 3.3: Peptide interactions that were lost, or gained by two or more TRIB3 variants | 70 |
| Table 3.4: Interactors affected by TRIB3 variants and involved in platelet-related processes | 755 |
| Table 4.1: Plasmids required for Protein Complementation Assays..... | 89 |

List of Abbreviations

| | |
|---------------|---|
| AD | Alzheimer's disease |
| ADP | Adenosine diphosphate |
| AKT | Protein kinase B |
| AML | Acute myeloid leukaemia |
| AMPK | AMP-activated protein kinase |
| APL | Acute promyelocytic leukaemia |
| ATF4 | Activating transcription factor 4 |
| ATP | Adenosine triphosphate |
| BSS | Bernard-Soulier syndrome |
| CAD | Coronary artery disease |
| CADD | Combined annotation dependent depletion |
| CD | Cluster of differentiation |
| Cdc25 | Cell division cycle 25 |
| COP1 | Constitutive photomorphogenic protein 1 |
| CVD | Cardiovascular disease |
| ECM | Extracellular matrix |
| eIF2 α | Eukaryotic initiation factor 2 alpha |
| EM | Electron microscopy |
| eNOS | Endothelial nitric oxide synthase |
| ER | Endoplasmic reticulum |
| ERK | Extracellular signal-regulated kinase |
| gnomAD | Genome Aggregation database |
| GP | Glycoprotein |
| GT | Glanzmann thrombasthenia |
| GWAS | Genome-wide association studies |
| HPS | Hermansky–Pudlak syndrome |

| | |
|----------------|--|
| HSC | Haematopoietic stem cells |
| iBAQ | Intensity-based absolute quantification |
| IGF-1 | Insulin-like growth factor-1 |
| IMT | Intima-media thickness |
| IPDs | Inherited platelet disorders |
| LB | Large bit |
| LTA | Light transmission aggregometry |
| MAF | Minor allele frequency |
| MAPK | Mitogen-activated protein kinase |
| MCAT | Malonyl coa-acyl carrier protein transacylase |
| MK | Megakaryocyte |
| mTORC1 | Mammalian target of rapamycin complex 1 |
| NF- κ B | Nuclear factor kappa-light-chain-enhancer of activated B cells |
| NGS | Next generation sequencing |
| NO | Nitric oxide |
| PAR-1 | Protease-activated receptors 1 |
| PAR-4 | Protease-activated receptors 4 |
| PCAs | Protein complementation assays |
| PD | Parkinson's disease |
| PDGF | Platelet-derived growth factor |
| PF4 | Platelet factor 4 |
| PI3K | Phosphoinositide 3-kinase |
| PPARs | Peroxisome proliferator-activated receptors |
| PPIs | Protein-protein interactions |
| SB | Small bit |
| SEM | Standard error of the mean |
| SNX2 | Sorting nexin 2 |

| | |
|------------------|--|
| SPTAN1 | Spectrin α -chain, non-erythrocytic 1 |
| STMN1 | Stathmin |
| T2DM | Type 2 diabetes mellitus |
| TF | Tissue factor |
| TIM | Translocase of the inner mitochondrial membrane |
| TIMM17B | Translocase of the inner mitochondrial membrane 17-B subunit |
| TOM | Translocase of the outer mitochondrial membrane |
| TPO | Thrombopoietin |
| TRAP | Thrombin receptor activating peptide |
| TRIB1 | Tribbles homologue 1 |
| TRIB2 | Tribbles homologue 2 |
| TRIB3 | Tribbles homologue 3 |
| TXA ₂ | Thromboxane A ₂ |
| UK-GAPP | The UK Genotyping And Phenotyping of Platelets |
| V1 | Venus1 |
| V2 | Venus2 |
| VWF | Von Willebrand factor |
| WES | Whole exome sequencing |
| ZIP | GCN4 leucine zipper |

Chapter 1:

General introduction

1.1 Platelets

Platelets (also called thrombocytes) are small cells (2-3 μm in diameter) that survive in the circulation for 7-9 days, and function to maintain normal blood flow by preventing blood loss into surrounding tissue when damage occurs to the vascular endothelium (Holinstat, 2017). Platelets normally circulate as quiescent discoid cells, but become rapidly activated when exposed to collagen at sites of vascular injury. Adhesion to collagen triggers intracellular signalling pathways that lead the platelets to change their shape, release the contents of their intracellular granules, and interact with other platelets to form a platelet plug that stems the bleeding. Therefore, defects giving rise to qualitative and/or quantitative abnormalities of platelets are associated with an increased tendency to bleed.

Platelets are produced through a process of megakaryocyte (MK) fragmentation, that maintains the platelet count in healthy individuals within the range of 150 to 450 $\times 10^9/\text{L}$ (Giles, 1981; Paulus, 1975). The bone-marrow-occupying MK precursors evolve to release 1×10^{11} mature platelets into the circulation every day, and the production rate can increase up to twenty-fold in response to a haemostatic challenge (Deutsch & Tomer, 2013; Kaushansky, 2008). MKs are derived from haematopoietic stem cells (HSC) through a process of differentiation (megakaryopoiesis) that takes place in the bone marrow. The main regulator of megakaryopoiesis is the circulating hormone thrombopoietin (TPO), levels of which are indirectly related to platelet count (McCarty et al, 1995). TPO is released into the bloodstream from the liver and kidney in response to a reduction in platelet count, which then induces HSC to differentiate to mature megakaryocytes and dispense new platelets into the circulation (Kaushansky, 2006).

The lung is also a site for resting MK precursors and platelet production as was described in a study by Zucker-Franklin and Philipp (2000) which examined sections of murine pulmonary capillaries that showed the MK progenitors and the demarcation membrane system, which is an indication of platelet assembly inside the MK cytoplasm (Zucker-Franklin & Philipp, 2000). Lately, Lefrançois et al (2017) published direct images of the murine pulmonary microcirculation highlighting the residence of MK progenitors and supported the observation by flow cytometric quantification of MK precursor and proplatelet formation markers (Lefrançois et al, 2017).

Most cells require a nucleus in order to guide the synthesis of functional proteins. Platelets are therefore unusual in being anucleated, though they are packed with ribosomes and mRNAs, which are derived from the mature MK during the process of

thrombopoiesis (Bugert et al, 2003; Rowley et al, 2012). The TPO-induced mature MKs undergo multiple cycles of endomitosis to become large polyploid cells that are responsible for synthesis of the proteins that are shuttled into the proplatelets prior to their extension into the bloodstream to release mature platelets (Machlus & Italiano, 2013).

White (1979) described platelet ultrastructure, dividing it into four regions: 1) the peripheral zone includes the outer membrane which is coated with a glycocalyx layer that contains several different glycoprotein (GP) receptors and encompasses the canalicular system which facilitates the release of the secretory contents of platelets; 2) the sol-gel zone comprises the cytoplasm and contains polymerised microtubules that support the platelet shape in resting and active states; 3) the organelle zone which includes mitochondria, lysosomes, glycogen, α and δ -granules; and 4) the membrane systems which consist of the dense tubular system where thromboxane A_2 (TXA₂) is synthesised and calcium is stored (Fig. 1.1) (White, 1979).

The shape of resting platelets is maintained by α - and β -microtubule fibres which assemble at the platelet margins, and also support the shape change in activated platelets (Radley & Hartshorn, 1987). The observation that mice deficient in β 1-tubulin, the major β -tubulin expressed in platelets, produced spherical platelets that showed a disorganised arrangement of marginal cytoskeletal microtubules during activation, supports the hypothesis that microtubules are essential for the discoid shape of platelets and the change in shape that occurs in response to agonist-induced activation (Italiano et al, 2003).

The platelet membrane contains several GPs including GP Ib-IX-V, GP VI, GP IIb/IIIa (also known as integrin $\alpha_{IIb}\beta_3$) and GP Ia/IIa (integrin $\alpha_2\beta_1$) that act as receptors for collagen, von Willebrand factor (VWF) and fibrinogen to mediate platelet adhesion, activation, aggregation, degranulation and the platelet-dependent inflammatory response. The interactions mediated by these receptors are essential for normal platelet function, and defects in these receptors have been associated with platelet bleeding disorders (Rivera et al, 2009). Platelet activation and aggregation rely on further intracellular signal transduction that is transmitted upon the interaction of soluble agonists with several G-protein coupled receptors which are also located on the platelet membrane. These seven transmembrane domain receptors include protease-activated receptors 1 and 4 (PAR-1 and PAR-4) which are activated by

thrombin, the ADP-activated P2Y₁ and P2Y₁₂ receptors, and the TXA₂/prostaglandin H₂ receptor (TP) which is activated by TXA₂ (Li et al, 2010).

The most potent effector molecules that are secreted from activated platelets are stored within the α - and the δ -granules. These granules are packed during thrombopoiesis, and their contents are released via the canalicular system to promote primary and secondary haemostasis (Eckly et al, 2014; White, 1979). The α -granule cargo includes molecules that enhance the adhesion of platelets and platelet-platelet interactions including VWF, P-selectin and fibrinogen (Maynard et al, 2007). They also contain cytokines and chemokines that are involved in inflammation and wound healing such as platelet-derived growth factor (PDGF), IL-8 and platelet factor 4 (PF4), while δ -granules contain small molecules such as ADP, ATP and calcium that are mainly required for platelet activation (Heijnen & van der Sluijs, 2015). Lysosomes are additional secretory granules in platelets, and their recognised secretions include acid hydrolases.

Due to the lack of a nucleus-controlled cell cycle, platelets are powered by five to eight mitochondria that are packaged during platelet biogenesis in megakaryocytes (Melchinger et al, 2019). In addition to generating adenosine triphosphate (ATP), studies have shown that the mitochondria are involved in platelet activation and apoptosis (Fuentes et al, 2019). Mitochondria import pre-packaged protein templates from the cytosol to transform them into the functional forms required to perform essential platelet and mitochondrial functions (Wiedemann & Pfanner, 2017).

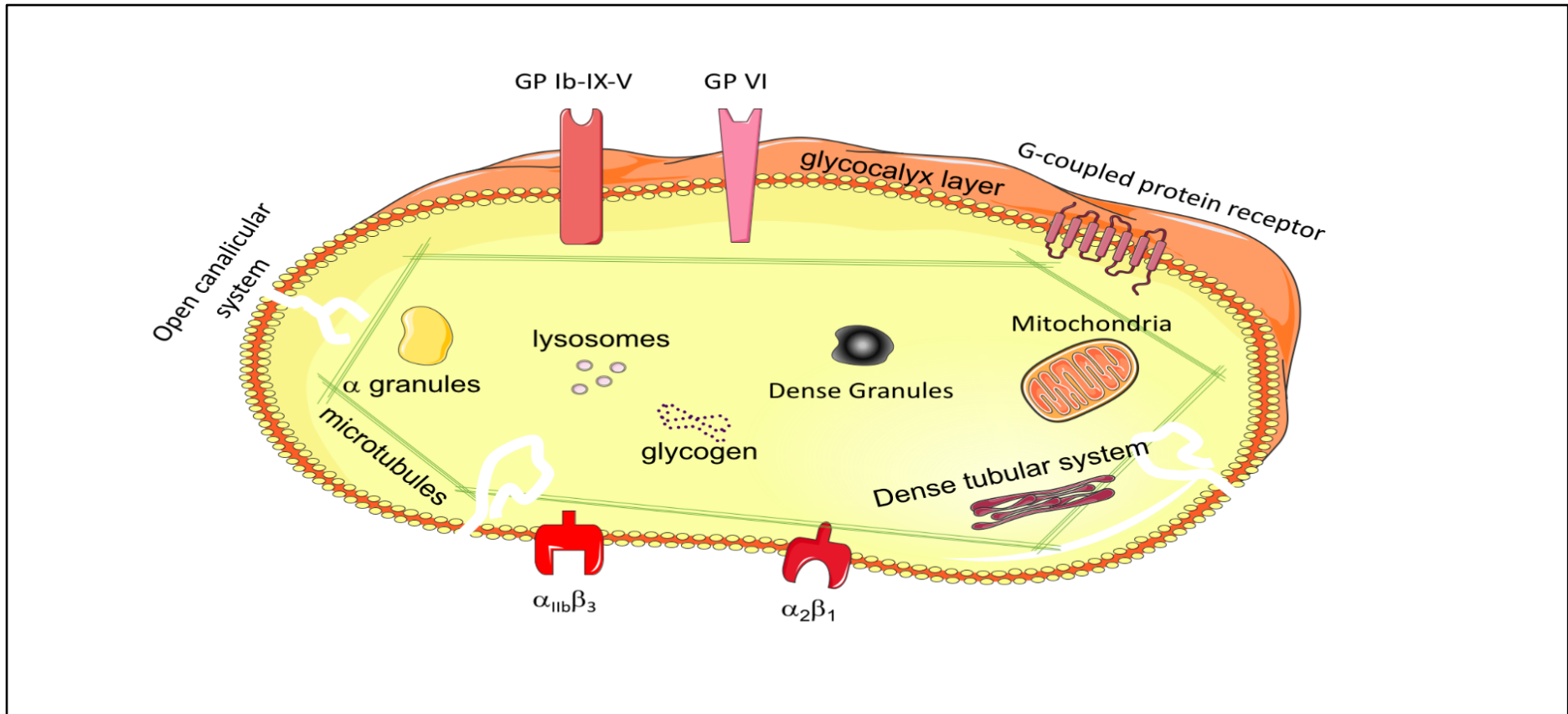


Figure 1.1: Platelet Ultrastructure

An illustration of the four zones of platelets; (i) the peripheral zone containing the glycocalyx layer, glycoprotein receptors, openings of the open canalicular system, and G-protein coupled receptors; (ii) the Sol-Gel zone comprises the microtubules; (iii) the organelle zone comprises the mitochondria, lysosomes, glycogen, alpha and dense granules and (iv) the dense tubular system of the membrane system. The contents used to construct the figure were adapted and modified from the publicly available Servier Medical Art, which is licensed under a Creative Commons Attribution 3.0 License. <https://smart.servier.com>.

(Note: the number and size of internal contents of the platelet is not proportional to the actual size, the components were enlarged for illustration purpose)

1.1.1 Normal physiological function of platelets

When damage occurs to the vascular endothelium, platelets adhere at the site of injury and rapidly become activated to prevent unopposed bleeding into the surrounding tissue. The platelet GP Ib-V-IX receptor mediates tethering of platelets to VWF that is bound to exposed collagen present in the sub-endothelium or so-called extracellular matrix (ECM) of the injured vessel wall (Falati et al, 1999). To strengthen platelet adhesion to the injury site, the platelet integrin $\alpha_2\beta_1$ and glycoprotein (GP) VI receptor interact directly with sub-endothelial collagen and trigger intracellular signalling pathways that activate the platelets (Gardiner & Andrews, 2014; Li et al, 2010). This results in a change in shape to a more dendritic form, release of the contents of the intracellular α - and δ -granules, and synthesis of TXA₂ (Varga-Szabo et al, 2008). Additionally, the exposure of tissue factor (TF) at the injury site leads to activation of the coagulation cascade, resulting in the generation of thrombin from its precursor, prothrombin, and the conversion of fibrinogen to fibrin (Rand et al, 1996). The adenosine diphosphate (ADP) which is released from dense granules, Thrombin and TXA₂ act as secondary mediators of platelet activation at the injured site, while fibrinogen, which is converted to polymerised fibrin upon interaction with thrombin, stabilises the growing platelet thrombus by crosslinking activated platelets through surface integrin $\alpha_{IIb}\beta_3$ receptors (Kashiwagi et al, 1997). Following the formation of the haemostatic plug, platelet activation is dampened in order to avoid blocking the flow of blood. The neighbouring intact endothelial cells release nitric oxide (NO) and prostacyclin that both inhibit transduction of activation signals and suppresses platelet activation (Smolenski, 2012).

Activated platelets also release angiogenesis promoting molecules such as PDGF at the injury site, thereby facilitating wound healing. In addition, molecules expressed and secreted upon activation of platelets such as P-selectin attract leucocytes to the injury site, initiating the inflammatory response (Nurden, 2011).

1.1.2 Intracellular signalling in platelets

Platelets are activated when they encounter subendothelial VWF and collagen, which trigger intracellular signal transduction through the GPIb-IX-V and GPVI receptors respectively. Signal transduction through the GPIb-IX-V receptor occurs sequentially through Src family kinase (SFK), phosphoinositide 3-kinase (PI3K), the Protein kinase B (PKB or AKT), endothelial nitric oxide synthase (eNOS), Soluble guanylate cyclase

(sGC), Cyclic guanosine monophosphate (cGMP), protein kinase G (PKG), and mitogen-activated protein kinase (MAPK) which regulates downstream pathways leading to platelet degranulation and TXA₂ synthesis. The direct interaction between collagen and platelet GPVI allows signal transduction through the FcR_γ subunit of GPVI to SFK which result in amplifying the downstream signalling pathways (Li et al, 2010) (Figure 1.2A).

Following degranulation of platelets, a second wave of signalling is initiated to sustain and amplify activation. ADP released from the dense granules binds to platelet receptors, P2Y₁ and P2Y₁₂, and TXA₂ binds to the platelet TXA₂/prostaglandin H2 receptor (TP) to transduce signals through cognate G-proteins, transducing the signals sequentially through PI3K, AKT, eNOS, and MAPK to promote shape change, TXA₂ synthesis, degranulation and aggregation (Li et al, 2010). In addition, thrombin generated through activation of coagulation binds to the protease-activated receptors 1 and 4 (PAR1 and PAR4), to further amplify activation through PI3K and MAPK (Li et al, 2010; Offermanns, 2006) (Figure 1.2B).

The signalling through the GPVI following collagen exposure leads to the phosphorylation of SFK. The use of SFK inhibitor (Dasatinib) showed a marked decrease in the platelet adhesion to the collagen-coated surface, which highlight the role of SFK in the activation signal transduction (Zhang & Diamond, 2020).

The PI3K/AKT signalling axis plays a key role in platelet activation downstream the SFK, and the use of PI3K inhibitor resulted in reduced AKT phosphorylation and affected platelet adhesion on collagen and VWF (Chen et al, 2019). Human and murine platelets express two isoforms of AKT (AKT1 and AKT2), with AKT1 being the predominant isoform expressed in human platelets (Kroner et al, 2000), in contrast to murine platelets where expression of Akt2 is higher than that of Akt1 (Woulfe et al, 2004). Kroner et al (2000) showed that AKT1 is phosphorylated in platelets following activation with thrombin, and that the level phosphorylation was proportional to the concentration of thrombin used. Similarly, phosphorylation of AKT correlates with platelet activation following signalling through the thrombin receptors PAR1 and PAR4, in response to the selective peptide agonists SFLLRN and AYPGKF respectively (Kim et al, 2004). Supporting these observations, Chen et al. (2004) demonstrated a reduction in platelet responses to thrombin activation in *Akt1*^{-/-} mice (Chen et al, 2004). Woulfe et al (2004) investigated the effects of deleting the two AKT isoforms from mice and found that platelets from *Akt2*^{-/-} mice exhibited a defect in platelet activation and

aggregation in response to thrombin and TxA₂. Interestingly, they also reported that the effect of reduced platelet response to thrombin in the *Akt1*^{-/-} mouse was only observed when accompanied by the deletion of one allele of AKT2 (*Akt2*^{+/-}) (Woulfe et al, 2004).

The role of the NO/sGC/cGMP/PKG axis in platelet activation or inhibition is controversial. Some studies concluded that low concentrations of eNOS were found to be associated with the transduction of the activation signal (Marjanovic et al, 2008), while the high concentration of eNOS was found to be involved in inhibiting the platelet activation (Emami et al, 2019). Similarly, studies are supporting the involvement of sGC, cGMP, PKG in either platelet activation or inhibition (Makhoul et al, 2018; Zhang et al, 2011). Lastly, the role of the cyclic adenosine monophosphate (cAMP)/ protein kinase A (PKA) axis in platelet signalling pathways was solely linked to platelet inhibition (Sepulveda et al, 2019)

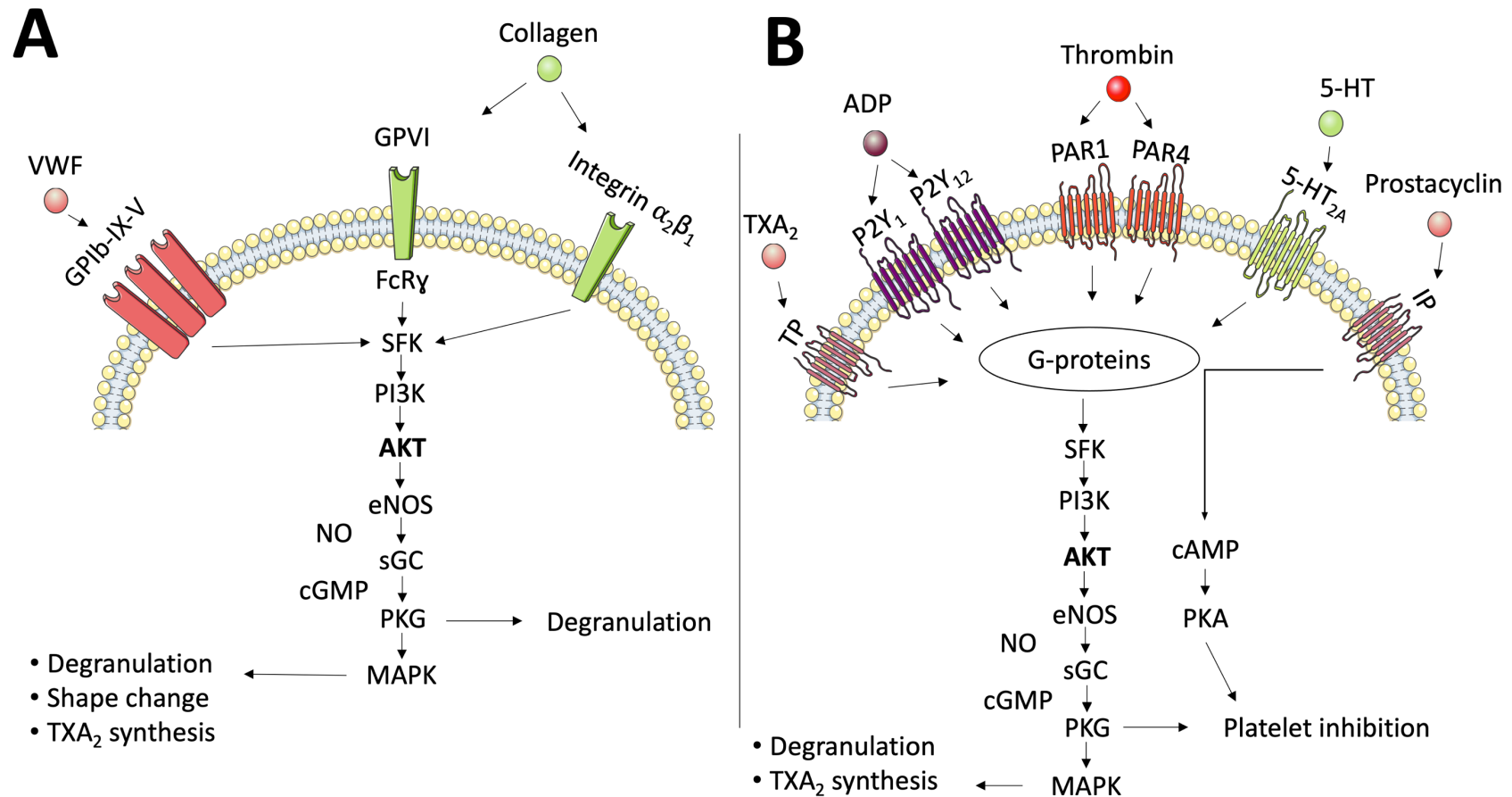


Figure 1.2: Platelet membrane receptors, agonists, and intracellular signalling pathways

(A) Platelet agonists that are exposed on the injured sub-endothelium and the receptors involved in transducing signals to amplify activation. Signalling also contributes to TXA₂ synthesis, shape change, and degranulation. **(B)** Platelet activation by signalling through G-protein coupled receptors. Signalling contributes to TXA₂ synthesis, degranulation, and also to platelet inhibition. Adapted with permission from (Li et al, 2010).

1.3 Platelet bleeding disorders

Platelet bleeding disorders are heterogeneous abnormalities caused by defects in platelet production and/or function. In 2019, published data relating to bleeding disorders in the UK recorded the registration of 149 cases with Glanzmann thrombasthenia (GT), 96 with Bernard-Soulier syndrome (BSS) and 741 with unclassified bleeding disorders (UKHCDO, 2019). The registry demonstrates a slight increase since 2011 in the number of patients having the well-characterised platelet bleeding disorders such as GT and BSS, while a more dramatic increase is observed in the number of patients registered with unclassified platelet disorders (Figure 1.3). These data highlight the increased interest in unexplained platelet bleeding disorders over the last decade, as well as advancements in gene sequencing that have facilitated the diagnosis of the less characterised disorders. The well-characterised disorders are readily diagnosed based on the laboratory phenotype of the platelets from affected patients. A typical diagnosis of a bleeding disorder commences with a clinical interview of the patient that includes an examination of their symptoms and details of their family history. Basic laboratory tests to determine platelet count, size and morphology then guide further specialised investigations that usually commence with platelet phenotyping (Gresele, 2015).

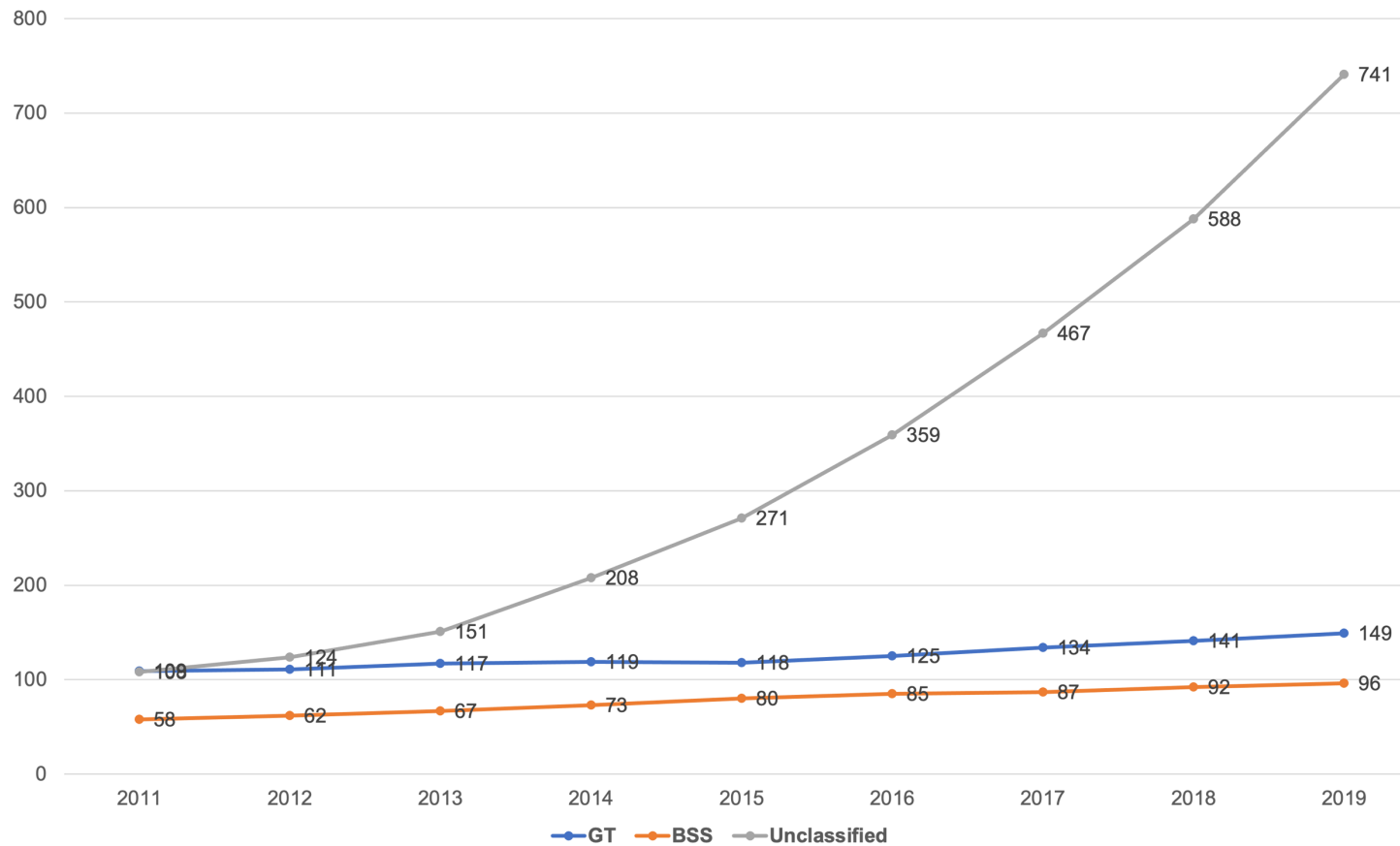


Figure 1.3: Platelet bleeding disorder data from 2011 to 2019.

Numbers of patients registered with UK Haemophilia Centres as having unclassified platelet disorders (grey), GT (blue) and BSS (orange) in the period from 2011 to 2019.

Data were obtained from the annual reports that are published by The United Kingdom Haemophilia Centre Doctors' Organisation (UKHCDO, 2019)

1.1.3.1 Phenotypic characterisation of platelets in bleeding disorders

The gold standard method for platelet phenotyping is light transmission aggregometry (LTA), which records the change in light transmission through a sample of platelet-rich plasma following exposure to different platelet activation agonists, including ADP, epinephrine, collagen, thrombin receptor activating peptide (TRAP), the TP receptor agonist U46619, arachidonic acid and ristocetin (Cattaneo et al, 2013). LTA can usually provide a definitive diagnosis for the well-characterised disorders of BSS and GT (Gresele et al, 2014). However, less-characterised inherited platelet disorders (IPDs) usually require further phenotypic investigation to aid diagnosis. These studies include the use of flow cytometry to quantify expression of cluster of differentiation (CD) markers expressed on the platelet membrane before and after agonist activation using antibodies recognising CD41 for GPIIb, CD61 for GPIIIa, CD42b for GPIb, CD42a for GPIb/IX, and CD62p for P-selectin (Curtis & McFarland, 2014; Gresele, 2015; Yun et al, 2016).

More extensive phenotyping would include assessment of the internal and external morphology of the platelets by electron microscopy (EM). This provides a visual indication of the presence or absence of internal components of platelets that can further aid diagnosis. For example, Bryan et al (2017) reported a patient with a diagnosis of von Willebrand disease which was revised to Hermansky–Pudlak syndrome (HPS) when EM examination revealed the absence of δ -granules from their platelets (Bryan et al, 2017).

Platelet phenotyping is useful in the diagnosis of well-characterised platelet bleeding disorders. However, in those cases where a diagnosis is not reached by phenotyping, the results can help to direct further investigations, in particular of candidate genes that may harbour underlying genetic defects.

1.1.3.2 Genetic investigations in patients with platelet bleeding disorders

Next generation sequencing (NGS) is a powerful tool which can be used to screen a panel of candidate genes for known or novel defects in patients referred for investigation of a platelet bleeding disorder. Ideally, genomic DNA from affected patients would be screened for alterations in those genes that are recognised to be associated with inherited platelet bleeding disorders (IPDs). Indeed this approach was adopted in the study by Downes et al (2019) which described the use of a panel of 96 IPD genes, defects in which were correlated previously to the development of IPDs (Downes et al, 2019). Sequencing of the panel of candidate genes succeeded in

identifying causative mutations in approximately half of the patients who had been diagnosed with unexplained platelet bleeding disorders that they studied (Downes et al, 2019). Another tool is whole exome sequencing (WES) which facilitated the identification of novel candidate genes that had no previous association with platelet bleeding disorders such as *SLFN14*, *FYB*, and *ETV6* (Almazni et al, 2019; Fletcher et al, 2015; Levin et al, 2015; Noetzli et al, 2015). However, with the use of both tools, the underlying genetic defects in approximately half of the patients with IPDs remain to be identified.

1.1.3.2.1 The UK-GAPP study

The UK Genotyping And Phenotyping of Platelets (UK-GAPP) study addressed the challenge of interpreting platelet phenotyping studies and correlating these with genetic data generated through WES analysis (Watson et al, 2013). The study, which was funded by the British Heart Foundation in the period from 2010 to 2015 and involved researchers from Birmingham, Bristol and Sheffield, recruited patients registered as having unexplained platelet bleeding disorders with Haemophilia Centres throughout the UK (<https://www.birmingham.ac.uk/research/cardiovascular-sciences/research/platelet-group/platelet-gapp/index.aspx>). Patients recruited to the study had a history of unusual bleeding with signs and symptoms that were compatible with a platelet function disorder, normal coagulation results and had not been diagnosed with an acquired platelet dysfunction disorder. In addition, they were not taking any medications that are known to affect platelet function at the time of investigation (Dawood et al, 2012).

The study developed a bioinformatic pipeline to identify candidate disease-causing genes following WES by first, aligning sequences to the latest version of the human genome (hg19), then identifying novel variants, use of reference sequence variation databases such as the 1000 genomes, gnomAD browser and an in-house exome sequence database (Johnson et al, 2016). Sequences were examined using either a candidate gene approach which involved selective examination of 358 genes which were previously associated with platelet bleeding disorders, or by applying the bioinformatic pipeline to identify novel candidate genes. The potential effects of candidate gene variants that were identified among patients using either approach were predicted using bioinformatic algorithms. Those variants which were predicted to be pathogenic, and were reported to have a minor allele frequency (MAF) of less than 0.01 in online databases were then targeted for further investigation (Daly et al, 2014; Johnson et al, 2016).

1.2 Mammalian Tribbles homologues

The *Tribbles* protein was first discovered in the fruit fly (*Drosophila*) where it was shown to regulate mitosis by interacting with the protein phosphatase cell division cycle 25 (Cdc25)/String, thereby regulating proliferation and morphogenesis at the early gastrulation stages of the fruit fly (Grosshans & Wieschaus, 2000; Mata et al, 2000; Seher & Leptin, 2000). In humans, *Tribbles* orthologues were identified to constitute a family of three members *TRIB1*, *TRIB2* and *TRIB3* that encode proteins which act mainly as intracellular signalling modulators to regulate diverse cellular processes including proliferation, differentiation, survival and apoptosis. There are three features that are shared by all Tribbles family members; an N-terminal domain that is rich in proline (P), glutamic acid (E), serine (S) and threonine (T) residues, the so-called PEST domain, that is suggested to have a role in determining the half-life of TRIB (Hegedus et al, 2007); a pseudokinase domain that lacks sequences which are essential for phosphorylation activity, and suggested to interact with protein kinases such as AKT to indirectly regulate target protein functions (Hegedus et al, 2007; Yokoyama & Nakamura, 2011) and; a C-terminal tail that contains two unique motifs that are involved in the interaction with MAPK and ubiquitin E3 ligase (Eyers et al, 2016) (Figure 1.4).

Although the Tribbles family members share similar features and show greater than 45% DNA sequence homology (Dedhia et al, 2010), they seem to engage in regulating different cellular mechanisms. Tribbles homologue 1 (*TRIB1*), which is encoded by a gene located at position *q24.13* on chromosome 8, was classified as an oncogene that enhances the phosphorylation of extracellular signal-regulated kinase (ERK), and consequently contributes to the survival of leukemic cells leading to acute myeloid leukaemia (AML) (Jin et al, 2007; Yokoyama et al, 2010). *TRIB1* was also linked to the pathogenesis of prostate cancer by exhibiting high expression levels prostate tumours in mice, and by showing interaction with cMYC proteins, that are known to contribute to the prostate cancer progression (Shahrouzi et al, 2020). *TRIB1* also has a possible role in maintaining low levels of hepatic and plasma cholesterol and triglycerides, as elevated lipid levels were observed in *Trib1* knockout mice (Burkhardt et al, 2010). Following observations supported the involvement of *TRIB1* in regulating lipid metabolism, which eventually contributes to the development of coronary artery disease (CAD) (Douvris et al, 2014; Johnston et al, 2018).

Tribbles homologue 2 (*TRIB2*), which is encoded by *TRIB2* on chromosome *2p24.3*, is considered an oncogene that inhibits CCAAT/enhancer-binding protein alpha

(C/EBP α) and suppresses apoptosis leading to AML (O'Connor et al, 2016; Rishi et al, 2014). The expression of *TRIB2* has been correlated with the progression of other cancers including liver cancer (Wang et al, 2013), lung cancer (Grandinetti et al, 2011; Liang et al, 2017), skin cancer (Chen et al, 2020; Zanella et al, 2010), colorectal cancer (Hou et al, 2018), and it has also been identified to be involved in resistance to anti-cancer therapies (Hill et al, 2017).

This study is investigating the potential role of Tribbles homologue 3 (TRIB3) in platelet function. This kinase-like protein, which is encoded by *TRIB3* on chromosome 20p13, has been associated with megakaryocyte differentiation (Butcher et al, 2017) and preliminary data from our group suggest that it also has a role in platelet function.

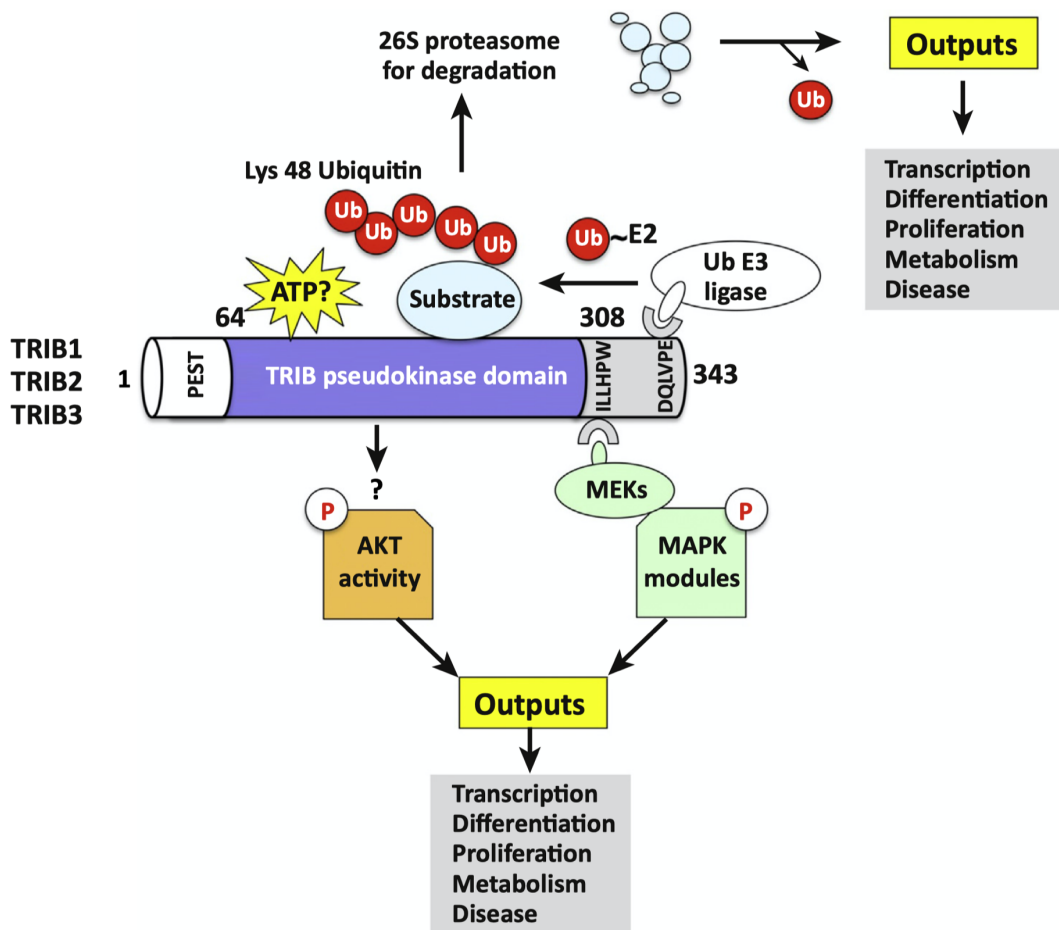


Figure 1.4: The three domains of TRIBBLES proteins and their functions

The figure shows the three features that are present in all three members of the TRIBBLES family (TRIB1, TRIB2, and TRIB3). The domains are (i) the N-terminal or PEST domain ; (ii) the pseudokinase domain that is suggested to interact with protein kinases such as AKT; (iii) the C-terminal tail that contains two unique motifs that are involved in the interaction with MAPK and ubiquitin E3 ligase. Adapted, with permission from Eyers et al (2016).

1.2.1 Tribbles homologue 3 (TRIB3)

TRIB3 encodes a 358-amino acid protein that possesses three distinct domains similar to the other Tribbles family members. The N-terminal domain, which comprises approximately 70 residues, has been shown to incorporate a PEST motif, which is suggested to regulate *TRIB3* degradation and stability (Ohoka et al, 2010; Zhou et al, 2008). The kinase-like domain, which has approximately 240 residues, mimics functional kinase domains but lacks consensus ATP-binding sequences that are essential for the kinase activity. The pseudokinase domain represents the majority of the protein and contains sequences that are suggested to regulate the interaction with AKT (Mondal et al, 2016). The short flanking C-terminal domain, which has approximately 45 residues, has binding sites for MAPK and the E3 ubiquitin ligase through which *TRIB3* promotes ubiquitination via constitutive photomorphogenic protein 1 (*COP1*) (Kiss-Toth et al, 2004; Mondal et al, 2016; Yokoyama & Nakamura, 2011; Zhou et al, 2008) (Fig. 1.5).

TRIB3 interacts with protein kinases to negatively control their phosphorylation in different cells including brain, liver and adipose tissues (Formoso et al, 2011; Kiss-Toth et al, 2004; Mondal et al, 2016; Prudente & Trischitta, 2015; Saleem & Biswas, 2017; Sun et al, 2017). The pseudokinase also suppresses the activity of several transcription factors including activating transcription factor 4 (*ATF4*), C/EBP α , nuclear factor kappa-light-chain-enhancer of activated B cells (*NF- κ B*) and peroxisome proliferator-activated receptors (*PPARs*), while silencing *TRIB3* was reported to increase the expression of transcription factors including GATA-binding factor 1 (*GATA1*), friend of GATA 1 (*FOG1*), friend leukaemia integration 1 (*FLI1*), and nuclear factor erythroid 2 (*NFE2*) (Butcher et al, 2017; Erazo et al, 2016; Mondal et al, 2016; Ord et al, 2014; Yokoyama & Nakamura, 2011).

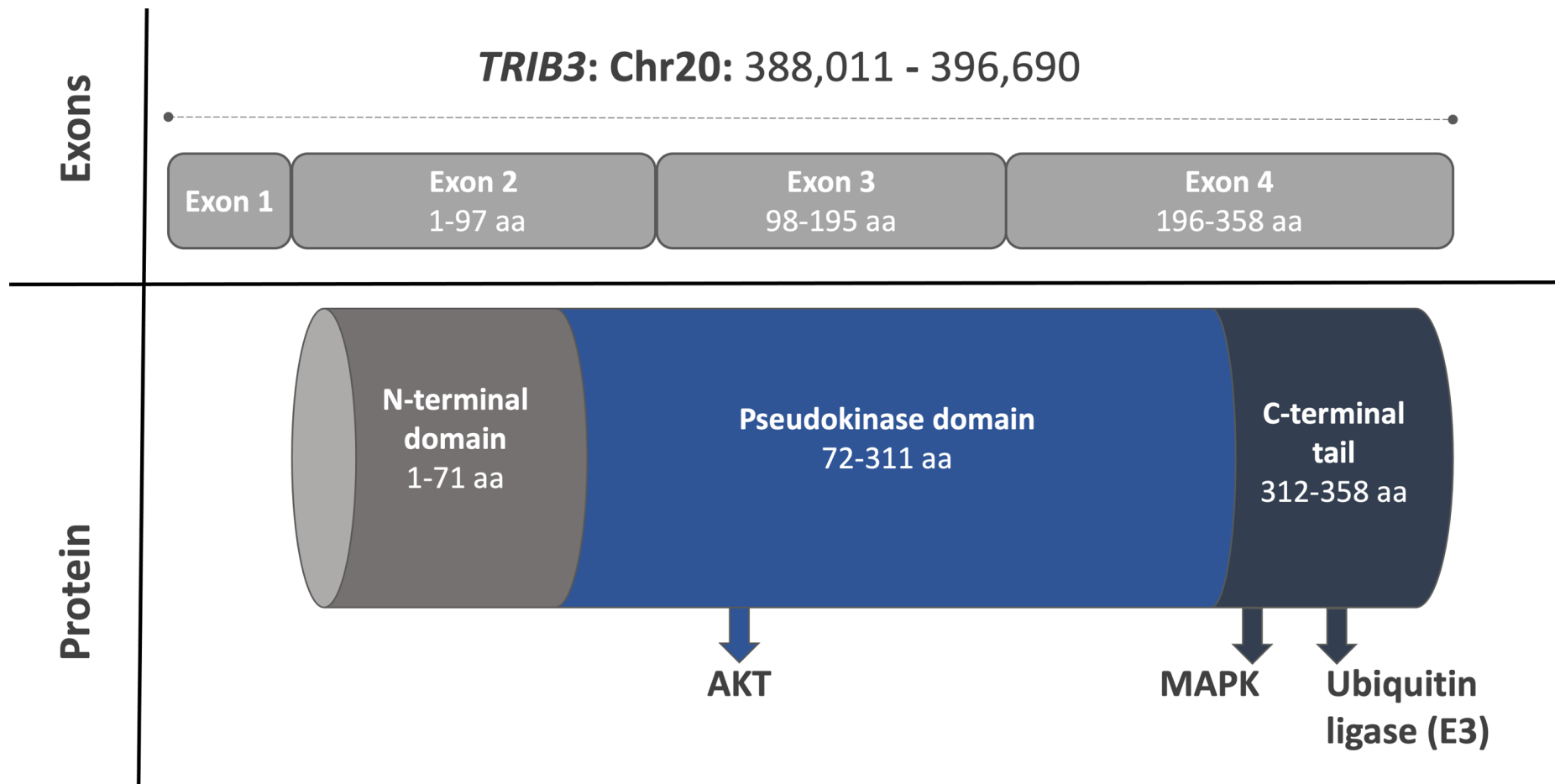


Figure 1.5: TRIB3 gene and protein domains

TRIB3 is located on chromosome 20 and comprises approximately 8,680 nucleotides of genomic DNA. Exons 2 to 4 of the gene encode the 358 residues that form the three domains of *TRIB3*.

1.2.2 TRIB3 in pathological situations and altered expression of TRIB3

Tribbles pseudokinase 3 has been reported to regulate insulin signalling in liver cells under starving conditions by interacting with AKT, to lower glucose uptake by cells and maintain normal glucose levels in the blood (Du et al, 2003). A common gain-of-function variant of *TRIB3*, in which the glutamine residue at amino acid position 84 is substituted by arginine (*c.A251G*, p.Q84R, rs2295490), has been reported to strengthen the interaction of TRIB3 with AKT and reduce its phosphorylation, resulting in less efficient insulin signalling and contributing to the development of insulin resistance (Prudente et al, 2005). Insulin resistance is reported to be a mediator of type 2 diabetes mellitus (T2DM), atherosclerosis, and impaired lipid metabolism (DeFronzo & Ferrannini, 1991). Investigation of the glucose profiles of healthy and diabetic patients found the Q84R variant of *TRIB3* to be associated with the development of T2DM (Prudente et al, 2005; Prudente et al, 2009). Examination of the association between the Q84R variant and atherosclerosis in endothelial cells revealed that inheritance of the R allele predisposed to endothelial dysfunction and cardiovascular disease (CVD) (Andreozzi et al, 2008). Moreover, an observational study investigating intima-media thickness (IMT) in a European cohort of 430 participants showed a significant increase in IMT in subjects expressing the R allele, which implies that carriers of this common variant are at higher risk for the development of CVD (Formoso et al, 2011).

TRIB3 is also associated with impaired lipid metabolism and obesity and a marked increase in hepatic *TRIB3* mRNA was observed in diabetic and obese patients that were scheduled to undergo weight-reducing surgery (Oberkofler et al, 2010). Moreover, silencing of *TRIB3* in diabetic and obese rats, led to activation of AMP-activated protein kinase (AMPK) and partial restoration of lipid and glucose metabolism (Sun et al, 2017). A further study, which emphasised the role of Trib3 in regulating lipid metabolism, showed markedly increased expression of *Trib3* in the skeletal muscle cells of obese mice which was accompanied by disrupted glucose homeostasis (Kwon et al, 2018).

TRIB3 is a cell stress regulator that has been shown to orchestrate cell survival and apoptosis in cancer cells. In breast cancer patients, increased expression of *TRIB3* in breast cancer tissue was correlated with longer survival and improved prognosis, and it was noted that tumours with elevated *TRIB3* levels were more susceptible to

treatments such as hypoxia and radiotherapy (Wennemers et al, 2011; Yu et al, 2019). Increased expression of TRIB3 was also associated with a good prognosis in patients with acute promyelocytic leukaemia (APL) (Li et al, 2017). Conversely, the downregulation of TRIB3 expression in Acute myeloid leukaemia (AML) cells was shown to trigger apoptosis and autophagy, suggesting that TRIB3 promotes the survival of AML tumour cells (Luo et al, 2020). TRIB3 has been shown to have a crucial role in tumour cell apoptosis as *Trib3*^{-/-} mice showed a failure to inhibit AKT/mammalian target of rapamycin complex 1 (mTORC1), which when repressed would trigger tumour cell autophagy and apoptosis (Salazar et al, 2013). A pharmacological study considered overexpressing TRIB3 in lung and pancreatic cancer cells to induce autophagy using an AKT/mTORC1 inhibitor, which showed an outstanding tumour cell death rates and supported the role of TRIB3 in tumour suppression (Erazo et al, 2016). TRIB3 showed upregulation and direct interaction with Parkin, a protein that promotes neuronal cell survival, in post-mortem samples from Parkinson's disease (PD) patients. The overexpression of *TRIB3* was proposed to induce neuronal cell death, which could contribute to development of the neurodegenerative disorder. Cultures of neuronal cell lines that act as in-vitro models of PD displayed extended neuron survival following *TRIB3* knockdown and higher cell death rates were observed following Parkin knockdown (Aime et al, 2015). A recent study using suppressors that target the TRIB3/Parkin interaction in *in-vitro* models of PD showed protective effects on neuron survival (Aime et al, 2020). Similarly, expression of *TRIB3* was correlated with the development of Alzheimer's Disease (AD). A report underlined an overexpression of *TRIB3* in response to the administration Amyloid- β , a key molecule in AD pathogenesis, which when overexpressed would block the AKT phosphorylation and allow the further transcription of pro-apoptotic genes (Saleem & Biswas, 2017). The contribution of TRIB3 to the development of neurodegenerative disorders highlights it as a possible pharmaceutical target for drug design.

The observation that *TRIB3* is overexpressed when megakaryopoiesis is inhibited in haematopoietic stem cells (Ahluwalia et al, 2015), and a following study which identified TRIB3 as a negative regulator of megakaryopoiesis in cell cultures of haematopoietic cell lines (Butcher et al, 2017) suggest a role for TRIB3 in platelets, though to date this has not yet been investigated.

1.3 Background, hypothesis and aims of the study

1.3.1 Background of this study

Prior to the work described in this thesis, research undertaken by a group in Cardiff Metropolitan University (Cardiff, UK) examined global gene expression in haematopoietic cells undergoing megakaryocyte differentiation in response to the selective megakaryopoiesis inhibitor, anagrelide. *TRIB3* was one of the 328 genes that was found to be differentially regulated by anagrelide, showing significantly increased expression, a finding that suggested it may play a role in the negative regulation of megakaryopoiesis. Pathway analysis and immunoblotting studies led the authors to propose that anagrelide suppressed megakaryopoiesis by increasing phosphorylation of eukaryotic initiation factor 2 alpha (eIF2 α), leading to increased levels of activating transcription factor 4 (ATF4), which is known to induce *TRIB3* (Ahluwalia et al, 2015).

The observations of Ahluwalia et al (2015) were explored further in the *Trib3* knockout (KO) mice by colleagues in our group at the University of Sheffield (Sheffield, UK), who observed that female *Trib3* knockout (KO) mice showed a marked reduction in platelet activation in response to the thrombin receptor activation peptide (TRAP), when compared to the male KO mice [unpublished].

These observations led us to hypothesise that variations in *TRIB3* may be associated with platelet function. This hypothesis was initially investigated by seeking variations in *TRIB3* in WES data from patients with unexplained platelet bleeding disorders who had been recruited to the UK GAPP study (Dawood et al, 2012). This analysis identified five rare non-synonymous single nucleotide variations in *TRIB3* predicting V107M, S146N, R149G, R153H and R181C amino acid substitutions in *TRIB3*. This finding supported the hypothesis that defects in *TRIB3* could contribute to a platelet function disorder.

As part of my MSc dissertation, I undertook preliminary studies to investigate the effects of the identified *TRIB3* variants, and observed that the R149G variant of *TRIB3* showed a diffuse pattern of expression in the nucleus of HeLa cells in contrast to the punctate expression pattern of wild-type *TRIB3* (Bukhari, 2016).

The Cardiff group has published further work on megakaryocyte production and *TRIB3* expression levels, and reported decreased *TRIB3* expression in response to TPO in a megakaryocytic cell line, increased megakaryocyte production with *TRIB3* silencing, and reduced megakaryopoiesis with overexpression of *TRIB3* (Butcher et al, 2017).

1.3.2 Hypothesis

We hypothesise that TRIB3 has a regulatory role in platelet function which, when altered, may be associated with an increased risk of bleeding

1.3.3 Aims

The aims of this study were to:

- (i) Use bioinformatic tools and mass spectrometric analysis to predict the effects of the rare non-synonymous *TRIB3* variants identified in patients with unexplained platelet bleeding disorders.
- (ii) Examine the expression of the *TRIB3* variants and their interactions with AKT isoforms using *in-vitro* approaches.
- (iii) Correlate *TRIB3* function with platelet function in the *Trib3* knockout mouse.

To accomplish these aims, predictive algorithms and structural analysis were used to predict the effects of the rare non-synonymous *TRIB3* variants, and the outcomes guided further exploration of interacting peptides using a mass spectrometric approach (see chapter 3). Protein complementation assays were used to examine the localisation and expression patterns of the variant forms of *TRIB3*, and their interactions with isoforms of *AKT*. The steps taken to optimise these assays are described in chapter 4. The protein complementation assays were then used to assess the effects of the rare variants on their cellular localisation and their interaction with key platelet signalling molecules, and an assessment of platelet function was performed to investigate platelet activation and secretion in *Trib3* knockout mice (see chapter 5). The potential involvement of *TRIB3* in mitochondrial function, which was identified through the mass spectrometric and cellular localisation studies, was explored in chapter 6.

Chapter 2:

Materials and Methods

2.1 Materials

2.1.1 Animals

Wild-type (WT) mice on a C57BL6/J background were obtained from Charles River Laboratories (Harlow, UK). The *Trib3*^{+/-} mice were generated by injecting *TRIB3* trapping vector (Salazar et al, 2015) into embryo mice, which were provided by Professor Endre Kiss-Toth (University of Sheffield, UK). The *Trib3*^{+/-} mice were used in mating to produce WT, *Trib3*^{+/-} and *Trib3*^{-/-} mice. Animals breeding, ear-clipping and experiments were executed in biological services unit facilities (University of Sheffield, UK). Genotyping from ear-clips was performed by the genomics core facility (University of Sheffield, UK) using primers listed in table 2.1. Animals at the age of 16 to 18 weeks were used for platelet function studies. The University of Sheffield and the UK Animals in Science Regulation Unit approved all murine experiments (Personal licence Category C #41779, Project licence #P5395C858).

2.1.2 Platelet collection and activation reagents

Mice were anaesthetized using IsoFlo[®] 100% w/w inhalation Vapour liquid Isoflurane, which was obtained from Zoetis UK Ltd. (London, UK). Anticoagulants including sodium citrate, which was provided by Dr Heather Judge (University of Sheffield, UK), and hirudin which was sourced from Canyon Pharmaceuticals (Columbia, MD, USA) were used for blood collection. Thrombin receptor-activating peptide (TRAP) was synthesised to order by Peptide 2.0 (Chantilly, VA, USA). Antibodies including fluorescein isothiocyanate (FITC)-conjugated rat anti-mouse CD62P sourced from BD Biosciences (San Jose, CA, USA), and phycoerythrin (PE)-conjugated rat anti-mouse Integrin $\alpha_{IIb}\beta_3$ (commonly referred to as CD41/61) purchased from Emfret Analytics (Eibelstadt, Germany) were used for flowcytometric detection. HEPES/Tyrod's (HT) buffer (129 mmol/L NaCl, 8.9 mmol/L NaHCO₃, 2.8 mmol/L KCL, 0.8 mmol/L KH₂PO₄, 5.6 mmol/L dextrose and 10 mmol/L HEPES) was provided by Dr. Heather Judge (University of Sheffield, UK). CHRONO-PAR Thrombin, and CHRONO-LUME[®] Luciferin Luciferase substrate were purchased from CHRONO-LOG Corp. (Havertown, PA, USA) for platelet secretion assay.

2.1.3 Plasmids

The identified *TRIB3* variants were introduced into the cDNA sequence of human *TRIB3* that was derived from HeLa cells and cloned using the TOPO™ method into a Gateway™ entry clone to make the h*TRIB3*-ENTR/D plasmid, which was provided by Professor Endre Kiss-Toth (University of Sheffield, UK). The Gateway™ entry clone, which is approximately 2.6kb in size and includes a Kanamycin-resistance cassette, was sourced from Invitrogen (Carlsbad, CA, USA) (Appendix 1). The entry clone was engineered to have two different backbones before introducing the *TRIB3* variants, one corresponding to the reference sequence of human *TRIB3* that is published on the UCSC genome browser (<https://genome.ucsc.edu>, version:GRCh38/hg38) (will be referred to as Q84/A171 wild-type), and a second, in which codons 84 and 171, of the *TRIB3* cDNA sequence were mutated to encode arginine and valine residues respectively (will be referred to as R84/V171 wild-type). Both versions were 3.655kb in size.

A Gateway™ destination vector which was 7.296 kb in size and allowed expression of *TRIB3* fused to YFP was obtained from Invitrogen (Carlsbad, CA, USA) (Appendix 2). The AKT1/Venus1 (V1) and *TRIB3*/Venus2 (V2) expression plasmids were 6.468kb and 6.696kb in size respectively. These were designed to encode a split YFP which emits a modified signal when V1 and V2 interact from both fusion proteins. These modified YFP destination vectors were supplied by Invitrogen (Carlsbad, CA, USA) (Appendix 3). The *TRIB3*/pBiT1.1C (*TRIB3*/LgBiT) and AKT1/pBiT2.1C (AKT1/SmBiT) expression plasmids are 5.038kb and 4.964kb in size respectively. These are designed to encode a split NanoLuc luciferase which emits a quantifiable luminance signal when the LgBiT and SmBiT from the two fusion proteins interact. The vectors expressing LgBiT and SmBiT of NanoLuc luciferase were supplied by Promega (Madison, WI, USA) (Appendix 4). All expression vectors include Ampicillin-resistance cassettes.

2.1.4 Oligonucleotide Primers

Oligonucleotide primers were designed to genotype *Trib3* from murine ear-clips, and introduce *TRIB3* variants into the wild-type *TRIB3* sequence in the h*TRIB3*-ENTR/D Gateway entry plasmid. The sequences of all primers used are shown in Table 2.1. Primers were ordered from Sigma-Aldrich (Darmstadt, Germany) and Eurofins Genomics (Ebersberg, Germany). Universal primers (M13 and BGH) and primers designed for the pBiT system (Split-NanoLuc system) were used to sequence

expression plasmids. Sequencing was carried out at the Source Bioscience sequencing facility (Nottingham, UK).

Table 2.1: Oligonucleotide primer sequences.

| Name | Sequence | Use |
|----------------|-----------------------------------|-------------|
| WT_Trib3_fw | 5' CCGCGACGAATGAAAGGTTTA 3' | Genotyping |
| WT_Trib3_rv | 5' AGACTCCGAGAGCTGCTCAGTTAGG 3' | Genotyping |
| KO_Trib3_fw | 5' CCGCGACGAATGAAAGGTTTA 3' | Genotyping |
| KO_Trib3_rv | 5' AAATGGCGTTACTTAAGCTAGCTTGC 3' | Genotyping |
| TRIB3_V107M_fw | 5' GGAAGCCCTGGCCATGCTGGAGCCCT 3' | Mutagenesis |
| TRIB3_V107M_rv | 5' AGGGCTCCAGCATGGCCAGGGCTTCC 3' | Mutagenesis |
| TRIB3_S146N_fw | 5' CCATGGGGACATGCAGAACCTGGTGCG 3' | Mutagenesis |
| TRIB3_S146N_rv | 5' CGCACCAGGTTGTGCATGTCCCATGG 3' | Mutagenesis |
| TRIB3_R149G_fw | 5' CACAGCCTGGTGGGAAGCCGCCACCG 3' | Mutagenesis |
| TRIB3_R149G_rv | 5' CGGTGGCGGCTTCCCACCAGGCTGTG 3' | Mutagenesis |
| TRIB3_R153H_fw | 5' CGAAGCCGCCACCATATCCCTGAGCC 3' | Mutagenesis |
| TRIB3_R153H_rv | 5' GGCTCAGGGATATGGTGGCGGCTTCG 3' | Mutagenesis |
| TRIB3_R181C_fw | 5' GTCTGGTCCTGTGTGATCTCAAG 3' | Mutagenesis |
| TRIB3_R181C_rv | 5' CTTGAGATCACACACAGGACCAGAC 3' | Mutagenesis |
| M13_fw | 5' TGTA AACGACGGCCAGT 3' | Sequencing |
| M13_rv | 5' CAGGAAACAGCTATGAC 3' | Sequencing |
| BGH_rv | 5' TAGAAGGCACAGTCGAGG 3' | Sequencing |
| BiT_fw | 5' CACCGAGCGACCCTGCAGCG 3' | Sequencing |
| BiT_rv | 5' CTTATCATGTCTGCTCGAAG 3' | Sequencing |

Oligonucleotides with WT and KO abbreviation were used to genotype murine samples. Mutagenesis primers were designed to introduce mutations using forward and reverse primers. M13 and BGH are universal primers used for sequencing. BiT primers are designed to sequence plasmids on the Split-NanoLuc system.

2.1.5 Mutagenesis, cloning, and DNA extraction kits

The QuikChange Lightning Site-Directed Mutagenesis kit was supplied by Agilent Technologies (Cedar Creek, TX, USA). The Gateway® LR Clonase™ II Enzyme Mix was supplied by Invitrogen (Carlsbad, CA, USA). The QIAprep® Spin Miniprep and EndoFree® Plasmid Maxi kits were purchased from Qiagen (Hilden, Germany), and the GenElute™ HP Plasmid Midiprep kit was sourced from Sigma-Aldrich (Darmstadt, Germany).

2.1.6 Electrophoresis reagents

Tris-Acetate EDTA (TAE) buffer (50X) was sourced from Geneflow Ltd. (Staffordshire, UK). Agarose powder was supplied by Fisher Scientific (Fair Lawn, NJ, USA). Ethidium bromide, at a concentration of 10 mg/ml, was purchased from Sigma-Aldrich (Steinheim, Germany). The Mini-Sub® Cell GT horizontal electrophoresis system and PowerPac 1000 power supply were both manufactured by Bio-Rad (USA).

2.1.7 Bacterial cultures

NYZ+ broth was sourced from Fisher Scientific (Fair Lawn, NJ, USA). LB agar was supplied by Merck (Darmstadt, Germany) and LB broth was obtained from Fisher BioReagents (Fair Lawn, NJ, USA). Kanamycin A and Ampicillin trihydrate were supplied as powders by the Sigma Chemical Co. (Steinheim, Germany), and dissolved in distilled water at a concentration of 50 µg/ml. Ethanol was supplied by VMR International Ltd. (Bedford, UK) and Isopropanol was obtained from Acros Organics (Geel, Belgium).

2.1.8 Cell lines, Tissue culture, and transfection reagents

Human embryonic kidney (HEK) 293T and cervical cancer cells (HeLa) were sourced from American Type Culture Collection (ATCC) (Manassas, VA, USA). Multiple culture mediums were used including Dulbecco's Modified Eagle Medium (DMEM) + GlutaMAX™-I, DMEM High Glucose (1X) Phenol red-free medium and Opti-MEM® Reduced serum (1X) Phenol red-free medium. All mediums were supplemented with 10% Fetal Bovine Serum (FBS) and 1% Antibiotic-Antimycotic (Anti-Anti) (100X). These reagents were sourced from Life Technologies Corporation (Grand Island, NY, USA). Trypsin-EDTA solution (1X) and Phosphate Buffered Saline (PBS) tablets were supplied by Sigma-Aldrich (St. Louis, MO, USA). Nunc™ EasY Flasks™ (75cm²) were

manufactured by Thermo Fisher Scientific (Roskilde, Denmark). DRAQ5 stain (5mM), diluted in Phenol red-free medium at a 1:2000 ratio, was supplied by Thermo Fisher (Waltham, MA, USA). Hoechst 33342 stain (10 mg/ml), diluted in Phenol red-free medium at a 1:2000 ratio, was supplied by Life Technologies (Eugene, OR, USA), and Dimethyl Sulfoxide (DMSO) was supplied by Sigma-Aldrich (St. Louis, MO, USA). Lipofectamine® 3000 Transfection reagent was purchased from Invitrogen (Carlsbad, CA, USA), while FuGENE HD transfection reagent and the Nano-Glo® Live Cell Assay system were supplied by Promega (Madison, WI, USA).

2.1.9 Protein extraction and blotting

Cells were lysed using Pierce® radioimmunoprecipitation assay buffer (RIPA) which was obtained from Thermo Scientific (Rockford, IL, USA). RIPA buffer was supplemented with 1% SIGMAFAST™ Protease Inhibitor Cocktail (PIC) and 1% PhosSTOP™ phosphatase inhibitor from Roche Diagnostics (Mannheim, Germany). The total protein extracted was quantitated using the Pierce BCA protein assay kit, which was supplied by Thermo Scientific (Rockford, IL, USA). Proteins were separated on NuPAGE™ 4-12% Bis-Tris gels using NuPAGE® LDS buffer (X4), NuPAGE® Sample Reducing Agent (10X), NuPAGE® MOPS SDS Running Buffer and an XCell SureLock™ Electrophoresis Cell system which were all sourced from Invitrogen (Carlsbad, CA, USA). Proteins were blotted using Nitrocellulose Regular Stacks sourced from Invitrogen (Kiryat Shmona, Israel) on an iBlot 2 system which was manufactured by Thermo Fisher (Waltham, MA, USA). Tris Buffered Saline (TBS) was purchased from Sigma-Aldrich (St. Louis, MO, USA) and Tween® 20 was sourced from Fisher BioReagents (Fair Lawn, NJ, USA). Odyssey® Blocking Buffer was supplied by LI-COR (Lincoln, NE, USA). Primary AKT and pAKT rabbit monoclonal antibodies were purchased from Cell Signalling (Danvers, MA, USA), and secondary IRDye® 680RD-conjugated Goat anti-Rabbit antibody was obtained from LI-COR (Lincoln, NE, USA). α Tubulin mouse monoclonal antibody was obtained from Santa Cruz Biotechnology (Heidelberg, Germany) and secondary IRDye® 800CW-conjugated Donkey anti-Mouse antibody was obtained from LI-COR (Lincoln, NE, USA). Membranes were imaged using a LI-COR Odyssey CLx machine that was manufactured by LI-COR (Lincoln, NE, USA).

2.1.10 Laboratory equipment

The Haemostasis laboratory is equipped with an accuSpin™ Micro bench-top microfuge manufactured by Thermo Electron Corporation (Osterode, Germany), a VortexGenie-2 from Scientific Industries (Bohemia, NY, USA), a SUB6 Water bath that was supplied by Grant Instruments (Cambridge, UK), a J2-21M/E centrifuge manufactured by Beckman Instruments (Glenrothes, UK), a block heater from Stuart Scientific (Stone, UK), and a Sysmex Automated Hematology Analyser Model KX – 21N manufactured by Sysmex Corporation (Kobe, Japan). Equipment used in other laboratories included a NanoDrop 1000 system supplied by Thermo Fisher Scientific (Waltham, Ma, USA), a class II Biological Safety Cabinet manufactured by Walker Safety Cabinets Ltd. (Glossop, UK), a Leica AF6000 Time-Lapse inverted wide-field fluorescence microscope supplied by Leica Microsystems (Wetzlar, Germany), a Multiphoton/Confocal Microscope LSM510 NLO Inverted manufactured by Zeiss (Oberkochen, Germany), a VIRIOSKAN FLASH plate reader from Fisher Scientific (Vantaa, Finland), a CHRONO-LOG aggregometer (Model 700) from CHRONO-LOG (Havertown, PA, USA) and an LSR II flow cytometer supplied by BD Biosciences (Franklin Lakes, NJ, USA).

2.1.11 Laboratory plastics

Plastics that were used included 5ml, 10ml, 25ml and 50ml Stripettes® supplied by Corning Incorporated (Corning, NY, USA), and thin-walled PCR tubes (0.2ml) sourced from Thermo Fisher Scientific (Loughborough, UK). CELLSTAR® tubes (15ml and 50ml) were sourced from Greiner Bio-One Ltd (Stonehouse, UK). Polypropylene Round-Bottom Tubes (14ml) were purchased from BD (Franklin Lakes, NJ, USA). Eppendorf Tubes® (1.5ml) were purchased from Eppendorf AG (Hamburg, Germany) and TipOne tips (10µl, 20µl, 200µl, 1000µl) were purchased from StarLab (Ahrensburg, Germany).

2.2 Methods

2.2.1 Site-directed mutagenesis of the *TRIB3* Entry clones

Site-directed mutagenesis was carried out using the QuikChange Lightning Site-Directed Mutagenesis Kit according to the manufacturer's instructions.

2.2.1.1 Designing mutagenic oligonucleotide primers

Oligonucleotide primers which had previously been designed to introduce single nucleotide variations into the *TRIB3* cDNA that predicted V107M, R149G, R153H and R181C amino acid substitutions in *TRIB3* were made available by Professor Endre Kiss-Toth (University of Sheffield, UK). The nucleotide change predicting the S146N substitution in *TRIB3* was introduced into the *TRIB3* cDNA using oligonucleotide primers which were designed at the outset of this study. All primers were designed according to the manufacturers' specifications. Thus, the desired point mutation was introduced in the middle of the primer or 10 to 15 nucleotides from either end. Primers were 25 to 45 nucleotides in length, had a melting temperature greater than or equal to 78° C and a GC content of at least 40%. The primers were supplied as stock solutions at a concentration of 100 pmol/μl, and the manufacturer provided a formula to calculate the volume of the stock solution that contained 125 ng as required for the thermocycling. The following formula is recommended by Agilent Technologies to calculate the dilution volumes:

$$\frac{\text{ng of oligo}}{330 \times \text{number of bases in oligo}} \times 1000 = \text{primer concentration in pmol}/\mu\text{l}$$

An example of the calculation for one of the S146N primers:

$$\frac{125 \text{ ng}}{330 \times 27} \times 1000 = 14.08 \text{ pmol}/\mu\text{l}$$

To prepare a 100μl of primer at 125ng, we diluted 14.08μl of the stock primer solution in 85.92μl of the diluent (distilled water). The 125ng is the recommended concentration of primer to be used at the thermocycling step of the mutagenesis.

2.2.1.2 Plasmid preparation

Mutagenesis was performed on the wild-type (WT) TRIB3 Gateway entry plasmids having the R84/V171 and Q84/A171 backbones (see section 2.1.2) to generate Gateway™ entry clones encoding the V107M, S146N, R149G, R153H and R181C variants of TRIB3. Prior to commencing the mutagenesis procedure, distilled water was used to dilute the two WT plasmids to a concentration of 100ng/μl.

2.2.1.3 Mutant strand synthesis

The 50μl reaction mixtures were prepared in thin-walled Eppendorf tubes to include 10x Reaction buffer, 100ng plasmid, 125ng of each primer, 1μl of dNTP mix and 1μl of the QuikChange Lightning enzyme (concentrations and enzyme activity are proprietary). Reaction mixtures were subjected to thermal cycling which comprised 18 cycles of denaturation at 95° C for 2 minutes, annealing at 60° C for 10 seconds and extension at 68° C for 2 minutes. The extension time was determined by the plasmid size as the manufacturer recommends allowing 30 seconds per kilobase of DNA. The hTRIB3-ENTR/D is 3.655 kb; therefore, 2 minutes were allowed for extension.

2.2.1.4 Digestion of parental strands

Following the mutagenesis step, the parental (non-mutated) strands were digested by adding 2μl of *Dpn* I, an enzyme which cuts at methylated GATC sequences (the concentration of the enzyme was proprietary), and incubating samples at 37° C for 15 minutes.

2.2.1.5 Transformation of ultracompetent cells

A 45μl aliquot of XL-10 Gold Ultracompetent cells was gently pipetted into a pre-chilled round-bottomed falcon tube containing 2μl of 2-Mercaptoethanol (β-ME). A 2μl sample of the *Dpn* I digested DNA was mixed with the cells and the sample incubated on ice for 30 seconds. The cells were then heat-shocked for precisely 30 seconds at 42° C, before incubation on ice for a further 2 minutes. A 0.5ml aliquot of pre-heated NYZ⁺ broth (prepared by dissolving 5.5g of NYZ⁺ broth powder in 250ml of distilled water) was then added and the cells were grown for 1 hour at 37° C with shaking at 200rpm. Cells were then plated on LB selective agar (prepared by dissolving 9.25g of LB agar powder in 250ml of distilled water) and incubated at 37° C overnight.

2.2.2 Entry clones DNA extraction and purification

Single colonies were picked from LB agar plates and used to inoculate LB broth (prepared by dissolving 6.25 g of LB broth powder in 250 ml of distilled water) containing 100 µg/ml ampicillin. Cultures were allowed to grow overnight at 37° C before extracting plasmid DNA using Qiagen extraction kits. The QIAprep® Spin Miniprep kit was used to extract plasmid DNA from 5ml cultures, while the EndoFree® Plasmid Maxi kit was used to extract plasmid DNA from 250ml cultures. The GenElute™ HP Plasmid Midiprep kit was used to extract DNA from 50ml cultures. All kits were used according to manufacturers' instructions.

2.2.2.1 DNA purification using QIAprep® Spin Miniprep kit

When purifying plasmid DNA using the QIAprep® Spin Miniprep kit, the 5ml bacterial suspension was first centrifuged at 13,000 rpm for 3 minutes before resuspending the bacterial pellet in the resuspension buffer. Bacterial membranes were then lysed using lysis buffer. The suspension was neutralised using neutralisation buffer before centrifuging at 13,000rpm for 10 minutes to precipitate cellular debris. The supernatant was then pipetted onto a QIAprep spin column. Binding buffer was used to enhance DNA binding to the beads, and the washing buffer was used to wash-out any unbound residues. The purified DNA was then harvested from the column using elution buffer and centrifugation at 13,000rpm for 1 minute.

2.2.2.2 DNA purification using GenElute™ HP Plasmid Midiprep kit

The DNA purification using the Midiprep kit uses 50ml bacterial suspension that was centrifuged at 2500rpm for 20 minutes. The bacterial pellet was then resuspended in resuspension solution before lysing bacterial membranes by the lysis buffer. The suspension was neutralised by a neutralization buffer. Binding buffer was added to the lysates before they were filtered using filter syringe into binding columns that were pre-treated by the column preparation solution. A vacuum was used to allow lysates through the column before the washing the unwanted residues using the washing solutions 1 and 2. The purified DNA was harvested using 1ml of elution buffer and centrifugation at 2500rpm for 8 minutes.

2.2.2.3 DNA purification using EndoFree® Plasmid Maxi kit

The Maxi kit was used to extract DNA from 250ml bacterial suspensions. The suspensions were centrifuged at 6000rpm for 15 minutes at 4° C before the bacterial

pellets were resuspended in the suspension buffer. The suspensions were neutralised before the lysates were filtered using Maxi Cartridges. The lysates were allowed to pass through Qiagen Tips before they were washed and the DNA was harvested using elution buffer. Isopropanol and centrifugation at 15,000rpm for 30 minutes at 4° C were used to precipitate the DNA. Ethanol (70%) and centrifugation at 15,000rpm for 10 minutes at 4° C were used to wash the DNA, which were then allowed to air-dry for one hour. The purified DNA was then resuspended in distilled water.

2.2.2.4 Assessment of purified mutated plasmids

DNA was quantitated in plasmid preparations using a NanoDrop 1000 system, which was blanked against the elution buffer for plasmid samples isolated using the Miniprep and Midiprep kits, and against distilled water for plasmids isolated using the Maxi kit.

The integrity of the hTRIB3-ENTR/D plasmid sequence was assessed following digestion with *Not* I and *Pst* I which were sourced from Promega (Madison, WI, USA), which cut the plasmid into two fragments of 862bp and 2,793bp in size. Restriction digestion was carried out in 15µl reactions that included buffer H, distilled water, *Not* I and *Pst* I (5U of each) and plasmid DNA. The reactions were incubated for one hour at 37° C before electrophoresis of samples in 1% Agarose (prepared by dissolving 1 g of agarose powder in 100ml of TAE buffer) containing 0.5 µg/ml Ethidium bromide.

Where the restriction digestion revealed fragments of the expected size, 100 ng of plasmid DNA was subjected to Sanger sequencing using universal M13 primers to confirm the presence of the modified nucleotide sequence.

2.2.3 Cloning mutated TRIB3 cDNA into expression vectors

2.2.3.1 Gateway cloning

The Gateway™ recombination cloning system allows the efficient transfer of a cDNA sequence from an entry clone to an expression vector without disrupting the reading frame of the sequence. To assess cellular localisation, wild-type and variant forms of the *TRIB3* cDNA were swapped from the Gateway™ entry plasmid into a destination vector that allowed their expression as YFP fusion proteins (TRIB3/YFP) in mammalian cells. To examine localisation of TRIB3 interactions with AKT, wild-type and variant *TRIB3* cDNAs were swapped into a destination vector and expressed as fusion proteins with either the N-terminal (Venus 1) or C-terminal (Venus 2) region of modified YFP (TRIB3/V1 and TRIB3/V2 respectively). To assess the strength of the interactions

between TRIB3 variants and AKT1, the wild-type and variant *TRIB3* cDNAs were swapped into a destination vector and expressed as fusion proteins with split fragments of the modified NanoLuc luciferase. The *TRIB3* cDNAs were inserted into an expression vector and expressed as fusion proteins with the C-terminal Large-BiT fragment of the modified NanoLuc (TRIB3-1.1C LgBiT) and the *Akt1* cDNA was expressed with the SmallBiT of the NanoLuc on the C-terminal (AKT1-2.1C SmBiT). The cloning reaction volumes were scaled-down from the manufacturers' recommendations and included 0.5 μ l of the expression vector at a concentration of 100ng/ μ l, 0.5 μ l Gateway™ LR Clonase™ II Enzyme Mix, 0.5 μ l distilled water and 0.5 μ l of the entry plasmid at a concentration of 100ng/ μ l. The reactions were incubated for 1 hour at 25° C before being terminated by the addition of 0.5 μ l of 2 μ g/ μ l Proteinase K solution and incubation for 10 minutes at 37° C. The recombinant plasmids were then transformed into competent Q5® cells. For each transformation reaction, 2 μ l of the recombinant plasmid was added to a 45 μ l aliquot of cells in a pre-chilled round bottomed falcon tube, and the mixture was incubated on ice for 2 minutes. The mixtures were then heat-shocked for precisely 30 seconds and incubated on ice for a further 2 minutes before adding 0.5ml of pre-heated NYZ⁺ broth. Cells were allowed to grow for 1 hour at 37° C on an orbital shaker at a setting of 200rpm before being plated on LB selective agar and incubated overnight at 30° C.

2.2.3.2 Assessment of purified recombinant plasmids

Recombinant plasmids were extracted (see section 2.2.2) from cells that had been grown at a temperature of 30° C in order to avoid undesirable recombination of the DNA. Digestion of the TRIB3/YFP constructs with *Kpn I* (8-12U/ μ l) (Promega, Madison, WI, USA) was expected to yield two fragments of 741bp and 6,555bp, while *Kpn I* digestion of the TRIB3/V1 or V2 constructs would generate fragments of 792bp and 5,676bp for the TRIB3/V1 construct, or 1,020bp and 5,676bp for the TRIB3/V2 construct. *Kpn I* digestions were performed in a final volume of 15 μ l that contained Buffer J (10x), distilled water, 1.5 μ l of *Kpn I* and 5 μ l of plasmid DNA. Digestion of the TRIB3-1.1C LgBiT constructs with *Acc 65I* was expected to yield two fragments of 1,275bp and 3,763bp. The *Acc 65I* digestions were performed in a final volume of 50 μ l that contained 5 μ l NEB3.1 buffer, distilled water, 1 μ l of *Acc 65I* and 5 μ l of plasmid DNA. All restriction reactions were incubated for 1 hour at 37° C before electrophoresis in 1% agarose gel.

Purified recombinant plasmids were sequenced using BGH universal primer to ensure the in-frame ligation of the TRIB3 sequence with the sequence encoding YFP or the split YFP (Venus) proteins. The pBiT primers were used to confirm the in-frame ligation of the TRIB3 sequence with the sequence encoding the LgBiT or the SmBiT fragments of the NanoLuc luciferase.

2.2.4 Cell line maintenance

2.2.4.1 Thawing cells

A cryotube of HeLa cells was retrieved from storage in liquid nitrogen and allowed to thaw in a 37° C water bath for less than a minute before seeding cells into fresh DMEM growth medium supplemented with 10% FBS and 1% Anti-Anti. HeLa Cells were allowed to grow for at least two weeks before commencing any transfection studies. HEK293T cells were thawed similarly but seeded into Opti-MEM growth medium containing 10% FBS and 1% Anti-Anti.

2.2.4.2 Passaging cells

Cells were maintained by providing sufficient nutrients and surface for growth. HeLa cells were passaged every four days by washing a sub-confluent T75 flask with PBS and incubating with 2ml of 1X Trypsin-EDTA for 5 minutes at 37° C in 5% CO₂ to detach the cells before re-suspending in 8ml of DMEM containing 10% FBS and 1% Anti-Anti. HEK293T cells were passaged similarly though the incubation with 1X Trypsin-EDTA was only for 1 minute and the cells were re-suspended in Opti-MEM supplemented with 10% FBS and 1% Anti-Anti.

2.2.4.3 Freezing cells

A stock of frozen cells having a low passage number was retained. Cells were counted, and aliquots of 5 x 10⁶ cells, suspended in freezing media (90% FBS, 10% DMSO), were dispensed into 1.8ml cryotubes. The cryotubes were stored at -80° C in a freezing container that maintains cell viability by slowly lowering the temperature of the cell suspension 1° C every minute. After 24 hours, cryotubes were transferred to liquid nitrogen for longer-term storage.

2.2.5 Expression and localisation of TRIB3 in HeLa cells

2.2.5.1 Seeding and transfecting HeLa cells

HeLa cells were transfected in 70-90% confluent 6- or 12-well plates. Cells were transfected for 24 hours at 37° C in the presence of 5% CO₂. In 6-well plate, 2ml of serum free medium containing 1,250 ng of the plasmid and 3µl of Lipfectamine™ 3000 was incubated, and in 12-well plate, 1ml of the serum free medium was incubated with 500ng of the plasmid and 1.5µl of Lipfectamine™ 3000. Following transfection, nuclei were stained by incubating cells with a 1:2,000 dilution of Hoechst stain for 10 minutes at 37° C in the presence of 5% CO₂. Before imaging the cells, the staining medium was removed and replaced with phenol-red free medium to reduce background fluorescence during microscopy.

In those experiments where cells were co-transfected with two plasmids expressing proteins that were known to interact, the total amount of DNA transfected remained the same but comprised equal amounts of the two plasmids being used.

2.2.5.2 Imaging transfected live cells

A Leica AF6000 Time-Lapse inverted wide-field fluorescence microscope was used to image transfected live cells. The microscope was programmed to allow both fluorescence and phase-contrast imaging. Dry lenses having 20x, 40x and 63x magnifications, were used to visualise cells, and images were taken using the 63x lens. Image acquisition required definition of the appropriate filter for each fluorophore (blue A4 for Hoechst stain, green L5 for GFP and YFP), and parameters were fixed (Exposure 350, Gain 7, Intensity 4) to standardise light transmission and detection measures across repeated transfections.

2.2.5.3 Quantification of fluorescence in transfected live cells and statistical analysis

Images were analysed to identify differences in the localisation of wild-type TRIB3 and TRIB3 variants. ImageJ software (Wayne Rasband, National Institutes of Health, USA) was used to quantitate fluorescence intensity, and statistical analysis was performed using GraphPad Prism version 7.02 (GraphPad Software, La Jolla California USA).

Fluorescence intensity values were collected for each variant (wild-type, V107M, S146N, R149G and R153H). To investigate the difference between the fluorescence intensity of all variants including the wild-type, a one-way-ANOVA test was used. However, testing the fluorescence intensity of each of the variants against the wild-

type is more relevant to the research scope, and therefore, Bonferroni's multiple comparisons test was used to check the difference between each of the variants when compared to the wild-type TRIB3.

To test the variability between the transfection repeats, fluorescence intensity values of the wild-type were collected from three independent transfections, and the results compared using a one-way-ANOVA.

2.2.6 Assessment of interaction strength of TRIB3/AKT1 complex in HEK293T using Protein complementation assay

HEK293T cells were seeded into a white flat-bottomed 96-well plate at a density of 17,000 cells/well and incubated overnight at 37° C in the presence of 5% CO₂ before transfection. Cells were incubated in 100µl of Opti-MEM supplemented with 10% FBS and 1% Antibiotic-Antimycotic (Anti-Anti). A transfection mixture containing 6µl of serum-free Opti-MEM medium, 1µl of each plasmid at 100ng concentration, and 0.6µl of the FuGENE HD transfection was prepared and added to each well. The plasmids used for this mixture were generated to express the split-NanoLuc system (LgBiT and SmBiT). Following transfection, cells were gently washed with warm PBS to avoid disrupting the monolayer, and 125µl of Nano-Glo[®] Live Cell substrate was added before reading the luminance signal using VIRIOSKAN FLASH plate reader.

The substrate was prepared by mixing one part of the Nano-Glo[®] Live Cell substrate with 19 parts of the Nano-Glo[®] LCS Dilution Buffer. For each well, 25µl of the diluted substrate was mixed with 100µl of Opti-MEM supplemented with 10% FBS and 1% Anti-Anti. The substrate is light-sensitive and must be covered in foil and added immediately before reading the luminance signal.

2.2.7 Electrophoresis and immunoblotting of phosphorylated AKT

2.2.7.1 Preparation of cell lysates

The adherent transfected HEK293T cells, in 6-well plates, were washed with PBS before being detached using 200µl of 1X Trypsin-EDTA and suspended in 800µl of Opti-MEM containing 10% FBS and 1% Anti-Anti. The cell suspension was centrifuged at 1,000rpm for 5 minutes, and the cells were washed with PBS before adding 50µl of the RIPA lysis buffer. Cells were sonicated for 15 seconds and placed on ice before centrifugation at 14,000rpm for 5 minutes at 4° C and collection of the supernatant. Cell lysates were split into aliquots and stored at -80° C before further analysis.

2.2.7.2 Measurement of total protein concentrations in cell lysates

The total protein concentrations of the cell lysates were determined from a standard curve using the BCA protein assay. The standards were prepared using RIPA lysis buffer to make serial dilutions of a 2 mg/ml solution of Bovine Serum Albumin (BSA) to obtain BSA concentrations (in $\mu\text{g/ml}$) of 2000, 1000, 500, 250, 125, 62.5, 31.25, 15.6, 7.8 and 0 (blank) in a 96-well plate. All standards were assayed in triplicate. Similarly, duplicate samples of the cell lysates were assayed after 1:2 dilution in lysis buffer. Pierce BCA protein assay solution was prepared by mixing 49 parts of reagent A with 1 part of reagent B (both reagents were supplied with the Pierce BCA protein assay kit) and 200 μl of the assay solution was added to 10 μl of the standards or test samples. The plate was incubated at 37° C for 30 minutes before stopping the reaction by cooling the plate on ice and then measuring the optical density in each well at 562nm using a VIRIOSKAN FLASH plate reader. The mean optical densities for the triplicate BSA standards were used to plot the standard curve using the Quantitative curve on the plate reader software, and the total protein concentrations of the test samples were determined by plotting the sample measurements against the standard curve.

2.2.7.3 Denaturing gel electrophoresis

Samples of cell lysates each containing 10 μg protein were diluted to 19.5 μl with RIPA lysis buffer and mixed with 7.5 μl of NuPAGE® LDS buffer (X4) and 3 μl of NuPAGE® Sample Reducing Agent (10X). Following denaturation by heating at 100° C for 10 minutes, 25 μl aliquots of the samples were loaded into the wells of NuPAGE™ 4-12% Bis-Tris gel and subjected to electrophoresis at 200V for 30 minutes in an XCell SureLock™ Electrophoresis Cell system filled with NuPAGE® MOPS SDS Running Buffer.

2.2.7.4 Protein blotting and detection

Following electrophoretic separation of the lysates, the gel was assembled on the iBlot® Nitrocellulose Regular Stacks and the separated proteins were transferred from the gel to the nitrocellulose membrane. The protein transfer was accomplished by subjecting the Nitrocellulose Regular Stacks to 20 volts and 1.2A current on the i-Blot 2 system. Following protein transfer, the membrane was incubated in 5ml of Odyssey® Blocking Buffer for 60 minutes to block remaining protein binding sites. The membrane was then incubated overnight at 4° C with monoclonal Rabbit antibody to human pAKT,

which was diluted 1:2000 in 5ml of Odyssey® Blocking Buffer. Excess primary antibody was removed by washing with TBST (prepared by dissolving 1 powder sachets of TBS in 1000ml distilled water and 1ml of Tween® 20), and the membrane was then incubated for 1 hour at room temperature with the secondary Goat anti-Rabbit antibody which was labelled with IRDye® 680RD and diluted 1:5000 in 5ml of Odyssey® Blocking Buffer. Following further washing with TBST, the membrane was imaged using the LI-COR Odyssey CLx machine.

Following detection of pAKT, the blot was incubated overnight at 4° C with a monoclonal Mouse anti-human α Tubulin antibody, diluted 1:1000 in Odyssey® Blocking Buffer. The membrane was then washed and incubated for 1 hour at room temperature with IRDye® 800CW-labelled Donkey anti-Mouse antibody diluted 1:5000 in 5ml of Odyssey® Blocking Buffer. The housekeeping protein was then visualised using the LI-COR Odyssey CLx machine

2.2.8 Assessment of murine platelet activation and ATP secretion

2.2.8.1 Quantifying platelet activation using activation markers

The anticoagulant hirudin was suspended in 500 μ l of normal saline. A 1:100 dilution of this stock solution was then prepared using normal saline for use as the working solution. Collection needles were pre-coated with 100 μ l hirudin and 900 μ l blood was collected via cardiac puncture from mice that were anaesthetized using isoflurane. Blood suspension was prepared by diluting 100 μ l of whole blood in 1.9ml of HT buffer and 20 μ l of 100mM CaCl₂. Platelets in 33 μ l of the blood suspension were activated with two concentrations of TRAP, 3mM and 10mM, and stained with 5 μ l of CD41/61 and 10 μ l of CD62p, which was diluted 1:200 in PBS. The amount of platelet activation was measured on the LSRII flow cytometer using the percentage of platelet showing both markers, CD62p and CD41/61, and the baseline reading was determined using unstimulated samples.

2.2.8.2 Assessment of ATP secretion from murine platelets

Whole blood was collected via cardiac puncture from mice that were anaesthetized by isoflurane, using needles pre-coated with 100 μ l of Sodium Citrate. Platelet-rich plasma (PRP) was prepared by centrifugation of the blood at 190g for 10 minutes and allow resting for 30 minutes in room temperature before collecting the PRP. Platelet counts were determined in whole blood and PRP samples using the Sysmex analyser, and

the count in PRP was adjusted to $10\text{-}25 \times 10^9/\text{L}$ using warm HT buffer. On the CHRONO-LOG aggregometer, $450\mu\text{l}$ of the PRP was stirred for 1 minute at 900rpm at 37°C , and then $50\mu\text{l}$ of the CHRONO-LUME® Luciferin Luciferase substrate was added and stirred for 1 minute. One unit ($50\mu\text{l}$) of the thrombin, a platelet activation agonist, was added and the ATP secretion was recorded. The ATP secretion reading was adjusted to the platelet count and reported as relative units of ATP/ $\times 10^9$ platelets.

Chapter 3:

***In-silico* predictions of the effects of non-synonymous *TRIB3* variants on *TRIB3* structure and function**

3.1 Introduction

Platelets are essential to maintaining haemostasis and required to prevent unopposed bleeding at sites of vascular injury (Margraf et al, 2019). In chapter one, the increase in the registered number of unexplained platelet bleeding disorders cases, and the genetic approaches that failed to identify the underlying genetic defects in ~50% of the cases were summarised.

TRIB3, and its potential role in regulating platelet biogenesis, was also introduced in chapter 1. In particular, previously published data supporting a role for TRIB3 in megakaryopoiesis, and unpublished findings from our group that suggest a potential role for TRIB3 in determining platelet function were summarised. In 2010, De Graaf et al listed *Trib3* among the down-regulated genes identified following microarray analysis of RNA from haematopoietic cells (LSK cells) collected from mice overexpressing human thrombopoietin (*TPO^{Tg}* mice). This work suggested that a reduction in *Trib3* expression correlated with the increased platelet production that was stimulated by the high levels of TPO, which is a primary regulator of platelet production (de Graaf et al, 2010). This suggestion was supported by a subsequent study which reported elevated expression of *TRIB3* in a microarray dataset generated from human megakaryocytes that were treated with the megakaryopoiesis inhibitor, anagrelide (Ahluwalia et al, 2015). Both studies linked the expression of *TRIB3* with megakaryocyte differentiation, which is required for normal platelet production.

The identification of TRIB3 as a potential regulator of megakaryopoiesis and platelet production led my colleague Dr Jessica Johnston (University of Sheffield, UK) to hypothesise that TRIB3 could also be involved in the regulation of platelet function. Dr Johnston explored this hypothesis by assessing platelet activation in the *Trib3* knockout mouse using flow cytometric analysis of platelet P-selectin (CD62p) expression in response to the platelet agonist, thrombin receptor activating peptide (TRAP). Interestingly, the results revealed a selective reduction in agonist-induced CD62p expression on platelets from female *Trib3^{-/-}* mice while platelets from male *Trib3^{-/-}* mice showed levels of CD62p expression that were comparable to those of wild-type platelets (unpublished data).

The differential platelet activation observed in the *Trib3* knockout mouse led us to investigate possible associations between TRIB3 and platelet function in humans. Examination of whole-exome sequence (WES) data from patients who were recruited to the UK-Genotyping and Phenotyping of Platelets (UK-GAPP) study for investigation

of an unexplained platelet bleeding disorder identified enrichment of rare non-synonymous *TRIB3* variants in the small cohort of patients, supporting a potential role for *TRIB3* in platelet function.

The work in this chapter describes the use of *in-silico* approaches to investigate the functional significance, if any, of the *TRIB3* variants that were enriched among patients with platelet bleeding disorders. The aims of the work described in this chapter were to:

- i. Use predictive algorithms to study the putative effects of the amino acid substitutions caused by the non-synonymous *TRIB3* variants on *TRIB3* function;
- ii. Use a three-dimensional model of *TRIB3* to predict the effects of the variants on the structure and conformation of *TRIB3*;
- iii. Compare the profiles of peptides interacting with wild-type and variant forms of *TRIB3* identified using mass spectrometry, and correlate any differences identified with platelet function.

3.2 Methods

3.2.1 Patients

Prior to this study, whole exome sequencing (WES) was undertaken on genomic DNA samples from thirty-four patients who were recruited to the UK-GAPP study for investigation of an unexplained inherited platelet bleeding disorder. Based on extensive platelet phenotyping, the patients were subgrouped according to whether their platelets displayed defects in Gi-signalling (12 patients), or dense granule secretion (22 patients) (Dawood et al, 2012). Venous blood samples were collected in S-Monovette® 0.106 mol L⁻¹ 3.2% trisodium citrate tubes (Sarstedt; Leicester, UK) from patients who passed the exclusion criteria for the UK-GAPP study (see section 1.1.3.2.1). Whole exome sequencing from extracted genomic DNA was performed by Dr Michael Simpson (Kings College, London, UK), and sequences were aligned with the reference genome, version GRCh37/hg19 (Leo et al, 2015). Raw sequence data was provided in a VCF file that included details of all variants detected in each exome including the nucleotide position and change, its associated rs number if previously identified, and its predicted effects on the protein. The WES data was mined for variants affecting *TRIB3*, and identified variants were confirmed in the latest reference human genome sequence available on the UCSC genome browser (<https://genome.ucsc.edu>, version:GRCh38/hg38). The minor allele frequencies of the identified *TRIB3* variants were obtained from the Genome Aggregation database (gnomAD) (<https://gnomad.broadinstitute.org/>).

Ethical approval for the UK-GAPP study was granted by the National Research Ethics Service Committee West Midlands-Edgbaston (REC reference: 06/MRE07/36), and following the guidelines of the Declaration of Helsinki, written informed consent was provided by all patients.

3.2.2 *In-silico* predictions of the effects of *TRIB3* variants

The Combined Annotation Dependent Depletion (CADD) v1.0 (Kircher et al, 2014) online prediction tool (<https://cadd.gs.washington.edu/>) was used to investigate the potential effects of *TRIB3* variants. This tool uses an algorithm that combines outcomes predicted by 63 annotations and considers multiple aspects of genetic variants such as degree of conservation, potential epigenetic modifications and functional effects, and genetic context (Rentzsch et al, 2019). The CADD tool provides two scores: (i) a raw score that is calculated from the annotations used, but does not

consider the reported SNVs in the reference genome databases; (ii) a PHRED-scaled score (CADD score) that considers the model calculations and ranks the variant among all reported SNVs in the reference database. In this sense, the CADD score is more meaningful to use, and according to the tool's publisher, a CADD score of 20 or more would mean that the algorithm ranks the deleteriousness of the variant among the top 1% of the ~ 8.6 billion SNVs reported to the GRCh37/hg19 reference dataset.

The cross-species conservation of TRIB3 sequences affected by *TRIB3* variants was investigated using sequences imported from the NCBI orthologs database (<https://www.ncbi.nlm.nih.gov/gene/57761/ortholog/>). Sequences were aligned using the alignment tool on EMBL-EBI (<https://www.ebi.ac.uk/Tools/msa/clustalo/>), and the BOXSHADE v3.21 tool (https://embnet.vital-it.ch/software/BOX_form.html) was used to highlight conserved residues.

In collaboration with Juan Salamanca Vioria (Barcelona, Spain), a three-dimensional (3D) structure of the pseudokinase domain of human TRIB3 was modelled using the crystallised TRIB1 protein as a template. The locations of the amino acid substitutions predicted by the *TRIB3* SNVs were identified using the educational version of the PyMOL Molecular Graphics System, Version 2.0 Schrödinger, LLC.

3.2.3 Mass spectrometry of peptides interacting with wild-type and variant forms of TRIB3

Peptides interacting with wild-type and variant forms of TRIB3 were identified by mass spectrometry in collaboration with Miguel Hernández-Quiles (Centre for Molecular Medicine, UMC Utrecht, Utrecht, Netherlands). Samples of expression plasmids encoding wild-type and variant forms of TRIB3 as fusion proteins with YFP were sent to Utrecht for use in the analysis. HEK293 cells were transfected overnight with the fusion constructs. As a control, cells were also transfected with a YFP expression plasmid to filter out peptides interacting with the YFP moiety of the fusion proteins. Transfected cells were then lysed and the anti-GFP coated beads that were supplied in the GFP-TRAP Agarose kit (ChromoTek GmbH; Planegg-Martinsried, Germany) were used to immunoprecipitate proteins fused to YFP from cell lysate. The eluted YFP-tagged proteins were purified and fractionated before being loaded into an LTQ Orbitrap Velos™ mass spectrometer (Thermo Fisher; Bremen, Germany). Details of the fractionation, mass spectrometry, and data analysis were supplied by Miguel Hernández-Quiles and were as follows: peptides were fractionated based on

their pH using Strong Anionic Exchange Chromatography, desalted, and acidified on a C-18 cartridge (3M, St. Paul, MN). C18-stagetips were activated with methanol and washed with buffer containing 0.5% formic acid in 80% acetonitrile (ACN) (buffer B) and then with 0.5% formic acid (buffer A). After loading of the digested sample, stagetips were washed with buffer A and peptides were eluted with buffer B, dried in a SpeedVac, and dissolved in buffer A. Peptides were separated on a 30 cm column (75 μ m ID fused silica capillary with emitter tip (New Objective, Woburn, MA)) packed with 3 μ m aquapur gold C-18 material (Dr Maisch, Ammerbuch-Entringen, Germany) using a 4-hour gradient (buffer A to buffer B), and delivered by an easy-nHPLC (Thermo Scientific). Peptides were electro-sprayed directly into a LTQ-Verlos-Orbitrap (Thermo Scientific) and analysed in data-dependent mode with the resolution of the full scan set at 60000, after which the top 10 peaks were selected for CID fragmentation in the ion trap with a target setting of 5000 ions. Raw files were analysed with Maxquant software version 1.5.1.0. For identification, the Human Uniprot 2012 database was searched with peptide and protein false discovery rates set to 1%. Proteins identified with two or more unique peptides were filtered for reverse hits, decoy hits and standard contaminants using Perseus software 1.3.0.4. Normalised ratios were used to quantify protein expression and further processed for comparative analysis of differential expression among the experimental conditions (Figure 3.1A).

Peptides quantified by the mass spectrometer were filtered to exclude: (i) peptides that were identified to interact with the YFP moiety, which were identified using the control YFP plasmid; (ii) peptides that were not consistently detected in all three repeats of the transfection. Following these exclusions, a list of interacting peptides with their corresponding intensity-based absolute quantification (iBAQ) values was compiled for each sample (wild-type TRIB3 and five TRIB3 variants). The Perseus software v1.3.0.4. was used to generate scatter plots comparing the iBAQ values of peptides detected as interacting with each of the TRIB3 variants with those of peptides interacting with wild-type TRIB3. The data was then exported to an excel sheet, and the difference in iBAQ values [$iBAQ_{\text{difference}} = iBAQ_{\text{wt}} - iBAQ_{\text{variant}}$] was determined for each peptide, in each of the plots. It is worth noting that the LTQ Orbitrap Velos mass spectrometer cannot accurately quantify peptides that have an iBAQ value of 15 or less. Therefore, peptides showing an iBAQ difference of 3 or more were considered in the further downstream analysis (the minimum detected iBAQ is 15; therefore, peptides with 18 or more were considered in the downstream analysis). Peptides showing a reduction in iBAQ value in cells expressing the variant forms of TRIB3 when compared

with cells expressing wild-type TRIB3 were considered to show a loss of interaction, while peptides showing an increase in iBAQ value were considered to have gained an interaction (Figure 3.1B).

Gene ontology analysis of the genes encoding peptides that consistently either gained or lost interactions with each of the TRIB3 variants, when compared with those that interacted with wild-type TRIB3, was undertaken. The analysis was performed using the GOrilla tool (<http://cbl-gorilla.cs.technion.ac.il/>) to predict processes and pathways that are regulated by the genes. Two lists were submitted to the tool for enrichment analysis; (i) a list of peptides that are sorted according to their iBAQ values (with an iBAQ_{difference} of 3 or more); (ii) the full list of detected peptides (including those having iBAQ_{difference} of less than 3) to aid in directing the enrichment algorithms (Figure 3.1B).

In, parallel, and to focus the predictions toward platelets, the list of peptides showing an iBAQ_{difference} of 3 or more that interacted with each TRIB3 variant was uploaded to the pathway browser on the Reactome database (<https://reactome.org/>), and a search performed to identify biological processes and pathways that were regulated by the submitted peptides. Pathways relating to haemostasis were selected from the output to identify the platelet-related processes that were predicted to be regulated by the peptides (Figure 3.1B).

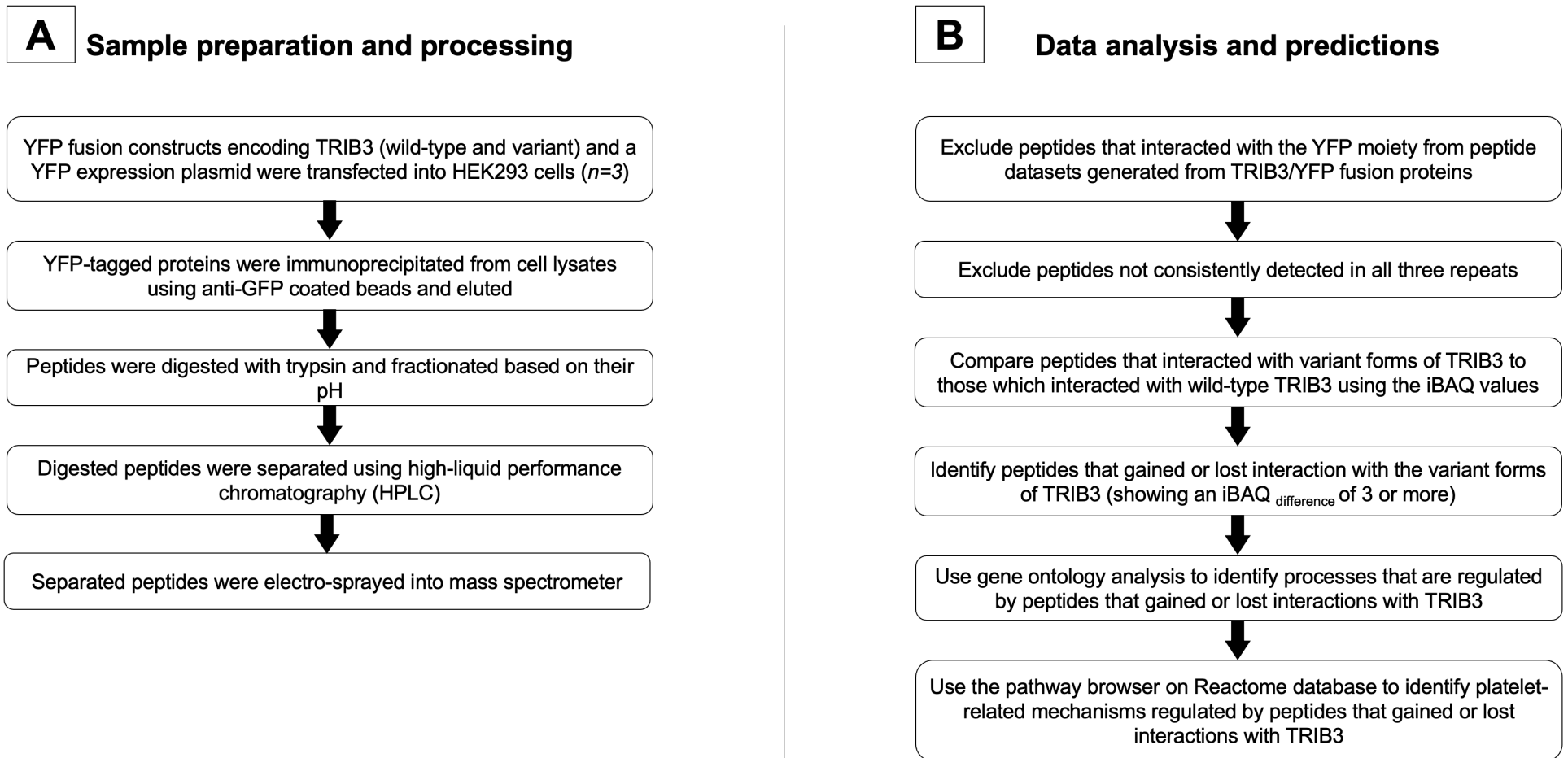


Figure 3.1: Pipelines for sample preparation and analysis of mass spectrometry data generated to identify peptides that interact differentially with variant forms of TRIB3

(A) The pipeline provides a brief description of the stages performed by Miguel Hernández-Quiles to prepare samples before mass spectrometry. **(B)** The pipeline describes the main stages of data analysis performed to predict pathways regulated by peptides that were interacting differentially with the variant forms of TRIB3.

3.3 Results

3.3.1 Identification of *TRIB3* variants and *in-silico* predictions

WES identified seven single nucleotide variants (SNVs) affecting *TRIB3* among five patients recruited to the UK-GAPP Study (cohort size = 34 patients), five of which were non-synonymous and predicted amino acid substitutions in *TRIB3* (Table 3.1). The minor allele frequencies (MAF) for the five non-synonymous variants [c.G319A (p.V107M), c.G436A (p.S146N), c.C445G (p.R149G), c.G458A (p.R153H), and c.C541T (p.R181C)], which had all been reported previously, were all <0.01 in the European population (Table 3.2). Moreover, all five non-synonymous variants were predicted to have deleterious effects on *TRIB3* using the CADD algorithm, which yielded CADD scores >20 in all cases (Table 3.2). The remaining two synonymous variants [c.T333C (p.Y111Y) and c.C969T (p.A323A)] were previously reported to have MAFs of >0.1 in the European population and were predicted to be benign using the CADD algorithm (CADD scores <20) (Table 3.2).

Multiple alignments of those *TRIB3* orthologs showing the greatest homology to human *TRIB3* [Chimpanzee 94%, Rhesus macaques (monkey) 94%, Cattle 83%, Dog 83%, Rat 73%, Mouse 74%] showed that amino acids 107, 146, 149 and 181 are all conserved across species. The Arginine residue at amino acid position 153 in human *TRIB3* is less conserved across species and is replaced by a proline residue in the chimpanzee sequence, and by a glycine residue in the rat and mouse sequences (Figure 3.2).

Structural predictions of the effects of the five SNVs on *TRIB3* were carried-out using a three-dimensional model of the protein. The five amino acids that are substituted in the variants are all predicted to be located on the surface of *TRIB3* where they could potentially affect protein folding or the interaction of *TRIB3* with other proteins (Figure 3.3). The substitution of a valine residue by a larger methionine residue at amino acid position 107 has the potential to promote additional hydrophobic interactions and thereby affect the pattern of protein expression. The serine residue at amino acid position 146 may be a site for phosphorylation. Its substitution with a larger asparagine residue could result in more hydrophilic interactions. The highly polar, and positively charged arginine residues at positions 149, 153 and 181 promote *TRIB3* stability through the formation of hydrogen bonds and salt bridges. Replacement of the arginine by the smaller, non-charged glycine at position 149, could potentially affect protein structure due to the loss of any salt bridges involving R149. The introduction of a

histidine residue at position 153 could create an interaction site for catalytic enzymes and may disturb protein folding due to the removal of any salt bridges created by the arginine residue that is normally present at that position. Replacing arginine with a cysteine residue at position 181 has the potential to disturb protein folding due to loss of positive charge and creating a site for disulfide bond formation with a proximal cysteine residue located at amino acid position 173.

Table 3.1: *TRIB3* variants identified in patients recruited to the UK-GAPP study

| Patient ID | Sex | Total number of variants * | Platelet phenotype | <i>TRIB3</i> Variants | Genotype | Exon: Nucleotide: AA |
|------------|-----|----------------------------|----------------------|--------------------------------|-------------------|---|
| S1008 | M | 24,739 | Secretion defect | <u>V107M</u> A323A Y111Y | Het Het Het | Exon3: G319A: V107M Exon4: C969T: A323A Exon3: T333C: Y111Y |
| JM-110111 | M | N/A | Secretion defect | <u>S146N</u> | Het | Exon3: G436A: S146N |
| S2142 | F | 15,981 | Secretion defect | <u>R149G</u> Y111Y | Het Hom | Exon3: C445G: R149G Exon3: T333C: Y111Y |
| S1013 | F | 24,438 | Gi-signalling defect | <u>R153H</u> Y111Y | Het Het | Exon3: G458A: R153H Exon3: T333C: Y111Y |
| S2134 | F | 26,259 | Secretion defect | <u>R181C</u> Y111Y A323A | Het Het Het | Exon3: C541T: R181C Exon3: T333C: Y111Y Exon4: C969T: A323A |

The table includes patients with non-synonymous *TRIB3* variants. M, male; F, female; Het, heterozygous; Hom, homozygous. * The total number of variants identified in each exome includes the following variant effects: frameshift deletion, non-frameshift deletion, frameshift insertion, non-frameshift insertion, frameshift substitution, non-frameshift substitution, splicing, stop-gain, stop-loss, synonymous, non-synonymous, and unknown effects.

Table 3.2: Single Nucleotide Variations identified by WES analysis of patients recruited to the GAPP study

| TRIB3 Variant | Nucleotide Change | Amino acid substitution | rs number* | Variant effect | MAF** | CADD score | Predicted effect |
|----------------------|--------------------------|--------------------------------|-------------------|-----------------------|--------------|-------------------|-------------------------|
| V107M | 20:372097 G>A | p.Val107Met | rs138380491 | Non- Synonymous | 0.004222 | 23.4 | Deleterious |
| Y111Y | 20:371972 T>C | p.Tyr111Tyr | rs6051637 | Synonymous | 0.5671 | 0.001 | Benign |
| S146N | 20:372076 G>A | p.Ser146Asn | rs41281850 | Non- Synonymous | 0.008546 | 26.8 | Deleterious |
| R149G | 20:372084 C>G | p.Arg149Gly | rs752911865 | Non- Synonymous | 0.0004575*** | 31 | Deleterious |
| R153H | 20:372097 G>A | p.Arg153His | rs35051116 | Non- Synonymous | 0.01446 | 22.7 | Deleterious |
| R181C | 20:372180 C>T | p.Arg181Cys | rs149447454 | Non- Synonymous | 0.001123 | 34 | Deleterious |
| A323A | 20:377226 C>T | p.Ala323Ala | rs6115830 | Synonymous | 0.4381 | 11.98 | Benign |

The table includes synonymous and non-synonymous *TRIB3* SNVs. *rs number obtained from the dbSNP database (<https://www.ncbi.nlm.nih.gov/snp/>) [last accessed 30/03/2020]. **minor allele frequencies (MAF) obtained from Genome Aggregation database (gnomAD) (<https://gnomad.broadinstitute.org/>) [last accessed 30/03/2020]. MAFs are primarily for the European non-Finnish population. *** the MAF for the R149G variant is for the South Asian population as the variant was not reported in the European population. Variants with CADD scores greater than 20 are predicted to be deleterious, while lower scores would indicate minor effects on the protein.

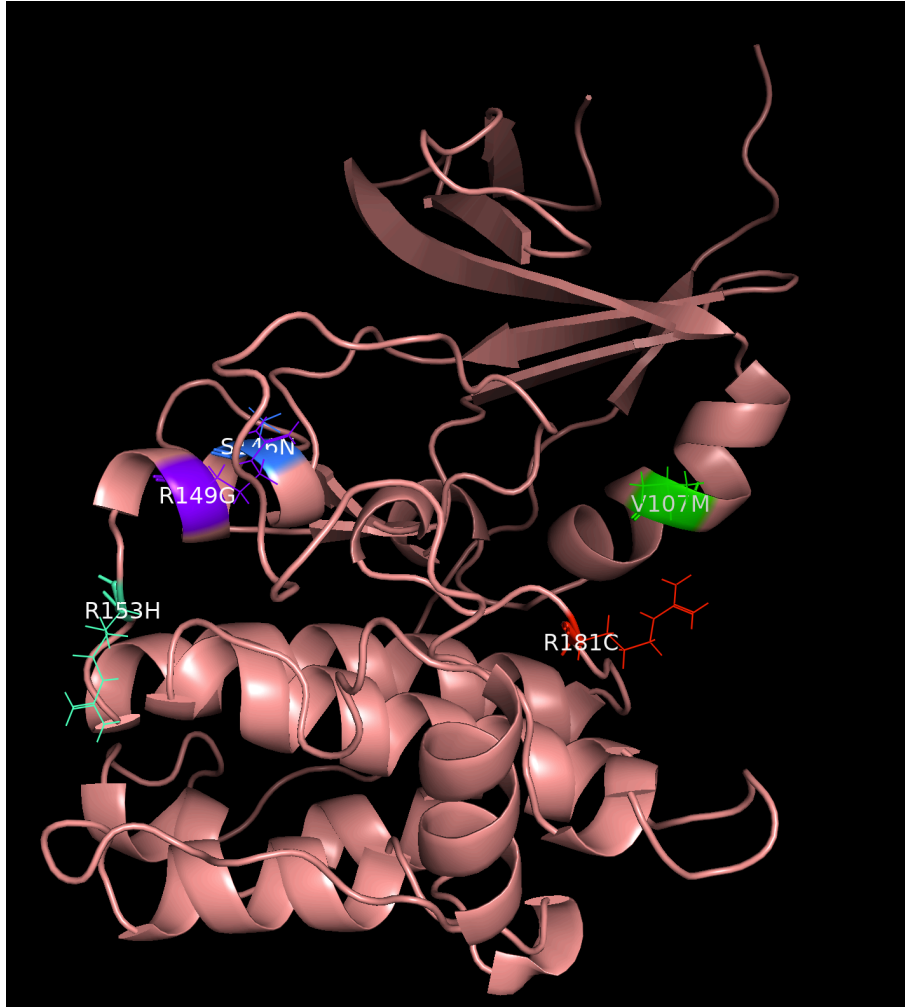


Figure 3.3: Predicted 3D structure of the pseudokinase domain of TRIB3

The model shows most of the pseudokinase domain of TRIB3, and commences from Serine 66 in the amino acid sequence. The residues that are substituted in the five variants are located to the protein surface and predicted to be able to affect the interactions of TRIB3 with other proteins. The model was created by Juan Salamanca Vilorio (Barcelona, Spain) based on a crystallised TRIB1 template. The locations of amino acids were predicted using the educational version of the PyMOL Molecular Graphics System, Version 2.0 Schrödinger, LLC.

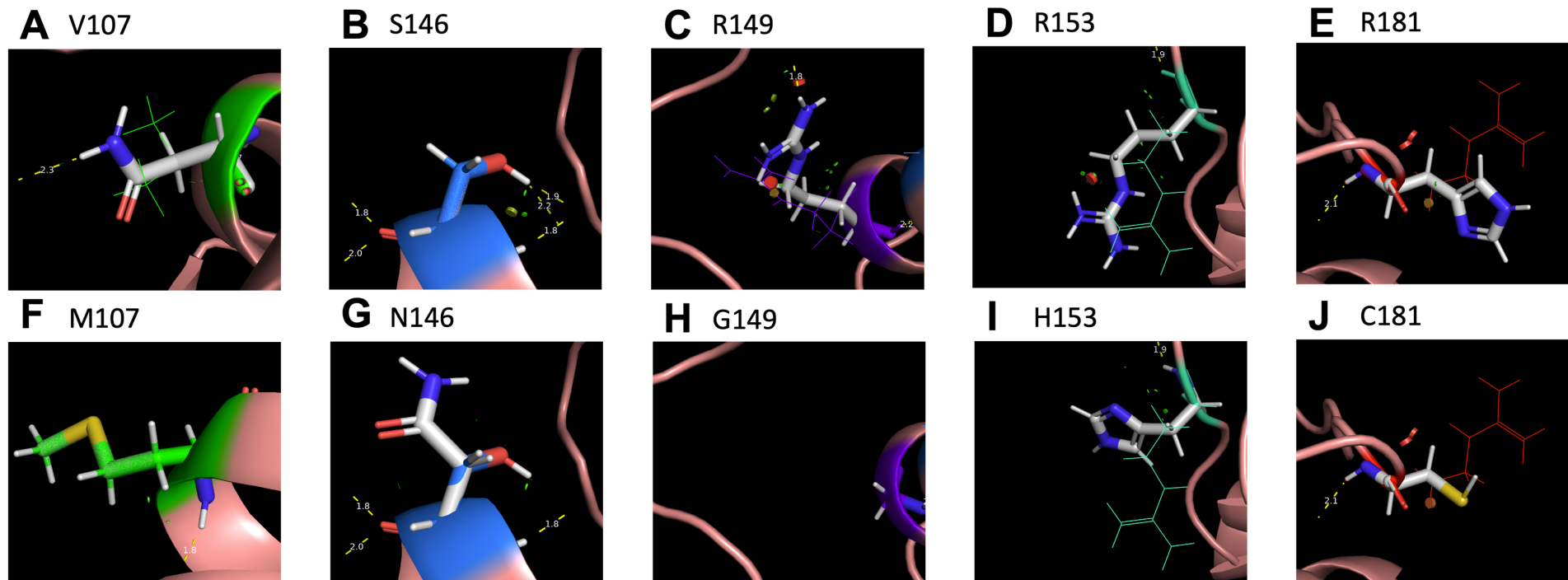


Figure 3.4: Amino acid substitutions on the surface of the pseudokinase domain of TRIB3

The substituted amino acid residues are predicted to be located on the surface of TRIB3. (A) V107 in wild-type TRIB3; (B) S146 in wild-type TRIB3; (C) R149 in wild-type TRIB3; (D) R153 in wild-type TRIB3; (E) R181 in wild-type TRIB3. The amino acid substitutions in TRIB3 are not predicted to change the protein conformation but could affect interactions with other proteins. (F) Substitution of residue 107 with methionine; (G) Substitution of residue 146 with asparagine; (H) Substitution of residue 149 with glycine; (I) Substitution of residue 153 with histidine; and (J) Substitution of residue 181 with cysteine.

3.3.3 TRIB3 interactors affected by *TRIB3* variants

The *in-silico* studies predicted that the rare non-synonymous *TRIB3* variants were likely to disturb the interactions of TRIB3 with other proteins. We used mass spectrometry to investigate the effects of the amino acid substitutions predicted by these variants on the interactions of TRIB3 with other proteins. Following lysis of HEK293 cells that were overexpressing either wild-type or variant forms of TRIB3/YFP fusion constructs, proteins fused to YFP were immunoprecipitated and subjected to mass spectrometry in collaboration with Miguel Hernández-Quiles (Utrecht, Netherlands). The results of the analysis were received as a data file which listed those peptides, and their iBAQ values, that were identified to interact with wild-type TRIB3 and each of the five TRIB3 variants studied. We used the Perseus software to compare the profiles of peptides interacting with wild-type TRIB3, and each of the variant TRIB3 molecules. This allowed grouping of peptides into three different categories; (i) peptides that gained interactions with one or more of the TRIB3 variants; (ii) peptides that lost interactions with one or more of the TRIB3 variants; and (iii) peptides that maintained their interactions with TRIB3 in both the wild-type and variant forms (Figure 3.5). Differences in iBAQ were used to compare the profiles of peptides that interacted with each of the five TRIB3 variants with that for wild-type TRIB3. Thus, the iBAQ value for each peptide that was identified to interact with a variant TRIB3 was subtracted from the iBAQ value reported for the same peptide when detected in cells expressing wild-type TRIB3 [$iBAQ_{\text{difference}} = iBAQ_{\text{wt}} - iBAQ_{\text{variant}}$]. The peptides that interacted with each variant were then ranked according to the difference in iBAQ. Peptides showing an $iBAQ_{\text{difference}}$ of 3 or lower were excluded from further consideration as their iBAQ values were close to the lower detection limits of the mass spectrometer.

Following the exclusion of peptides where the $iBAQ_{\text{difference}}$ was 3 or less, the analysis showed that the V107M variant gained 82 peptide interactions and lost 28 peptide interactions when compared with the wild-type TRIB3. The S146N variant gained interactions with 108 peptides and lost interactions with 9 peptides. The R149G variant gained 104 peptide interactions and lost 324 interactions, and interestingly, TRIB3 was one of the peptides that lost interaction with the TRIB3 R149G. The R153H variant gained interactions with 73 peptides and lost interactions with 40 peptides compared to the wild-type molecule, while the R181C variant showed a gain of 109 peptide interactions and a loss of interaction with 113 peptides. Table 3.3. lists those peptide interactions that were lost, or gained by two or more of the TRIB3 variants (Appendix 6 shows complete list of peptides with their iBAQ scores).

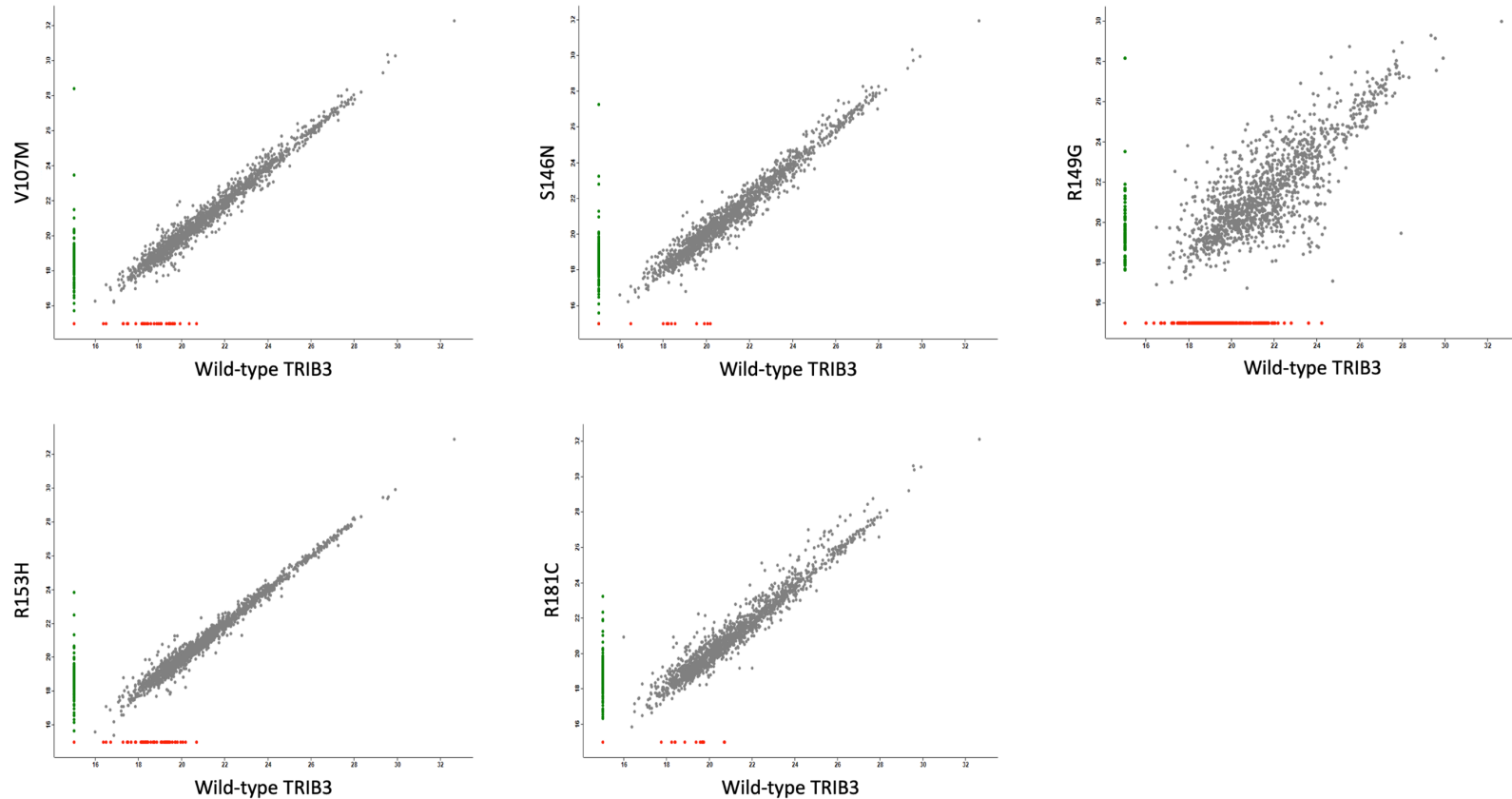


Figure 3.5: Scatter plots of peptides that interacted with wild-type and variant TRIB3 molecules quantified using mass spectrometry

YFP-tagged wild-type and variant TRIB3 molecules were overexpressed in HEK293 cells. The YFP tag was used to immunoprecipitate the TRIB3 proteins from cell lysates and the samples were subjected to mass spectrometry to identify peptides that interacted with TRIB3. Scatter plots were generated using the Perseus software to compare iBAQ values of peptides that interacted with wild-type TRIB3 (X-axis) with those of peptides that interacted with each of the TRIB3 variants (Y-axis). Peptides that gained interactions with the variant TRIB3 are shown in green, and peptides that lost interactions with the variant TRIB3 are shown in red.

Table 3.3: Peptide interactions that were lost, or gained by two or more TRIB3 variants

| V107M | | | S146N | | | R149G | | | R153H | | | R181C | | |
|-----------------|----------------|---|-----------------|----------------|---|-----------------|----------------|---|-----------------|---------------|--|-----------------|----------------|---|
| iBAQ difference | Gene | Protein name | iBAQ difference | Gene | Protein name | iBAQ difference | Gene | Protein name | iBAQ difference | Gene | Protein name | iBAQ difference | Gene | Protein name |
| 13.4 | <i>TIMM17B</i> | Mitochondrial import inner membrane translocase subunit Tim17-B | 12.3 | <i>TIMM17B</i> | Mitochondrial import inner membrane translocase subunit Tim17-B | 13.2 | <i>TIMM17B</i> | Mitochondrial import inner membrane translocase subunit Tim17-B | 8.8 | <i>MCAT</i> | Malonyl-CoA-acyl carrier protein transacylase, mitochondrial | 8.3 | <i>MCAT</i> | Malonyl-CoA-acyl carrier protein transacylase, mitochondrial |
| 8.5 | <i>MCAT</i> | Malonyl-CoA-acyl carrier protein transacylase, mitochondrial | 8.3 | <i>MCAT</i> | Malonyl-CoA-acyl carrier protein transacylase, mitochondrial | 8.5 | <i>DENR</i> | Density-regulated protein | 7.5 | <i>RPL10</i> | 60S ribosomal protein L10 | 7.3 | <i>RPL10</i> | 60S ribosomal protein L10 |
| 6.5 | <i>RPL3L</i> | 60S ribosomal protein L3-like | 7.8 | <i>RPL10</i> | 60S ribosomal protein L10 | 6.7 | <i>Sep-06</i> | Septin-6 | 6.4 | <i>DENR</i> | Density-regulated protein | 6.9 | <i>TIMM17B</i> | Mitochondrial import inner membrane translocase subunit Tim17-B |
| 6.0 | <i>DENR</i> | Density-regulated protein | 6.3 | <i>DENR</i> | Density-regulated protein | 6.6 | <i>HINT1</i> | Histidine triad nucleotide-binding protein 1 | 5.7 | <i>MRPL57</i> | Ribosomal protein 63, mitochondrial | 6.3 | <i>DENR</i> | Density-regulated protein |
| 5.3 | <i>MRPL57</i> | Ribosomal protein 63, mitochondrial | 6.0 | <i>RPL3L</i> | 60S ribosomal protein L3-like | 5.4 | <i>APEX1</i> | DNA-(apurinic or apyrimidinic site) lyase | 5.6 | <i>RPL3L</i> | 60S ribosomal protein L3-like | 6.1 | <i>RPL3L</i> | 60S ribosomal protein L3-like |
| 5.2 | <i>MED12</i> | Mediator of RNA polymerase II transcription subunit 12 | 5.1 | <i>SPTLC1</i> | Serine palmitoyltransferase 1 | 5.2 | <i>COA3</i> | Cytochrome c oxidase assembly factor 3 homolog, mitochondrial | 5.0 | <i>MED12</i> | Mediator of RNA polymerase II transcription subunit 12 | 5.2 | <i>SPTLC1</i> | Serine palmitoyltransferase 1 |
| 5.2 | <i>SPTLC1</i> | Serine palmitoyltransferase 1 | 5.0 | <i>HINT1</i> | Histidine triad nucleotide-binding protein 1 | 4.5 | <i>AP2B1</i> | AP-2 complex subunit beta | 4.9 | <i>APEX1</i> | DNA-(apurinic or apyrimidinic site) lyase | 5.1 | <i>REEP4</i> | Receptor expression-enhancing protein 4 |
| 4.9 | <i>GATAD2B</i> | Transcriptional repressor p66-beta | 5.0 | <i>REEP4</i> | Receptor expression-enhancing protein 4 | 4.3 | <i>ATP5C1</i> | ATP synthase subunit gamma, mitochondrial | 4.7 | <i>REEP4</i> | Receptor expression-enhancing protein 4 | 4.9 | <i>ATP5C1</i> | ATP synthase subunit gamma, mitochondrial |
| 4.9 | <i>APEX1</i> | DNA-(apurinic or apyrimidinic site) lyase | 4.9 | <i>MRPL57</i> | Ribosomal protein 63, mitochondrial | 3.4 | <i>SPTAN1</i> | Spectrin alpha chain, non-erythrocytic 1 | 4.5 | <i>AP2B1</i> | AP-2 complex subunit beta | 4.8 | <i>MED12</i> | Mediator of RNA polymerase II transcription subunit 12 |
| 4.5 | <i>REEP4</i> | Receptor expression-enhancing protein 4 | 4.8 | <i>MED12</i> | Mediator of RNA polymerase II transcription subunit 12 | - | - | - | 4.2 | <i>Sep-06</i> | Septin-6 | 4.8 | <i>GATAD2B</i> | Transcriptional repressor p66-beta |

| | | | | | | | | | | | | | | |
|-----|--------|---|-----|---------|---|---|---|---|-----|--------|--|-----|--------|---|
| 4.3 | COA3 | Cytochrome c oxidase assembly factor 3 homolog, mitochondrial | 4.8 | GATAD2B | Transcriptional repressor p66-beta | - | - | - | 5.7 | STMN1 | Stathmin | 4.7 | MRPL57 | Ribosomal protein 63, mitochondrial |
| 4.2 | AP2B1 | AP-2 complex subunit beta | 4.8 | APEX1 | DNA-(apurinic or apyrimidinic site) lyase | - | - | - | 5.2 | MZT1 | Mitotic-spindle organizing protein 1 | 4.7 | COA3 | Cytochrome c oxidase assembly factor 3 homolog, mitochondrial |
| 5.7 | STMN1 | Stathmin | 4.5 | COA3 | Cytochrome c oxidase assembly factor 3 homolog, mitochondrial | - | - | - | 5.0 | KPRP | Keratinocyte proline-rich protein | 4.5 | AP2B1 | AP-2 complex subunit beta;AP-2 complex subunit beta |
| 4.6 | PEBP1 | Phosphatidylethanolamine-binding protein 1 | 4.4 | ATP5C1 | ATP synthase subunit gamma, mitochondrial | - | - | - | 4.6 | PEBP1 | Phosphatidylethanolamine-binding protein 1 | 4.4 | APEX1 | DNA-(apurinic or apyrimidinic site) lyase |
| 3.4 | SNX2 | Sorting nexin-2 | 4.4 | AP2B1 | AP-2 complex subunit beta | - | - | - | 3.4 | SNX2 | Sorting nexin-2 | 5.7 | STMN1 | Stathmin |
| 3.4 | SPTAN1 | Spectrin alpha chain, non-erythrocytic 1 | 4.1 | Sep-06 | Septin-6 | - | - | - | 3.4 | SPTAN1 | Spectrin alpha chain, non-erythrocytic 1 | 4.6 | PEBP1 | Phosphatidylethanolamine-binding protein 1 |
| 3.2 | SH3GL1 | Endophilin-A2 | 5.2 | MZT1 | Mitotic-spindle organizing protein 1 | - | - | - | 3.2 | SH3GL1 | Endophilin-A2 | 3.4 | SNX2 | Sorting nexin-2 |
| | | | 5.0 | KPRP | Keratinocyte proline-rich protein | | | | | | | | | |
| | | | 3.4 | SNX2 | Sorting nexin-2 | | | | | | | | | |
| | | | 3.2 | SH3GL1 | Endophilin-A2 | | | | | | | | | |

The table includes peptide interactions that were lost, or gained by two or more TRIB3 variants. Peptides that gained interactions with TRIB3 are shown in regular font and at the top of the column. Peptides that lost interactions with TRIB3 are shown in bold font and toward the end of the columns. The iBAQ difference is the difference between iBAQ values for each interacting peptide when detected in cells expressing the variant TRIB3 and wild-type TRIB3.

Gene ontology analysis of the genes encoding the peptides (iBAQ difference of 3 or more) identified as either gaining or losing interactions with each of the TRIB3 variants showed that they were involved in a diversity of cellular processes and pathways (Figure 3.6). Peptides that gained interactions with the V107M variant were involved in maintaining the cell membrane and the integral components attached to the membrane of cellular organelles. Compared to wild-type TRIB3, the V107M variant lost interactions with peptides that are involved in the regulation of G protein-coupled receptor binding, serine-type endopeptidase inhibitor activity, nitric oxide binding and chemokine receptor binding. Peptides that gained interactions with the S146N variant were involved in regulating functions of the endoplasmic reticulum membrane protein complex, and this variant lost interactions that were involved in microtubule nucleation which were possessed by wild-type TRIB3. The R149G variant gained interactions that are normally involved in ATP biosynthesis and in the metabolism of NAD and pyruvate, and lost interactions with peptides involved in multiple stages of mitochondrial translation, cellular protein complex/component disassembly, regulation of target of rapamycin (TOR) signalling, and of endothelial and epithelial cell proliferation. The R153H variant gained interactions with peptides involved in lipid biosynthesis and metabolism, purine and nucleoside metabolic processes, and in the regulation of chromosome segregation, and showed a loss of interactions with peptides involved in serine-type endopeptidase inhibitor activity, transferase activity and nitric acid binding. The R181C variant gained interactions with peptides involved in the catabolic process of purine-containing compounds and processes relating to lipid biosynthesis, and lost interactions with peptides involved in maintaining homeostasis in multicellular organisms and in the regulation of endopeptidase activity (Figure 3.6).

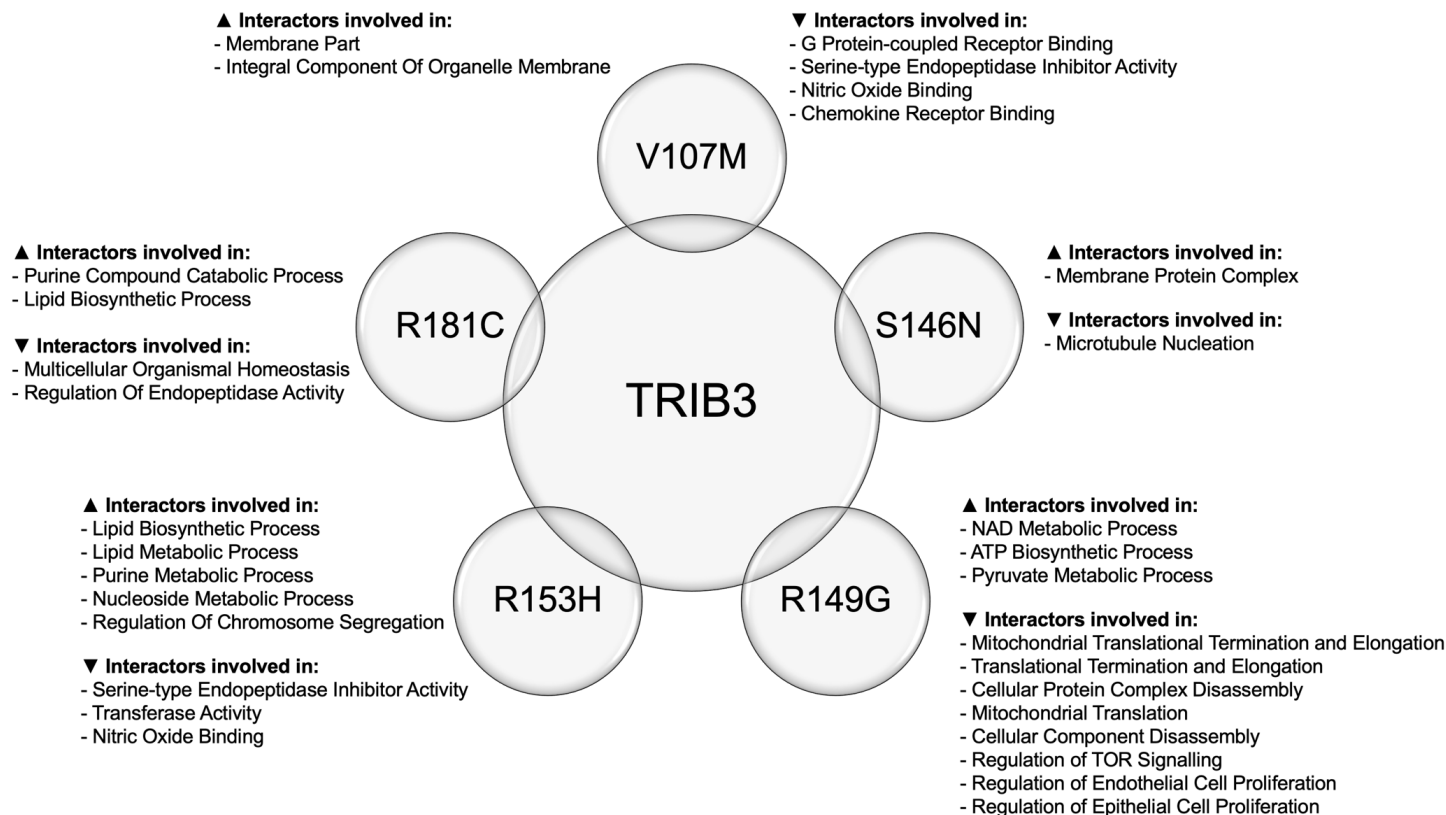


Figure 3.6: Gene ontology analysis to identify processes that may be affected by TRIB3 variants

The genes encoding peptides (showing an iBAQ difference of 3 or more) identified as either gaining or losing interactions with each of the TRIB3 variants were analysed using the GOrilla tool (<http://cbl-gorilla.cs.technion.ac.il/>) [last accessed 30/03/2020] (Eden et al, 2009) to predict processes and pathways that are regulated by those genes. ▲ Indicates processes regulated by peptides that gained interactions with the TRIB3 variant; ▼ indicates processes regulated by peptides that lost interactions with the TRIB3 variant.

Lists of those peptides that gained or lost interactions with TRIB3 as a result of the V107M, S146N, R149G, R153H and R181C substitutions were submitted to the browser of the Reactome pathway database, and the search limited to platelet-related processes. The outcomes for each peptide list were classified into different properties of haemostasis including: (i) Thrombin signalling through proteinase-activated receptors (PARs); (ii) GPVI-mediated activation cascade; (iii) Platelet aggregation; (iv) Cell surface interactions at the vascular wall; (v) Platelet homeostasis; (vi) Platelet adhesion to exposed collagen; (vii) GPIb-IX-V activation signalling; (viii) Signal amplification; (ix) Response to elevated platelet cytosolic Ca²⁺; (x) Formation of fibrin clot; (xi) Factors involved in megakaryocyte development and platelet production; (xii) Dissolution of fibrin clot and (xiii) Platelet activation, signalling and aggregation (Table 3.4).

Table 3.4: Interactors affected by *TRIB3* variants and involved in platelet-related processes

| TRIB3 Variant | Affected platelet-related process | Interactors affected |
|---|---|---|
| V107M | Thrombin signalling through proteinase activated receptors (PARs) | ▲ HSPA8, PIK3R2, AP2B1 |
| | GPVI-mediated activation cascade | ▲ SRP68, AP2B1 ▼ SGTA, SNX2, SPTAN1 |
| | Platelet Aggregation | ▲ PIK3R2, AP2B1, SRP68 ▼ SNX2, SPTAN1 |
| | Cell surface interactions at the vascular wall | ▲ DRAP1, ZNF593, EXOSC5 ▼ SGTA, PEBP1 |
| | Platelet Adhesion to exposed collagen | ▼ PDCD6IP |
| | GP1b-IX-V activation signalling | ▼ PEBP1 |
| | Response to elevated platelet cytosolic Ca ²⁺ | ▼ PFN1 |
| | Dissolution of Fibrin Clot | ▼ SGTA |
| S146N | Thrombin signalling through proteinase activated receptors (PARs) | ▲ CTTN, PIK3R2, AP2B1 ▼ S100A9 |
| | GPVI-mediated activation cascade | ▲ AP2B1 ▼ SNX2 |
| | Platelet Aggregation | ▲ PIK3R2, AP2B1 ▼ SNX2 |
| | Cell surface interactions at the vascular wall | ▲ DRAP1, EIF1AD, ZNF593, EXOSC5, AP2B1, RRP8 ▼ SUPT5H |
| | Factors involved in megakaryocyte development and platelet production | ▲ SUMO1, KIF3A, PPP1CA |
| R149G | Thrombin signalling through proteinase activated receptors (PARs) | ▲ CTTN, HDGFRP2, AP2B1 ▼ ZBTB43 |
| | GPVI-mediated activation cascade | ▲ LDHA, MSN, DSTN, AP2B1, SPTAN1, SPTBN1 ▼ PSMD3, ZNF655 |
| | Platelet Aggregation | ▲ AP2B1, LDHA, MSN, SPTAN1, SPTBN1 ▼ BCR, USP9X, ABL2 |
| | Cell surface interactions at the vascular wall | ▲ DRAP1, EIF1AD, AP2B1, RRP8 ▼ SCNM1, USP9X, UTP3, ZBTB24, ABL2, CDK2AP1, FAM207A, MCM10, BYSL |
| | Platelet homeostasis | ▼ APC, MKNK2, OBSL1 |
| | Platelet Adhesion to exposed collagen | ▼ HNRNPK |
| | GP1b-IX-V activation signalling | ▼ PPP2CA, ARAF, IRS2 |
| | Signal amplification | ▼ PRDX4, MKNK2, OBSL1 |
| | Response to elevated platelet cytosolic Ca ²⁺ | ▼ SGPL1, PSMA3 |
| | Formation of Fibrin Clot (Clotting Cascade) | ▼ MTIF3 |
| Factors involved in megakaryocyte development and platelet production | ▼ KANK2, MRPS17, SUN2, PCM1, KIF3B, FOXK2, ASH2L, ZNF689, ECT2, SHB, SCAPER, BYSL | |

| | | |
|--------------|---|---|
| R153H | GPVI-mediated activation cascade | ▲ SRP68, AP2B1 ▼ SNX2, SPTAN1 |
| | Platelet Aggregation | ▲ PIK3R2, AP2B1, SRP68 ▼ SNX2, SPTAN1 |
| | Cell surface interactions at the vascular wall | ▲ DRAP1, ZNF593, EXOSC5, AP2B1, RRP8 ▼ SCNM1, CANX, CDK2AP1, PEBP1 |
| | Factors involved in megakaryocyte development and platelet production | ▲ SUMO1, KIF3A, PPP1CA ▼ CREBBP |
| | Platelet activation, signaling and aggregation | ▼ PEBP1, SNX2, SPTAN1 |
| | GP1b-IX-V activation signalling | ▼ PEBP1 |
| R181C | Thrombin signalling through proteinase activated receptors (PARs) | ▲ HSPA8, CTTN, PIK3R2, AP2B1 |
| | GPVI-mediated activation cascade | ▲ AP2B1 ▼ SNX2 |
| | Platelet Aggregation | ▲ PIK3R2, AP2B1 ▼ SNX2 |
| | Cell surface interactions at the vascular wall | ▲ DRAP1, EIF1AD, ZNF593, EXOSC5, AP2B1, RRP8 ▼ PEBP1 |
| | Factors involved in megakaryocyte development and platelet production | ▲ SUMO1, KIF3A, ZNF436, PPP1CA |
| | Platelet homeostasis | ▼ MKNK2 |
| | GP1b-IX-V activation signalling | ▼ PEBP1 |
| | Signal amplification | ▼ MKNK2 |

Platelet-related gene lists were obtained from the Reactome database (<https://reactome.org/>) [last accessed 30/03/2020] (Fabregat et al, 2018). The ▲ symbol indicates peptides that gained interactions with the TRIB3 variant, compared to wild-type TRIB3, and ▼ indicates peptides that lost interactions with the TRIB3 variant, compared to wild-type TRIB3.

3.4 Discussion

Prior to this study, the expression level of *TRIB3* was reported to be negatively correlated with platelet biogenesis (Ahluwalia et al, 2015; Butcher et al, 2017). Previous studies had also identified both common and rare single nucleotide variants of *TRIB3* that were associated with the development of T2DM and CVD (Andreozzi et al, 2008; Formoso et al, 2011; Prudente et al, 2015; Prudente et al, 2009). However, a potential role for *TRIB3* in platelets had not been investigated. Our observations of an overrepresentation of rare *TRIB3* variants among 34 patients with unexplained platelet bleeding disorders, and an aberrant response to TRAP-induced platelet activation in platelets from female *Trib3*^{-/-} mice suggested a role for *TRIB3* in platelet function. The work described in this chapter aimed to investigate the effects, if any, of the rare *TRIB3* variants on *TRIB3* structure and function, and to correlate any changes in protein-protein interactors predicted to arise as a result of the *TRIB3* variants with platelet function.

The non-synonymous rare *TRIB3* variants predict substitutions of amino acids which are located within the highly-conserved pseudokinase domain that encompasses amino acids 95 to 342 of *TRIB3* (V107M, S146N, R149G, R153H and R181C). They were all predicted to be deleterious using the CADD algorithm. Two further common synonymous SNVs affecting codon positions 111 and 323 of *TRIB3* were predicted to have benign effects.

The valine and serine residues at amino acid positions 107 and 146, and the positively charged arginine residues at positions 149 and 181, are conserved in mammalian *TRIB3* sequences. This suggests that these residues are required for physiological *TRIB3* function and that substitutions at these positions are likely to alter the structure or function of the protein. On the other hand, the arginine residue at amino acid position 153 is less conserved and replaced by proline and glycine residues in the chimpanzee and mouse *TRIB3* respectively. This indicates that the protein can tolerate variation at this position, though proline and glycine are small amino acids and possibly less disruptive than a histidine residue, which was predicted to have a deleterious effect in human *TRIB3*.

Structural studies using a 3D model of *TRIB3* indicated that all five variants predicted substitutions of amino acids that are located on the surface of *TRIB3*, which increases the likelihood of them affecting the interaction of *TRIB3* with other proteins. *AKT* is a

known partner of TRIB3. It was surprising therefore, that the mass spectrometric analysis of the peptides that interacted with wild-type or variant forms of TRIB3 in transfected HEK293 cells did not identify any of the AKT isoforms. This may reflect sensitivity issues for the mass spectrometry as it is well known that without prior fractionation, abundant proteins are more likely to dominate the peptide signals. Nevertheless, AKT remains an important candidate for further investigation of the potential effects of the *TRIB3* variants due to the recognised interaction between TRIB3 and AKT1 in serum-deprived HEK293 cells, and the established role of AKT in regulating platelet function (Chen et al, 2019; Du et al, 2003; Woulfe et al, 2004). The effects of the *TRIB3* variants on the interaction of the corresponding TRIB3 molecules with AKT were therefore examined further and the results are presented in chapter 5 of this thesis.

The differences in the profiles of interacting peptides that were detected by mass spectrometry between wild-type TRIB3 and the five TRIB3 variants suggest that the amino acid substitutions in the variants may be disrupting interactions with other proteins, potentially leading to either a gain or loss of function. There was no expectation of the TRIB3 interacting partners other than the known partners as no previous publication was listing the TRIB3 interactions with other proteins using the mass spectrometric approach. Therefore, to improve the reliability and reproducibility of the mass spectrometric findings, the proteins considered for further analysis were limited to proteins that showed more than three peptides interacting with TRIB3. Additionally, the minimum iBAQ_{difference} was set to 3 to remove peptides that were close to the lower detection level of the mass spectrometer, and only peptides showing robust and consistent iBAQ values across all three repeat transfections were considered.

Interestingly, four of the TRIB3 variants (R181C, V107M, S146N and R149G) gained interactions with TIMM17B (Mitochondrial import inner membrane translocase subunit Tim17-B), a protein that mediates the translocation of mitochondrial pre-proteins from the cytosol and the mitochondrial outer membrane to the mitochondrial inner matrix to allow mitochondrial protein synthesis (Bauer et al, 1999). Furthermore, the R181C, V107M, S146N and R153H variants gained interactions with MCAT (Malonyl-CoA-Acyl Carrier Protein Transacylase), a protein that is found exclusively in the mitochondrion where it is suggested to be part of the malonyl-CoA/acyl carrier protein-dependent fatty acid synthase system which supports mitochondrial function (Zhang et al, 2003). The

increased interaction of all five variants with mitochondrial peptides suggest that TRIB3 might be involved in regulating mitochondrial processes, a finding that will be explored further in chapter 6.

Peptides that lost interactions with two or more of the TRIB3 variants when compared to wild-type TRIB3 included Stathmin (STMN1), Spectrin α -chain, non-erythrocytic 1 (SPTAN1), and Sorting nexin 2 (SNX2). STMN1 is a cytosolic phosphoprotein that has been described previously to be involved in the regulation of microtubules during the early stages of megakaryopoiesis, and *STMN1* expression was correlated to megakaryocyte polyploidisation (Iancu-Rubin et al, 2010; Rubin et al, 2003). Non-erythroid Spectrin α -chain (SPTAN1) was identified to have a significant role in maintaining membrane stability in megakaryocytes and platelets, and was also identified to be essential for proplatelet formation (Fox et al, 1987; Patel-Hett et al, 2011). Studies investigating the role of sorting nexin 2 (SNX2) suggest that it has a role in retromer function, which involves regulation of transmembrane trafficking and cargo transportation between endosomes and the trans-Golgi network (Rojas et al, 2007). While there is no published evidence for the involvement of SNX2 in platelet secretion, another member of the sorting nexin family, SNX1, has been shown to be involved in the regulation of lysosome degranulation from platelets (Wang et al, 2002), and the functions of SNX1 and SNX2 have been suggested to overlap, which could indicate a role for SNX2 in regulating platelet secretion (Rojas et al, 2007).

The set of peptides that lost interactions with the R149G TRIB3 variant included a peptide derived from TRIB3, which suggests that the amino acid substitution at position 149 may affect protein dimerisation. Previous unpublished work in our laboratory indicated that TRIB3 would form a dimer when overexpressed in HEK293 cells, and our mass spectrometric data supported this by showing an interaction between wild-type and variant forms of TRIB3 (except R149G TRIB3) with a peptide derived from TRIB3. Interestingly, R149 has been predicted to be a hot spot for the interaction between TRIB3 and AKT using *in-silico* simulation of the protein interaction [performed by Juan Salamanca Vilorio (Barcelona, Spain)] (unpublished). Therefore, the initial anticipation is that the R149G variant would behave differently compared to other variants.

Gene ontology analysis of the peptides that showed a gain or loss of interaction with the TRIB3 variants predicted a range of pathways and processes that could be

disturbed. A more targeted search of the Reactome database focused on platelet-related genes and on those peptides that could be regulating platelet function. This analysis highlighted genes such as *SNX2*, *SPTAN1* and *AP2B1* to be involved in different platelet-related processes including the GPVI-mediated platelet activation cascade, platelet aggregation, thrombin signalling through PARs, and surface interactions at the vascular wall. The *AP2B1* gene was previously listed in a meta-analysis of genome-wide association studies (GWAS) to be associated with platelet disorders (Bunimov et al, 2013), and the possible involvement of *SPTAN1* and *SNX2* in regulating several aspects of platelet function (Patel-Hett et al, 2011; Rojas et al, 2007; Wang et al, 2002) support the notion that these might be disrupted in the presence of a variant form of *TRIB3*. These findings support the potential role of *TRIB3* in platelet function and a possible contribution from the five variants studied here to the increased bleeding tendency that was observed in the UK-GAPP study patients.

The outcomes of the *in-silico* predictions and the analysis of the mass spectrometric data, combined with previous knowledge of *TRIB3*, form the basis for further hypotheses about *TRIB3* and its potential role in platelets. Firstly, we hypothesise that *TRIB3* variants predicting amino acid substitutions in *TRIB3* will affect the localisation, structure, conformation, and aggregation of *TRIB3*, and the interactions of *TRIB3* with other proteins. This hypothesis will be investigated further in chapter 5 of this thesis. Secondly, the detection of several *TRIB3*-interacting peptides that are involved in mitochondrial translocation and biosynthesis lead us to hypothesise that variants of *TRIB3* could disrupt mitochondrial function. This hypothesis will be explored in work described in chapter 6 of this thesis.

Chapter 4:

Gateway cloning of *TRIB3* variants and optimisation of protein complementation assays to investigate the interaction between TRIB3 and AKT

4.1 Introduction

It is well recognised that defects in genes regulating megakaryopoiesis can be associated with platelet bleeding disorders (Almazni et al, 2019; Bianchi et al, 2016). *TRIB3* was suggested to be involved in regulating megakaryopoiesis following the observation of high expression levels of *TRIB3* in cells treated with an inhibitor of megakaryopoiesis (Anagrelide) (Ahluwalia et al, 2015), and a high megakaryocyte differentiation rate in cells treated with a *TRIB3* silencing agent (*TRIB3* short_interfering_RNA) (Butcher et al, 2017). In chapter 3, I described the identification of five nonsynonymous variants of *TRIB3* in patients with platelet bleeding disorders, and I showed using structural modelling, and predictive algorithms, that these variants could affect protein-protein interactions (PPIs) as they affected amino acids that are predicted to reside in regions on the surface of *TRIB3*. AKT is a well-studied interactor of *TRIB3*, and previous reports have shown that the *TRIB3* SNV *c.251A>G* (rs2295490, p.Q84R) has a gain-of-function effect on the interaction with AKT, which leads to the disruption of intracellular signalling and contributes to the development of T2DM and cardiovascular diseases (Prudente & Trischitta, 2015). Therefore, investigating the interactions between the *TRIB3* molecules encoded by the nonsynonymous variants and AKT could provide insights into their potential functional effects, and explain their identification in patients with platelet bleeding disorders. We proposed investigating the impact of these variants on *TRIB3* function using protein complementation assays to examine cellular localisation of the *TRIB3*/AKT complex and measure the strength of their interaction with AKT. In this chapter, I describe the development of the tools necessary for these studies.

Protein complementation assays are widely used to detect and assess protein-protein interactions (PPIs) (Shekhawat & Ghosh, 2011). In this study, a split-YFP system was used to investigate localisation of the *TRIB3*/AKT1 complex, and a split-luciferase system was used to quantify the interaction between *TRIB3* and either AKT1 or AKT2.

In this chapter, the generation of plasmids encoding the five *TRIB3* variants introduced in chapter 3 is described. The use of Gateway cloning to generate a panel of expression plasmids suitable for use in split-YFP and split-luciferase protein complementation assays and the experimental work carried out to determine the optimal orientations of these expression plasmids are also described. The optimal orientations will then be adopted to generate expression plasmids of the *TRIB3*

variants that will be used to investigate their interactions with AKT which will be described in the subsequent chapter.

4.1.1 Gateway™ cloning technology

The *in-vitro* investigation of protein expression and function is greatly facilitated by the use of recombinant DNA technology to engineer expression plasmids for the proteins of interest. The Gateway™ cloning system streamlined the process of cloning through the use of recombination sites that allow an instant transfer of DNA sequences from so-called Entry vectors into expression vectors without affecting the sequence of the introduced DNA fragment (Hartley et al, 2000). Early cloning strategies were dependent on the identification of suitable restriction sites and the use of ligation enzymes to introduce the DNA fragment of interest into the reading frame of the expression vector. They were time-consuming procedures in contrast to Gateway™ cloning which allows quick and precise generation of expression vectors with greater than 95% efficiency (Sasaki et al, 2004). Additionally, the Gateway™ systems support high-throughput cloning, facilitating the investigation of wild-type and variant forms of proteins such as TRIB3 using multiple expression vectors. LR Gateway™ cloning allows the transfer of a gene positioned between attL sites on an Entry clone to expression vectors that incorporate attR recombination sites (Figure 4.1). This system was suitable for this study as it allows the generation of expression vectors that can be used to study protein localisation and facilitates protein complementation assays that investigate the localisation and strength of PPIs. Prior to commencing these studies, it was necessary for the genes encoding the proteins of interest to be cloned into the Entry vector of the Gateway system. At the outset of this study, an Entry vector (*TRIB3-ENTR/D*) containing the wild-type human *TRIB3* cDNA cloned between two attL sites was made available by Professor Endre Kiss-Toth (University of Sheffield, UK). Site-directed mutagenesis was then used to introduce the single nucleotide changes predicting V107M, R149G, S146N, R153H and R181C amino acid substitutions in TRIB3 into *TRIB3-ENTR/D*.

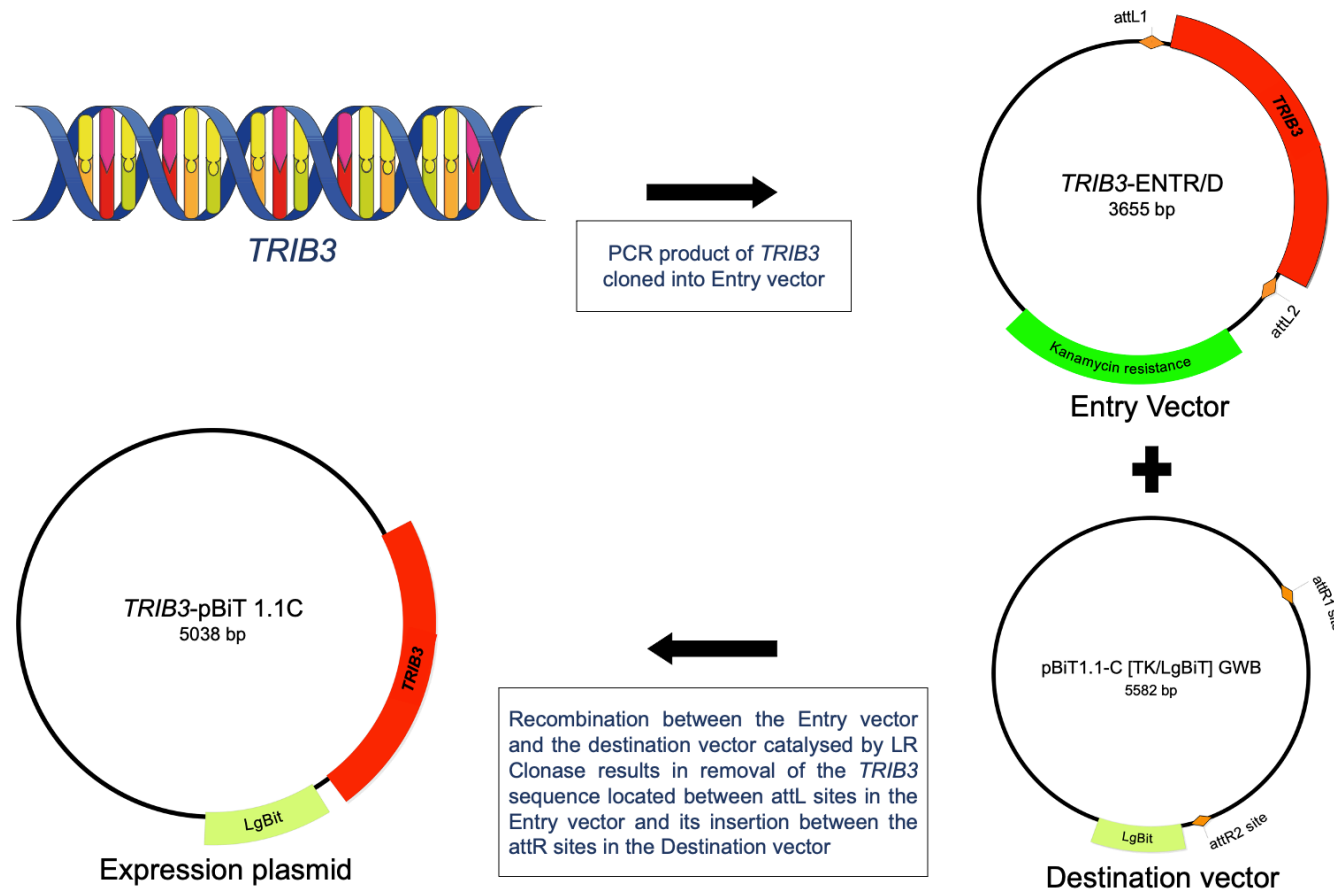


Figure 4.1: LR Gateway™ cloning strategy

LR Gateway™ cloning requires the presence of an entry vector and a destination vector in the LR reaction. The entry vector contains the *TRIB3* positioned between two *attL* sites. The destination vector encompasses features used to study specific aspects of the protein encoded by the gene of interest, and *attR* sites to allow recombination during the LR reaction. In this example, the destination vector incorporates sequence encoding the LgBiT fragment of luciferase and two *attR* sites. The LR reaction will instantly transfer the *TRIB3* cDNA using the *attL* sites and recombine it with the destination vector using the *attR* sites to create an expression plasmid expressing h*TRIB3* fused to the LgBiT.

4.1.2 Protein fragment complementation assays

The use of protein fragment complementation assays to assess the interaction of two proteins is well established (Remy & Michnick, 2007). It requires having the cDNAs of the two interacting proteins cloned immediately up- or downstream of matching fragments of a reporter gene on the destination vector. To study the effects of the selected *TRIB3* variants on the interaction of TRIB3 with AKT, Gateway cloning was used to transfer wild-type and mutated *TRIB3* variants from entry vectors to destination vectors encoding fragments of either NanoLuc or YFP.

4.1.2.1 Investigation of the interaction between TRIB3 and either AKT1 or AKT2 using a Split-NanoLuc luciferase complementation assay

To investigate the interaction between TRIB3 and either AKT1 or AKT2, a Split-NanoLuc luciferase complementation assay was developed. This required two expression vectors that incorporated the cDNAs of TRIB3 and either AKT1 or AKT2 (referred to as A and B respectively in figure 4.2), fused to fragments of the cDNA encoding NanoLuc, which could then be co-transfected to assess the extent of the interaction between TRIB3 and AKT (Dixon et al, 2016). In developing this complementation assay, it was crucial to ensure that fusion of either of the two fragments of the NanoLuc protein [Large Bit (LB) and Small Bit (SB)] to TRIB3 or AKT did not alter their expression or interaction. Therefore, to identify optimal conditions for the assay, it was advisable to test the interactions using vectors that expressed fusion proteins of TRIB3 and AKT having the NanoLuc fragments at either the amino (N-) or the carboxy (C-) terminus (Lepur & Vugrek, 2018). In order to test the different combinations, TRIB3 and AKT were each expressed as four separate fusion proteins, two with LB (both N- and C-termini) and two with SB (both N- and C-termini), resulting in eight possible vector combinations (Figure 4.2). The basal luminance signal was set to be that obtained by co-transfecting the expression plasmid encoding the LB fragment with the NanoBiT Negative Control plasmid which, according to the manufacturer (Promega, Madison, USA), is designed to generate a minimal signal. Additionally, in this study, the known strong interaction between Rel-A SB-C and $\text{I}\kappa\text{B}\alpha$ LB-C provided a positive control for the test. Use of high-throughput Gateway cloning allows the rapid generation of expression vectors tagged with LB and SB in all possible orientations. The combination of plasmids that generates the highest luminance signal

when TRIB3 and AKT interact was then identified following co-transfection of mammalian cells and assay of luciferase activity.

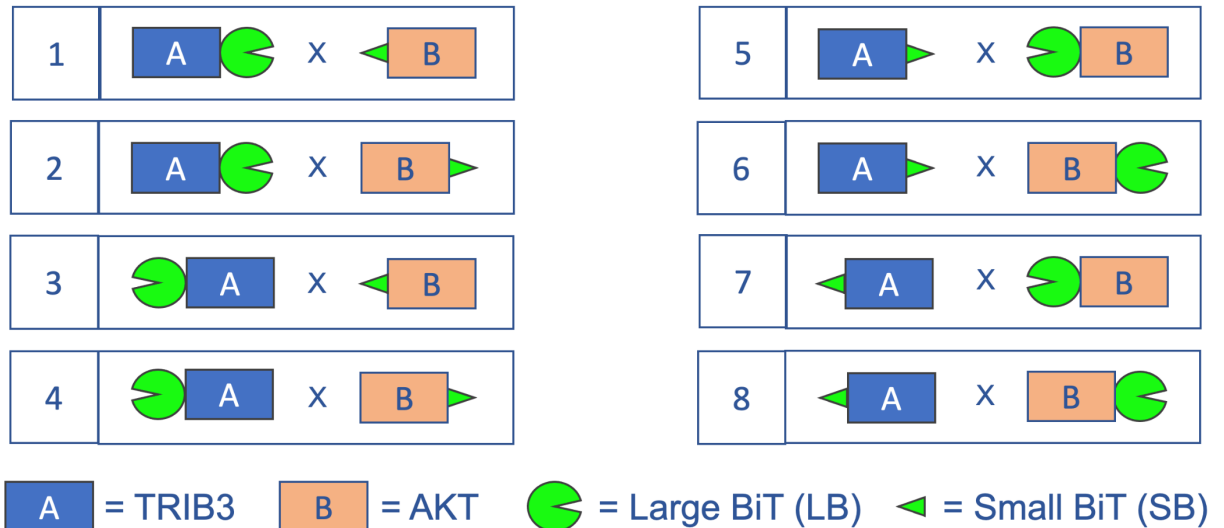


Figure 4.2: Optimisation of the Split-NanoLuc fragment complementation assay

To determine the optimal combination of fusion proteins for the assay, four different possible fusions are generated; Protein A (or TRIB3) tagged with either LB or SB on either the C- or N- terminus and Protein B (or AKT1/2) tagged with either LB or SB on either the C- or N- terminus. Every combination tested includes both LB and SB to generate NanoLuc activity through the physical interaction of the two proteins. Therefore, the eight possible combinations are shown. Adapted from the manufacturer's protocol for the Nano-Glo[®] Live Cell Assay system (Catalogue number: N2011) (Copyright – Promega Corporation, Madison, WI, USA. 2020).

4.1.2.2 Localisation of TRIB3/AKT1 interactions using a Split-YFP fragment complementation assay

The use of Split-fluorescent proteins allows examination of the subcellular localisation of PPIs. The Split-YFP complementation assay relies on having two expression plasmids that incorporate sequences encoding the two proteins of interest fused to non-fluorescent fragments of YFP (Figure 4.3). Co-transfection and expression of the two plasmids then allow localisation of any interactions between the two proteins within the transfected cells. It is crucial to ensure that fusion of the YFP fragments, Venus-1 (V1) or Venus-2 (V2), to the proteins of interest does not alter their expression or trafficking within the cell (Lepur & Vugrek, 2018). The destination vectors that were used in this study allowed the expression of TRIB3 and AKT1 fused to either V1 or V2 at the carboxy (C-) terminus. The optimal combination of vectors was then determined by co-transfecting TRIB3-V1 with AKT1-V2 and AKT1-V1 with TRIB3-V2. The commonly used positive control plasmid encodes a leucine-rich dimerisation domain derived from the yeast GCN4 transcriptional activator (Galarneau et al, 2002; Remy & Michnick, 2004). Complementary sequences of the GCN4 dimer-forming motif fused to complementary YFP fragments (V1 and V2) were therefore generated. The positive control plasmids used in this study were provided by Professor Endre Kiss-Toth (University of Sheffield, UK).

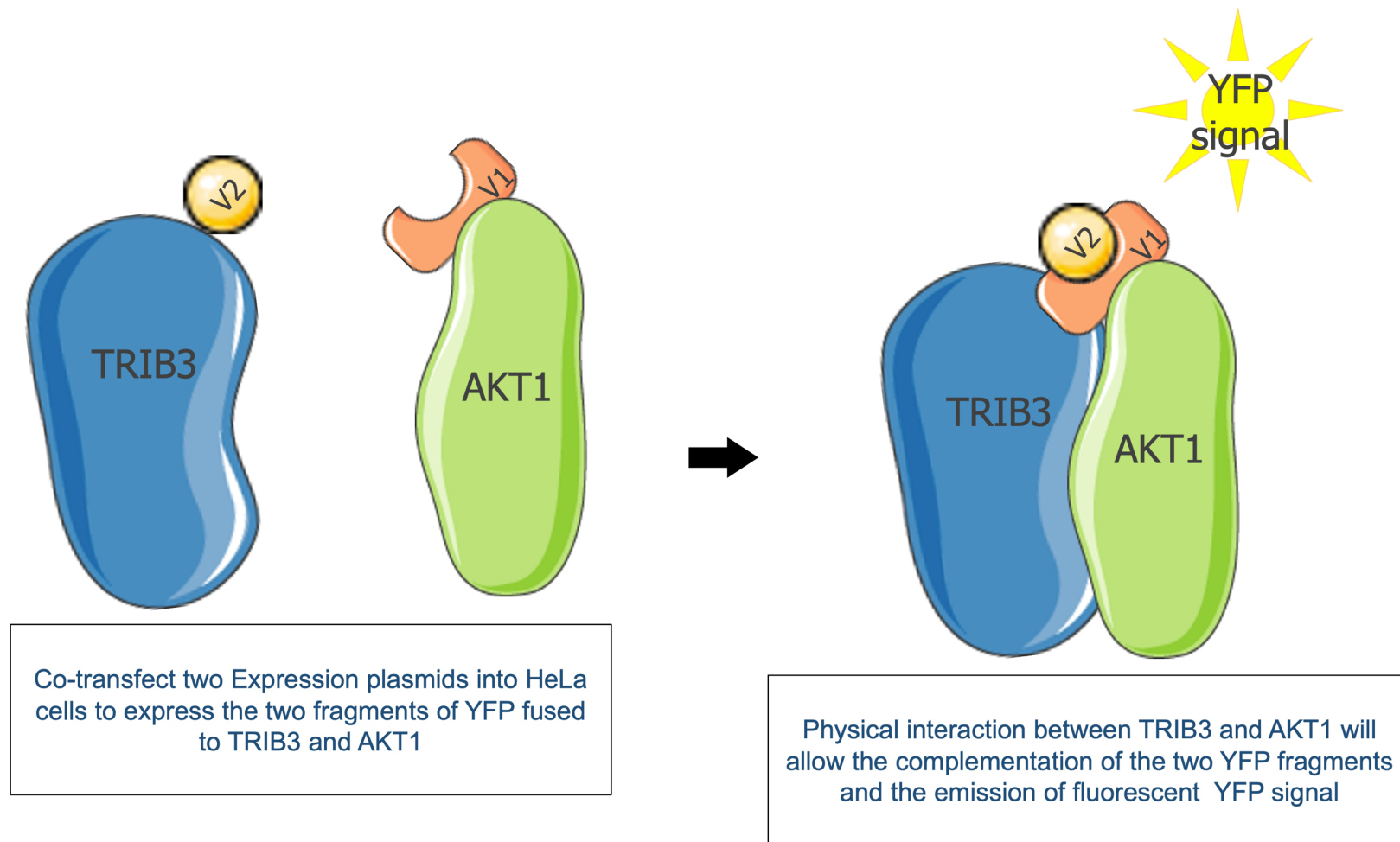


Figure 4.3: The Split-YFP fragment complementation assay

The two fragments of YFP (V1 and V2) are fused to the two interacting proteins (TRIB3 and AKT1) at their C-termini. When the two proteins interact, and the two YFP fragments (V1 and V2) come into close proximity, the YFP will emit a fluorescent signal. The localisation of the interaction is then assessed by fluorescence microscopy.

4.2 Methods

Optimisation of the protein complementation assays (PCAs) described above required the generation of plasmids expressing different proteins, or fragments thereof, which are listed in table 4.1. Details of the cloning protocols that were used to derive new plasmids are included in section 2.2.3.

Table 4.1: Plasmids required for Protein Complementation Assays

| Name | Use | Source |
|----------------------------|--|--------|
| TRIB3-ENTR/D | Entry plasmid encompassing wild-type <i>TRIB3</i> cDNA. Used to clone <i>TRIB3</i> into expression vectors using LR Gateway cloning. | IH |
| TRIB3-V1 | Expression plasmid used in the optimisation of the split-YFP PCA to study the localisation of the TRIB3/AKT1 complex. The plasmid encodes TRIB3 fused to the Venus 1 fragment of YFP at its C-terminus | SC |
| TRIB3-V2 | Encodes TRIB3 fused to the Venus 2 fragment of YFP at its C-terminus | SC |
| AKT1-V1 | Encodes murine AKT1 fused to the V1 fragment at its C-terminus | IH |
| AKT1-V2 | Encodes murine AKT1 fused to the V2 fragment at its C-terminus | IH |
| ZIP-V1 | Encodes V1 fragment fused to the GCN4 Leucine zipper (ZIP) dimerisation domain. The plasmid was used as a positive control for the split-YFP PCA when co-transfected with ZIP-V2 | IH |
| ZIP-V2 | Encodes V2 fragment fused to the GCN4 Leucine zipper (ZIP) dimerisation domain and used as a positive control | IH |
| TRIB3 SB-N | Expression plasmid used in the optimisation of the split-NanoLuc PCA to study the interaction between TRIB3 and either AKT1 or AKT2. The plasmid encodes TRIB3 fused to the Small BiT (SB) fragment of the NanoLuc protein at its N-terminus | SC |
| TRIB3 SB-C | Encodes TRIB3 fused to the Small BiT (SB) fragment of the NanoLuc protein at its C-terminus | SC |
| TRIB3 LB-N | Encodes TRIB3 fused to the Large BiT (LB) fragment of the NanoLuc protein at its N-terminus | SC |
| TRIB3 LB-C | Encodes TRIB3 fused to the Large BiT (LB) fragment of the NanoLuc protein at its C-terminus | SC |
| AKT1(or 2) SB-N | Encodes either murine AKT1 or AKT2 fused with SB fragment of the NanoLuc protein at its N-terminus | IH |
| AKT1(or 2) SB-C | Encodes either murine AKT1 or AKT2 fused with SB fragment of the NanoLuc protein at its C-terminus | IH |
| AKT1(or 2) LB-N | Encodes either murine AKT1 or AKT2 fused with LB fragment of the NanoLuc protein at its N-terminus | IH |
| AKT1(or 2) LB-C | Encodes either murine AKT1 or AKT2 fused with LB fragment of the NanoLuc protein at its C-terminus | IH |
| NanoBiT | Negative control for the split-NanoLuc PCA that is expected to generate a minimal signal when co-transfected with the plasmid expressing the LB | PM |
| Rel A SB-C | Expression plasmid that encodes murine <i>RelA</i> (a transcription factor also known as NF κ B) fused to the SB at its C-terminus. The plasmid was used as a positive control for the split-NanoLuc system when co-transfected with I κ B α LB-C | IH |
| I κ B α LB-C | Encodes murine I κ B α (which is an inhibitor of NF κ B) fused to LB at its C-terminus | IH |

IH: previously developed in-house by Professor Endre Kiss-Toth; SC: generated and subcloned during the course of this study; PM: purchased from the manufacturer.

4.3 Results

4.3.1 Generation of Gateway entry plasmids and expression vectors encoding wild-type and variant forms of TRIB3

Site-directed mutagenesis was used to introduce the single nucleotide changes predicting V107M, R149G, S146N, R153H and R181C amino acid substitutions in TRIB3 into a Gateway Entry plasmid encoding wild-type TRIB3 (hTRIB3-ENTR/D). Entry plasmids for the V107M, R149G, R153H and R181C variants were generated previously as part of my MSc project, and the S146N variant was added and generated during the course of this study (see section 2.2.1). The integrity of the recombinant plasmids was examined by restriction digestion using *Not* I and *Pst* I. The wild-type *TRIB3* entry plasmid is 3,655bp in size, and the expected fragments of 2,793bp and 862bp were generated following restriction digestion of the recombinant plasmids generated (Fig. 4.4). The presence of the desired nucleotide changes was confirmed in the recombinant plasmids by direct sequencing and alignment of the plasmid sequences with the reference human *TRIB3* cDNA sequence (version GRCh38/hg38) available at the UCSC Genome Browser (<https://genome.ucsc.edu>) (Fig. 4.4).

The Gateway™ cloning system (LR Clonase™ II Enzyme Mix kit) was used to transfer wild-type and variant *TRIB3* cDNAs from entry plasmids to a destination vector that incorporated a YFP cassette downstream of the inserted cDNA, thus allowing their expression as YFP fusion proteins (see section 2.2.3.1). Restriction of the resulting 7,296bp YFP expression plasmids with *Kpn* I yielded the expected fragments of 741bp and 6,555bp (Fig 4.5 A). Sanger sequencing confirmed the integrity of the *TRIB3* sequence and the YFP fusion cassette.

Similarly, the variant *TRIB3* cDNAs from mutagenised entry plasmids were subcloned into destination vectors that incorporated the cDNA encoding either the V1 or V2 fragments of YFP downstream of the inserted cDNA to allow expression of the YFP fragment fused to *TRIB3* (see section 2.2.3.1). The size of the *TRIB3*/V1 plasmid is 6,468bp, and digestion with *Kpn* I resulted in the expected fragments of 792bp and 5,676bp in size (Fig 4.5 B). Digestion of the 6,696bp *TRIB3*/V2 plasmid with *Kpn*I yielded the anticipated fragments of 1,020bp and 5,676bp (Fig 4.5 C). The integrity of the *TRIB3* sequence, and fusion with the V1 or V2 sequence, were confirmed by Sanger sequencing.

Wild-type and variant *TRIB3* cDNAs were also transferred from entry clones to destination vectors that allowed their expression as proteins having LB (also denoted as 1.1C or 1.1N), or SB (also denoted as 2.1C or 2.1N) fused to either the N- or C-terminal of *TRIB3* (see section 2.2.3.1). The resulting vectors encoding wild-type or variant forms of *TRIB3* with a C-terminal LB tag were 5,004bp as expected, and *Acc65I* digestion yielded the expected fragments of 1257bp and 3747bp (Fig 4.5 D). Likewise, the vectors encoding SB fused to the N-terminal of wild-type or variant *TRIB3* molecules were the expected size of 4,591bp and yielded fragments of 1,332bp and 3,259bp when digested with *Acc65I* (Fig 4.5 E).

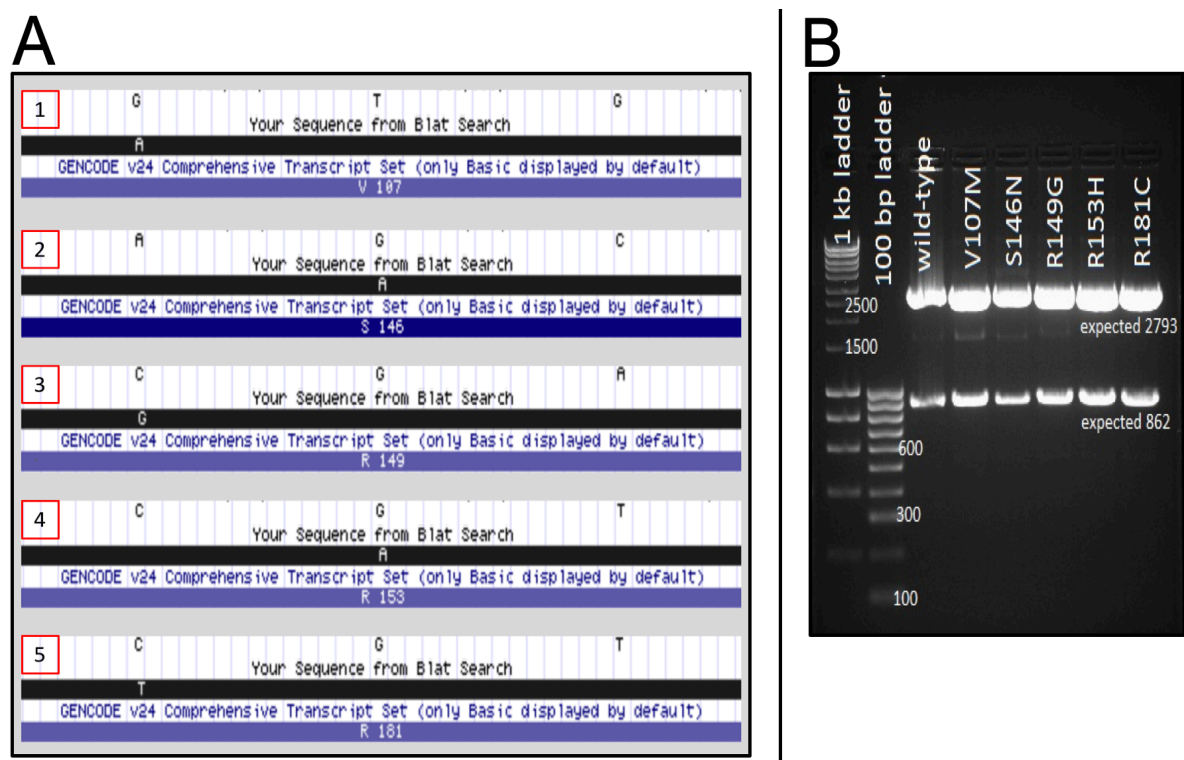


Figure 4.4: Analysis of variant *TRIB3* entry plasmids

(A) Alignment of *TRIB3* entry plasmid sequences with the reference *TRIB3* sequence following site-directed mutagenesis to introduce: (1) a c.G319A transition predicting the p.V107M substitution; (2) a c.G437A transition predicting a p.S146N substitution; (3) a c.C445G transversion predicting the p.R149G substitution; (4) a c.G458A transition in codon 153 predicting a p.R153H substitution; (5) a c.C541T transition predicting a p.R181C substitution. **(B)** Recombinant *TRIB3* entry plasmids were digested with *Not I* and *Pst I* following mutagenesis and subjected to electrophoresis in 1% agarose alongside samples of 1kb and 100bp DNA ladders. Fragments of the expected sizes of 2,793bp and 862bp were observed following digestion of the wild-type and variant forms of the entry plasmid.

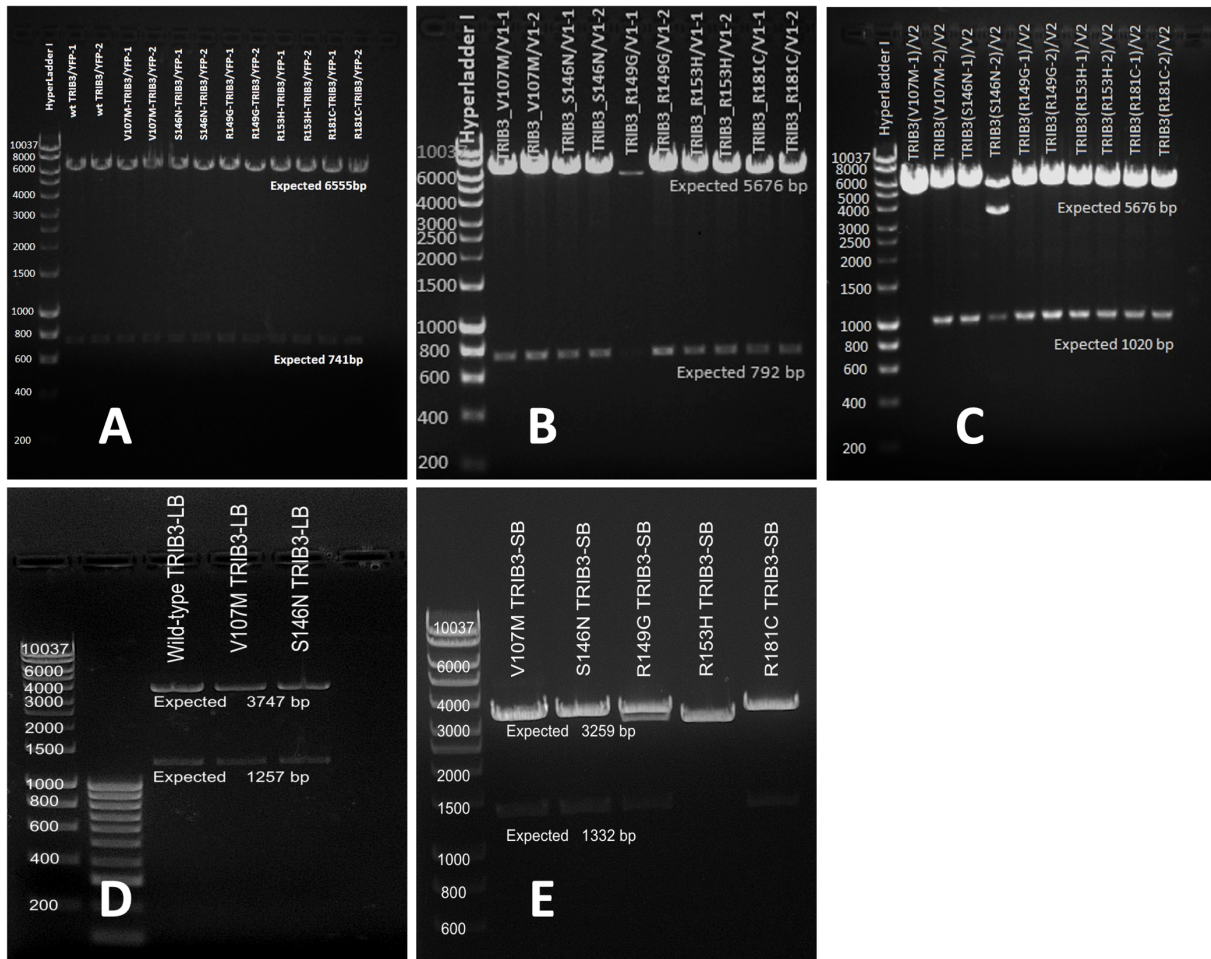


Figure 4.5: Restriction analysis of TRIB3 expression plasmids

(A) Plasmids encoding either wild-type or mutated TRIB3 variants fused to YFP were digested with *Kpn* I to yield the expected fragments of 6,555bp and 741bp. **(B)** Plasmids encoding either wild-type or mutated TRIB3 variants fused to the V1 fragment of YFP were digested with *Kpn* I to yield the expected fragments of 792bp and 5676bp. **(C)** Plasmids encoding wild-type or mutated TRIB3 variants fused to the V2 fragment of YFP were digested with *Kpn* I to yield the expected fragments of 1020bp and 5676bp. **(D)** Examples of plasmids encoding wild-type and the indicated TRIB3 variants with an LB tag were digested with *Acc65*I yielding the expected fragments of 1,257bp and 3,747bp. **(E)** Examples of plasmids encoding mutated TRIB3 with an SB tag were digested with *Acc65* I to produce the expected fragments of 1,332bp and 3,259bp. Restriction digests were electrophoresed in 1% agarose along with a sample of a 10kb DNA ladder.

4.3.2 Optimisation of the split-NanoLuc complementation assay of the TRIB3/AKT interaction

Following confirmation of the plasmid sequences, the eight combinations of plasmids shown in figure 4.2 were transfected into HEK293 cells. The cells were incubated for 24 hours with the transfection mixtures before adding Nano-Glo® Live Cell substrate and measuring luciferase activity (see section 2.2.6). Experiments to test different combinations of plasmids expressing TRIB3 with either AKT1 or AKT2 were carried out three times, and all plasmid combinations were transfected in triplicate in each repeat experiment.

Luciferase activity was measured in cells transfected with plasmids encoding fusion proteins of wild-type TRIB3 and AKT1 tagged with LB or SB at either the C- or the N-terminal. As a positive control, cells were co-transfected with two vectors encoding Rel-A SB-C and I κ B α LB-C, which are known to interact strongly. Basal luciferase activity was measured in cells co-transfected with the NanoBiT negative control plasmid and a plasmid encoding TRIB3 fused to the LB at its C-terminus (TRIB3 LB-C). The luciferase activity in cells transfected with each of the plasmid combinations was compared with that in control cells using Dunnett's multiple comparisons test. Luciferase activity was similar to or below basal levels in cells transfected with the majority of plasmid combinations tested ($P>0.05$; Fig. 4.6). Maximum luciferase activity, reflecting the optimal conditions for TRIB3 to interact with AKT1, was observed in cells expressing TRIB3 with a C-terminal LB tag, and AKT1 with an N-terminal SB tag which showed an approximate two-fold difference in luciferase activity over background ($P=0.098$).

Similarly, luciferase activity was measured in cells transfected with plasmids encoding fusion proteins of TRIB3 and AKT2 tagged with LB or SB at either the C- or the N-terminal. The Rel-A SB-C and I κ B α LB-C plasmids were included as a positive control, and the background signal was determined by the activity measured in cells transfected with the NanoBiT and I κ B α LB-C plasmids. Five of the test plasmid combinations resulted in luciferase activity levels that were similar to or below the basal levels ($P=>0.05$) (Fig. 4.7), and the remaining three combinations led to significant increases in luciferase activity over basal levels. The Dunnett's multiple comparisons test was used to identify the combination that allows the optimal interaction between TRIB3 and AKT2. The combination where the SB was fused to TRIB3 at the N-terminal

(TRIB3 SB-N) and the LB was fused to AKT2 at the C-terminal (AKT2 LB-C) resulted in maximum luciferase activity ($P=0.0001$). The two combinations (TRIB3 LB-C with AKT2 SB-N, and TRIB3 SB-C with AKT2 LB-C) also significantly increases luciferase activity over basal levels ($P=0.022$, 0.032 , respectively) but the TRIB3 SB-N with AKT2 LB-C combination of plasmids provided the broadest range above background and was therefore considered to be the optimal combination for detecting differences (if any) between wild-type and variant forms of TRIB3.

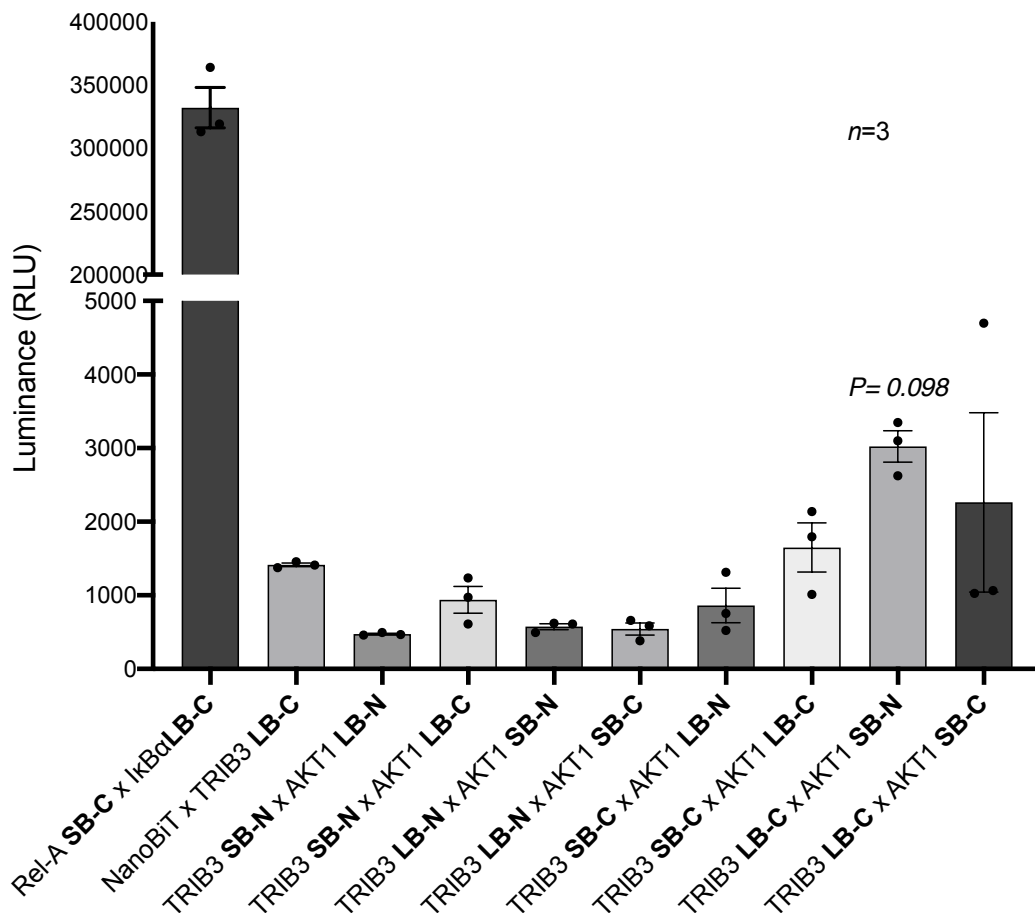


Figure 4.6: Nano-Luciferase activity in HEK293 cells transfected with plasmids encoding TRIB3 and AKT1 tagged with LB or SB luciferase fragments.

HEK293T cells were co-transfected with the indicated combinations of plasmids allowing the expression of TRIB3 and AKT1 tagged with the LB or SB fragments of luciferase. The tags were present on either the C- or N-terminal of TRIB3 and AKT1. Cells were co-transfected with Rel-A SB-C and IκBα LB-C expression plasmids as a positive control and the luciferase activity in cells co-transfected with NanoBIT and TRIB3 LB-C expression plasmids was considered to be the baseline level. Each point on the graph represents a biological repeat of the experiment ($n=3$), which was performed in triplicate for each repeat. Error bars represent +/- the standard error of the mean (SEM). Dunnett's multiple comparisons test was used to compare luminance levels for each of the plasmid combinations to baseline. $P>0.05$ for all comparisons, unless otherwise indicated.

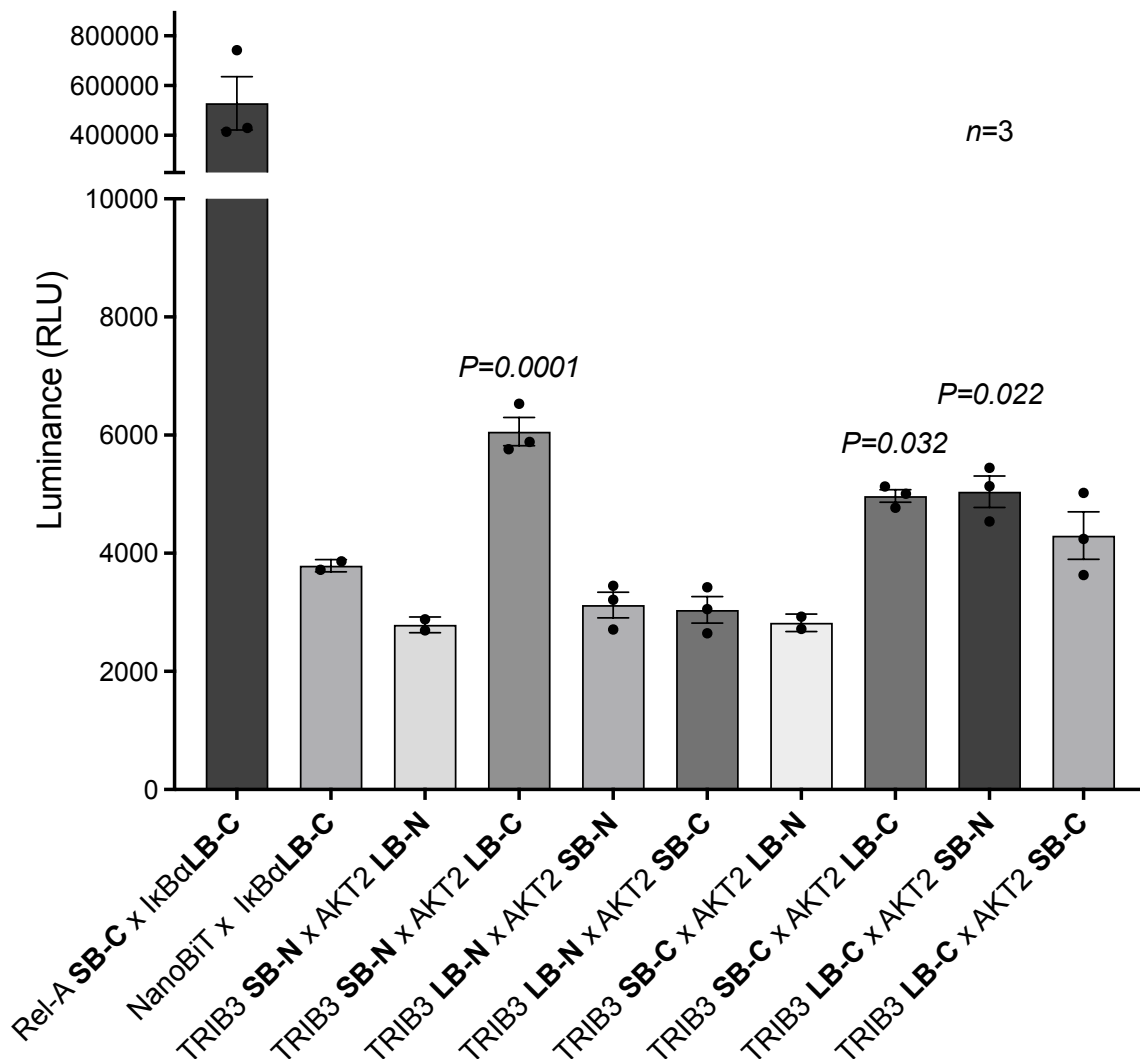


Figure 4.7: Nano-Luciferase activity in cells transfected with TRIB3 and AKT2 plasmids tagged with LB or SB luciferase fragments.

HEK293T cells were co-transfected with the indicated combinations of plasmids allowing the expression of TRIB3 and AKT2 tagged with the LB or SB fragments of luciferase. The tags were present on either the C- or N-terminal of TRIB3 and AKT2. Cells were co-transfected with Rel-A SB-C and IκBα LB-C expression plasmids as a positive control and the luciferase activity in cells co-transfected with NanoBiT and IκBα LB-C expression plasmids was considered to be the baseline level. Each point on the graph represents a biological repeat of the experiment ($n=3$), which was performed in triplicate for each repeat. Error bars represent +/- the standard error of the mean (SEM). Dunnett's multiple comparisons test was used to compare luminance levels for each of the plasmid combinations to baseline. $P>0.05$ for all comparisons, unless otherwise indicated.

4.3.3 Optimisation of the split-YFP complementation assay for localisation of TRIB3/AKT1 interactions

Four plasmids were generated as previously described (see section 2.2.3.1) to allow expression of TRIB3 and AKT1 tagged with either the V1 or V2 fragments of YFP. The two combinations tested were TRIB3-V1 with AKT1-V2 and TRIB3-V2 with AKT1-V1. The plasmids were co-transfected into HeLa cells, and following an overnight incubation, cells were incubated for ten minutes with the 1:2000 diluted Hoechst 33342 stain before proceeding to microscopy (see section 2.2.5). The YFP signal intensities of eleven cells captured from three independent transfections were quantified to determine the combination providing the brightest signal that would allow the greatest differentiation of expression pattern differences (if any) caused by TRIB3 variants. Cells were also transfected with plasmids encoding complementary fragments of the GCN4 leucine zipper tagged with YFP fragments (ZIP-V1 and ZIP-V2) as a positive control. For negative control, only ZIP-V1 was transfected into HeLa cells, and no fluorescence was detected from those cells (not shown).

The fluorescence intensities from cells expressing each of the two combinations of TRIB3 and AKT, TRIB3-V1/AKT1-V2 and TRIB3-V2/AKT1-V1, were analysed using ImageJ software. The cells expressing the TRIB3-V2/AKT1-V1 combination of plasmids showed a wider range of fluorescent intensity when compared to those expressing the TRIB3-V1/AKT1-V2 combination (unpaired t-test $P=0.0003$) (Fig. 4.5), and the next chapter will use this combination to study the effects of *TRIB3* variants on the localisation of the TRIB3/AKT1 complex.

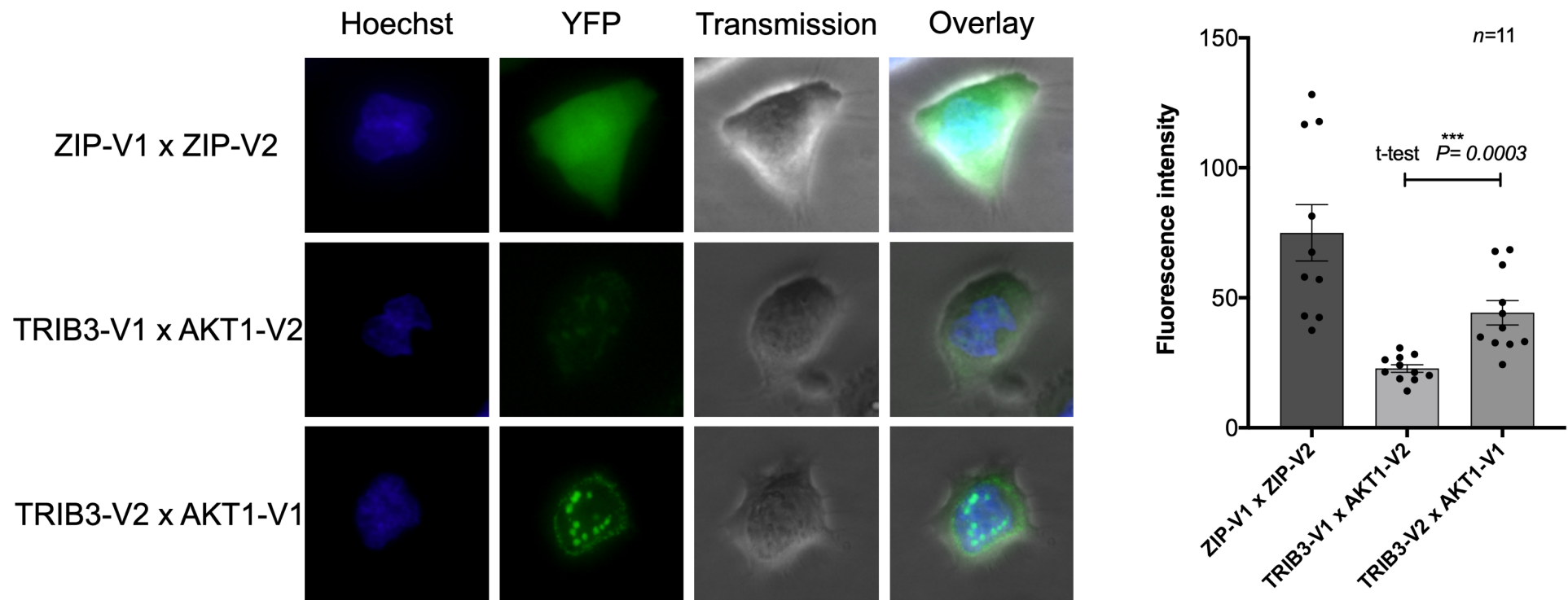


Figure 4.8 Split-YFP fluorescence in cells co-transfected with TRIB3 and AKT1 plasmids tagged with V1 or V2 YFP fragments

HeLa cells were co-transfected three times with plasmids expressing wild-type TRIB3 and AKT1 fused to either V1 or V2 to determine the combination of plasmids that allows visualisation of the complex with minimum artificial effects. Fluorescence images were captured from eleven cells using the X63 objective lens on a Leica AF6000 inverted wide-field fluorescence microscope. The ZIP-V1/ZIP-V2 combination was used as a positive control for the experiment. The Hoechst 33342 stain was used to visualise nuclei for live-cell imaging, which appear blue. Unpaired t-test was used to compare YFP fluorescence intensities from the TRIB3/AKT1 combinations (t-test $P=0.0003$), which appears green. Error bars represent +/- the SEM.

4.4 Discussion

In this chapter, the use of Gateway cloning to derive a panel of TRIB3 plasmids for use in studies described in chapter 5 was summarised. I have also described the steps taken to optimise the split-YFP and split-NanoLuc complementation assays.

Use of the Gateway cloning system facilitated the rapid generation of plasmids that were required to optimise the split-NanoLuc and split-YFP PCAs that were designed to investigate the interactions between TRIB3 and either AKT1 or AKT2. In this study, Gateway cloning was used to generate TRIB3/YFP fusion constructs encoding the V107M, S146N, R149G, R153H and R181C variants. Thus, Gateway cloning enabled the generation of a large number of plasmids with ease and high fidelity.

Optimisation of the split-NanoLuc assay required the generation of plasmids encoding fusion proteins of wild-type TRIB3, AKT1 and AKT2. More specifically, four versions of each protein were required which were; (i) tagged with LB at the C-terminal; (ii) tagged with LB at the N-terminal; (iii) tagged with SB at the C-terminal; (iv) tagged with SB at the N-terminal. Wild-type TRIB3 was used to identify the optimal combination, and once identified, the expression vector with the appropriate tag was used to produce expression plasmids encoding the five *TRIB3* variants. Similarly, Gateway cloning was also used to generate plasmids that were required to determine the optimal combination of plasmids for the split-YFP assay. Previous work in the lab which had explored the interaction between TRIB3 and AKT1 had shown that fusion of YFP fragments to the N-terminal of these two proteins would greatly restrict their interaction (unpublished). Therefore, expression plasmids encoding wild-type TRIB3 fused to either V1 or V2 at the C-terminus were generated. Again, following the identification of the optimal orientation of the split-YFP fragments, plasmids encoding the five TRIB3 variants tagged with the appropriate YFP fragment were generated.

Transfection of the eight combinations of wild-type TRIB3 and AKT1 expression plasmids designed for the split-NanoLuc PCA and measurement of luciferase activity revealed the TRIB3 LB-C and AKT1 SB-N combination to generate the highest luciferase activity when compared to other combinations. The high luminance signal observed suggests that the SB and LB tags caused the least restriction to the interaction between wild-type TRIB3 and AKT1 with this combination. Additionally, the high signal provides a broader range that is more likely to allow discrimination of any effects the *TRIB3* variants may have on the interaction of TRIB3 with AKT1. The luciferase activity levels observed after transfection of the alternative plasmid

combinations suggest that fusion of either SB or LB to the N- terminus of TRIB3 restricts interactions with AKT1. Interestingly, while the fusion of the SB to the N-terminus of AKT1 did not appear to disrupt the interaction of AKT1 with TRIB3, this was not the case when the AKT1 had an N-terminal LB tag. A possible explanation for this is the difference in the size of the LB (17.6kDa) and SB (11 amino acids) tags. Following these findings, the five *TRIB3* variants were subcloned into the vector that allowed expression of TRIB3 with a C-terminal LB tag for use in further studies to explore their effects on the interaction with AKT1. The results of these studies are described in chapter 5.

Transfection studies with the equivalent eight combinations of plasmids designed to explore the interaction between wild-type TRIB3 and AKT2 using the split-NanoLuc system suggested that the sites where TRIB3 interacts with AKT2 differ from those where it interacts with AKT1. Thus, although the combination of plasmids that was considered optimal for assessing the TRIB3/AKT1 interaction (TRIB3 LB-C x AKT2 SB-N) led to a significant increase in luciferase activity over background ($P=0.022$), the highest activity was observed using the TRIB3 SB-N x AKT2 LB-C combination ($P=0.0001$). This observation suggests that fusing the SB-N to TRIB3 and the LB-C to the AKT2 affected the least the interaction between these two proteins. Following identification of the optimal combination, the expression vector that incorporated the SB-N tag was used to subclone the *TRIB3* variants and subsequent studies assessing their effects (if any) on the interaction with AKT2. The results will be described in the next chapter.

Transfection of the different combinations of plasmids that were designed to explore the interaction of TRIB3 with AKT1 using a split-YFP PCA revealed the greatest fluorescence intensity to be generated using the TRIB3-V2 x AKT-V1 combination. The lower intensity observed in cells co-transfected with the TRIB3-V1 x AKT-V2 combination of plasmids suggests that fusing V1 to TRIB3 and/or V2 to AKT1 interferes with the interaction sites on either/or both proteins. Therefore, the five *TRIB3* variants were subcloned into expression plasmids expressing the V2 fragment fused to TRIB3 to test their effects on the localisation of the TRIB3/AKT1 complex. The results of these studies will be described in the following chapter.

Chapter 5:

TRIB3 is an intracellular signalling regulator for platelet activation and secretion

5.1 Introduction

Several compelling arguments support a role for TRIB3 in regulating platelet function, one of which is the clustering of five rare non-synonymous *TRIB3* variants among 34 patients who were recruited to the UK-GAPP study for investigation of unexplained platelet bleeding disorders. In chapter 3, I summarised the results of *in-silico* studies aimed at predicting the effects of these five variants on TRIB3 structure and function. The online Combined Annotation Dependent Depletion (CADD) tool predicted all five variants to be deleterious, each having a CADD score over 20. Structural analysis using a 3D model of TRIB3 showed that the V107M, S146N, R149G, R153H, and R181C amino acid substitutions predicted by the five *TRIB3* variants all involved residues which are located towards the surface of TRIB3. The substituted residues are also located within the pseudokinase domain, which interacts with AKT, raising the possibility that the substitutions may affect the interaction of TRIB3 with AKT and possibly other proteins. The latter possibility was supported by data gained by mass spectrometry analysis which identified several peptides that lost and gained interactions with each of the five TRIB3 variants when compared to wild-type TRIB3.

As described in chapter 1, AKT is a key signalling molecule that participates in the intracellular signalling pathways leading to platelet adhesion and activation (Chen et al, 2004; Chen et al, 2019; Du et al, 2003; Formoso et al, 2011; Prudente & Trischitta, 2015; Yin et al, 2008). Two isoforms of AKT (AKT1 and AKT2) can be detected in human and murine platelets (Kroner et al, 2000; Woulfe et al, 2004). Chapter 4 detailed the experimental work undertaken to optimise protein complementation assays (PCA) which were established to compare the cellular distribution of wild-type and variant forms of TRIB3 complexed with AKT1 and to derive a functional readout of the interaction between wild-type and variant TRIB3 molecules with both AKT1 and AKT2.

A preliminary investigation performed by Dr Jessica Johnston (University of Sheffield, UK) using whole blood from *Trib3*^{-/-} mice reported a selective reduction in the expression of a platelet activation marker (P-Selectin or CD62p) on platelets from female mice in response to thrombin receptor activating peptide (TRAP) (unpublished). This observation supported the involvement of TRIB3 in regulating platelet function.

In this chapter, we aim to (i) investigate the expression and subcellular localisation of the variant forms of TRIB3; (ii) investigate the subcellular localisation of the complex formed by the interaction between variant forms of TRIB3 and AKT1; (iii) investigate

the interaction between variant forms of TRIB3 with AKT1 and AKT2; (iv) examine platelet activation and ATP secretion in *Trib3^{-/-}* and *Trib3^{+/-}* mice.

5.2 Methods

5.2.1 Mice

The University of Sheffield and the UK Animals in Science Regulation Unit approved all murine experiments (PPL: P5395C858). Wild-type mice on a C57BL6/J background were sourced from Charles River Laboratories (Harlow, UK) and crossbred with *Trib3^{-/-}* mice, which were generated using a Gene Trapping technique that was developed by Lexicon Pharmaceuticals (Texas, USA). Details of how the *Trib3* gene was targeted were published previously (Salazar et al, 2015). The heterozygous male and female *Trib3^{+/-}* littermates were used as breeders to derive wild-type, *Trib3^{+/-}* and *Trib3^{-/-}* mice in which platelet activation and secretion were subsequently investigated.

5.2.2 Localisation of TRIB3 variants using TRIB3/YFP fusion proteins and TRIB3/AKT1 complexes using the split-YFP PCA system

Expression plasmids encoding wild-type and variant forms of TRIB3 fused with YFP and with the Venus 2 YFP fragment (V2) were generated using the Gateway[®] system following the identification of the optimal orientation of the plasmids as described earlier (see section 4.3.3). An expression plasmid encoding AKT1 fused with the Venus 1 YFP fragment (V1) was previously generated in-house by Professor Endre Kiss-Toth and made available for use in this study. Transfection mixtures, which included the TRIB3/YFP expression plasmids, were incubated overnight with confluent HeLa cells as described in section 2.2.5. To obtain higher resolution images, co-transfection of expression plasmids encoding TRIB3 and AKT1 on the split-YFP PCA system was carried out on cells growing in 8-well glass chambers. Transfection in 8-well chambers was carried out with 70-90% confluent cells, which were incubated overnight with 500 μ l of serum-free medium containing a total of 250ng of both plasmids and 0.75 μ l of Lipofectamine[™] 3000m. Live HeLa cells were imaged using a Leica AF6000 Time Lapse inverted wide field fluorescence microscope using the acquisition parameters detailed in section 2.2.5.2. Localisation of TRIB3 variants was evaluated using the YFP signal from TRIB3/YFP fusion proteins, and the nuclear territories that were marked using the Hoechst 33342 stain as described in section 2.2.5.1. Similarly, the

expression patterns of the TRIB3/AKT1 complex were assessed using the YFP signal emitted through the interaction of V1 and V2 from both fusion proteins, and the Hoechst 33342 nuclear stain. ImageJ software (Wayne Rasband, National Institutes of Health, USA) was used to quantify fluorescence intensity in cells expressing TRIB3/YFP fusion proteins, and Dunnett's multiple comparisons test was performed using GraphPad Prism version 7.02 (GraphPad Software, La Jolla California USA). The expression patterns of TRIB3/AKT1 complexes were compared using the Chi-square test available in GraphPad Prism.

5.2.3 Assessment of the interaction between TRIB3 variants and either AKT1 or AKT2 using the Nano-Luc PCA system

Expression plasmids encoding AKT1, AKT2, and wild-type and variant forms of TRIB3 fused with complementary fragments of the NanoLuc protein (LB and SB) were generated following the identification of the optimal orientation of the plasmids as described earlier (see section 4.3.2). Transfection mixtures were incubated overnight with confluent HEK293T cells as described in section 2.2.6, and luciferase activity was measured using a VIRIOSKAN FLASH plate reader (see section 2.2.6). A one-way ANOVA and Dunnett's multiple comparisons test were used to assess the effects of TRIB3 variants on the interaction with either AKT1 or AKT2.

5.2.4 Assessment of murine platelet function

Platelets were collected from wild-type and *Trib3*^{+/-} mice and P-selectin expression in response to TRAP quantified using flow cytometry as described in section 2.2.8.1. The used TRAP agonist would initiate the activation signal through the PAR4 receptor as murine platelets lack the expression of the PAR1 receptor. The quantification of CD62p median fluorescence was performed using the Floreada.io tool (<https://floreada.io/>), and power calculations were performed using the G*power software v3.1 (<https://gpower.hhu.ed>). A two-way ANOVA and Sidak's multiple comparisons test were used to confirm observed differences in membrane P-selectin expression in platelets in response to different concentrations of TRAP. In parallel, platelet-rich plasma was collected for measurement of thrombin-induced ATP secretion as described in section 2.2.8.2., and an unpaired t-test was used to statistically confirm the observed defect in ATP secretion.

5.3 Results

5.3.1 Variants of TRIB3 show altered expression patterns

We confirmed the previously reported nuclear localisation and dot-like (or punctate) expression pattern of wild-type TRIB3 in HeLa cells (Xu et al, 2007). Expression of all five TRIB3 variants was also confined to the nucleus, indicating no effect of the *TRIB3* variants on the nuclear localisation of TRIB3 (Figure 5.1A). However, there were some differences in the expression patterns of three of the variants when compared with the cells expressing wild-type TRIB3. Thus, more than half of the cells expressing the V107M and R181C variants displayed a diffuse pattern of nuclear expression, while the majority of cells expressing the R149G variant showed a diffuse pattern of nuclear expression (89%). The S146N and R153H variants both showed similar patterns of expression to that of wild-type TRIB3 with 100% of the cells showing a punctate pattern (Figure 5.1B). The possibility that the differences in expression pattern could be due to differences in the efficiency of transfection was explored by quantifying the fluorescence intensity from 30 cells (10 cells from each independent transfection), which showed that there was no difference in the transfection efficiency of the wild-type or variant TRIB3 expression plasmids (Figure 5.1C). This data also confirms the reproducibility of the expression patterns.

5.3.2 The TRIB3/AKT1 complex shows four different patterns of expression

We used a split-YFP complementation assay to investigate the effect of *TRIB3* variants on the localisation of the interaction between TRIB3 and AKT1. Fluorescence microscopy of the transfected cells revealed the two proteins to interact physically and showed four different distribution patterns of the complex (Figure 5.2A). The wild-type TRIB3/AKT1 complex showed a punctate pattern of expression which was localised to the perinuclear region in the majority (45.4%) of cells. However, cells showing a more diffuse distribution of the complex in either the nucleus (27.3%) or the cytoplasm (1.3%) were also observed. In the remainder of cells, the complex showed a punctate distribution pattern in the cytoplasm (26%) (Figure 5.2C). The variant TRIB3/AKT1 complexes showed similar distribution patterns to that of the wild-type TRIB3/AKT1 complex (Chi-square test $P > 0.05$ for each TRIB3 variant vs wild-type TRIB3) (Figure 5.2B).

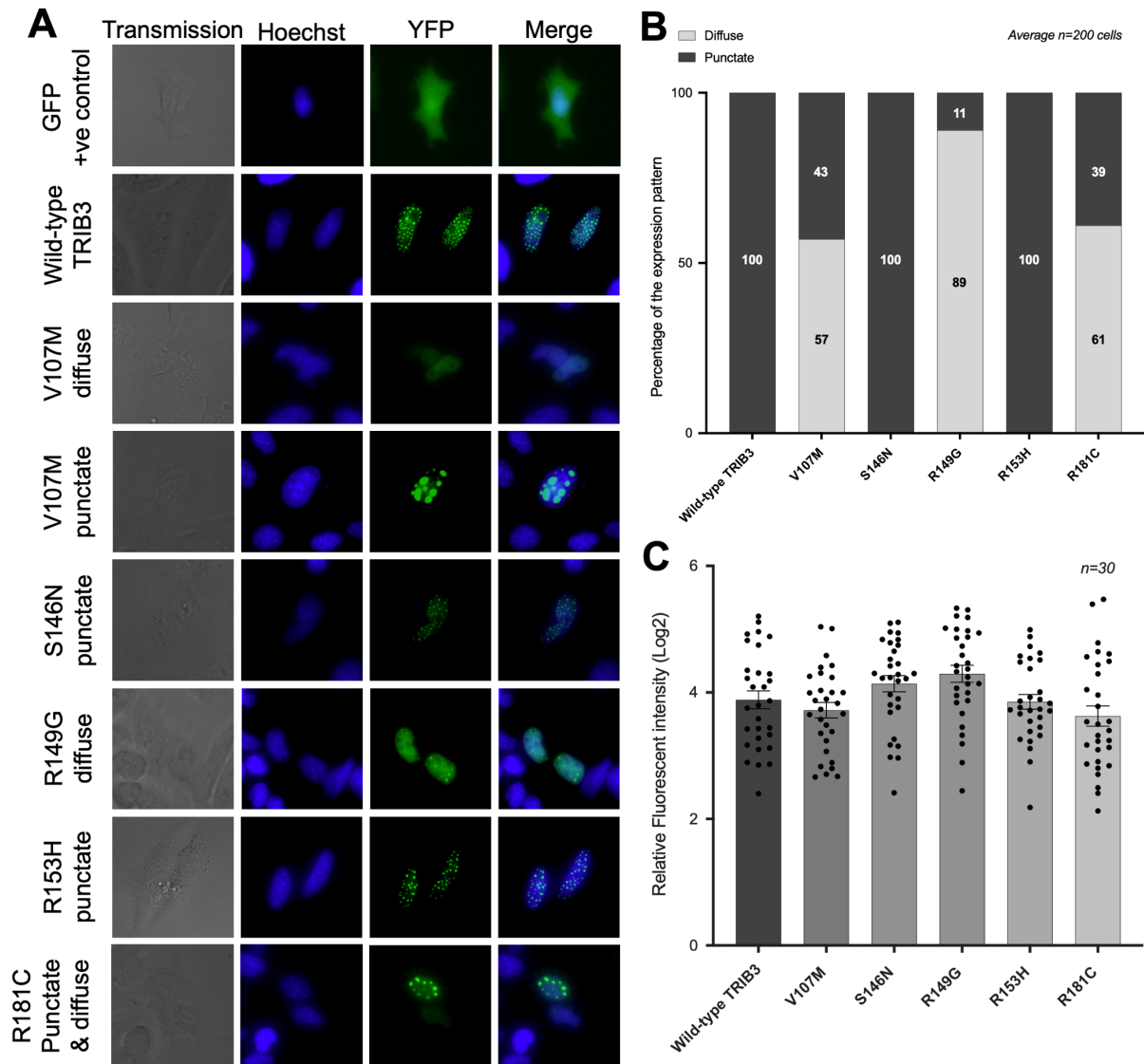


Figure 5.1: Expression patterns of wild-type and variant forms of TRIB3 fused to YFP in HeLa cells

HeLa cells were transfected with plasmids expressing wild-type and variant forms of TRIB3 fused with YFP. **(A)** Fluorescence images were captured using the X63 objective lens on the Leica AF6000 inverted wide-field fluorescence microscope. The transmission images show the cell shape using light transmission and appear grey. Hoechst 33342 stain was used to visualise nuclei, which appear blue. YFP fluorescence appears green. The merged images combine the Hoechst 33342 and YFP images to confirm nuclear localisation. **(B)** The percentage of cells displaying the indicated expression patterns was calculated from an average of 200 cells for three repeats of the transfection. Wild-type TRIB3, and the S146N and R181C variants show a punctate pattern of expression in all cells. The V107M and R181C variants display a diffuse expression pattern in more than 50% of the cells enumerated (57 and 61%, respectively). The R149G variant displays a diffuse expression pattern in the majority of the cells analysed (89%). **(C)** Quantification of fluorescence intensity in 30 cells from three transfections shows no statistical difference in overall expression between the wild-type TRIB3 and the variant forms of TRIB3. Error bars represent the mean and SEM. Dunnett's multiple comparisons test was used to compare signals for each of the TRIB3 variants with the wild-type, and all multiple comparisons resulted in $P > 0.05$.

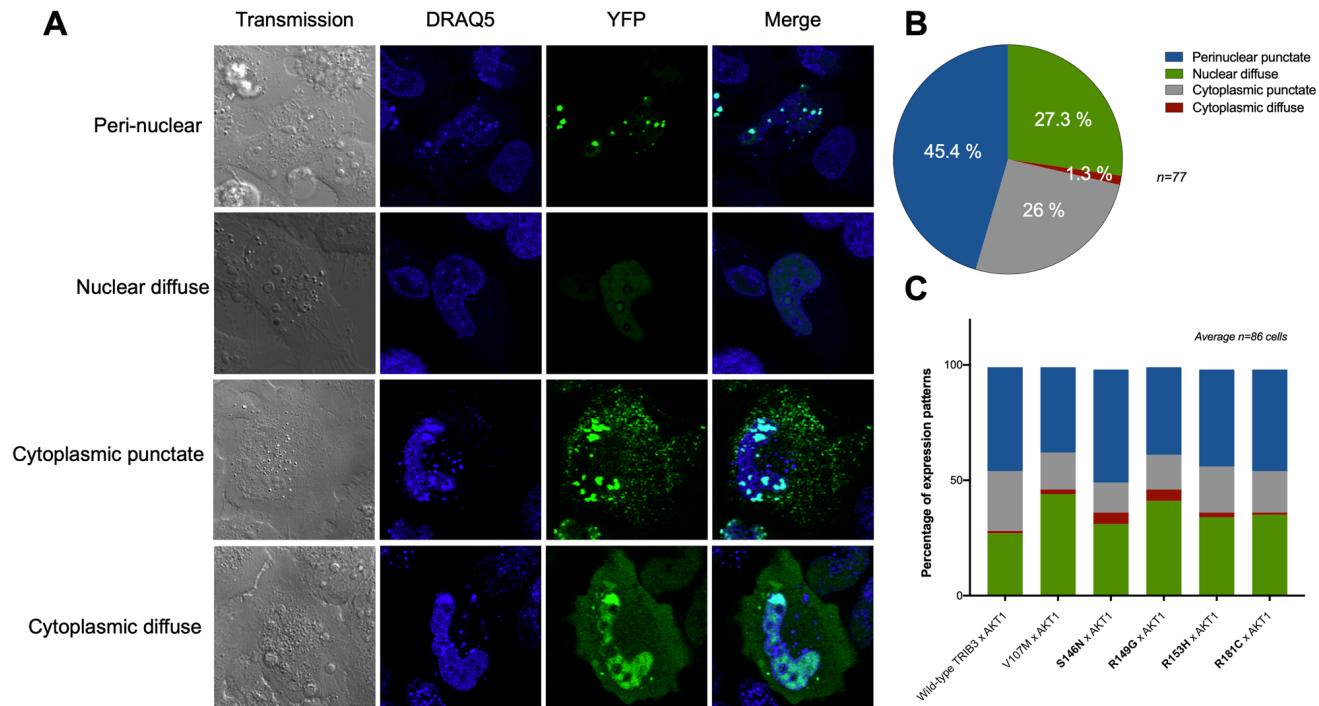


Figure 5.2: Distribution of the TRIB3/AKT1 complex

HeLa cells were co-transfected with plasmids encoding TRIB3 (wild-type and variant) and AKT1 fused to fragments of YFP (V2 and V1, respectively) to investigate the effect of TRIB3 variants on localisation of the TRIB3/AKT1 complex. **(A)** Fluorescence images were captured using the X63 objective lens on a Leica AF6000 inverted wide-field fluorescence microscope. The transmission images outline the cells, which appear grey by light transmission. Hoechst 33342 stain was used to visualise the nuclei, which appear blue. YFP generated from the interaction between TRIB3 and AKT1, through complementation of the two YFP fragments, appears green. The Hoechst 33342 and YFP images are merged in the 'merge' images. **(B)** Distribution of the wild-type TRIB3/AKT1 complex in HeLa cells. The majority (45.4%) is localised to the perinuclear region and expressed in a punctate pattern. The remainder is distributed between the nucleus where it displays a diffuse pattern of expression (27.3%), and the cytoplasm where it displays either punctate (26%) or diffuse (1.3%) expression patterns. **(C)** The wild-type and variant TRIB3/AKT1 complex expression patterns were assessed in an average of 86 cells. Chi-square testing showed that the TRIB3 variants did not affect the distribution of the TRIB3/AKT1 complex ($P>0.05$).

5.3.3 Interaction of TRIB3 variants with AKT1 and AKT2

The interactions between wild-type and variant forms of TRIB3 with AKT1 and AKT2 were investigated using a split-NanoLuc complementation assay. The transfections were repeated five times to examine the interaction with AKT1 and six times to examine the interaction with AKT2, with each repeat performed in triplicate.

Comparison of luciferase levels in samples from cells expressing AKT1 along with either wild-type TRIB3 or a TRIB3 variant showed increased luciferase activity in samples expressing all of the TRIB3 variants, suggesting a gain of interaction with AKT1, which was significant in the case of the R149G, R153H, and R181C variants ($P=0.0485$, 0.0001 , 0.0029 , respectively). The V107M and S146N variants also showed an increase in the average signal compared with wild-type TRIB3 though this did not achieve statistical significance ($P=0.9267$, 0.6997 , respectively) (Figure 5.3A).

In contrast, comparison of luciferase activity in cells co-expressing AKT2 with either wild-type TRIB3 or a TRIB3 variant showed similar luciferase activity levels in all samples, suggesting that the amino acid substitutions in the variants do not affect the interaction of TRIB3 with AKT2 ($P>0.05$) (Figure 5.3B).

Since the R149G, R153H and R181C TRIB3 variants showed a gain-of-function in their interaction with AKT1, further work was carried out to examine whether this was associated with a difference in AKT phosphorylation. Cells were co-transfected and cell lysates were subjected to electrophoresis and western blotting as described in section 2.2.7. Western blotting for pAKT detected a single protein of the expected size of 70 kDa in all samples (Figure 5.4A). Densitometric analysis was used to quantify the pAKT, which was then normalised to the signal obtained for the housekeeping protein, α -Tubulin. The quantification showed no statistical difference in total AKT phosphorylation between cells expressing wild-type TRIB3 and any of the variant forms of TRIB3 ($P>0.05$) (Figure 5.4B).

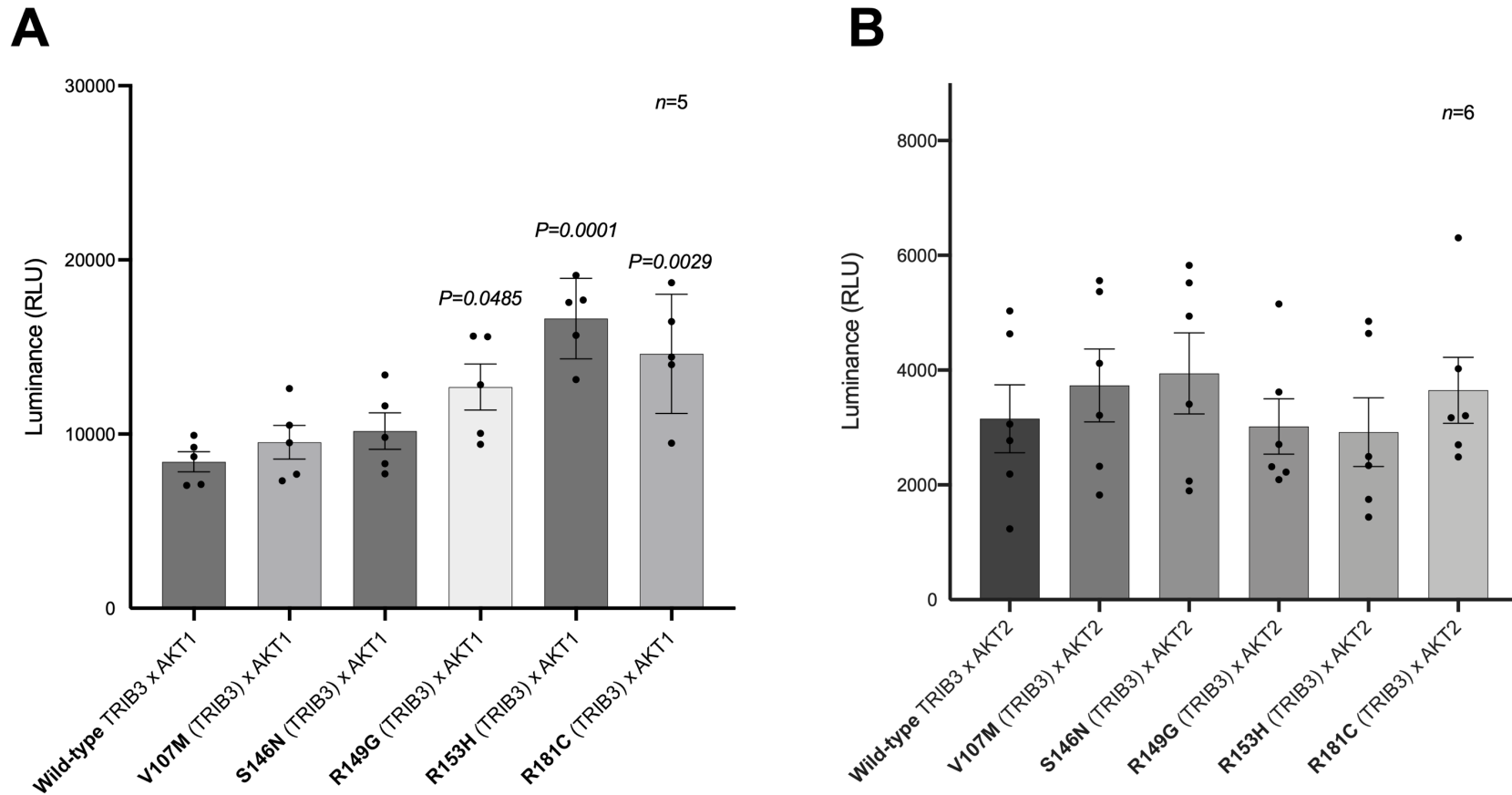


Figure 5.3: Luciferase activity in cells co-expressing wild-type or variant forms of TRIB3 and AKT1 (A) or AKT2 (B)

HEK293T cells were co-transfected with plasmids expressing wild-type or variant forms of TRIB3 and either AKT1 (A) or AKT2 (B) on the Split-NanoLuc complementation system, and luciferase activity was measured after overnight incubation. The luciferase activity was proportional to the detected luminance signal. **(A)** Luciferase activity in cells co-expressing wild-type or variant TRIB3 with AKT1 show the R149G, R153H, and R181C have a gain-of-function with AKT1 [One-way ANOVA with Dunnett's multiple comparisons test ($P=0.0485$, $P=0.0001$, $P=0.0029$, respectively)]. The interaction of the V107M and S146N variants with AKT1 is similar to that of wild-type TRIB3 ($P>0.05$). **(B)** Luciferase activity from cells co-expressing wild-type or variant forms of TRIB3 with AKT2 show no effect of the TRIB3 variants on this interaction (One-way ANOVA with Dunnett's multiple comparisons test $P>0.05$).

The error bars represent the mean and SEM, and each point represents a transfection, which was performed in triplicate.

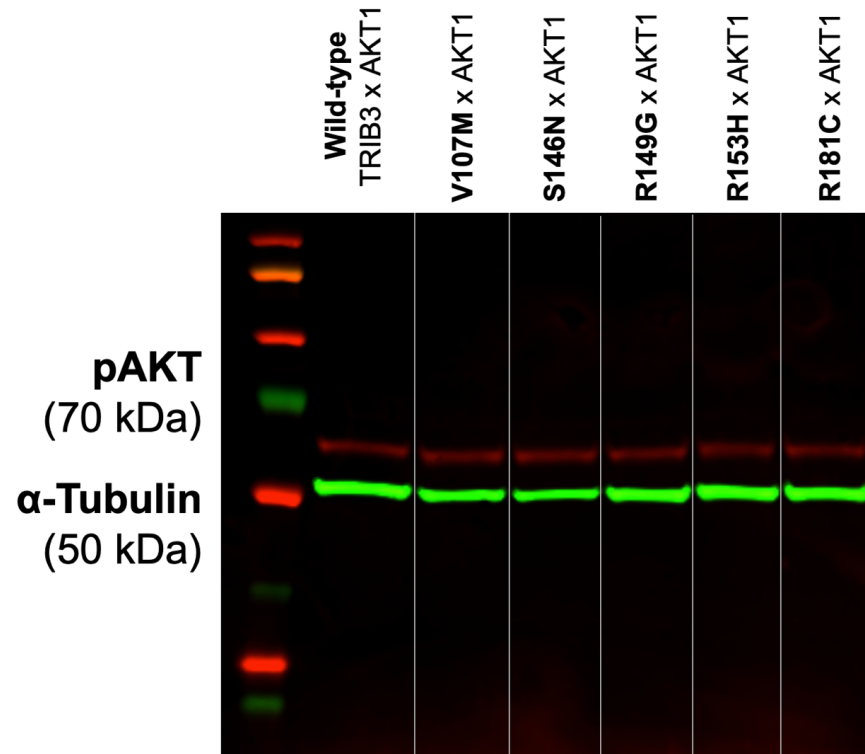
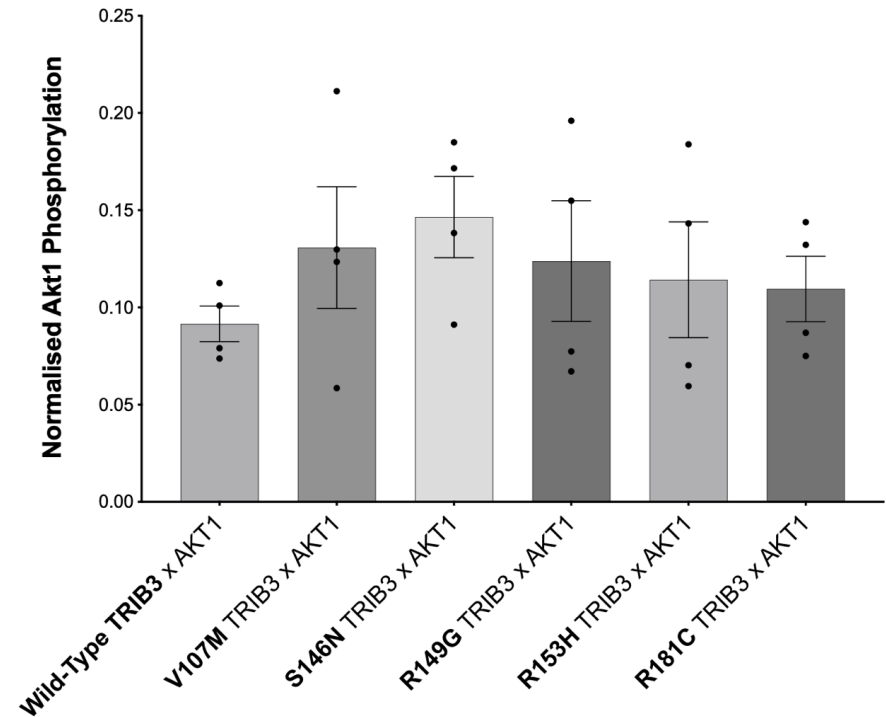
A**B**

Figure 5.4: Detection and quantification of phosphorylated AKT in cells co-expressing AKT1 and wild-type or variant forms of TRIB3

HEK293T cells were co-transfected with plasmids expressing wild-type or variant forms of TRIB3 and AKT1. **(A)** Detection of pAKT by western blotting following electrophoresis of cell lysates. α -Tubulin was detected as a control housekeeping protein. **(B)** pAKT was quantified using densitometric analysis and the values were normalised using the values determined for α -Tubulin. A one-way ANOVA and Dunnett's multiple comparisons test showed no statistical difference in pAKT levels between cells expressing the wild-type and variant forms of TRIB3 ($P > 0.05$).

5.3.4 Altered platelet activation in female *Trib3* knockout mice

We assessed platelet activation *ex-vivo* in whole blood samples from homozygous (*Trib3*^{-/-}) and heterozygous (*Trib3*^{+/-}) *Trib3* knockout mice by quantifying the expression of the platelet activation marker, CD62p (P-selectin), in response to varying concentrations of thrombin receptor activating peptide (TRAP). The work performed by Dr Jessica Johnston (University of Sheffield, UK) showed that CD62p expression on platelets from male *Trib3*^{-/-} (*n*=6) mice was similar to that on platelets from wild-type male mice (*n*=4) at concentrations of TRAP used (Figure 5.5A). Interestingly, the results for P-selectin expression in blood from female *Trib3*^{-/-} mice (*n*=6) showed ~ 52% (*P*<0.0001) reduction with 3 mmol/L TRAP and ~ 45% (*P*=0.0029) reduction with 10 mmol/L TRAP when compared to the expression in blood from wild-type female mice (*n*=3) (Figure 5.5B). Our preliminary data on P-selectin expression in a blood sample from female *Trib3*^{+/-} mice (*n*=6) indicated that there is ~ 84% reduction with 3 mmol/L TRAP and ~ 80% reduction with 10 mmol/L TRAP when compared to the expression in samples from wild-type female mice (*n*=1) (Figure 5.5C). However, the small numbers of the wild-type female mice refrained us from drawing conclusions or perform statistical analysis within the timeframe of my project.

We also investigated platelet dense granule secretion by measuring the release of ATP from platelets activated with 1 unit (50 µl) of thrombin. The platelet-rich plasma from female *Trib3*^{-/-} (*n*=3) showed ~20% reduction in ATP secretion (unpaired t test *P*=0.0362), while male platelets showed similar ATP secretion when compared to the secretion levels from wild-type platelets (*n*=3) (unpaired t test *P*>0.05) (Figure 5.5D).

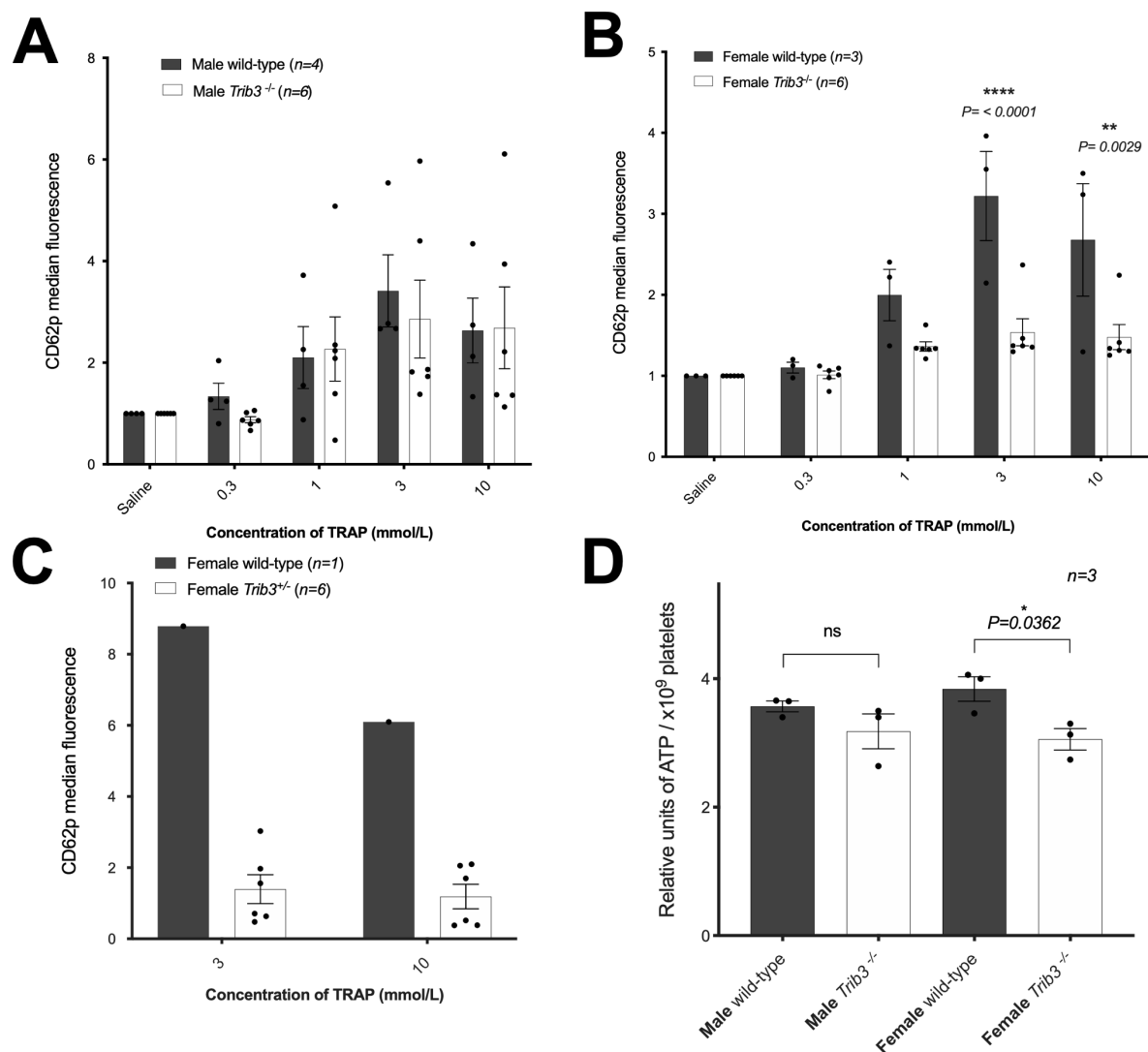


Figure 5.5: Gender-specific activation defect in platelets from *Trib3*^{-/-} and *Trib3*^{+/-} mice

(A) CD62p expression on platelets in whole blood in response to TRAP, which was collected from male *Trib3*^{-/-} ($n=6$) and wild-type ($n=4$) mice. Two-way ANOVA with Sidak's multiple comparisons test shows $P>0.05$ for comparisons between wild-type and *Trib3*^{-/-} platelets at all TRAP concentrations tested. (B) CD62p expression in response to TRAP on platelets from female *Trib3*^{-/-} ($n=6$) and wild-type ($n=3$) mice. Two-way ANOVA with Sidak's multiple comparisons test shows $P<0.0001$ with 3 mM TRAP and $P=0.0029$ with 10mM TRAP for comparisons between wild-type and *Trib3*^{-/-} platelets and $P>0.05$ at other concentrations tested. (C) CD62p expression in response to TRAP on platelets from female *Trib3*^{-/-} ($n=6$) and wild-type mice. Only one wild-type mouse was studied, precluding statistical analysis. (D) ATP secretion measurement from platelet-rich plasma collected from male and female wild-type and *Trib3*^{-/-} mice in response to 1 unit of thrombin (50 μ l). Error bars represent the mean \pm SEM. An unpaired t-test was used to compare data obtained for the male ($P=0.2424$) and female ($P=0.0362$) wild-type and *Trib3*^{-/-} mice.

5.4 Discussion

The exploration and discovery of novel molecules that regulate platelet signalling could potentially lead to the identification of therapeutic targets for platelet signalling defects. Prior to this study, the potential role of TRIB3 in platelet function has not been studied, but several studies had reported an association between TRIB3 and megakaryopoiesis which was evidenced by the increased expression of *TRIB3* in cultured megakaryocytic cells that were treated with an inhibitor of megakaryopoiesis, and by the increased megakaryocyte differentiation following the knock-down of *TRIB3* (Butcher et al, 2017; Takaishi et al, 2020). The findings described here provide preliminary evidence for the involvement of TRIB3 in platelet activation and dense granule secretion, and we anticipate that this is happening through the regulation of AKT phosphorylation.

The observed altered expression (diffuse expression pattern) of the V107M, R149G, and R181C variants using TRIB3/YFP fusion constructs could be because the amino acid substitutions affect the capability of the protein to interact with other proteins. Moreover, the majority of the cells expressing the R149G TRIB3/YFP fusion construct showed diffuse expression (89%), and the mass spectrometric analysis showed that the variant affected protein dimerisation. There are no published studies reporting TRIB3 dimerisation, but mass spectrometric analysis showed that the wild-type and the remaining four variants (V107M, S146N, R153H, and R181C) interacted with peptides of TRIB3. Moreover, a preliminary investigation in our group identified a TRIB3/TRIB3 interaction using the split-NanoLuc assay (unpublished). If the loss of interaction with other TRIB3 molecules is the sole reason for the observed diffuse pattern, the loss of interaction with other proteins could also be the reason for the diffuse patterns observed with the other two variants (V107M and R181C).

The observed diffuse expression pattern was reported to occur within the nucleus of HeLa cells, and platelets are known for lacking the nucleus. However, our data shows that the variants affected the protein interaction and the protein expression, which would lead us to speculate that they could, in theory, affect TRIB3 functions in different cells including platelets.

The altered expression pattern (diffuse pattern) was observed only when TRIB3 was expressed as a fusion protein with YFP, while when the TRIB3 was co-expressed with AKT1, the expression patterns observed for the complex were not affected by the amino acid substitutions predicted by the five *TRIB3* variants. Indeed, our data showed four distinct patterns of expression for the complex (cytoplasmic punctate, cytoplasmic

diffuse, nuclear diffuse, and perinuclear punctate), which could represent the different stages of AKT translocation during phosphorylation. It is well established that AKT is synthesised in the endoplasmic reticulum (ER) and translocates to the plasma membrane where it is phosphorylated before it translocates to different subcellular compartments including the nucleus, the mitochondrial membrane and the cytosol (Calleja et al, 2007; Sugiyama et al, 2019). The work in chapter 6 examines the association which may occur between the pattern of expression of the TRIB3/AKT1 complex and its localisation to the mitochondria.

The split-Nanoluc complementation assay showed a gain-of-function effect for three of the TRIB3 variants (R149G, R153H, and R181C) on the interaction with AKT1, but not AKT2. Inversely, western blotting to quantify pAKT in cells overexpressing the TRIB3/AKT1 complex showed similar phosphorylation levels for all of the variant forms of TRIB3. AKT was expected to show reduced phosphorylation with the TRIB3 variants as TRIB3 was previously shown to reduce AKT phosphorylation when expressing a gain-of-function in the case of the Q84R variant (Andreozzi et al, 2008). However, the typical way of assessing AKT phosphorylation involves stimulation of the cells before collecting the lysates. To illustrate, Andreozzi et al. (2008) stimulated endothelial cells using insulin to quantitate pAKT in cells overexpressing Q84R TRIB3, and Butcher et al. (2017) used TPO to stimulate a megakaryocytic progenitor cell line to investigate the effect of silencing *TRIB3* on pAKT levels (Andreozzi et al, 2008; Butcher et al, 2017). Therefore, to perform a reliable pAKT quantification, the HEK293 cells should have been stimulated before lysis, and this could explain the contradicting results obtained from the PCA studies and the pAKT quantification.

We also noted from the split-NanoLuc data that replacing any one of three arginine (R) residues (R149G, R153H, and R181C) in the pseudokinase domain (where the interaction with AKT happens) resulted in a gain-of-function effect on the interaction with AKT1 but not AKT2. A gain-of-function effect on the interaction with AKT was previously reported with a common TRIB3 variant (Q84R), where the substitution of glutamine by arginine enhanced the interaction with AKT and disrupted the insulin signalling pathway (Andreozzi et al, 2008). Moreover, the arginine residue at amino acid position 149 was predicted to be a hotspot for the interaction with AKT [unpublished data performed by Juan Salamanca Vilorio (Barcelona, Spain)]. The diffuse expression pattern of R149G TRIB3 when expressed as a YFP fusion protein, along with the gain-of-function when interacting with AKT1, make it an interesting

variant for further studies. The work in chapter 6 examines the difference in mitochondrial localisation of the TRIB3/AKT1 complex when using wild-type and R149G TRIB3.

The selective reduction in P-selectin expression observed in platelets from female *Trib3*^{-/-} mice in response to 3mM and 10 mM TRAP suggests that TRIB3 has a gender-specific effect on platelet function. This observation could be explained by the published correlation between *TRIB3* expression and the female hormone, estrogen. This correlation was established following the identification of *TRIB3* as one of the genes that showed an elevated expression in microarray analysis of cells treated with estrogen-like compounds (Ise et al, 2005). Additionally, an unpublished analysis performed by Miguel Hernández-Quiles (Centre for Molecular Medicine, UMC Utrecht, Utrecht, Netherlands) discovered that the *TRIB3* promoter encompasses a binding site for estrogen receptor. Moreover, a recent study reported that platelet activation signalling through PAR1, a thrombin receptor, is increased in healthy women and female mice, when compared with signalling through PAR1 in healthy men and male mice (Soo Kim et al, 2020).

To determine whether the selective effects of *Trib3* knockout on female murine platelets is a dominant trait, we examined expression of CD62p in response to TRAP on platelets from female *Trib3*^{+/-} mice. The preliminary data suggest a dominant effect of *Trib3* knockout on platelet activation in the female mice, but these experiments were not sufficiently powered to be conclusive. The sample size calculations to detect a 20% difference in the expression of CD62p and to have 80% power concluded the need for 26 animals in each group, while the current number of tested animal (wild-type $n=1$, *Trib3*^{+/-} $n=6$) achieves only 9.3% power.

The reduced ATP secretion from platelets in female *Trib3*^{-/-} mice again highlights the possible role of TRIB3 in the regulation of platelet intracellular signalling in response to thrombin. The exact effector of TRIB3 in platelet signalling remains to be identified, but TRIB3 is known to regulate two key signalling molecules, AKT and extracellular-signal-regulated kinase (ERK), in platelet activation (Li et al, 2010). When Butcher et al. silenced *TRIB3* in a megakaryocytic cell line (UT7/mpl cells), they observed increased phosphorylation of ERK, while phosphorylation of AKT was unaffected (Butcher et al, 2017). Therefore, in a cellular environment that is closer to platelets, TRIB3 was shown to regulate the phosphorylation of ERK, and the observed defect in platelet activation could be a result of disrupted ERK signalling.

Further investigations to increase the power of the study assessing CD62p expression in platelets from female Trib3^{+/-} mice, and to examine AKT phosphorylation post-stimulation in cells expressing variant forms of TRIB3 and AKT1 would aid in explaining the role of TRIB3 in platelet function. Additionally, further studies investigating the effect of TRIB3 variants on the interaction with ERK may form a basis for further characterisation of the role of TRIB3 in platelet function and could lead to a better understanding of the platelet signalling pathways.

Chapter 6:

Mitochondrial localisation of the TRIB3/AKT1 complex

6.1 Introduction

Examination of platelet ultrastructure (see chapter 1, Figure 1.1) reveals the presence of mitochondria and lysosomes in the organelle zone, and the dense tubular system, which is the platelet equivalent of the endoplasmic reticulum (ER) present in nucleated cells (Gerrard et al, 1978). The studies to investigate localisation of the TRIB3/AKT1 complex in HeLa cells which were described in chapter 5, which showed that the complex was formed at different subcellular locations including the nucleus, the perinucleus, and the cytoplasm (see figure 5.2). The presence of the complex in the cytoplasm suggests that it might be recruited to subcellular organelles. Our data and previous reports showed that TRIB3 is localised to the nuclei (Xu et al, 2007), but when interacting with AKT1, it shows four different localisation patterns (see figure 5.1). In nucleated cells, the majority of AKT occurs in the cytoplasm, but when cells are treated with platelet-derived growth factor- (PDGF), there is a marked increase in AKT translocation to the nucleus (Borgatti et al, 2000). Moreover, AKT showed a five-fold increase in translocation to mitochondria in HEK293 cells when treated with Insulin-like growth factor-1 (IGF-1) (Bijur & Jope, 2003). Additionally, mammalian target of rapamycin (mTOR), which is a kinase that facilitates AKT phosphorylation, was shown to reside at the surface of the endoplasmic reticulum and it could become activated through interaction with lysosomes (Boulbes et al, 2011; Korolchuk et al, 2011). Those studies derived the suggestion of the observed cytoplasmic punctate expression pattern of the TRIB3/AKT1 complex being a representation of the complex translocation to subcellular organelles such as mitochondria, ER, and lysosomes.

Chapter 3 described the mass spectrometric analysis of peptides which interacted with wild-type and variant forms of TRIB3. The results revealed a gain-of-interaction with several mitochondrial peptides including the translocase of the inner mitochondrial membrane 17-B subunit (TIMM17B) for the V107M, S146N, R149G, and R181C variants, and with the mitochondrial malonyl CoA-acyl carrier protein transacylase (MCAT) for the R153H and R181C variants (see 3.3.3). Moreover, *in-silico* studies performed by Miguel Hernández-Quiles (Centre for Molecular Medicine, UMC Utrecht, Utrecht, Netherlands) predicted that TRIB3 encompasses mitochondrial import sequences that bind the TIM/TOM complex (unpublished data), which function to facilitate protein translocation from the cytosol into the mitochondria (Rehling et al, 2001). The mitochondrial ultra-structure consists of four compartments that are the outer membrane, the intermembrane space, the inner membrane, and the matrix (Frey

& Mannella, 2000). The process of importing a protein commences with the binding of the mitochondrial import sequence of the protein to the translocase of the outer mitochondrial membrane (TOM) channel, before the remainder of the protein is pulled into the mitochondrial matrix through the intermembrane space to the translocase of inner mitochondrial membrane (TIM) channel (Wiedemann & Pfanner, 2017) (Fig. 6.1). Platelets are anucleate cells that use the mitochondria to provide the energy required to function (Fuentes et al, 2019), and disrupted mitochondrial activity has been shown affected platelet activity and was linked to the development of cardiovascular disease (Fuentes et al, 2019; Wang et al, 2017). A study reported an association between platelet hyperactivation in patients with type-2 diabetes mellitus (T2DM) and an increase in glucose trafficking into mitochondria, which would accelerate platelet activation events (Guo et al, 2010).

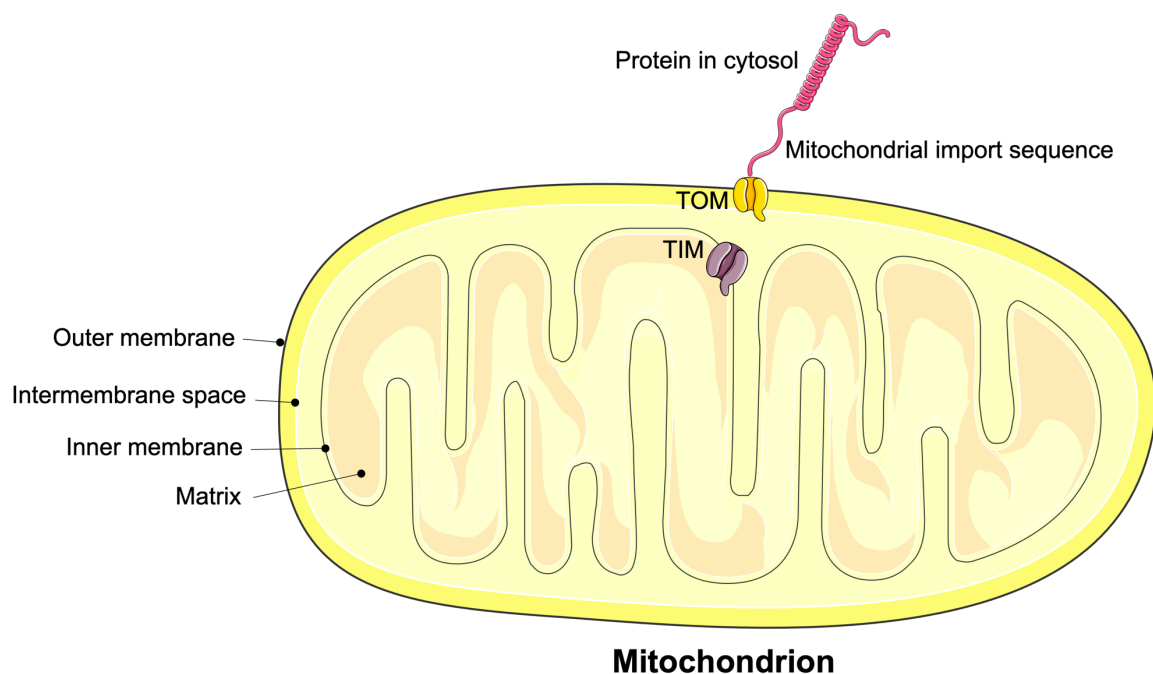


Figure 6.1: Protein import into mitochondria

An illustration of the four compartments of mitochondria that are involved in the protein import process. (i) the outer membrane contains the translocase of the outer mitochondrial membrane (TOM) that acts as a receptor for the mitochondrial import sequences on proteins in the cytosol; (ii) the intermembrane space functions to direct imported proteins to the inner membrane; (iii) the inner membrane encompasses the translocase of the inner mitochondrial membrane (TIM) that pulls the protein from the TOM into the mitochondrial matrix and (iv) the matrix contains mitochondrial DNA and machinery used for protein synthesis (Frey & Mannella, 2000).

The contents used to construct the figure were adapted and modified from the publicly available Servier Medical Art, which is licensed under a Creative Commons Attribution 3.0 License. <https://smart.servier.com>.

6.1.1 Hypothesis and Aims

The translocation of activated AKT to multiple subcellular compartments including mitochondria, ER, and lysosomes, to reach the optimal phosphorylation level derived us to consider investigating the co-localisation of the TRIB3/AKT1 complex to those compartments. However, the combined evidence from the mass spectrometric analysis that showed a gain-of-interaction with mitochondrial proteins, and the *in-silico* identification of binding motifs on TRIB3 for the mitochondrial TIM/TOM complex, guided us to prioritise the testing of the localisation of the TRIB3/AKT1 complex to mitochondria rather than ER or lysosomes. We hypothesise that the TRIB3/AKT1 complex might translocate to mitochondria in order to process the AKT1 phosphorylation and to explore this hypothesis we quantified the percentage of the TRIB3/AKT1 complex that was co-localised to the stained mitochondria using confocal microscopy. The aims of the work of this chapter are to:

- i. Examine localisation of the TRIB3/AKT1 complex with the mitochondria.
- ii. Examine the effect of R149G TRIB3 on the translocation of the TRIB3/AKT1 complex into the mitochondria (if the complex showed mitochondrial localisation) as the R149G variant was shown to lose interaction with a peptide of TRIB3 (see section 3.3.3), and shown to impose a gain-of-function effect on the interaction with AKT1 (see section 5.3.3).

6.2 Methods

6.2.1 Staining subcellular compartments

HeLa cells were seeded in 6-well plates and incubated at 37° C in the presence of 5% CO₂ until they had reached 70-90% confluency. For mitochondrial staining, cells were washed and incubated at 37° C in the presence of 5% CO₂ for ten minutes with warm PBS containing mitochondrial stain (Mitochondrial Staining Reagent, #ab176833, Abcam, Cambridge, UK) diluted 1:500 and nuclear stain (Hoechst 33342) diluted 1:2000. The manufacturers' protocol suggests incubating cells with stains for 30 minutes to 2 hours. However, even the 30 minutes incubation was toxic to the cells. Reducing the incubation to ten minutes showed minimum toxicity and imaging showed a sufficient signal for both stains.

For lysosomal staining, cells were washed and incubated at 37° C in the presence of 5% CO₂ for 30 minutes with Lysosomal stain (Lysosomal Staining Kit, #ab112137, Abcam, Cambridge, UK) diluted 1:500 in live cell staining buffer (supplied with the kit) and a 1:2000 dilution of Hoechst stain. Further dilutions of the stain (1:2, 1:4, 1:8, 1:16, 1:32) in live cell staining buffer were performed to reduce the cell death rate, but images showed a faint signal and uneven distribution of the stain in cells. However, the step that showed the finest images was restricting the incubation period to 30 minutes (the manufacturer suggested 30 minutes – 2 hours incubation).

To stain the endoplasmic reticulum, cells were washed and incubated at 37° C in the presence of 5% CO₂ for 15 minutes with ER stain (ER Staining Kit, #ab139482, Abcam, Cambridge, UK) diluted 1:1000 in 1x assay buffer (supplied with the kit) and Hoechst stain diluted 1:1000. This protocol showed a high cell death rate, and further dilutions were performed to reach the non-toxic concentration. We found that 1:5 dilution in warm PBS (from the dye working solution), and maintaining the incubation period to 15 minutes (the manufacturer suggested 15 – 30 minutes) would reduce the cell death rate to the minimum.

Before imaging using all cytopainters, cells were washed with warm PBS and wells were replenished with a warm phenol-red free medium.

6.2.2 Staining of Mitochondria in transfected HeLa cells

HeLa cells were seeded on a glass-bottom culture plate and incubated at 37° C in the presence of 5% CO₂. Plasmids encoding TRIB3 and AKT1 tagged with the two fragments of the split-YFP system were transfected into cells. The Leucine Zippers (ZIP-V1 and ZIP-V2) were used as a positive control for the split-YFP system, and ZIP-V1 was included as a negative control for the assay. The transfection mixture contained 125µl of serum-free medium, 1,250ng DNA of each plasmid, 5µl of Lipofectamine™ 3000 and 6µl of P3000 reagent (see details in section 2.2.5.1). Following transfection and overnight incubation, cells were stained using the mitochondrial staining reagent as described above.

6.2.3 Confocal imaging of mitochondria in live cells

The Confocal Microscope (LSM510 NLO Inverted) was used to image transfected live cells at multiple depths. The microscope was programmed to allow both fluorescent and phase-contrast imaging. A water lens having 40x magnification was used to image cells. Image acquisition required the setup of the appropriate filter for each fluorophore. The YFP signal was detected following excitation using the 488nm laser, and the emission (Green) was detected using the 500-550nm filter. The Mitochondrial stain was detected following the use of 543nm laser for excitation, and the signal (Red) was detected using a 560nm filter.

6.2.4 Quantification of YFP fluorescence localised to mitochondria using Pixel analysis

ImageJ software (Wayne Rasband, National Institutes of Health, USA) was used to quantitate pixels corresponding to the YFP signal (Green channel) and the Mitochondrial signal (Red channel). Channels were split using the split-channels tool, and the colour was transformed into a greyscale using the threshold tool. Cells were selected using the freehand selection tool, and the pixel count was quantitated using the histogram tool. Pixel counts from the red (mitochondria) and green (YFP) channels were used to calculate the percentage of the TRIB3/AKT1 complex that was localised to mitochondria. Statistical analysis was performed using GraphPad Prism version 8.3.0 (GraphPad Software, La Jolla California USA).

6.3 Results

6.3.1 Optimising mitochondrial, ER, and lysosomal stains

HeLa cells were dual-stained using staining kits targeting nuclei, mitochondria, lysosomes, and ER. The stained cells were imaged from 6-well plates using the 40x objective lens on the Leica AF6000 Time-Lapse inverted wide-field fluorescence microscope. The images obtained using the above staining protocols for the three subcellular compartments showed that the cells tolerated the stains with minimal toxicity (Figure 6.2). However, the imaging resolution was not to the quality that would allow quantifying the co-localisation of the TRIB3/AKT1 complex to the subcellular compartment at multiple depths, and Therefore, the use of confocal imaging was suggested.

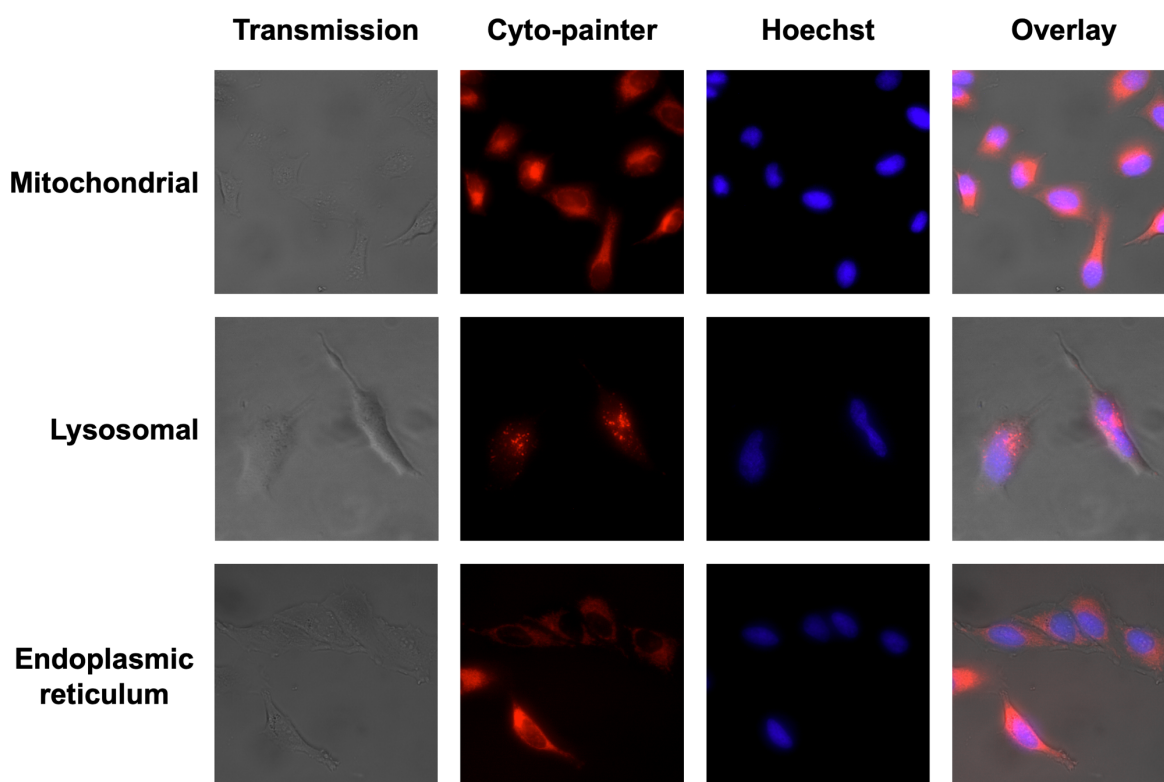
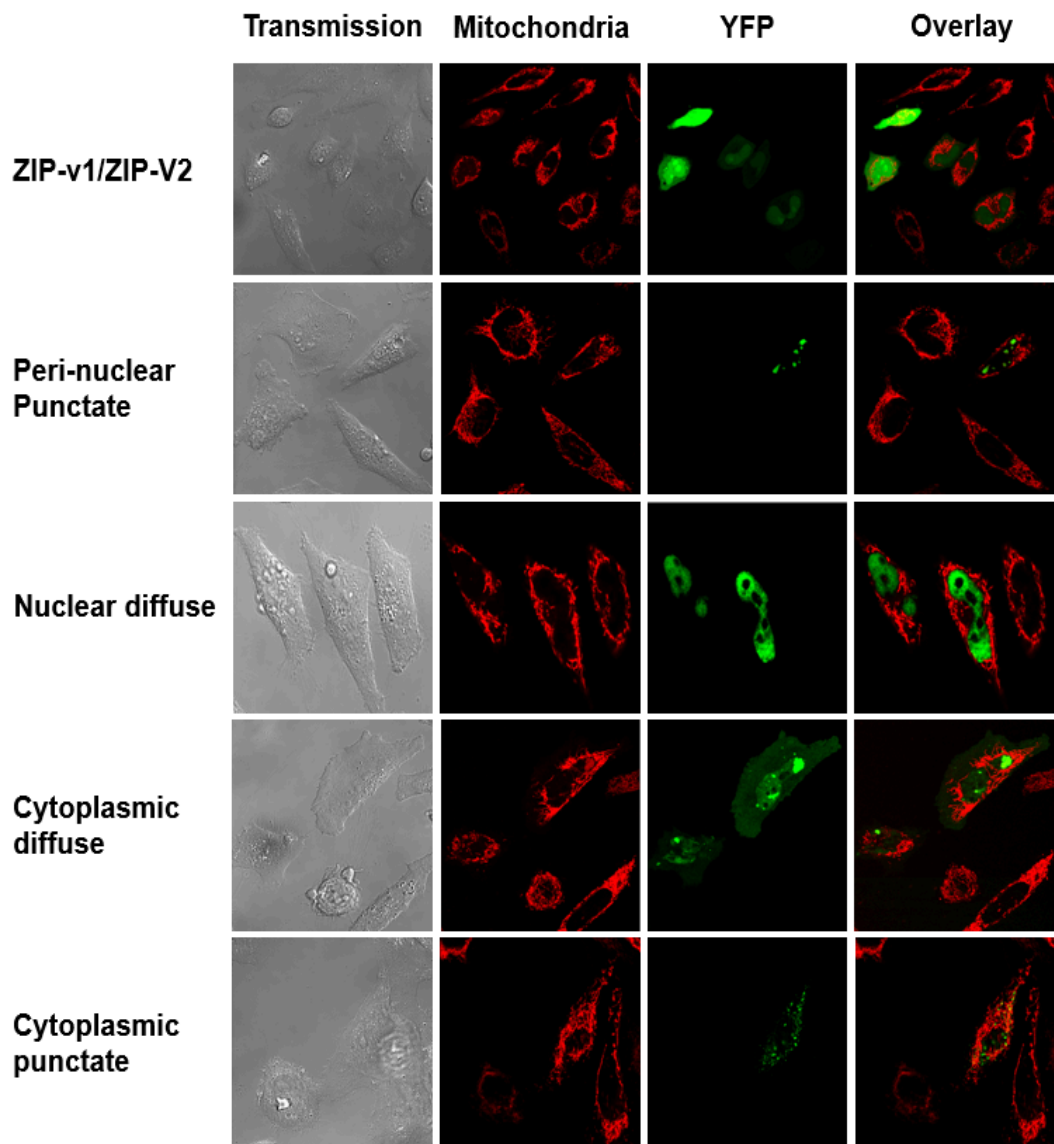


Figure 6.2: Staining of subcellular compartments

HeLa cells were seeded and allowed to reach confluency before dual staining the indicated subcellular compartments (cyto-painters) and nuclei (Hoechst) and then imaging the cells. Fluorescence images were captured using the 40x objective lens on a Leica AF6000 inverted wide-field fluorescence microscope.

6.3.2 TRIB3/AKT1 complex localised to mitochondria only when expressed in a cytoplasmic punctate pattern

HeLa cells were co-transfected with the TRIB3-V2 and AKT1-V1 plasmids, and allowed to recover overnight before the mitochondria were stained and the cells imaged by confocal microscopy. Imaging revealed the four expression patterns of the TRIB3/AKT1 complex that were observed previously (see section 5.3.2) (Figure 6.3). Pixel analysis was performed to measure the percentage of the wild-type TRIB3/AKT1 complex that was co-localised with the mitochondrial territories, which were marked using the mitochondrial staining reagent (Figure 6.4). Co-localisation to mitochondria was detected only in the cytoplasmic punctate expression pattern.



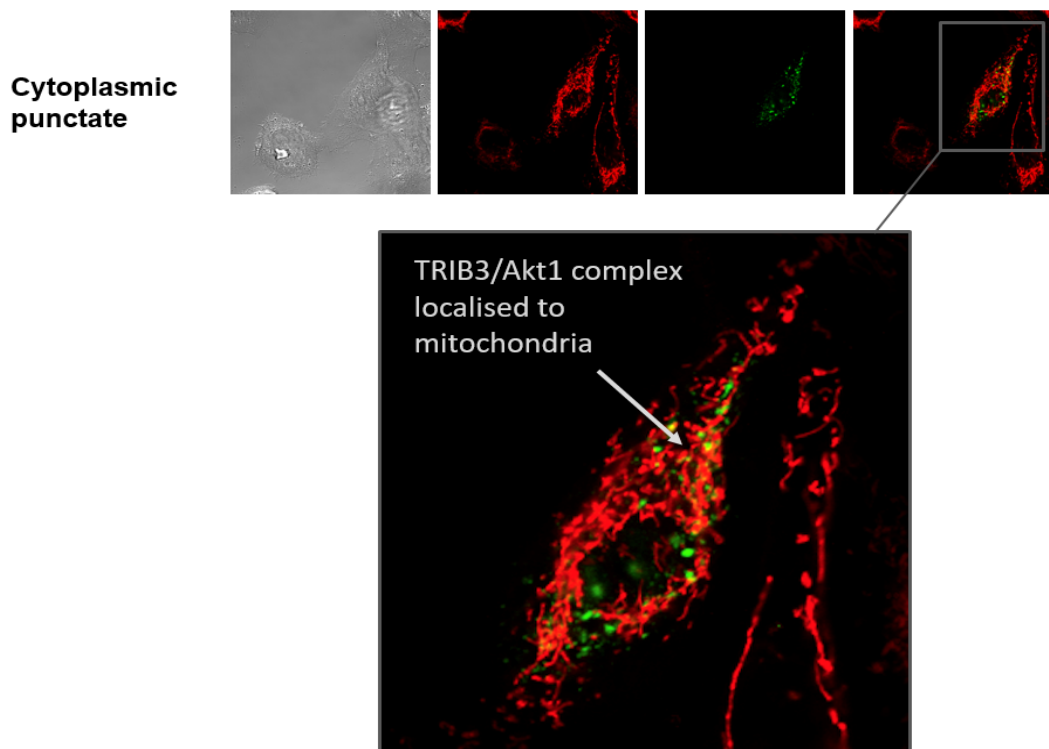


Figure 6.3: Localisation of TRIB3/AKT1 complex to mitochondria in cytoplasmic punctate expression pattern

HeLa cells were co-transfected with YFP complementation plasmids (TRIB3-V1 and AKT1-V2) to examine localisation of the TRIB3/AKT1 complex (Green). The mitochondria were stained (Red) and localisation of the complex assessed by confocal imaging. The TRIB3/AKT1 complex showed four expression patterns, and the cytoplasmic punctate expression pattern corresponded with the complex being localised to the mitochondria. The ZIP-V1/ZIP-V2 complex was used as a positive control for the split-YFP system.

6.3.2 The R149G variant did not affect the translocation of the TRIB3/AKT1 complex to mitochondria

Following confirmation of the translocation of the TRIB3/AKT1 complex to mitochondria, the effect of the R149G variant on this localisation was investigated. Localisation of the TRIB3/AKT1 complex was examined in seventeen cells expressing the wild-type TRIB3/AKT1 complex and thirty cells expressing the R149G TRIB3/AKT1 complex (Figure 6.4). The percentage of the complex that showed mitochondrial localisation was slightly greater for the R149G form than for the wild-type form but this did not reach statistical significance (Unpaired t-test $P=0.1326$).

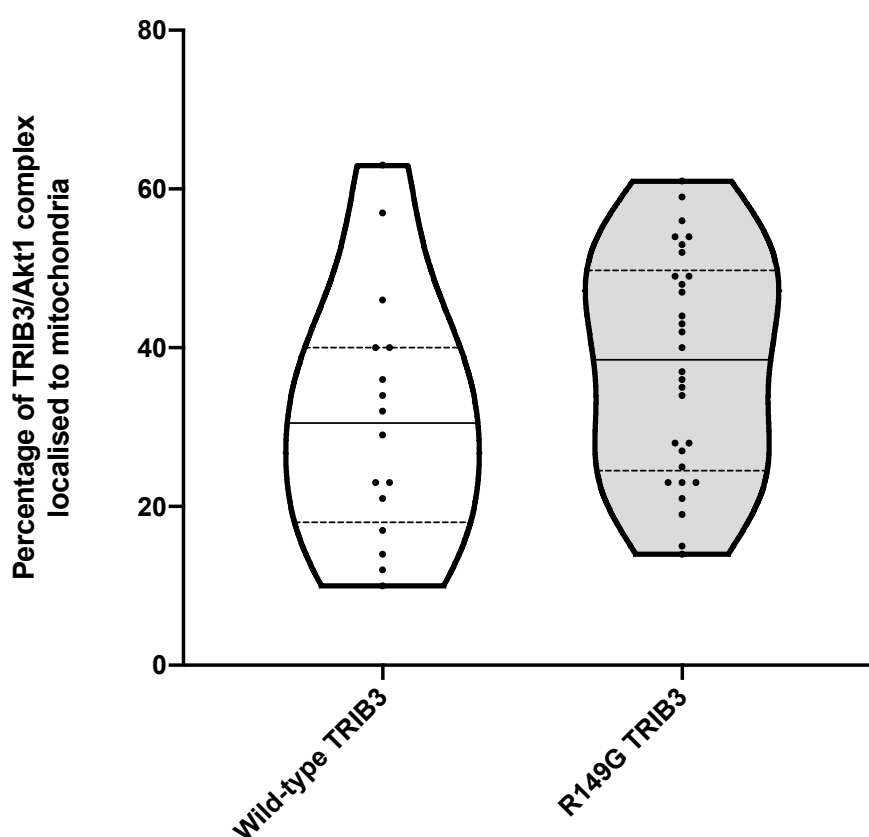


Figure 6.4: Violin plots comparing mitochondrial localisation of the wild-type TRIB3/AKT1 and the R149G TRIB3/AKT1 complexes

HeLa cells were co-transfected with the TRIB3/AKT1 complexes encoding two forms of TRIB3; wild-type ($n=17$) and R149G ($n=30$). Confocal images were analysed using ImageJ software to quantify pixels and determine the percentage of the TRIB3/AKT1 complex localised to the mitochondria. The solid horizontal line represents the median, and the dotted lines represent the quartiles. The width of the violin plot is proportional to the number of the points at the level, and the whole shape provides an idea of the overall distribution. Statistical analysis using an unpaired t-test showed no significant difference between the two TRIB3 forms ($P=0.1326$).

6.4 Discussion

We demonstrated the physical protein-protein interaction (PPI) between TRIB3 and AKT1 using the split-YFP system and showed that the complex is expressed in four different expression patterns (nuclear diffuse, peri-nuclear, cytoplasmic diffuse, and cytoplasmic punctate). Those locations were suggested to represent phosphorylation sites for AKT1 including the nucleus, the nuclear membrane, and the cytoplasm or subcellular organelle including mitochondria, endoplasmic reticulum, and lysosomes (Bijur & Jope, 2003; Boulbes et al, 2011; Sugiyama et al, 2019). Our observations relating to TRIB3 localisation (see section 5.3.1) confirm those of a previous study by (Xu et al, 2007) which concluded that TRIB3 is localised to the nucleus when expressed by itself. Unphosphorylated AKT1 is mostly localised to the cytoplasm, and upon stimulation, AKT1 migrates to the cell membrane where the majority of the phosphorylation takes place (Saji et al, 2005). However, further phosphorylation of AKT1 has been reported to occur in the nucleus and in other subcellular compartments, including mitochondria (Szymonowicz et al, 2018).

In this chapter, I optimised staining of the mitochondria, the ER, and the lysosomes to facilitate co-localisation studies, and investigated the translocation of the TRIB3/AKT1 complex into the mitochondria. The mitochondrial localisation was investigated using pixel analysis of confocal images that were taken of HeLa cells transfected with TRIB3 and AKT1 plasmids on the split-YFP complementation system and stained mitochondria. The TRIB3/AKT1 complex displayed the four expression patterns that were observed previously, and the cytoplasmic punctate expression pattern of the complex corresponds with mitochondrial staining.

Mass spectrometric analysis of the peptides interacting with the variant TRIB3 molecules predicted a gain-of-interaction with mitochondrial peptides such as TIMM17B, and MCAT (See section 3.3.3), which implies that the variants are forming novel mitochondrial interactions and therefore, expected to show increased mitochondrial localisation. The R149G variant was selected for further analysis because of the loss-of-interaction detected with peptides of the TRIB3, which implies that the R149G substitution affects the ability of TRIB3 to form a dimer. Additionally, the *in-silico* studies performed by Juan Salamanca Vilorio (Barcelona, Spain), highlighted the R149 residue as a hot spot for the interaction between TRIB3 and AKT1 (unpublished). The pixel quantification of cells co-transfected with AKT1 and either wild-type TRIB3 or R149G TRIB3 showed a slight increase in mitochondrial localisation

of the complex formed with the R149G variant ($P=0.1326$). This analysis uses Mander's overlap coefficient (MOC) with the ImageJ software to detect and quantify the co-occurrence for each pixel (Dunn et al, 2011). This approach is useful for detecting co-localisation, but other approaches that allow quantification of the fraction of the fluorescence that shows co-localisation such as Mander's co-localisation coefficient (MCC) would be more accurate for our comparison (Dunn et al, 2011). The MCC approach would allow detection of differences in the levels of expression of the complex localised to the mitochondria between the wild-type-TRIB3/AKT1 and the R149G TRIB3/AKT1 rather than quantifying the overlapping between the two fluorescence probs.

The expression of TRIB3 was associated with downregulation of AKT phosphorylation (Prudente et al, 2005), and AKT is known to be an important molecule downstream of the PI3K signalling pathway (Bos, 1995). Active signal transduction through the PI3K/AKT pathway acts to maintain cell viability and block the translocation of pro-apoptotic proteins from the cytoplasm to the mitochondria (Takino et al, 2019). Additionally, studies have identified the migration of AKT1 into mitochondria as a crucial mechanism for maintaining cell proliferation and regulating apoptosis (Arciuch et al, 2009; Feng et al, 2013). Therefore, the observed slight increase in mitochondrial localisation of the TRIB3 R149G/AKT1 complex could provide a basis for further studies looking at the apoptosis rate in cells expressing the R149G TRIB3 variant.

The survival and activity of platelets are maintained by the appropriate functioning of the mitochondria, and mitochondrial defects were previously correlated with shortened platelet half-life and with defects in platelet activation (Avila et al, 2012; Baaten et al, 2018). Studies have shown that the PI3K/AKT pathway is crucial during thrombin-induced platelet activation that maintains ATP synthesis by regulating glycolysis and Oxidative phosphorylation (OXPHOS) in platelet mitochondria (Adam et al, 2003; de la Pena et al, 2017). Our work showed that TRIB3 is interacting with AKT, to form a complex that translocates to mitochondria. Further investigations are required to identify if TRIB3 is involved in maintaining AKT activity in platelet mitochondria.

Additional work is required to investigate the role of TRIB3 in mitochondria, and to examine the effects of the remaining four TRIB3 variants studied here on mitochondrial functions. Also examination of platelet survival, AKT phosphorylation, and mitochondrial function in *Trib3* knockout mice could provide further insights into the role of TRIB3 in platelet function.

Chapter 7:

General Discussion, Final Summary, and Future Work

Platelets function to maintain vascular integrity by adhering at sites of injury and forming platelet thrombi that stem bleeding. To fulfil this role, the number of circulating platelets should be maintained within the normal range, and each platelet should be capable of achieving optimal activation upon encountering haemostatic challenges. TRIB3 has been associated with the regulation of megakaryopoiesis, which is the primary process in platelet biogenesis (Ahluwalia et al, 2015; Butcher et al, 2017). However, the potential role of TRIB3 in the regulation of platelet function remains to be clarified. The work described in this thesis explored the involvement of TRIB3 in the regulation of thrombin-induced platelet activation and degranulation. Additionally, the effects of five rare non-synonymous TRIB3 variants that were identified among patients recruited to the UK-GAPP study with unexplained platelet bleeding disorders were explored using different approaches including; in-silico predictions, structural analysis, assessment of interacting peptides, cellular localisation, interaction with AKT, and translocation to subcellular compartments.

We identified clustering of five rare non-synonymous TRIB3 variants (predicting V107M, S146N, R149G, R153H, and R181C amino acid substitutions) in a cohort of 34 patients recruited to the UK-GAPP study. Four of the five variants (V107M, S146N, R153H, and R181C) were significantly associated with coronary artery disease among Italian T2DM patients (Prudente et al, 2015). The fifth variant (R149G) was not previously reported in the European population but was reported in the South Asian population (see table 3.2). Each of the five variants was predicted to have a deleterious effect on TRIB3 (CADD score >20), and the 3D model of TRIB3 predicted the five variants to affect amino acids that are located toward the protein surface (see Figure 3.4).

The predicted deleterious effects of the five variants, and the surface location of the amino acids that were substituted in TRIB3 as a result, suggested that they may disturb the interaction of TRIB3 with other proteins. Hence, we investigated TRIB3 interactors using mass spectrometric analysis, and the outcomes showed that those variants trigger gain and loss-of-interaction with other peptides (see Figure 3.5). We observed a shared gain-of-interaction in mass spectrometric profiles with peptides that are associated with mitochondrial functions (see Table 3.3), and interestingly, the R149G variant showed a loss of interaction with a peptide of TRIB3 among other peptides. Our data showed distorted expression of the R149G variant (89% of the cells displayed a diffuse pattern), and also the V107M and the R181C variants (more than half of the

cells displayed a diffuse pattern), which could be related to the loss of interaction with other proteins. The altered expression of the R149G variant was proposed to be associated with defective TRIB3 dimerization (see section 3.3.3), which is essential for some protein functions (Marianayagam et al, 2004). Further investigation of TRIB3 dimerization and of its interaction with peptides that were shown to gain or lose interactions with the variant forms of TRIB3 could provide insights into the effects of TRIB3 on different cellular processes in general, and on platelet-related-processes in particular.

The protein complementation assays (PCA) performed to assess the interaction between TRIB3 and either AKT1 or AKT2 showed that the R149G, the R153H, and the R181C variants had gain-of-function effects on the interaction with AKT1, while the interaction with AKT2 was not disturbed by any of the variants (see Figure 5.3). However, quantification of phosphorylated AKT in cells transfected with the TRIB3 variants and AKT1 did not show the expected reduction (see Figure 5.4). We propose that these contradicting findings are because our experiment did not include compounds to induce AKT phosphorylation. Nevertheless, the gain-of-function effects on the interaction with AKT1 could, in theory, extend to affecting platelet function. Moreover, additional testing of other known effectors of TRIB3, such as ERK, that are known to be involved in regulating platelet signalling would contribute to the identification of the platelet signalling axis that is regulated by TRIB3.

Gene ontology analysis of peptides interacting with wild-type and variant forms of TRIB3 which were identified by mass spectrometry predicted these to be involved in multiple cellular processes (see Figure 3.6) including platelet function mechanisms (see Table 3.4). The observed reduction in TRAP-induced CD62p expression in platelets from *Trib3*^{-/-} female mice, and also the reduction in ATP secretion from those platelets supported our hypothesis that TRIB3 is involved in regulating platelet function (see Figure 5.5). The gender-specific effect of TRIB3 on platelet reactivity could be explained by the fact that the promotor of *TRIB3* encompasses a binding site for estrogen receptor (unpublished), and also by the overexpression of *TRIB3* detected upon stimulation with an estrogen-like compound (Ise et al, 2005). We hypothesise that the reduced activity in platelets from female mice could be linked to the proposed involvement of estrogen in regulating platelet activation (Figure 7.1). However, our data for the wild-type mice did not show a significant difference between the two genders. This observation could be explained by an earlier study that highlighted the gender

differences in murine platelet reactivity is declining with the use of higher concentrations of PAR4 agonist (Leng et al, 2004), which we did not measure in our study. Nevertheless, the three patients who were heterozygous carriers of the variants that showed a gain-of-function effect on the interaction with AKT1 (R149G, R153H, R181C) were all females (see Table 3.1). Further studies investigating the phosphorylation of kinases such as AKT and ERK in platelets from these patients could yield insights into the potential gender-specific role of TRIB3 in the development of their bleeding phenotype. Additionally, knocking out/down TRIB3 in stem cells, and differentiating them to megakaryocytes and then platelets would facilitate investigating the role of TRIB3 in megakaryopoiesis, thrombopoiesis and platelet function. Further to this approach, introducing *TRIB3* variants to stem cells and differentiate them would enable examining their effects on platelet functions.

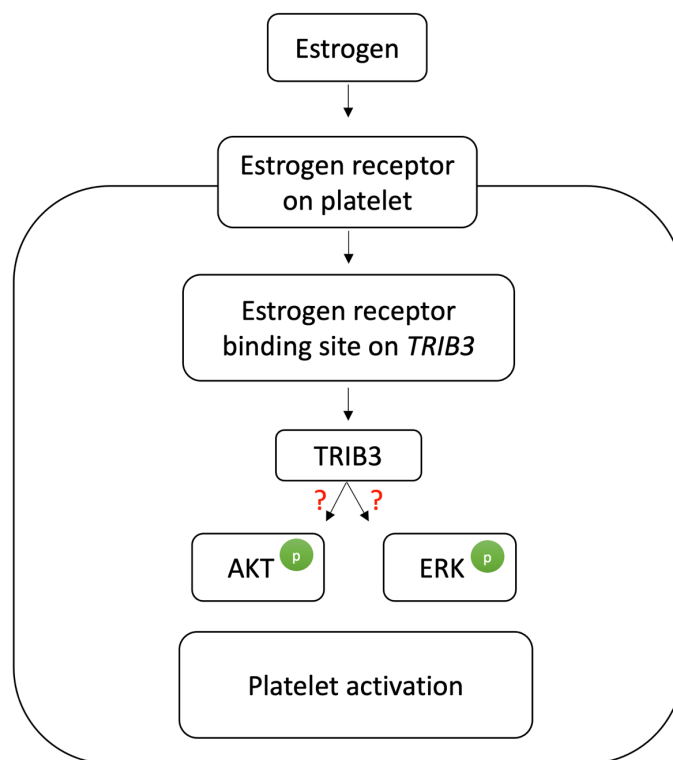


Figure 7.1: Proposed mechanism of the role of estrogen in regulating platelet activation through TRIB3

The diagram shows the proposed scenario of the involvement of the female hormone (Estrogen) in regulating platelet activation. Estrogen is proposed to promote the expression of TRIB3, which regulate the phosphorylation of kinases that are known to have a key role in platelet intracellular signalling pathways.

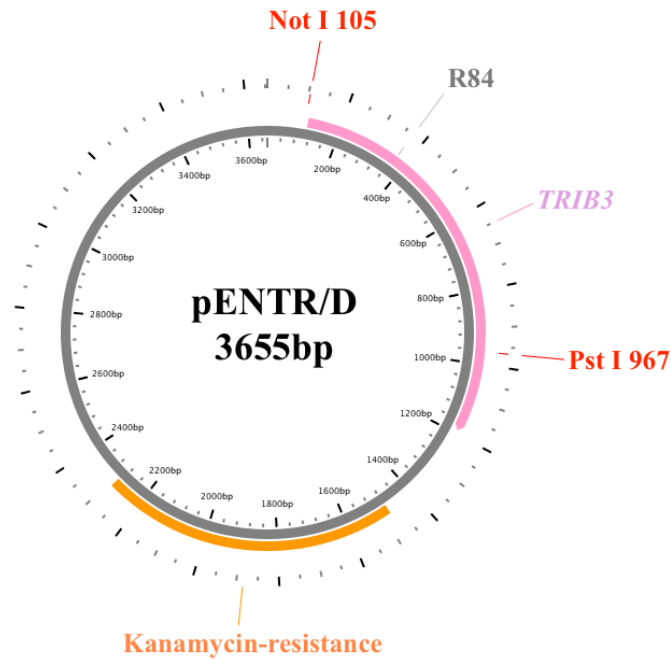
We observed from the interaction between TRIB3 and AKT1 that the complex displayed four different expression patterns, two of which were cytoplasmic. We suggested that the cytoplasmic localisation of the TRIB3/AKT1 complex represented a translocation to subcellular compartments. Thus, we optimised the staining of mitochondria, ER, and lysosomes in HeLa cells to investigate co-localisation of the TRIB3/AKT1 complex to those compartments (see Figure 6.2). The gain-of-interaction with mitochondrial peptides observed with all five variant forms of TRIB3 (see Table 3.3) studied suggested that these variants might show an increased translocation to mitochondria. Indeed, we confirmed that the cytoplasmic punctate expression pattern of the wild-type TRIB3/AKT1 complex was partially co-localised to the mitochondria (see Figure 6.3). Furthermore, we also compared the proportions of the complex that were co-localised to mitochondria for wild-type TRIB3 and the R149G variant, and although the R149G TRIB3/AKT1 complex appeared to show an increased association with the mitochondria when compared to the wild-type complex, this did not reach statistical significance (see Figure 6.4). However, the method we used to quantify the co-localisation (pixel analysis) counts pixels that are positive for both fluorophores (Mitochondrial and YFP) without considering the amount of those fluorophores (the expression level). Thus, more accurate quantification may show a distinct difference that might reach statistical significance. Nevertheless, the mitochondrial co-localisation of the TRIB3/AKT1 complex aids in understanding the role of TRIB3 in regulating cellular functions, which could also apply to platelets.

In our study, we used either HeLa or HEK293T cells, which do not simulate the microenvironment of the platelet, and they have a nucleus while platelets are anucleate cells. Nevertheless, the experiments that were undertaken using those cell lines provided an indication of the effects the *TRIB3* variants may have on the expression of TRIB3 and its interaction with AKT1 in platelets. Additionally, the slight increase in the localisation of the R149G TRIB3/AKT1 complex to mitochondria, which was supported by the mass spectrometric analysis, provided another indication of the effects that a TRIB3 variant may have on a cellular compartment that is crucial for the normal platelet functions. The different cellular environment is a limitation of this study, and in an effort to resolve this limitation, we attempted transfecting megakaryocytic cell lines (DAMI and Meg-01 cells). However, those transfections showed extremely low transfection efficiency (<1%) using different transfection reagents including; Lipofectamine 3000, Lipofectamine LTX, Xfect, and jetPEI.

In our measurement of ATP secretion from platelet-rich-plasma collected from mice we did not use an ATP standard. Usually, the quantification of ATP secretion from murine platelets requires pooled samples from 5-15 animals to have sufficient volume to plot the ATP standard and then quantify ATP secretion (Hughes, 2018; Jirouskova et al, 2007). However, we showed that using samples that were diluted to have similar platelet counts was sufficient to provide an indication of the differences in ATP secretion without the use of an ATP standard. This approach was suggested to reduce animal numbers to the minimum and to adhere to the best practice proposed by the National Centre for the Replacement, Refinement and Reduction (NC3Rs) of animals in research.

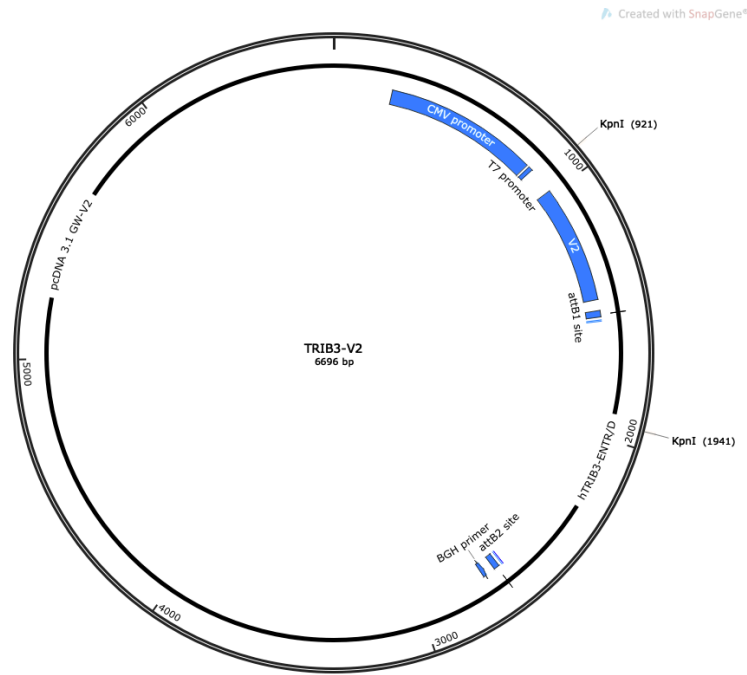
Appendices

Appendix 1. hTRIB3-ENTR/D plasmid sequence



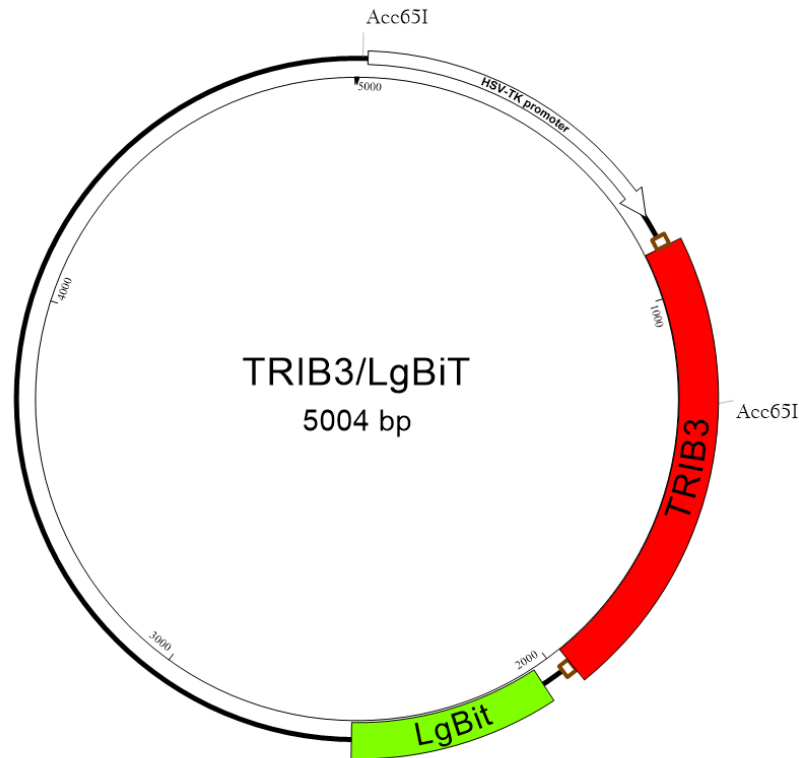
CAAATAATGATTTTATTTTGACTGATAGTGACCTGTTCTGTTGCAACAAATTGATGAGCAATGCTTTTTTATAATGCCAACTTTGTACAAAAAGCAGGCTCCGCGGGCCG
 CCCCCTTACCATGCGAGCCACCCCTCTGGTGCTCCTGCGGGTCCCTGTCAGGAAGAAGCGGTTGGAGTTGGATGACAACTTAGATACCGAGCGTCCCGTCCAGAA
 ACGAGCTCGAAGTGGGCCCCAGCCAGACTGCCCCCTGCCTGTTGCCCTGAGCCCACTACTGCTCCAGATCGTGCAACTGCTGTGGCCACTGCCTCCGCTTTGGG
 CCCTATGCTCCTCGAGCCGAGGAGGGCGGGCGGGCTACCGGGCCCTGCATGCCCTACAGGCATGAGTATACCTGCAAGGTGTACCCCGTCCAGGAAGCCCTGG
 CCGTGTGGAGCCCTACGCGCGGCTGCCCGGCACAAGCATGTGGCTCGGCCACTGAGGTCCTGGCTGGTACCCAGCTCCTACGCTTTTCACTCGGACCCATGG
 GGACATGCACAGCTGGTGCAGAACGCCACCGTATCCCTGAGCCTGAGGCTGCGGTGCTCTCCGCCAGATGGCCACCGCCCTGGTGCACTGTACCAGCACGGTCTG
 GTCCTGCGTGATCTCAAGCTGTGTGCTTTGTCTTCGCTGACCGTGAGAAGAAGAAGCTGGTGCTAGAGAACCTGGAGGACTCTGCGTGCTGACTGGGCCAGATGATT
 CCCTGTGGGACAAGCACGCGTGCACAGCTACGTGGGACTGAGATACTCAGCTCAGGGCCCTCATACTCGGGCAAGGCAGCCGATGTCTGGAGCTGGGCGTGGCGCT
 CTTACCATGCTGGCCGCCACTACCCCTCCAGGACTCGGAGCCTGTCCTGCTCTCGGCAAGATCCGCCCGGGGCTACGCCCTGCTGCGAGCCTCTCGGCCCT
 GCCCGCTGTCTGGTTCGCTGCTCCTTCGTCGGGAGCCAGCTGAACGGCTCACAGCCACAGGCATCCTCCTGCACCCCTGGCTGCGACAGGACCCGATGCCCTTAGCTC
 CAACCCGATCCCATCTCGGGAGGCTGCCAGGTGGTCCCTGATGGACTGGGGCTGGACGAAGCCAGGGAAGAGGAGGAGACAGAGAAGTGGTCTGTATGGCCAAGG
 GTGGGCGCGCCAGCCAGCTTTCTTGTACAAAAGTTGGCATTATAAGAAAAGCATTGCTTATCAATTTGTTGCAACGAACAGGCTCAGTCAAAAATAAATCATTAT
 TTGCCATCCAGCTGATATCCCTATAGTGAGTCGATTACATGGTCAATAGCTGTTTCTGGCAGCTCTGGCCGTGCTCAAAATCTCTGATGTTACATTGCACAAGAT
 AAAAATATATCATCATGAACAATAAACTGTCTGCTTACATAAACAGTAAACAAGGGGTGTTATGAGCCATATTCACCGGGAAACGTCGAGGCCGCGATTAAATCCA
 ACATGGATGCTGATTTATATGGGTATAAATGGGCTCGCGATAATGTCGGGAATCAGGTGCGACAATCTATCGCTTGTATGGGAAGCCCGATGCGCCAGAGTTGTTTCT
 GAAACATGGCAAAGGTAGCGTTGCCAATGATGTTACAGATGAGATGGTCAGACTAACTGGCTGACGGAATTTATGCGCTCTCCGACCATCAAGCATTATCCGTA
 CCTGATGATGATGCTGTTACTCACCCTGCGATCCCGGAAAAACAGCATTCCAGGTATTAGAAGAATCCTGATTCAGGTGAAAAATTTGTTGATGCGCTGGCAGTGT
 TCCTGCGCCGGTTGCAATTCGATTCTGTTTGTAAATGTCCTTTAACAGCGATCGCGTATTTCTGCTCAGGCGCAATCACGAATGAATAACGGTTTGGTTGATGC
 GAGTGTATTTGATGACGAGCGTAATGGCTGGCCTGTTGAACAAGTCTGGAAGAATAATGATAAACTTTTGGCATTCTCACCAGGATTCAGTCGCTACTCATGGTATTT
 TCACCTGATAACCTTATTTTACGAGGGGAAATTAATAGGTTGATTGATGTTGGACGAGTGGGAATCGCAGACCGATACCAGGATCTTCCATCTATGGAAGTCC
 TCGGTGAGTTTTCTCCTTATTACAGAAACGGCTTTTTCAAAAATATGGTATTGATAATCCTGATATGAATAAATGCAAGTTTCAATTTGATGCTCGATGAGTTTTCTA
 ATCAGAATGGTTAATTTGTTGTAACACTGGCAGAGCATTACGCTGACTTGCAGGGACGGCGCAAGCTCATGACCAAAATCCCTAACGTGAGTTACGCGCTGTTCCAC
 TGAGCGTCAGACCCCGTAGAAAAGATCAAGGATCTTCTTGGATCCTTTTTTCTGCGGTAATCTGCTGCTTGCACAAAAAACACCGCTACCAGCGTGGTTTT
 GTTTGCCGGATCAAGAGCTACCAACTCTTTTCCGAAGGTAAGTGGCTTACGAGAGCGCAGATACCAAACTACTGCTTCTAGTGTAGCCGTAGTTAGGCCACCCTT
 CAAGAACTCTGTAGCACCGCTACATACCTCGCTCTGTAATCCTGTTACCAAGTGGCTGCTGCCAGTGGCGATAAGTCTGCTTACCAGGTTGGACTCAAGAGCATTAG
 TTACCGGATAAGGCGCAGCGGTGGGCTGAACGGGGGTTCTGTCACACAGCCAGCTTGGAGCGAACGACCTACACCGAAGTACAGTACCTACAGCGTGGCATTGAG
 AAAGCGCCACGCTTCCCGAAGGGAGAAAAGCGGACAGGTATCCGGTAAGCGGCAAGGTCGGAACAGGAGAGCGCACGAGGGAGCTTCCAGGGGAAACCGCTGGTATCT
 TTATAGTCTGTCGGGTTCCGCCACTCTGACTTGAAGCGTCGATTTTGTGATGCTGCTCAGGGGGCGGAGCCTATGGAAAAACGCCAGCAACGCGGCTTTTACGG
 TTCTGGCCTTTTGTGGCCTTTTGTCTACATGTTCTTCTGCTGTTATCCCTGATCTGTGGATAACCGTATTACCAGCTTTGAGTGTAGCTGATACCGCTCGCCGCA
 GCCGAACCGCAGCGCCAGCGAGTCAAGTGTGAGCGAGGAAAGCGGAAGAGCGCCCAATACGCAAAACCGCTTCCCGCGCGTTGGCGGATTCATTAATGCAAGTGGCAGCA
 CAGGTTTCCGACTGGAAGCGGGCAGTGTGAGCGCAACGCAATTAATACGCTGACTGAGCAGGAAAGGTTTGTAGAAAACGAAAAAGGCCATCCGTCAGGATGGCCT
 TCTGCTTAGTTGATGCTGGCAGTTTATGGCGGGCGTCTGCGCCGCAACCTCCGGGCGGTTGCTTCAACAGTTCAAAATCCGCTCCCGCGGATTTGTCTACTCAG
 GAGAGCGTTACCAGCAAAACAGATAAAACGAAAGGCCAGTCTCCGACTGAGCCTTTCGTTTTTATTTGATGCTGGCAGTCCCTACTCTCGGTTAACGCTAGC
 ATGGATGTTTTCCAGTCACGACGTTGATAAACGACGGCCAGTCTTAAGCTCGGGCC

Appendix 3. Schematic representation of TRIB3/V2 plasmid



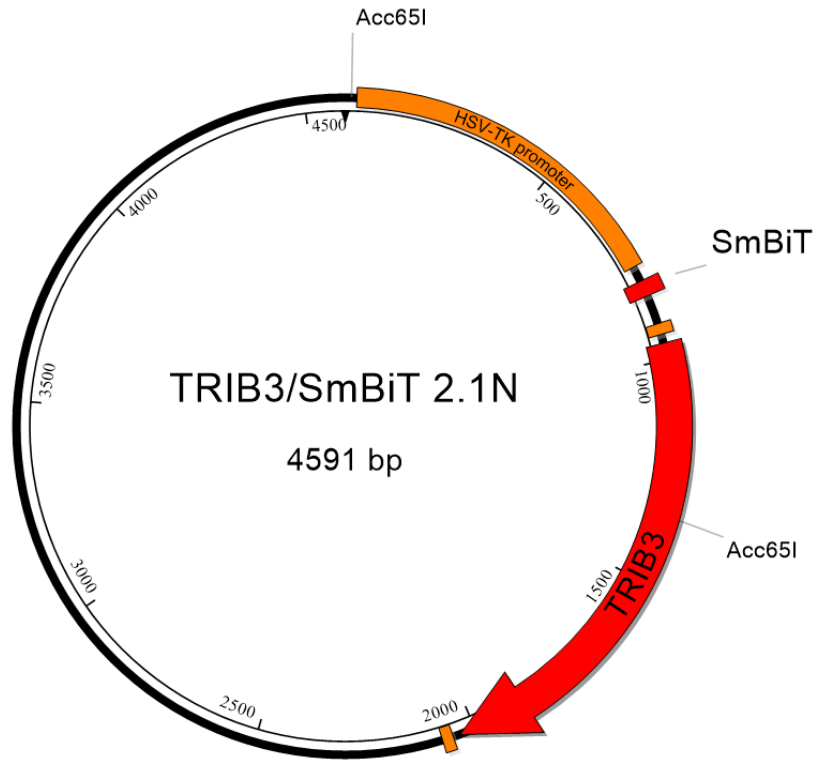
GACGGATCGGGAGATCTCCCGATCCCTATGGTGCAGTCTCAGTACAATCTGCTCTGATGCCGATAGTTAAGCCAGTATCTGCTCCCTGCTGTGTGTGGAGGTCGCTGAGTAGTGCAGGCA
AAATTTAAGCTACAACAAGGCAAGGCTTGACCGACAATTGCATGAAGAATCTGCTTAGGGTTAGGCGTTTGGCGTGTCTCGCGATGTACGGGCGAGATATACCGTGTGACATTTGATTATTGACTA
GTTTAAATAGTAATCAATACGGGGTCATTAGTTTCATAGCCCATATATGGAGTTCGGCGTTACATAAATACGGTAAATGGCCCGCTGGCTGACCGCCCAACGACCCCGCCATTGACGTCAA
TAATGACGTATGTTCCATAGTAACGCCAATAGGGACTTTCATTGACGCTCAATGGGTGGACTATTACGGTAAATGCCACTTGGCAGTACATCAAGTGATCATATGCCAAGTACGCCCCCTA
TGACGTCATGACGCTAAATGGCCGCTGGCATTATGCCAGTACATGACCTTATGGGACTTTCCTACTTGGCAGTACATCTAGTATTAGCTATTACCATGGTGTGCGGTTTGGC
AGTACATCAATGGGCGTGGATAGCGGTTTGAATCTCACGGGATTTCAAAGTCTCCACCCATTGACGCTCAATGGGAGTTTGTGGTGGCACCACAAATCAACGGGACTTCCAAAAATGCGTAACT
CGGCCCCATTGACGCAAAATGGGCGTAGGCGTGTACGGTGGGAGGTTCTATAAGCAGAGCTCTGGCTAACTAGAGAACCCACTGCTTACTGGCTTATCGAAATTAATACGACTCACTATAGGG
AGACCAAGCTGGTAGCTTAAACTTAAGCTTGGTACCGAGCTCGGATCCACTAGTCCAGTGGTGGTAAATTCGACAGATATCCAGCAGATGGCGGCGCACCATTGGTGAAGCAGGGGAGGA
GCTGTTACCAGGGGTGGTCCCATCTGGTTCGAGCTGGACGGCAGCTAAACGGCCACAAGTTCAGCGTTCGGCGAGGGCGAGGGCGATGCCACTACGGCAAGCTGACCTGAAGCTGATCTG
CACCACGGCAAGCTGCCGTTGCCCTGGCCACCCCTGTCGACCACTGGGCTACGGCTGCAAGTGTCTGCCCGCTACCCGACACATGAAGCAGCAGCAGCTTCTCAAGTCCGCCATGCCCGCA
AGGCTACGTCAGGAGCGCACCATCTTCTCAAGGACGACGGCACTACAAGACCCGCGGAGGTGAAGTTCGAGGGCGACACCCTGGTGAACCGCATCGAGCTGAAGGGCATCGACTCAAGGA
GGACGGCAACATCTGGGGCACAAAGCTGGAGTACAACACAGCCACAACGCTATATACCCCGCAGCAAGCAGATCGATGGTGGCGTGGCTTCGGAGGTGGTGGGCTCCCGGATCAACAAG
TTGTACAAAAAAGCAGGCTCCGCGGCGCCCTTACCATGCGAGCCACCCTTGGCTGCTCTCGGGTTCCTGTCCAGGAAGAAGCGGTGGAGTTGGATGACAACCTAGATACCAGGCG
TCCCGTCCAGAAAGAGCTCGAAGTGGGCGCCAGCCAGACTGCCCCCTGCCGTTGGCCCTGAGCCCACTACTGCTCCAGATCGTGAACCTGCTGGCCACTGCCCTCCGCTTTGGGCGCTA
GTCCCTCGAGAAAGTGGTGTATCTAGAGGGCCGTTAAACCCGCTGATCAGCTCGACTGGCTTCTAGTTGGCCAGCCATCTGTTGTTGGCCCTCCCGCTGCTTCCAGCCCTGA
GTCCCTCGAGGGCCGAGGAGGGCGGGCGGGCTACCAGGCTGCACTGCCCTACAGGCACTGAGTATACCTGCAAGGTGATCCCGCTCAGGAAGCCCTGGCGTGTGGAGCCCTACGCGCG
GCTGCCCCGCAACAGCATGTGGCTGGCCACTGAGGCTCTGGCTGGTACCCAGCTCTTACGCTCTTTCCTCAGTCCGACCCATGGGGACATCACAGCTGGTGGCAGGCGCCACCTATCCC
TGAGCTGAGGCTGCCGCTCTCCGCGAGTGGCCACCCTGGTGCATGTACCAGCAGCGTCTGGTCTGGCTGATCTCAAGCTGTGCTGCTTGTCTCGTACCCTGAGAGAAAGAA
GCTGGTCTAGAGAACCTGGAGACTCTCGCTGCTGACTGGGCGAGATGATTCCTGTTGGGCAAGCAGCGGTCGCCACGCTACGTTGGGACTGAGATACTCACTCACGGGCTCATACTCGG
CAAGCAGCCGATGTCTGGAGCTGGGCGTGGCGCTCTTACCATGCTGGCGGGCACTACCCTTCCAGGACTCGGAGCTGTCTGCTCTTCGGCAAGATCCCGCGGGGCGCTACGCTTGGC
TGCAGGCTCTGGCCCTGCCGCTGTCTGGTTCGCTGCTCTTCTGCTGGGAGCAGCTGAACGGCTCACAGCCACAGGCACTCTCTGCAACCCTGGCTGGCAGAGACCCGATGCCCTTAGC
TCCAACCCGATCCCATCTCTGGAGGCTGCCAGGTGGTCCCTGATGGACTGGGCTGGACGAAGCCAGGGAAGGAGGAGAGAGAAAGTGGTCTGATGGCCAAAGGTTGGGCGCGGAC
CGCAGCTGACCCGCTACACTTGGCCAGCCCTAGCGCCGCTCCTTTCGCTTCTCCCTTCCCTTTCGCGCCAGTTCGCGGCTTCCCGCTCAAGCTTCCCGCTGAGCTTCCCTTAGGGTT
CGGATTTAGTGCTTTACGGCACCTCGACCCAAAAAATTGATAGGGTATGGTTACAGTGGGCGCATCGCCGTAGTAGAGCGGTTTTTCGCTTTCGAGCTTGAAGTCCACGTTCTTTAATAG
TGGACTCTGTTTCAAACTGGAACAACACTCAACCCTATCTGGTCTAATCTTTGATTTAAGGGATTTGGGGATTTGGGGATTTGGGGATTTGGCAAAAAAAGTGGGAGCTTGTATATCCATTTT
GAATTAATCTGTGGAATGTGTGAGTATGGGTGGAAAGTCCCAGGCTCCCAGGCGAGGAGTATGCAAAAGTGCATCTCAATTAGTCAAGCAACAGGTGTGAAAGTCCCAGGCTC
CCCAGCGGAGAAAGTATGCAAAAGTGCATCTCAATTAGTCAAGCAACATAGTCCGCCCCAATCCGCCCCAATCCGCCCCAATCCGCCCCAATCCGCCCCAATCCGCCCCAATCCGCCCCA
AATTTTTTTTTTATGAGAGGGCCGAGGCGGCTCTGGCTCTGAGCTATTCCAGAGTAGTGAAGGATTTGGGGATTTGGGGATTTGGGGATTTGGCAAAAAAAGTGGGAGCTTGTATATCCATTTT
CGGATCTGATCAGCAGCTGTGACAATAATCATCGGCATAGTATATCGGCATAGTATAACGCAAGGTGAGGAACATAAACCATGGCAAGTTGACCAAGTGGCTTCCGTTCCGTTCCGCTCAGCTGCTGCT
GACGTCGCGGGAGCGGTGAGTTCGACCCGACCGGCTCGGTTCTCCGGGACTTCGTTGGAGGACGACTTCGCGGTTGGTCCGGGACGACGTCGACCTGTTTCATCAGCGCGTCCAGGACAG
GTGGTGGCCGACAAACCTTGGCTGGGTGGGTGGCGGCTGGACGAGTGTACGGCAGTGGTGGAGGTCGAGGTCGAGGATTCGCGGACGCTTCCGGGCGGCTTCCGCGGCGGCTGACCGAGATCGGC
GAGCAGCCGTGGGGCGGAGTTCGCTTCCGCGACCCGCGGCACTGCTGCACTTCGTTGGCGAGGAGCAGGACTGACAGCTGCTACGAGATTTGATTCACCCGCGCTTCTATGAAAGG
TTGGCTCTGGAAATGTTTTCCGGGAGCCGCGCTGGATGATCTCCAGCGCGGGACTCATAGCTGGAATTTCTCCGCCACCCCAACTTGTTTTTGCGCACTTAAATGGTTAACAATAAAGCAAT
AGCATCACAAATTTACAATAAAGCATTTTTTTACTGCTATTAGTGTGGTTTGTCAAACCTCATCAATGTATCTTATCATGTCTGTATACCTGCGACTTACGTAGAGCTTGGCGTAATCA
TGGTCAATAGCTTCTGCTGTGAAATTTGATCCGCTCAACAATCCACACAACATACGAGCCGGAAGCATAAAGTGAAGGCTGGGGTGCATTAAGTGAAGTAACTCACATTAATTTGGCTG
CGCTCACTGCCCCTTCCAGTCGGGAACCTGCTGTCGAGCTCATTAAATGAATCGGCCAACCGCGGGGAGAGGCGGTTTTGCGTATTGGGCGCTTTCGCTTCTCCGCTCACTGACTCGCTG
CGCTCGGTGTTCCGCTGGCGGAGCGGTATCAGCTCACTCAAAGCGGTAATACGGTTATCCACAGAATCAGGGGATAACGCAAGAAAGCAATGTGAGCAAAAGGCGCAGAAAAGCCAGGAAC
CGTAAAAAGGCGGCTGCTGGGCTTTTCCATAGGCTCCGCCCCCTGACGAGCATCAAAAAATCGAGCTCAAGTCAAGAGTGGCAGAAACCCGACAGGACTATAAAGATACCGGCGTTCCTCC
CCTGGAAGCTCCCTCGTGGCTCTCTGTTCCGACCTCGCGCTTACCAGATACCTGCGCTTTTCCCTTCCGGAAGCGTGGCGCTTCTCAATGCTCAGCGTGTAGGATCTCAAGTTCCGGT
TAGGCTGTTGCTCAAGCTGGGCTGTGTGCACGAACCCCGGTTACGGCCAGCCGCTGCGCTTATCCGGTAACATCTGCTTGAATCAACCCGTTAAGACAGCAGCTTATCGCCACTGGCAGCA
GCCACTGGTAACAGGATAGCAGAGCAGGATGTAGGCGGTGTACAGAGTCTTGAAGTGGTGGCTCACTACGCTACAGTGAAGGACAGTATTTGGTATCTGCTGCTGCTGAGCCAGT
ACCCTTCGGAAGAGTGGTGGTACTTGTATCCGCAAAACAAACCAACCCGCTGGTAGCGGTTGTTTTTGTGTTGCAAGCAGCAGATACGCGCAGAAAAAAGGACTCAAGAAGATCTTTTGATC
TTTTACGGGCTCTGACGCTCAGTGGAAAGCAAACTCAGGTTAAGGGATTTTGGTCAATGAGATATCAAAAAAGGACTTCACTAGATCTTTAAATAAAAATGAAGTTTAAATCAATCAAA
AGTATATAGAGTAACTTGGTTCAGACTTACCAATGCTTAAATCAGTGAAGCCACTTCACTGAGGCTGTCTGCTTCTGCTTCAATGCTTCAATGCTTCAATGCTTCAATGCTTCAATGCTTCAATGCT
CGGAGGGCTTACCATCTGGCCAGTGTGCAATGATACCGCGAGACCCAGCTCACCGGCTCCAGATTATCAGCAATAAACAGCCAGCCGGAAGGGCGGAGCGCAAGTGGTCTGCAACT
TTATCCGCTCCATCCAGTCTAATTTGTTGCGGGAAAGTGAAGTGGTTCGCGAGTTAATAGTTTGGCGCAAGCTTGTGCAATTGCTACAGGACTCGTGGTGTGACGCTGCTGTTGTTGTT
ATGGCTTCAATCAGCTCCGTTCCCAACGATCAAGCGAGTACATGATCCCCATGTTGTGCAAAAAAGGCGGTTAGCTCCTCGTCTCGTCTCGTCTCGTCTCGTCTCGTCTCGTCTCGTCTCGTCTCGT
TCACTCATGTTATGGCAGCACTGCAATAATCTTACTGTCATGCCATCCGTAAGTGTCTTCTGTGACTGGTGGTACTCAACCAAGTCACTTGAAGTATGTTGCGGCGACCGAGTTCG
TCTTGGCCGCGCTCAATACGGGATAATACCGGCCACATAGCAGAACTTAAAGGTGCTCATATGGAAAAAGCTTCTCGGGCGCAAACTCAAGGACTTACCCTGTTGAGATCCAGTTCG
ATGTAACCCCACTGTCACCAACTGATCTTCAAGTCTTTTACTTCCAGCGGTTTCTGGGTGAGCAGAAACAGGAAGGCAAAATGCCGCAAAAAAGGGAATAGGGGCAACAGGAAATGTTGA
ATACTCATCTCTCTTTTCAATATATTGAAGCATTATCAGGGTATTGCTCATGAGCGGATACATATTTGAATGATTTAGAAAAATAAACAAATAGGGGTTCCGCGCATTTCGCCGA
AAAGTCCACTGACGCT

Appendix 4. Schematic representation of TRIB3/LgBiT 1.1C plasmid



GGCCTAACTGGCCGTTACTGAGTCTAAATGAGTCTTCGGACCTCGCGGGGGCCGCTTAAGCGGTGGTATAGGTTTGTCTGACGCGGGGGGAGGGGGAAGAACAAACACTCTCATTCCGAGGGC
GCTCGGGTTTGGTCTTGGTGGCCACGGGACGACAGAAGAGCGCCGCGATCCTTAAAGACCCCCCGCCCTCGTGGAGCGGGGTTTGGTGGCGGGTGGTAACTGGCGGGCCGCTGACTCG
GGCGGGTCCGCGGCCAGAGTGTGACCTTTTCGGTCTGCTCGCAGACCCCGGGCGGGCCGCGCCGCGGCGCCAGCGGGCTCGTGGTCTTAGGCTCCATGGGGACCGTATACGTGGACAGGCTC
TGGAGCATCCGCACGACTGCGGTGATATTACGGGAGACTTCTGCGGGACGAGCCGGGTACGCGGCTGACCGGGAGCGTCCGTTGGGCGACAAACACAGGACGGGGCACAGGTACACTATCTTG
TACCCGGAGGCGGAGGGACTCGAGGACTTCAGGAGTGGCGCAGCTGCTTCATCCCCGTGGCCGTTGCTCGCTTTGCTGGCGGTGCCCGGAAGAAATATATTTGATGTCTTTAGTTCT
ATGATGACACAAACCCGCCAGCGTCTTGTATTGGCGAAGTCAACACGAGATGCACTGGGGCGGCGCGTCCAGGTCACCTTCGCATATTAAGTGAACGCGTGTGGCCTCGAACCCGAG
CGACCTGACGCGACCCGCTTAAAGCTTGGCAATCCGGTACTGTTGGTAAAGCCACAGATCTGCTAGCGATCGCTAAGTGGGAGCTCAGGGGAATATCAACAAGTTGTACAAAAAAGCAGG
CTCCGGCGCCGCCCTTACCATGCGAGCCACCCCTGGTCTGCTCGCGGTTCCCTGTCAGGAAGAAGCGGTTGGAGTGGATGACAACCTAGATACCGAGCGTCCCGCCAGAAACGAGC
TGAAGTGGGCCAGCCAGACTGCCCTGCTTGGCCCTGAGCCCACTACTGCTCCAGATCGTCAACTGCTGGCCACTGCTCCCGCTTGGGCCCTATGCTCTCTGGAGCCGA
GGAGGGCGGGCGGCTACCGGCCCTGCCTACAGGCACTGAGTATACCTGCAAGGTGTACCCGTCAGGAAGCCCTGGCCGCTGGAGCCCTACGCGGGCTGCCCCGACAAAGCA
TGTGGCTCGGCCACTGAGGCTCTGGTGTACCCAGCTCCTACGCTTTTTACTCGGACCCATGGGACATGACAGCCCTGGTGGAGGCCCGCCAGCTATCCCTGAGCTGAGGCTGCCGT
GCTCTTCCGCGAGATGGCCACCGCCCTGGTGCCTGACAGCAGGCTGGTCTGCGTGTCTCAAGCTGTGTGCTTTGCTTTCGCTGACCGTGAAGAAGAAGCTGGTCTAGAGAACCT
GGAGGACTCCTGCTGCTGACTGGCCAGATGATTCCTGTGGGACAAGCAGCGTCCAGCTACGTTGGGACCTGAGATACCTAGCTCACGGCCCTCACTCGGGCAAGGACGCGATGCTG
GAGCTGGGCGTGGCGCTTCCACATGCTGGCCGGCCACTACCCCTCCAGGACTCGGAGCTGCTGCTCTTCGGCAAGATCCGCGCGGGGCCCTACGCTTGCCTGACGGCTCTCGGGCC
TGCCCGTGTCTGGTTCGCTGCCCTCTCGTGGGAGCCAGTGAACGGCTCACAGCCACAGGATCCCTCGACCCCTGGCTGCGACAGACCCGATCCCTTAGCTCAACCCGATCCCATCT
CTGGGAGGCTGCCAGGTGGTCCCTGATGGACTGGGCTGGACGAAGCAGGGGAAGGAGGAGACAGAGAAGTGGTCTGTATGGCCAAAGGTTGGGCGCCGACCCAGCTTTCTTTGACAAAG
TGGTTGATAAATCTGGCTCGAGCGTGGTGGCGGAGCGGAGGTGGAGGGTCTGAGGTCTTCACTCGAAGATTCGTTGGGACTGGGAACAGACAGCCGCTACAACCTGGACCAAGTCC
TTGAACAGGGAGGTGTCCAGTTTGTGTCAGAACTCGCCGTGTCGTAACCTCCGATCCAAAGGATGTCCGAGCGGTGAAAAATGCCCTGAAGATCGACATCCATGTATCCCTGATGAAG
GTCGAGCGCCGCAAAATGGCCAGATCGAAGAGGTGTTAAAGTGGTGTACCTGTGGATGATCATCTTTAAAGTGTCTGCTTTCGGCAAGATCCGCTATGGCACACTGTAATCGACGGGGTACGCGCAACA
TGCTGAACATTTTCGACGGCGGTATGAAGGATCGCCGTGTTTCGAGGGCAAAAAGATCACTGTAACAGGGACCCGTGGAAACGGCAACAAAATATCGACGAGCCGCTGATCACCCTGAGCGGT
CCATGCTTCCGAGTAACCATCAACAGCTAATCTAGAGTCGGGGCGCCGCGCTTCGAGCAGACATGATAAGATACATTTGATGAGTTGGACAAACCAACTAGAATGCAAGTGAAGAAAAATG
CTTTATTTGTAATTTGATGCTATTGCTTTATTTGTAACCATATAAGTGAATAAACAAGTTAAACAACAACATTTGATTCATTTATGTTTCAGGTTACGGGGAGGTGGTGGGAGTTT
TTAAAGCAAGTAAAACTTACAAATGTGTAATAATCGATAAGGATCCGTCGACCGATGCCCTTAGAGAGCTTCAACCCAGTCAAGCTCTCCGGTGGGCGGGGGCATGACTATCGTCGCGCAC
TTATGACTGTCTTTATCATGCAACTCGTAGGACAGGTGCCGCGACGCTCTTCGCTTCCCTGCTCACTGACTCGCTGCGCTCGGTGCTTCGCTGCGGCGAGCGGTATCAGCTCACTCAAAG
CGGTAATACGGTTATCCACAGAATCAGGGATAACGCAAGAAAGAACATGTGAGCAAAAGCCAGCAAAAGCCAGGAACCGTAAAAGGCCGCTGTGCTGGCGTTTTCCATAGGCTCCGCCC
CCTGACGAGCATCAAAAAATCGAGCTCAAGTCAAGGTGGCGAAACCCGACAGGACTATAAAGATCAGGGCTTTCCCTGGAAAGCTCCCTCGTGGCTCTCTGTTCCGACCTCGCGCTT
ACCGGATACCTGTCCGCTTTCTCCCTTCGGGAAGCGTGGCGCTTTCTCATAGCTCAAGCTGTAGGTATCTCAGTTCCGGTGTAGGTGCTTCGCTCAAGCTGGGCTGTGTGACAAACCCCGCT
CAGCCGACCCGCTGCGCTTATCCGGTAACTATCGCTTGGAGTCCAACCCGTAAGACAGCACTTATCGCCACTGGCAGCAGCCACTGGTAAACAGGATAGCAGAGCGAGGTATGAGCGGTGCT
ACAGAGTCTTGAAGTGGTGGCTAACTACGGCTACACTAGAAGAACAGTATTTGGTATCTGCGCTCTGCTGAAGCCAGTACCTTCGAAAAAGAGTGGTAGCTCTTGATCGGCAAAACAACC
ACCGTGGTAGCGGTGGTTTTTTTGTGTAAGCAGCAGATACCGCGCAAAAAAAGGATCTCAAGAAGATCCTTTGATCTTTTACGGGGTCTGACCTCAGTGGAAACGAAAACTCAGTTAA
GGGATTTTGGTCAAGATATCAAAAAGGATCTTCACTAGATCCTTTTAAATAAAAATGAAGTTTAAATCAATCAAAGTATATAGATAAATTTGGTCTGACAGCGGGCCGAAATGCTAA
ACCCTGCAAGTGGTTACCAAGTCTGATCAGTGGGACCGATCTCAGCGATCTGCTTTCGTTGCTCCATAGTGGCTGACTCCCGCTCGTGTAGTCACTACGATTCGTGAGGGCTTACCAT
CAGGCCCCAGCGCAGCAATGATGCCGCGAGAGCCGCTTACCAGCCCGGATTTGTGCAAGTGAACAGCCAGCAGCGAGGGAGGGCCGAGCGAAGAGTGGTCTGCTACTTTGTCCGCTCCATCC
AGTCTATGAGCTGCTGCTGATGCTAGAGTAAGAAGTTCGCCAGTGAAGTATTTCCGAAGAGTTGGCCATTTGCTACTGGCATCGTGGTATCACGCTCGCTTGGTATAGGCTTCGTTCAACT
CTGGTTCACAGCGGTCAAGCCGGTACATGATCACCATATTATGAAGAAATGCACTGCTTTCAGGGCCCTCCGATCGTTGTCAGAAAGTAAAGTGGCCCGGTTGTGCTCATGGTAAATGG
CAGACACACAATTTCTTACCGTATGCCATCCGTAAGTGCCTTTCCGTCGACCGGAGTACTCAACAAGTCTGTTTTGTAGTATGTATACGGGCAACAAGCTGCTTCCCGCGCTTA
TACGGGACAACACCGCCACATAGCAGTACTTTGAAAGTGTCTCATCGGAAATCGTTTTCGGGGCGAAAGACTCAAGGATCTTGGCGCTATTGAGATCCAGTTGATATAGCCACTTTCG
CACCAGTGTATCTCAGCATCTTTTACTTTTCCAGCGTTCGGGGTGTGCAAAAACAGGCAAGCAAAATGCCGCAAAAGAGGGAATGAGTGGACACGAAAAATGTTGGATGCTCATACTCGTCC
TTTTTCAATATTAAGCAATTTATAGGGTACTAGTACGCTCTCAAGGATAAGTAAAGTAAATTAAGGTACGGGAGTATGGACAGGCCCAATAAAAATCTTTATTTTTCATTACATCTG
TGTGTTGGTTTTTGTGTAATCGATAGTACTAACATACGCTCTCATCAAAAACAAACGAAACAAACAACTAGCAAAATAGGCTGTCCCGTGAAGTGCAGGTTGCCAGAACATTTCTCT

Appendix 5. Schematic representation of TRIB3/SmBiT 2.1N plasmid



GGCCTAACTGGCCGTACCTGAGTCTAAATGAGTCTTCGACCTCGCGGGGCGCTTAAGCGGTGGTTAGGGTTTGTCTGACGCGGGGGAGGGGGAAGAAACGAAACTCTCATTGCGAGGCG
GCTCGGGGTTTGGTCTTGGTGGCCACGGGACGCGAGAAGAGCGCCGCGATCTCTTAAGCACCCCGCCCTCCGTGGAGGCGGGGTTTGGTGGCGGGTGGTAACCTGGCGGGCGCTGACTCG
GGCGGGTGGCGGCGCCAGAGTGTGACCTTTTCGGTGTGCTCGCAGACCCCGGGCGGCGCCCGCGGCGGCGACGGGCTCGTGGGCTTAGGCTCCATGGGACCGTATACGTGGACAGGCTC
TGGAGCATCCGCACGACTGCGGTGATATACCGGAGACTTCTGCGGGACGAGCCGGGTACGCGGGTACGCGGGAGCGTCCGTTGGGCGACAAACACAGGACGGGGACAGGTACACTATCTTG
TCACCCGGAGGCGGAGGGACTCGAGGAGCTTCAGGGAGTGGCGCAGCTTTCATCCCGTGGCCGTTGCTCGCGTTTGGTGGCGGTCCCGGAAAGAAATATATTGCAATGCTTTAGTTCT
ATGATGACACAAACCCGCCAGCGTCTTGTCAATGGCGAAGTCGAACACGAGATCGAGTCGGGGCGGCGGTTCCAGGTCCACTTCGCATATAAAGTGACGCGTGTGGCCTCGAACCCAG
CGACCTGACGAGCCGCTTAAAGCTTGGCAATCCGGTACTGTGGTAAAGCCACAGATCTGCTAGCGATCGCTAAAGTGGGAGCTCAGGGGAATATCAACAAGTTGTACAAAAAGCAGGC
TCCCGGGCGCCCCCTTACCATGCGAGCCACCCCTTGGCTGCTCCTGCGGGTCCCTGTCCAGGAAGAAGCGTGGAGTTGGATGACAACCTAGATACCGAGCGTCCCGTCCAGAAACGAGCT
CGAAGTGGGCGCCAGCCAGACTGCCCTTGCCTGTGCGCTGAGCCACCTACTGCTCAGATCGTCAACTGCTGCGCAACTGCTGTGGCCACTGCCCTCCGCTTGGGCGCTATGCTCCTGGAGCCGAG
GAGGCGGGCGGGCTACCGGGCCCTGCACTGCCCCACAGGCACTGAGTATACCTGCAAGGTGTACCCCGTCCAGGAAGCCCTGGCGGTGCTGGAGCCCTACGCGCGGCTCCCGCCGCAAGCAT
GTGGCTCGGCCACTGAGGCTTGGCTGTTACCCAGCTCTCTACGCCTTTTCTACTCGGACCCATGGGACATGCACAGCTGGTGGCAAGCGCCACCGTATCCCTGAGCTGAGGCTGCCGTG
CTCTTCGCGCAGATGGCCACCGCCCTGGTGCATGTACCAGCAGCGTGTGGTCTGCGTGATCTCAAGCTGTGTCGTTTTGCTTCGCTGACCGTGAAGAAGAAGCTGGTGTAGAGAACCTG
GAGGACTCTGCGTGTGACTGGCCAGATGATTCCTGTGGGACAAGCAGCGTGGCCAGCTACGTGGGACTGAGATACTCAGCTCACGGGCTCATACTCGGGCAAGGACGCGATGTCTGG
AGCTGGGCGTGGCGCTTTCACATGCTGGCCGCACTACCCCTTCCAGGACTCGGAGCTGTCTGCTCTTGGCAAGATCCGCCGGGGCTACGCCCTTGCCTGCAAGGCTCTCGGCCCT
GCCCGTGTCTGGTTGCTGCTCTCTCGTGGGAGCCAGTGAACGGCTCACAGCCACAGGCACTCTCTGCACCCCTGGTGGCAGGACCCGATGCCCTTAGCTCCAACCCGATCCCATCTC
TGGGAGGCTGCCAGGTGGTCCCTGATGGACTGGGCTGGACGAAGCCAGGGAAGAGGAGGAGAGACAGAGAAGTGGTTGTATGGCCAAGGGTGGCGCGCCGACCCAGCTTCTTGTACAAAAT
GGTGTATAATCTGGCTCGAGCGGTGGTGGCGGAGCGGAGTGGAGGGTGTGAGTGTGACCGGCTACCGGCTGTTGAGGAGATCTGTAATCTAGAGTGGGGCGCGCGCCGCTTCGAGCA
GACATGATAAGATACATGATGAGTTGGACAACCAACTAGAAATGCAGTGAAGAAATGCTTATTTGTGAAATTTGTGATGCTATTGCTTTATTTGTAACCATATAAGCTGCAATAAACA
GTTAACAACAACAATGCAATCATTATGTTTTCAGGTTCAAGGGGAGGTGTGGGAGGTTTTTAAAGCAAGTAAACCTTACAAAATGTGGTAAAATCGATAAGGATCCGTGCACCGATGCCCTT
GAGAGCCTTCAACCCAGTCACTCTCCGGTGGGCGCGGGGATGACTATCGTGGCGCACTTACTGCTGCTCTTATCATGCAACTGTAAGGACAGGTGCCGCGCAGCGCTTCCGCTTCTC
CGCTCACTGACTCGCTGCGCTCGGTGCTGGCTGGCGGAGCGGTATCAGTCACTCAAGGGCGGTAATACGGTTATCCACAGAATCAGGGGATAACGCAAGAAAGAACATGTGAGCAAAAGGCC
AGCAAAAGGCCAGGAACCGTAAAAGGGCGGTTGCTGGCGTTTTCCATAGGCTCCGCCCCCTGACGAGCATCACAAAATCGAGCTCAAGTCAAGGTTGGCAGAACCCGACAGGACTATAAA
GATACGAGGCTTTCCCGTGAAGCTCCCTGTCGCTCTCTGTTCCGACCTGGCGCTTACCAGGATACCTGTCCGCTTCTCCCTTCGGGAAGCGTGGCGCTTCTCATAGCTCAGCTGTA
GGTATCTCAGTTCCGTTAGGTGCTGCTCAAGCTGGGCTGTGTCAGCAACCCCGTTCAGCCGACCGCTGCGCTTATCCGGTAACTATCGTCTTGAAGTCAAACCGGTAAAGACAGGACT
TATGCCACTGGCAGCAGCACTGGTAAAGGATAGCAGAGCAGGATGTAGGCGGTGCTACAGAGTCTTGAAGTGGTGGCTAACTACGGCTACACTAGAAGAAGATTTGGTATCTGCG
CTCTGCTGAAGCCAGTTACCTCGGAAAAAGAGTTGGTAGCTCTTGTCCGGCAACAAACCCGCTGGTAGCGGTGGTTTTTGTGTAAGCAGCAGATACCGCGAGAAAAAAGGATCTC
AAGAAGATCCTTTGATCTTTTACGGGGTCTGACGCTCAGTGGAAACGAAAACCTACGTTAAGGGATTTTGGTTCATGAGATATCAAAAAGGATCTCACCTAGATCCTTTAAATAAAAATGAA
GTTTTAAATCAATCTAAAGTATATAGTAAACTTGGTCTGACAGCGGCGCAAGTGTAAACCACTGCAAGTGGTACCAGTGTGATCAGTGGGACCGGATCTCAGCGATCGCTTATTTCCG
TTCCGCTAAGTGGCTGACTCCCGCTGCTGATGATCACTACGATTCTGTGAGGGCTTACCTACGGCCCAAGCAATGATGCCGCGAGAGCCGCTTTCCCGGCGCCGATTTGTGAGCAAT
GAACAGCCAGCAGGAGGGCGGAGCAAGAAGTGGTCTGCTACTTTTCCGCTCCATCCAGTCTATGAGCTGCTGCTGATGCTAGAGTAAAGAGTTCGCCAGTGGTGGTTCGGAAGT
TGTGGCCATTGCTACTGGCATCGTGGTATCAGCTCGTCTGCTGATGGCTCGTCAACTCGTTCAGCGGTCAGCCGGTCAAGCCGGTCAATGATCACCCATATATGAAGAAATGCAAGTCAAGCTC
CTTAGGGCTCCGATCGTTGTAGAAAGTAAAGTTGGCGCGGTGTTGCTGCTCATGGTAAATGGCAGCACTACACAATCTCTAACGTCATGCCATCGTAAGATGCTTTTCCGTGACCGCGAGTA
CTCAACCAAGTCTTTTGTGAGTGTATACGGCGACCAAGCTGCTTGGCCGGGCTATACGGGCAACBCTACCGCGCCACATAGCAGTACTTTGAAAGTGTCTCATCGGGAATCGTTC
TTGCGGGCGGAAAGACTCAAGGATCTTGGCGCTATTGAGATCCAAGTTCGATATAGCCCACTTTCACCCAGTGTGATCTTCAAGTCTTACCTTCCAGGCTTTCCGGGTGTGCAAAAACAGG
CAAGCAAAATGCCCAAAAGAGGAAATGAGTGCACACGAAAATGTGGATGCTCATACTGCTCTTTTCAAATATATTGAAGCAATTTACAGGGTACTAGTACGCTCTCAAGGATAAGTAAG
TAATATAAGGTACGGAGGATTTGGCAGGCGCAATAAAATATCTTTATTTCAATCATCTGTGTGTTGTTTTGTGTGTAATCGATAGTACTAACATACGCTCTCCATCAAAAACAAAACGA
AACAAAACAACTAGCAAAATAGGCTGTCCCGAGTCAAGTGCAGGTGCCAGAACATTTCTCT

Appendix 6. iBAQ values, protein and gene names of peptides identified by mass spectrometry as interacting with wild-type and variant forms of TRIB3

| WT | V107M | S146N | R149G | R153H | R181C | Protein names | Gene names |
|------|-------|-------|-------|-------|-------|---|----------------|
| 20.4 | 20.2 | 19.9 | 20.1 | 20.3 | 20.1 | [3-methyl-2-oxobutanoate dehydrogenase [lipoamide]] kinase, mitochondrial | <i>BCKDK</i> |
| 18.3 | 18.1 | 18.0 | 15.0 | 17.8 | 18.3 | 1-phosphatidylinositol 4,5-bisphosphate phosphodiesterase eta-1 | <i>PLCH1</i> |
| 21.1 | 20.0 | 20.9 | 23.5 | 20.5 | 20.5 | 10 kDa heat shock protein, mitochondrial | <i>HSPE1</i> |
| 21.8 | 21.7 | 21.8 | 21.6 | 21.8 | 21.8 | 116 kDa U5 small nuclear ribonucleoprotein component | <i>EFTUD2</i> |
| 18.9 | 19.0 | 19.5 | 21.2 | 19.0 | 19.6 | 14-3-3 protein beta/alpha | <i>YWHAB</i> |
| 22.1 | 21.2 | 21.7 | 22.7 | 21.3 | 22.2 | 14-3-3 protein epsilon | <i>YWHAE</i> |
| 20.0 | 19.9 | 20.1 | 20.7 | 19.9 | 20.0 | 14-3-3 protein eta | <i>YWHAH</i> |
| 21.7 | 21.6 | 21.7 | 22.2 | 21.8 | 21.7 | 14-3-3 protein theta | <i>YWHAQ</i> |
| 22.0 | 21.7 | 22.2 | 23.4 | 21.7 | 22.1 | 14-3-3 protein zeta/delta | <i>YWHAZ</i> |
| 15.0 | 16.2 | 16.1 | 15.0 | 15.7 | 16.6 | 2-5A-dependent ribonuclease | <i>RNASEL</i> |
| 19.8 | 20.6 | 20.9 | 20.3 | 19.7 | 20.6 | 2,3-cyclic-nucleotide 3-phosphodiesterase | <i>CNP</i> |
| 20.7 | 20.9 | 21.1 | 20.9 | 20.9 | 20.7 | 2,4-dienoyl-CoA reductase, mitochondrial | <i>DECR1</i> |
| 23.9 | 24.6 | 24.7 | 22.2 | 24.2 | 24.9 | 26S protease regulatory subunit 10B | <i>PSMC6</i> |
| 23.9 | 24.6 | 24.6 | 22.3 | 24.3 | 24.5 | 26S protease regulatory subunit 4 | <i>PSMC1</i> |
| 24.6 | 24.9 | 24.7 | 22.4 | 24.7 | 25.0 | 26S protease regulatory subunit 6A | <i>PSMC3</i> |
| 23.6 | 24.2 | 24.1 | 21.8 | 23.8 | 24.1 | 26S protease regulatory subunit 6B | <i>PSMC4</i> |
| 24.0 | 24.4 | 24.3 | 21.8 | 24.3 | 24.5 | 26S protease regulatory subunit 7 | <i>PSMC2</i> |
| 24.0 | 24.6 | 24.6 | 22.2 | 24.3 | 24.7 | 26S protease regulatory subunit 8 | <i>PSMC5</i> |
| 21.5 | 21.7 | 21.7 | 15.0 | 21.4 | 21.8 | 26S proteasome non-ATPase regulatory subunit 1 | <i>PSMD1</i> |
| 22.6 | 23.1 | 23.2 | 20.1 | 22.7 | 23.3 | 26S proteasome non-ATPase regulatory subunit 11 | <i>PSMD11</i> |
| 21.0 | 21.2 | 21.1 | 15.0 | 21.1 | 21.4 | 26S proteasome non-ATPase regulatory subunit 12 | <i>PSMD12</i> |
| 21.1 | 21.7 | 21.0 | 19.1 | 21.5 | 21.7 | 26S proteasome non-ATPase regulatory subunit 13 | <i>PSMD13</i> |
| 15.0 | 18.0 | 18.2 | 15.0 | 18.2 | 18.8 | 26S proteasome non-ATPase regulatory subunit 14 | <i>PSMD14</i> |
| 22.6 | 22.9 | 22.8 | 20.8 | 22.9 | 23.1 | 26S proteasome non-ATPase regulatory subunit 2 | <i>PSMD2</i> |
| 21.3 | 21.5 | 21.3 | 15.0 | 21.2 | 21.5 | 26S proteasome non-ATPase regulatory subunit 3 | <i>PSMD3</i> |
| 24.0 | 24.5 | 24.0 | 21.4 | 23.9 | 24.3 | 26S proteasome non-ATPase regulatory subunit 4 | <i>PSMD4</i> |
| 24.3 | 24.7 | 24.4 | 22.9 | 24.3 | 24.4 | 26S proteasome non-ATPase regulatory subunit 6 | <i>PSMD6</i> |
| 21.5 | 22.0 | 21.8 | 19.6 | 21.6 | 21.8 | 26S proteasome non-ATPase regulatory subunit 7 | <i>PSMD7</i> |
| 21.9 | 22.1 | 22.9 | 25.1 | 22.3 | 22.2 | 28 kDa heat- and acid-stable phosphoprotein | <i>PDAP1</i> |
| 21.9 | 21.7 | 21.2 | 15.0 | 22.0 | 21.4 | 28S ribosomal protein S10, mitochondrial | <i>MRPS10</i> |
| 23.4 | 23.0 | 22.8 | 20.2 | 23.6 | 22.8 | 28S ribosomal protein S11, mitochondrial | <i>MRPS11</i> |
| 21.5 | 21.3 | 21.1 | 21.1 | 21.0 | 21.5 | 28S ribosomal protein S12, mitochondrial | <i>MRPS12</i> |
| 23.6 | 22.9 | 22.4 | 15.0 | 23.6 | 22.6 | 28S ribosomal protein S14, mitochondrial | <i>MRPS14</i> |
| 21.6 | 21.1 | 21.1 | 18.7 | 21.4 | 20.5 | 28S ribosomal protein S15, mitochondrial | <i>MRPS15</i> |
| 24.0 | 22.9 | 23.6 | 18.8 | 23.5 | 23.6 | 28S ribosomal protein S16, mitochondrial | <i>MRPS16</i> |
| 24.0 | 23.7 | 23.3 | 20.9 | 24.3 | 23.5 | 28S ribosomal protein S17, mitochondrial | <i>MRPS17</i> |
| 21.6 | 21.6 | 20.6 | 20.2 | 21.7 | 21.1 | 28S ribosomal protein S18a, mitochondrial | <i>MRPS18A</i> |
| 23.6 | 23.7 | 23.6 | 19.2 | 24.1 | 23.3 | 28S ribosomal protein S18b, mitochondrial | <i>MRPS18B</i> |

| | | | | | | | |
|------|------|------|------|------|------|---|-----------------|
| 22.9 | 22.3 | 22.0 | 19.5 | 22.7 | 22.0 | 28S ribosomal protein S18c, mitochondrial | <i>MRPS18C</i> |
| 21.9 | 21.9 | 21.4 | 15.0 | 22.3 | 21.5 | 28S ribosomal protein S2, mitochondrial | <i>MRPS2</i> |
| 23.7 | 22.7 | 22.4 | 20.2 | 23.7 | 22.5 | 28S ribosomal protein S21, mitochondrial | <i>MRPS21</i> |
| 24.2 | 23.7 | 23.5 | 20.9 | 24.2 | 23.6 | 28S ribosomal protein S22, mitochondrial | <i>MRPS22</i> |
| 24.5 | 24.0 | 23.6 | 22.0 | 24.6 | 23.7 | 28S ribosomal protein S23, mitochondrial | <i>MRPS23</i> |
| 23.9 | 23.7 | 23.6 | 21.0 | 24.1 | 23.3 | 28S ribosomal protein S25, mitochondrial | <i>MRPS25</i> |
| 24.0 | 23.7 | 23.2 | 20.9 | 24.1 | 23.7 | 28S ribosomal protein S26, mitochondrial | <i>MRPS26</i> |
| 21.2 | 20.8 | 20.9 | 15.0 | 21.1 | 20.7 | 28S ribosomal protein S27, mitochondrial | <i>MRPS27</i> |
| 24.2 | 23.1 | 22.6 | 19.4 | 24.1 | 23.0 | 28S ribosomal protein S28, mitochondrial | <i>MRPS28</i> |
| 20.2 | 20.0 | 19.8 | 15.0 | 20.2 | 19.8 | 28S ribosomal protein S29, mitochondrial | <i>DAP3</i> |
| 20.6 | 20.2 | 19.3 | 15.0 | 20.4 | 19.7 | 28S ribosomal protein S30, mitochondrial | <i>MRPS30</i> |
| 23.2 | 22.9 | 22.5 | 20.3 | 23.6 | 22.8 | 28S ribosomal protein S31, mitochondrial | <i>MRPS31</i> |
| 23.9 | 23.2 | 23.0 | 20.1 | 24.1 | 23.0 | 28S ribosomal protein S33, mitochondrial | <i>MRPS33</i> |
| 24.1 | 23.5 | 23.4 | 18.8 | 24.0 | 23.4 | 28S ribosomal protein S34, mitochondrial | <i>MRPS34</i> |
| 23.7 | 23.1 | 23.0 | 19.0 | 23.7 | 23.0 | 28S ribosomal protein S35, mitochondrial | <i>MRPS35</i> |
| 22.2 | 22.0 | 21.9 | 15.0 | 22.5 | 21.7 | 28S ribosomal protein S5, mitochondrial | <i>MRPS5</i> |
| 23.3 | 22.6 | 22.6 | 19.8 | 23.4 | 22.4 | 28S ribosomal protein S6, mitochondrial | <i>MRPS6</i> |
| 24.4 | 23.9 | 23.6 | 20.9 | 24.3 | 23.7 | 28S ribosomal protein S7, mitochondrial | <i>MRPS7</i> |
| 24.3 | 23.9 | 23.7 | 21.8 | 24.4 | 23.7 | 28S ribosomal protein S9, mitochondrial | <i>MRPS9</i> |
| 15.0 | 18.4 | 18.5 | 19.1 | 18.2 | 18.8 | 3-hydroxyacyl-CoA dehydrogenase type-2 | <i>HSD17B10</i> |
| 19.6 | 19.5 | 18.9 | 18.9 | 19.9 | 19.7 | 39S ribosomal protein L1, mitochondrial | <i>MRPL1</i> |
| 23.5 | 23.5 | 23.0 | 22.4 | 23.6 | 23.1 | 39S ribosomal protein L11, mitochondrial | <i>MRPL11</i> |
| 24.0 | 23.9 | 23.2 | 21.9 | 24.0 | 23.7 | 39S ribosomal protein L12, mitochondrial | <i>MRPL12</i> |
| 20.5 | 20.3 | 19.4 | 15.0 | 20.3 | 19.9 | 39S ribosomal protein L13, mitochondrial | <i>MRPL13</i> |
| 15.0 | 18.1 | 15.0 | 15.0 | 18.0 | 17.6 | 39S ribosomal protein L14, mitochondrial | <i>MRPL14</i> |
| 22.7 | 22.7 | 21.8 | 20.5 | 22.9 | 22.3 | 39S ribosomal protein L15, mitochondrial | <i>MRPL15</i> |
| 22.1 | 21.7 | 20.7 | 20.0 | 22.1 | 21.0 | 39S ribosomal protein L16, mitochondrial | <i>MRPL16</i> |
| 21.9 | 21.6 | 21.1 | 19.5 | 22.0 | 21.4 | 39S ribosomal protein L17, mitochondrial | <i>MRPL17</i> |
| 21.1 | 20.7 | 20.0 | 19.3 | 21.1 | 20.6 | 39S ribosomal protein L18, mitochondrial | <i>MRPL18</i> |
| 21.3 | 21.0 | 19.9 | 15.0 | 21.3 | 20.3 | 39S ribosomal protein L2, mitochondrial | <i>MRPL2</i> |
| 19.8 | 19.6 | 18.6 | 18.0 | 19.7 | 19.2 | 39S ribosomal protein L20, mitochondrial | <i>MRPL20</i> |
| 20.5 | 20.5 | 19.4 | 19.2 | 20.2 | 19.9 | 39S ribosomal protein L21, mitochondrial | <i>MRPL21</i> |
| 21.8 | 21.3 | 20.7 | 20.5 | 21.7 | 20.8 | 39S ribosomal protein L22, mitochondrial | <i>MRPL22</i> |
| 22.0 | 21.7 | 20.5 | 19.9 | 22.0 | 21.2 | 39S ribosomal protein L23, mitochondrial | <i>MRPL23</i> |
| 22.1 | 22.1 | 21.1 | 19.6 | 22.3 | 21.6 | 39S ribosomal protein L24, mitochondrial | <i>MRPL24</i> |
| 22.1 | 21.6 | 21.1 | 20.2 | 22.2 | 21.7 | 39S ribosomal protein L27, mitochondrial | <i>MRPL27</i> |
| 22.2 | 22.4 | 21.1 | 18.8 | 22.6 | 21.3 | 39S ribosomal protein L28, mitochondrial | <i>MRPL28</i> |
| 20.7 | 20.8 | 20.4 | 15.0 | 21.1 | 20.4 | 39S ribosomal protein L3, mitochondrial | <i>MRPL3</i> |
| 20.2 | 20.0 | 20.1 | 15.0 | 20.6 | 19.8 | 39S ribosomal protein L30, mitochondrial | <i>MRPL30</i> |
| 20.6 | 19.7 | 20.0 | 15.0 | 19.9 | 19.8 | 39S ribosomal protein L32, mitochondrial | <i>MRPL32</i> |
| 20.9 | 20.5 | 20.3 | 19.9 | 20.9 | 20.5 | 39S ribosomal protein L33, mitochondrial | <i>MRPL33</i> |
| 21.1 | 20.7 | 19.5 | 15.0 | 21.1 | 20.1 | 39S ribosomal protein L35, mitochondrial | <i>MRPL35</i> |
| 20.9 | 20.8 | 20.4 | 15.0 | 20.8 | 20.2 | 39S ribosomal protein L37, mitochondrial | <i>MRPL37</i> |
| 21.5 | 21.0 | 19.9 | 15.0 | 21.2 | 20.7 | 39S ribosomal protein L38, mitochondrial | <i>MRPL38</i> |
| 22.2 | 21.7 | 21.1 | 20.2 | 22.1 | 21.4 | 39S ribosomal protein L39, mitochondrial | <i>MRPL39</i> |
| 20.1 | 20.0 | 19.7 | 19.1 | 20.3 | 19.7 | 39S ribosomal protein L4, mitochondrial | <i>MRPL4</i> |
| 21.9 | 21.6 | 20.9 | 20.7 | 21.8 | 21.3 | 39S ribosomal protein L40, mitochondrial | <i>MRPL40</i> |
| 20.7 | 20.5 | 19.7 | 19.2 | 20.7 | 20.4 | 39S ribosomal protein L41, mitochondrial | <i>MRPL41</i> |
| 21.7 | 21.2 | 20.3 | 20.0 | 21.6 | 20.7 | 39S ribosomal protein L43, mitochondrial | <i>MRPL43</i> |

| | | | | | | | |
|------|------|------|------|------|------|--|---------------|
| 19.3 | 19.7 | 18.9 | 17.9 | 19.6 | 19.2 | 39S ribosomal protein L44, mitochondrial | <i>MRPL44</i> |
| 22.8 | 22.5 | 21.4 | 20.5 | 22.8 | 22.0 | 39S ribosomal protein L45, mitochondrial | <i>MRPL45</i> |
| 21.9 | 21.9 | 21.2 | 20.6 | 22.0 | 21.6 | 39S ribosomal protein L46, mitochondrial | <i>MRPL46</i> |
| 22.3 | 22.2 | 21.2 | 19.9 | 22.3 | 21.6 | 39S ribosomal protein L47, mitochondrial | <i>MRPL47</i> |
| 20.4 | 20.1 | 19.9 | 19.6 | 20.5 | 20.0 | 39S ribosomal protein L48, mitochondrial | <i>MRPL48</i> |
| 21.7 | 21.9 | 20.8 | 19.9 | 22.2 | 21.2 | 39S ribosomal protein L51, mitochondrial | <i>MRPL51</i> |
| 24.0 | 23.0 | 22.7 | 20.2 | 23.5 | 23.4 | 39S ribosomal protein L53, mitochondrial | <i>MRPL53</i> |
| 21.6 | 21.3 | 20.7 | 20.1 | 21.7 | 21.2 | 39S ribosomal protein L55, mitochondrial | <i>MRPL55</i> |
| 21.4 | 21.3 | 20.7 | 15.0 | 21.7 | 20.7 | 39S ribosomal protein L9, mitochondrial | <i>MRPL9</i> |
| 25.2 | 24.9 | 25.1 | 24.4 | 25.2 | 24.9 | 40S ribosomal protein S10 | <i>RPS10</i> |
| 27.7 | 27.6 | 27.6 | 27.4 | 27.7 | 27.6 | 40S ribosomal protein S11 | <i>RPS11</i> |
| 26.2 | 26.1 | 26.2 | 25.0 | 26.1 | 26.1 | 40S ribosomal protein S12 | <i>RPS12</i> |
| 26.3 | 26.3 | 26.3 | 25.8 | 26.4 | 26.2 | 40S ribosomal protein S13 | <i>RPS13</i> |
| 27.1 | 27.2 | 27.0 | 26.8 | 27.2 | 27.0 | 40S ribosomal protein S14 | <i>RPS14</i> |
| 22.6 | 23.0 | 23.0 | 22.6 | 22.6 | 22.6 | 40S ribosomal protein S15 | <i>RPS15</i> |
| 24.7 | 24.7 | 24.7 | 23.5 | 24.8 | 24.6 | 40S ribosomal protein S15a | <i>RPS15A</i> |
| 27.2 | 27.3 | 27.1 | 26.9 | 27.2 | 27.1 | 40S ribosomal protein S16 | <i>RPS16</i> |
| 26.8 | 26.7 | 26.5 | 25.9 | 26.9 | 26.5 | 40S ribosomal protein S17 | <i>RPS17</i> |
| 27.2 | 27.3 | 27.1 | 26.6 | 27.1 | 27.0 | 40S ribosomal protein S18 | <i>RPS18</i> |
| 27.8 | 27.8 | 27.7 | 27.4 | 27.9 | 27.7 | 40S ribosomal protein S19 | <i>RPS19</i> |
| 27.6 | 27.5 | 27.5 | 26.4 | 27.6 | 27.4 | 40S ribosomal protein S2 | <i>RPS2</i> |
| 26.4 | 26.4 | 26.6 | 26.8 | 26.6 | 26.4 | 40S ribosomal protein S20 | <i>RPS20</i> |
| 20.4 | 20.4 | 20.5 | 22.7 | 20.3 | 20.1 | 40S ribosomal protein S21 | <i>RPS21</i> |
| 26.6 | 26.8 | 26.7 | 26.4 | 26.8 | 26.6 | 40S ribosomal protein S23 | <i>RPS23</i> |
| 25.8 | 25.9 | 25.7 | 24.8 | 25.9 | 25.8 | 40S ribosomal protein S24 | <i>RPS24</i> |
| 26.5 | 26.3 | 26.3 | 26.5 | 26.3 | 26.3 | 40S ribosomal protein S25 | <i>RPS25</i> |
| 26.0 | 26.0 | 25.7 | 25.6 | 25.9 | 25.7 | 40S ribosomal protein S26 | <i>RPS26</i> |
| 25.1 | 25.7 | 25.9 | 26.1 | 25.4 | 26.1 | 40S ribosomal protein S27 | <i>RPS27</i> |
| 19.8 | 20.4 | 20.8 | 15.0 | 20.3 | 21.4 | 40S ribosomal protein S27 | <i>RPS27L</i> |
| 24.2 | 24.1 | 23.9 | 24.4 | 24.0 | 23.8 | 40S ribosomal protein S28 | <i>RPS28</i> |
| 26.4 | 26.5 | 26.2 | 25.8 | 26.5 | 26.0 | 40S ribosomal protein S29 | <i>RPS29</i> |
| 26.3 | 26.3 | 26.1 | 25.2 | 26.3 | 26.1 | 40S ribosomal protein S3 | <i>RPS3</i> |
| 24.9 | 24.8 | 24.7 | 24.9 | 24.7 | 24.6 | 40S ribosomal protein S30 | <i>FAU</i> |
| 27.9 | 27.9 | 27.9 | 27.2 | 27.8 | 27.7 | 40S ribosomal protein S3a | <i>RPS3A</i> |
| 27.0 | 27.1 | 27.1 | 26.5 | 27.0 | 26.9 | 40S ribosomal protein S4, X isoform | <i>RPS4X</i> |
| 26.7 | 26.8 | 26.7 | 25.5 | 26.8 | 26.4 | 40S ribosomal protein S5 | <i>RPS5</i> |
| 27.0 | 27.1 | 27.0 | 26.8 | 27.1 | 26.8 | 40S ribosomal protein S6 | <i>RPS6</i> |
| 26.8 | 26.8 | 27.0 | 26.4 | 26.8 | 26.8 | 40S ribosomal protein S7 | <i>RPS7</i> |
| 28.3 | 28.2 | 28.1 | 27.2 | 28.3 | 28.1 | 40S ribosomal protein S8 | <i>RPS8</i> |
| 25.9 | 25.8 | 26.1 | 24.3 | 25.8 | 25.7 | 40S ribosomal protein S9 | <i>RPS9</i> |
| 21.9 | 21.4 | 21.5 | 22.6 | 21.7 | 21.6 | 40S ribosomal protein SA | <i>RPSA</i> |
| 18.6 | 15.0 | 18.4 | 15.0 | 15.0 | 19.0 | 45 kDa calcium-binding protein | <i>SDF4</i> |
| 21.1 | 21.0 | 20.9 | 15.0 | 21.1 | 21.0 | 5-3 exoribonuclease 1 | <i>XRN1</i> |
| 22.9 | 22.9 | 22.7 | 22.0 | 23.2 | 22.6 | 5-3 exoribonuclease 2 | <i>XRN2</i> |
| 29.5 | 30.4 | 30.4 | 29.2 | 29.4 | 30.6 | 60 kDa heat shock protein, mitochondrial | <i>HSPD1</i> |
| 15.0 | 18.0 | 18.2 | 15.0 | 15.0 | 18.2 | 60 kDa SS-A/Ro ribonucleoprotein | <i>TROVE2</i> |
| 26.1 | 26.2 | 26.3 | 24.8 | 26.2 | 26.1 | 60S acidic ribosomal protein P0 | <i>RPLP0</i> |
| 27.2 | 26.6 | 26.8 | 25.9 | 26.6 | 26.4 | 60S acidic ribosomal protein P1 | <i>RPLP1</i> |
| 23.9 | 23.7 | 23.9 | 23.3 | 23.9 | 23.8 | 60S acidic ribosomal protein P2 | <i>RPLP2</i> |
| 27.0 | 27.2 | 27.1 | 26.8 | 27.0 | 26.9 | 60S ribosomal protein L10 | <i>RPL10</i> |

| | | | | | | | |
|------|------|------|------|------|------|--|----------------|
| 26.1 | 26.0 | 26.1 | 25.0 | 26.1 | 25.9 | 60S ribosomal protein L10a | <i>RPL10A</i> |
| 26.9 | 27.0 | 27.0 | 26.7 | 27.1 | 26.9 | 60S ribosomal protein L11 | <i>RPL11</i> |
| 26.3 | 26.2 | 26.2 | 25.3 | 26.5 | 26.1 | 60S ribosomal protein L12 | <i>RPL12</i> |
| 27.4 | 27.4 | 27.4 | 27.4 | 27.5 | 27.2 | 60S ribosomal protein L13 | <i>RPL13</i> |
| 24.9 | 25.0 | 25.2 | 24.6 | 24.9 | 24.9 | 60S ribosomal protein L13a | <i>RPL13A</i> |
| 27.0 | 26.9 | 26.7 | 26.4 | 26.9 | 26.6 | 60S ribosomal protein L14 | <i>RPL14</i> |
| 26.0 | 26.1 | 26.0 | 25.4 | 26.0 | 25.9 | 60S ribosomal protein L15 | <i>RPL15</i> |
| 26.7 | 26.7 | 26.6 | 26.5 | 26.6 | 26.4 | 60S ribosomal protein L17 | <i>RPL17</i> |
| 26.4 | 26.4 | 26.6 | 25.6 | 26.5 | 26.2 | 60S ribosomal protein L18 | <i>RPL18</i> |
| 27.2 | 27.1 | 27.2 | 27.1 | 27.2 | 27.0 | 60S ribosomal protein L18a | <i>RPL18A</i> |
| 26.5 | 26.6 | 26.6 | 25.8 | 26.6 | 26.4 | 60S ribosomal protein L19 | <i>RPL19</i> |
| 27.4 | 27.6 | 27.7 | 27.4 | 27.6 | 27.5 | 60S ribosomal protein L21 | <i>RPL21</i> |
| 25.9 | 26.0 | 26.1 | 26.3 | 25.9 | 25.9 | 60S ribosomal protein L22 | <i>RPL22</i> |
| 19.4 | 20.0 | 20.3 | 21.0 | 20.1 | 20.1 | 60S ribosomal protein L22-like 1 | <i>RPL22L1</i> |
| 26.2 | 26.3 | 26.1 | 25.1 | 26.1 | 26.3 | 60S ribosomal protein L23 | <i>RPL23</i> |
| 23.2 | 23.3 | 23.5 | 23.0 | 23.1 | 23.5 | 60S ribosomal protein L23a | <i>RPL23A</i> |
| 26.6 | 26.8 | 26.5 | 26.2 | 26.8 | 26.5 | 60S ribosomal protein L24 | <i>RPL24</i> |
| 22.3 | 22.6 | 22.9 | 22.9 | 22.4 | 22.3 | 60S ribosomal protein L26 | <i>RPL26</i> |
| 27.2 | 27.1 | 27.0 | 26.6 | 27.0 | 26.8 | 60S ribosomal protein L26-like 1 | <i>RPL26L1</i> |
| 25.9 | 26.0 | 26.1 | 25.8 | 26.1 | 26.0 | 60S ribosomal protein L27 | <i>RPL27</i> |
| 26.8 | 26.8 | 26.8 | 27.0 | 26.9 | 26.6 | 60S ribosomal protein L27a | <i>RPL27A</i> |
| 26.1 | 26.2 | 26.0 | 26.1 | 26.2 | 25.8 | 60S ribosomal protein L28 | <i>RPL28</i> |
| 25.8 | 25.9 | 26.1 | 26.3 | 25.7 | 25.5 | 60S ribosomal protein L29 | <i>RPL29</i> |
| 27.1 | 27.1 | 27.3 | 26.7 | 27.1 | 27.0 | 60S ribosomal protein L3 | <i>RPL3</i> |
| 15.0 | 21.5 | 21.0 | 15.0 | 20.6 | 21.1 | 60S ribosomal protein L3-like | <i>RPL3L</i> |
| 26.6 | 26.6 | 26.8 | 27.1 | 26.6 | 26.5 | 60S ribosomal protein L30 | <i>RPL30</i> |
| 26.7 | 26.8 | 26.4 | 26.2 | 26.7 | 26.3 | 60S ribosomal protein L31 | <i>RPL31</i> |
| 26.8 | 26.8 | 26.8 | 26.9 | 26.8 | 26.8 | 60S ribosomal protein L32 | <i>RPL32</i> |
| 25.7 | 25.7 | 25.6 | 25.7 | 25.8 | 25.6 | 60S ribosomal protein L34 | <i>RPL34</i> |
| 26.2 | 25.9 | 26.0 | 26.0 | 26.0 | 25.8 | 60S ribosomal protein L35 | <i>RPL35</i> |
| 25.6 | 25.6 | 25.5 | 25.3 | 25.6 | 25.3 | 60S ribosomal protein L35a | <i>RPL35A</i> |
| 26.0 | 25.8 | 25.8 | 25.6 | 26.0 | 25.8 | 60S ribosomal protein L36 | <i>RPL36</i> |
| 24.8 | 24.8 | 24.8 | 24.1 | 24.7 | 24.6 | 60S ribosomal protein L36a | <i>RPL36A</i> |
| 18.0 | 18.3 | 19.1 | 18.1 | 18.4 | 18.1 | 60S ribosomal protein L36a-like | <i>RPL36AL</i> |
| 21.4 | 21.3 | 21.3 | 20.3 | 21.1 | 20.9 | 60S ribosomal protein L37 | <i>RPL37</i> |
| 26.2 | 26.3 | 26.3 | 26.4 | 26.2 | 26.0 | 60S ribosomal protein L37a | <i>RPL37A</i> |
| 24.9 | 24.6 | 24.5 | 25.7 | 24.7 | 24.6 | 60S ribosomal protein L38 | <i>RPL38</i> |
| 27.8 | 27.8 | 27.8 | 27.4 | 27.7 | 27.7 | 60S ribosomal protein L4 | <i>RPL4</i> |
| 25.0 | 24.7 | 24.5 | 24.7 | 24.8 | 24.6 | 60S ribosomal protein L5 | <i>RPL5</i> |
| 26.7 | 26.8 | 26.9 | 26.5 | 26.8 | 26.7 | 60S ribosomal protein L6 | <i>RPL6</i> |
| 26.1 | 26.3 | 26.4 | 25.8 | 26.1 | 26.1 | 60S ribosomal protein L7 | <i>RPL7</i> |
| 19.3 | 19.0 | 18.9 | 18.9 | 19.1 | 18.8 | 60S ribosomal protein L7-like 1 | <i>RPL7L1</i> |
| 27.3 | 27.4 | 27.5 | 27.6 | 27.5 | 27.2 | 60S ribosomal protein L7a | <i>RPL7A</i> |
| 27.7 | 27.8 | 27.8 | 27.8 | 27.8 | 27.6 | 60S ribosomal protein L8 | <i>RPL8</i> |
| 26.3 | 26.4 | 26.2 | 24.7 | 26.7 | 26.1 | 60S ribosomal protein L9 | <i>RPL9</i> |
| 26.0 | 25.9 | 25.7 | 25.9 | 26.0 | 26.1 | 78 kDa glucose-regulated protein | <i>HSPA5</i> |
| 20.2 | 19.4 | 19.1 | 15.0 | 20.1 | 19.0 | 7SK snRNA methylphosphate capping enzyme | <i>MEPCE</i> |
| 19.4 | 19.9 | 19.9 | 19.6 | 19.4 | 21.2 | A-kinase anchor protein 13 | <i>AKAP13</i> |
| 18.5 | 18.3 | 18.6 | 15.0 | 18.5 | 18.4 | A-kinase anchor protein 17A | <i>AKAP17A</i> |

| | | | | | | | |
|------|------|------|------|------|------|---|-----------------|
| 23.7 | 24.0 | 23.7 | 20.3 | 23.8 | 24.1 | A-kinase anchor protein 8 | <i>AKAP8</i> |
| 22.9 | 23.3 | 23.2 | 21.6 | 23.4 | 23.6 | A-kinase anchor protein 8-like | <i>AKAP8L</i> |
| 19.1 | 18.7 | 19.1 | 15.0 | 18.7 | 18.7 | Abelson tyrosine-protein kinase 2 | <i>ABL2</i> |
| 19.3 | 18.7 | 19.4 | 20.6 | 18.8 | 19.5 | Acetyl-CoA acetyltransferase, mitochondrial | <i>ACAT1</i> |
| 15.0 | 19.0 | 18.6 | 15.0 | 19.0 | 18.9 | Acetyl-CoA carboxylase 1 | <i>ACACA</i> |
| 21.4 | 21.6 | 21.0 | 21.8 | 21.7 | 21.5 | Acidic leucine-rich nuclear phosphoprotein 32 family member A | <i>ANP32A</i> |
| 19.7 | 19.7 | 19.4 | 21.0 | 19.9 | 15.0 | Acidic leucine-rich nuclear phosphoprotein 32 family member B | <i>ANP32B</i> |
| 20.4 | 20.6 | 19.9 | 21.4 | 20.9 | 20.0 | Acidic leucine-rich nuclear phosphoprotein 32 family member E | <i>ANP32E</i> |
| 17.5 | 15.0 | 17.7 | 15.0 | 17.2 | 18.0 | Actin filament-associated protein 1-like 1 | <i>AFAP1L1</i> |
| 19.1 | 19.1 | 19.2 | 19.8 | 18.9 | 19.0 | Actin-binding protein anillin | <i>ANLN</i> |
| 19.1 | 18.5 | 18.7 | 15.0 | 19.5 | 18.7 | Actin-like protein 6A | <i>ACTL6A</i> |
| 23.9 | 23.4 | 24.1 | 25.8 | 23.5 | 23.9 | Actin, cytoplasmic 2 | <i>ACTG1</i> |
| 24.2 | 24.0 | 24.7 | 27.4 | 24.3 | 24.2 | Activated RNA polymerase II transcriptional coactivator p15 | <i>SUB1</i> |
| 18.4 | 18.2 | 18.9 | 15.0 | 17.9 | 19.1 | Activating molecule in BECN1-regulated autophagy protein 1 | <i>AMBRA1</i> |
| 21.7 | 21.2 | 21.1 | 20.3 | 21.6 | 20.9 | Activating signal cointegrator 1 | <i>TRIP4</i> |
| 20.1 | 19.8 | 20.0 | 19.9 | 19.6 | 19.7 | Activating signal cointegrator 1 complex subunit 2 | <i>ASCC2</i> |
| 19.7 | 19.6 | 19.5 | 19.4 | 19.8 | 19.3 | Activating signal cointegrator 1 complex subunit 3 | <i>ASCC3</i> |
| 21.5 | 21.7 | 21.4 | 20.1 | 21.7 | 21.4 | Activator of basal transcription 1 | <i>ABT1</i> |
| 15.0 | 19.3 | 19.1 | 15.0 | 19.6 | 19.3 | Active regulator of SIRT1 | <i>RPS19BP1</i> |
| 21.1 | 21.2 | 21.2 | 20.9 | 21.3 | 21.1 | Activity-dependent neuroprotector homeobox protein | <i>ADNP</i> |
| 20.8 | 21.1 | 21.4 | 21.6 | 20.9 | 21.1 | Acyglycerol kinase, mitochondrial | <i>AGK</i> |
| 18.8 | 19.2 | 18.7 | 15.0 | 18.7 | 19.2 | Adenomatous polyposis coli protein | <i>APC</i> |
| 15.0 | 15.0 | 18.6 | 19.7 | 15.0 | 18.8 | Adenosylhomocysteinase | <i>AHCY</i> |
| 20.1 | 18.8 | 19.7 | 22.1 | 18.9 | 20.0 | Adenylate kinase 2, mitochondrial | <i>AK2</i> |
| 18.4 | 18.5 | 18.2 | 18.4 | 18.1 | 18.3 | ADP-ribosylation factor GTPase-activating protein 3 | <i>ARFGAP3</i> |
| 20.5 | 19.3 | 20.8 | 23.2 | 20.5 | 20.6 | ADP-ribosylation factor-like protein 6-interacting protein 4 | <i>ARL6IP4</i> |
| 24.1 | 24.0 | 24.3 | 23.3 | 24.2 | 24.5 | ADP/ATP translocase 2 | <i>SLC25A5</i> |
| 23.2 | 23.8 | 23.9 | 22.7 | 23.5 | 23.7 | ADP/ATP translocase 3 | <i>SLC25A6</i> |
| 21.3 | 21.3 | 21.6 | 20.9 | 21.2 | 21.4 | AFG3-like protein 2 | <i>AFG3L2</i> |
| 20.0 | 20.3 | 19.7 | 20.9 | 20.0 | 20.0 | AH receptor-interacting protein | <i>AIP</i> |
| 20.8 | 20.6 | 20.5 | 21.5 | 20.4 | 20.4 | Alpha-adducin | <i>ADD1</i> |
| 15.0 | 15.0 | 18.2 | 19.4 | 18.3 | 17.9 | Alpha-endosulfine | <i>ENSA</i> |
| 22.8 | 21.4 | 22.5 | 24.6 | 21.3 | 22.8 | Alpha-enolase | <i>ENO1</i> |
| 15.0 | 15.0 | 18.7 | 17.9 | 17.8 | 18.0 | Alpha-globin transcription factor CP2 | <i>TFCP2</i> |
| 19.1 | 19.1 | 19.0 | 15.0 | 19.0 | 18.7 | Alpha-ketoglutarate-dependent dioxygenase alkB homolog 2 | <i>ALKBH2</i> |
| 21.7 | 21.9 | 22.1 | 23.0 | 21.9 | 21.9 | Alpha-taxilin | <i>TXLNA</i> |
| 18.3 | 18.5 | 18.5 | 15.0 | 18.4 | 18.4 | Alpha-tubulin N-acetyltransferase 1 | <i>ATAT1</i> |
| 18.7 | 19.0 | 19.6 | 19.2 | 18.6 | 18.9 | Amino acid transporter | <i>SLC1A5</i> |
| 23.0 | 23.1 | 22.9 | 23.3 | 22.8 | 22.8 | Aminoacyl tRNA synthase complex-interacting multifunctional protein 1 | <i>AIMP1</i> |
| 21.3 | 21.8 | 21.6 | 22.2 | 21.7 | 21.2 | Aminoacyl tRNA synthase complex-interacting multifunctional protein 2 | <i>AIMP2</i> |
| 21.1 | 21.0 | 20.7 | 15.0 | 21.2 | 20.9 | Anaphase-promoting complex subunit 1 | <i>ANAPC1</i> |
| 18.8 | 18.8 | 19.1 | 15.0 | 18.9 | 18.6 | Anaphase-promoting complex subunit 10 | <i>ANAPC10</i> |
| 15.0 | 19.3 | 19.5 | 15.0 | 19.4 | 19.2 | Anaphase-promoting complex subunit 7 | <i>ANAPC7</i> |
| 18.4 | 18.7 | 18.6 | 18.3 | 18.5 | 18.6 | Ancient ubiquitous protein 1 | <i>AUP1</i> |
| 22.7 | 23.1 | 23.0 | 24.0 | 22.8 | 23.0 | Angiomotin | <i>AMOT</i> |

| | | | | | | | |
|------|------|------|------|------|------|---|----------------|
| 23.4 | 23.8 | 23.3 | 21.0 | 23.1 | 23.5 | Ankyrin repeat and KH domain-containing protein 1 | <i>ANKHD1</i> |
| 18.3 | 18.9 | 18.7 | 15.0 | 18.4 | 18.9 | Ankyrin repeat and LEM domain-containing protein 2 | <i>ANKLE2</i> |
| 19.3 | 19.5 | 19.4 | 15.0 | 19.6 | 19.1 | Ankyrin repeat and zinc finger domain-containing protein 1 | <i>ANKZF1</i> |
| 21.4 | 22.2 | 21.7 | 20.0 | 21.2 | 22.1 | Ankyrin repeat domain-containing protein 17 | <i>ANKRD17</i> |
| 23.8 | 23.8 | 23.9 | 24.1 | 24.2 | 24.0 | Antigen KI-67 | <i>MKI67</i> |
| 18.9 | 19.6 | 19.4 | 18.7 | 19.4 | 19.3 | AP-2 complex subunit alpha-1 | <i>AP2A1</i> |
| 15.0 | 19.2 | 19.4 | 19.5 | 19.5 | 19.5 | AP-2 complex subunit beta | <i>AP2B1</i> |
| 20.4 | 20.3 | 20.1 | 20.9 | 20.3 | 20.0 | AP-2 complex subunit mu | <i>AP2M1</i> |
| 19.2 | 19.2 | 19.7 | 19.6 | 19.5 | 19.2 | AP-3 complex subunit delta-1 | <i>AP3D1</i> |
| 19.7 | 20.0 | 19.9 | 15.0 | 19.5 | 19.8 | APC membrane recruitment protein 1 | <i>AMER1</i> |
| 25.4 | 26.4 | 26.1 | 23.7 | 25.6 | 26.7 | Apoptosis-inducing factor 1, mitochondrial | <i>AIFM1</i> |
| 26.4 | 26.1 | 26.0 | 27.5 | 26.6 | 25.8 | Apoptotic chromatin condensation inducer in the nucleus | <i>ACIN1</i> |
| 19.1 | 18.8 | 18.7 | 19.2 | 18.9 | 18.8 | Arf-GAP with GTPase, ANK repeat and PH domain-containing protein 3 | <i>AGAP3</i> |
| 21.0 | 21.0 | 21.2 | 23.4 | 20.9 | 21.0 | Arginine and glutamate-rich protein 1 | <i>ARGLU1</i> |
| 21.7 | 21.7 | 21.6 | 22.1 | 21.6 | 21.4 | Arginine--tRNA ligase, cytoplasmic | <i>RARS</i> |
| 20.4 | 20.9 | 20.7 | 22.1 | 20.7 | 20.3 | Arginine/serine-rich coiled-coil protein 2 | <i>RSRC2</i> |
| 19.4 | 15.0 | 19.4 | 19.6 | 19.1 | 19.2 | Asparagine--tRNA ligase, cytoplasmic | <i>NARS</i> |
| 21.2 | 21.4 | 21.3 | 21.8 | 21.3 | 21.0 | Aspartate--tRNA ligase, cytoplasmic | <i>DARS</i> |
| 21.2 | 21.4 | 21.2 | 20.6 | 20.9 | 21.4 | Aspartyl/asparaginyl beta-hydroxylase | <i>ASPH</i> |
| 19.2 | 18.7 | 19.2 | 19.0 | 19.8 | 19.2 | AT-rich interactive domain-containing protein 1A | <i>ARID1A</i> |
| 19.3 | 19.0 | 19.4 | 19.3 | 19.5 | 19.0 | AT-rich interactive domain-containing protein 3B | <i>ARID3B</i> |
| 21.9 | 22.0 | 22.0 | 22.2 | 22.0 | 21.7 | Ataxin-2 | <i>ATXN2</i> |
| 22.3 | 22.2 | 22.1 | 23.0 | 22.2 | 22.0 | Ataxin-2-like protein | <i>ATXN2L</i> |
| 17.7 | 18.2 | 18.7 | 15.0 | 18.8 | 15.0 | Atherin | <i>SAMD1</i> |
| 22.6 | 22.9 | 23.2 | 23.9 | 22.8 | 22.9 | ATP synthase subunit alpha, mitochondrial | <i>ATP5A1</i> |
| 23.2 | 23.5 | 23.6 | 24.0 | 23.1 | 23.4 | ATP synthase subunit beta, mitochondrial | <i>ATP5B</i> |
| 20.5 | 20.7 | 20.5 | 20.5 | 20.7 | 20.7 | ATP synthase subunit d, mitochondrial | <i>ATP5H</i> |
| 19.1 | 19.5 | 19.6 | 20.5 | 19.6 | 19.5 | ATP synthase subunit e, mitochondrial | <i>ATP5I</i> |
| 15.0 | 19.0 | 19.4 | 19.3 | 18.8 | 19.9 | ATP synthase subunit gamma, mitochondrial | <i>ATP5C1</i> |
| 20.5 | 20.7 | 20.9 | 21.8 | 20.6 | 20.7 | ATP synthase subunit O, mitochondrial | <i>ATP5O</i> |
| 15.0 | 15.0 | 18.2 | 15.0 | 15.0 | 18.4 | ATP synthase subunit s-like protein | <i>ATP5SL</i> |
| 17.3 | 17.3 | 17.1 | 15.0 | 16.6 | 16.9 | ATP-binding cassette sub-family D member 3 | <i>ABCD3</i> |
| 20.2 | 20.4 | 20.7 | 20.1 | 19.6 | 20.3 | ATP-binding cassette sub-family E member 1 | <i>ABCE1</i> |
| 22.4 | 22.4 | 22.6 | 23.1 | 22.4 | 22.3 | ATP-binding cassette sub-family F member 1 | <i>ABCF1</i> |
| 22.7 | 23.0 | 22.9 | 22.3 | 22.8 | 22.8 | ATP-binding cassette sub-family F member 2 | <i>ABCF2</i> |
| 20.8 | 20.3 | 20.9 | 21.7 | 20.4 | 20.6 | ATP-citrate synthase | <i>ACLY</i> |
| 18.1 | 18.3 | 18.1 | 18.1 | 17.8 | 18.3 | ATP-dependent Clp protease ATP-binding subunit clpX-like, mitochondrial | <i>CLPX</i> |
| 18.8 | 18.9 | 18.9 | 17.9 | 18.9 | 18.8 | ATP-dependent DNA helicase Q4 | <i>RECQL4</i> |
| 25.4 | 25.3 | 25.3 | 24.2 | 25.4 | 25.1 | ATP-dependent RNA helicase A | <i>DHX9</i> |
| 23.0 | 23.1 | 22.9 | 22.3 | 23.1 | 22.7 | ATP-dependent RNA helicase DDX1 | <i>DDX1</i> |
| 21.6 | 21.7 | 21.8 | 15.0 | 21.9 | 21.5 | ATP-dependent RNA helicase DDX18 | <i>DDX18</i> |
| 21.6 | 21.1 | 21.6 | 20.9 | 21.4 | 21.3 | ATP-dependent RNA helicase DDX24 | <i>DDX24</i> |
| 24.5 | 24.1 | 24.2 | 24.5 | 24.5 | 24.1 | ATP-dependent RNA helicase DDX3X | <i>DDX3X</i> |
| 23.5 | 23.5 | 23.3 | 22.4 | 23.6 | 23.2 | ATP-dependent RNA helicase DDX50 | <i>DDX50</i> |
| 19.2 | 19.1 | 19.0 | 19.2 | 19.3 | 18.9 | ATP-dependent RNA helicase DDX51 | <i>DDX51</i> |

| | | | | | | | |
|------|------|------|------|------|------|--|-----------------|
| 22.2 | 22.0 | 22.0 | 21.7 | 22.1 | 21.6 | ATP-dependent RNA helicase DDX54 | <i>DDX54</i> |
| 19.7 | 19.8 | 19.7 | 19.0 | 19.5 | 19.5 | ATP-dependent RNA helicase DDX55 | <i>DDX55</i> |
| 20.7 | 20.7 | 20.8 | 20.1 | 20.6 | 20.5 | ATP-dependent RNA helicase DHX29 | <i>DHX29</i> |
| 22.1 | 21.9 | 22.1 | 20.9 | 21.9 | 22.0 | ATP-dependent RNA helicase DHX36 | <i>DHX36</i> |
| 15.0 | 18.4 | 18.5 | 18.3 | 18.6 | 18.3 | ATP-dependent RNA helicase DHX8 | <i>DHX8</i> |
| 15.0 | 18.9 | 19.5 | 15.0 | 19.1 | 18.5 | ATP-dependent zinc metalloprotease YME1L1 | <i>YME1L1</i> |
| 23.6 | 23.7 | 24.2 | 22.5 | 23.5 | 23.6 | ATPase family AAA domain-containing protein 3A | <i>ATAD3A</i> |
| 20.4 | 20.2 | 20.9 | 19.2 | 20.3 | 20.5 | ATPase family AAA domain-containing protein 3B | <i>ATAD3B</i> |
| 19.1 | 18.8 | 18.9 | 21.2 | 18.6 | 18.3 | ATPase inhibitor, mitochondrial | <i>ATPIF1</i> |
| 19.7 | 19.8 | 19.8 | 19.6 | 19.8 | 19.9 | Aurora kinase B | <i>AURKB</i> |
| 15.0 | 15.0 | 15.0 | 15.0 | 18.3 | 18.4 | B-cell lymphoma/leukemia 11A | <i>BCL11A</i> |
| 24.2 | 25.0 | 24.8 | 22.2 | 24.1 | 25.5 | BAG family molecular chaperone regulator 2 | <i>BAG2</i> |
| 22.0 | 21.8 | 21.2 | 15.0 | 21.8 | 21.7 | BAG family molecular chaperone regulator 4 | <i>BAG4</i> |
| 21.9 | 22.3 | 22.2 | 19.7 | 21.4 | 22.8 | BAG family molecular chaperone regulator 5 | <i>BAG5</i> |
| 18.9 | 20.6 | 21.1 | 20.7 | 20.4 | 20.4 | Barrier-to-autointegration factor | <i>BANF1</i> |
| 20.8 | 20.6 | 20.2 | 19.7 | 20.2 | 20.4 | BCL-6 corepressor | <i>BCOR</i> |
| 24.3 | 24.4 | 24.3 | 25.0 | 24.1 | 24.2 | Bifunctional glutamate/proline--tRNA ligase | <i>EPRS</i> |
| 20.6 | 20.1 | 19.9 | 21.1 | 20.2 | 20.1 | Bifunctional methylenetetrahydrofolate dehydrogenase/cyclohydrolase, mitochondrial | <i>MTHFD2</i> |
| 15.0 | 15.0 | 18.6 | 20.3 | 15.0 | 15.0 | Bifunctional purine biosynthesis protein PURH | <i>ATIC</i> |
| 19.5 | 19.6 | 19.5 | 19.3 | 19.5 | 19.2 | Bloom syndrome protein | <i>BLM</i> |
| 19.8 | 19.5 | 19.8 | 22.3 | 19.8 | 19.5 | BoIA-like protein 2 | <i>BOLA2</i> |
| 19.8 | 20.0 | 20.1 | 20.9 | 19.9 | 19.8 | Brain-specific angiogenesis inhibitor 1-associated protein 2-like protein 1 | <i>BAIAP2L1</i> |
| 20.2 | 20.3 | 20.4 | 19.1 | 20.4 | 20.5 | BRCA1-A complex subunit RAP80 | <i>UIMC1</i> |
| 18.9 | 18.6 | 18.9 | 15.0 | 18.3 | 19.3 | Breakpoint cluster region protein | <i>BCR</i> |
| 19.2 | 18.9 | 18.4 | 15.0 | 15.0 | 19.1 | Breast cancer type 1 susceptibility protein | <i>BRCA1</i> |
| 19.5 | 19.5 | 19.2 | 15.0 | 19.6 | 18.9 | Bromodomain adjacent to zinc finger domain protein 1A | <i>BAZ1A</i> |
| 23.7 | 23.7 | 23.0 | 18.8 | 24.1 | 23.1 | Bystin | <i>BYSL</i> |
| 22.8 | 22.7 | 23.0 | 24.1 | 22.9 | 22.9 | C-1-tetrahydrofolate synthase, cytoplasmic | <i>MTHFD1</i> |
| 18.0 | 18.0 | 18.2 | 15.0 | 17.9 | 18.4 | C-myc promoter-binding protein | <i>DENND4A</i> |
| 20.3 | 20.3 | 20.4 | 20.8 | 20.3 | 20.3 | C-Myc-binding protein | <i>MYCBP</i> |
| 23.0 | 24.1 | 23.6 | 22.6 | 22.9 | 24.0 | CAD protein | <i>CAD</i> |
| 19.8 | 20.0 | 19.7 | 20.5 | 20.0 | 19.6 | Calcium homeostasis endoplasmic reticulum protein | <i>CHERP</i> |
| 19.1 | 19.7 | 19.9 | 19.9 | 19.7 | 19.7 | Calcium-binding mitochondrial carrier protein Aralar2 | <i>SLC25A13</i> |
| 18.6 | 18.6 | 18.6 | 19.1 | 18.5 | 18.4 | Calcium/calmodulin-dependent protein kinase type II subunit gamma | <i>CAMK2G</i> |
| 19.4 | 20.3 | 20.6 | 22.6 | 19.6 | 20.1 | Calcyclin-binding protein | <i>CACYBP</i> |
| 23.4 | 23.6 | 23.7 | 23.4 | 23.6 | 23.3 | Calmodulin-regulated spectrin-associated protein 1 | <i>CAMSAP1</i> |
| 18.4 | 15.0 | 17.8 | 15.0 | 18.4 | 18.3 | Calmodulin-regulated spectrin-associated protein 2 | <i>CAMSAP2</i> |
| 20.5 | 20.6 | 20.5 | 20.4 | 20.6 | 20.3 | Calmodulin-regulated spectrin-associated protein 3 | <i>CAMSAP3</i> |
| 18.1 | 18.3 | 18.4 | 18.8 | 15.0 | 18.9 | Calnexin | <i>CANX</i> |
| 20.2 | 20.4 | 20.4 | 15.0 | 20.2 | 20.7 | cAMP-dependent protein kinase type I-alpha regulatory subunit | <i>PRKAR1A</i> |
| 20.2 | 19.8 | 19.7 | 19.6 | 20.0 | 20.1 | cAMP-dependent protein kinase type II-alpha regulatory subunit | <i>PRKAR2A</i> |
| 23.7 | 24.3 | 24.2 | 24.0 | 23.8 | 24.7 | Cancer-related nucleoside-triphosphatase | <i>NTPCR</i> |

| | | | | | | | |
|------|------|------|------|------|------|---|-----------------|
| 18.2 | 19.0 | 18.7 | 19.5 | 15.0 | 18.5 | Cap-specific mRNA (nucleoside-2-O-)-methyltransferase 1 | <i>CMTR1</i> |
| 23.4 | 23.5 | 23.1 | 22.8 | 23.7 | 23.2 | Caprin-1 | <i>CAPRIN1</i> |
| 20.2 | 20.1 | 20.5 | 20.4 | 19.8 | 20.1 | Carnitine O-palmitoyltransferase 1, liver isoform | <i>CPT1A</i> |
| 18.8 | 18.7 | 18.9 | 19.3 | 18.8 | 19.0 | Casein kinase I isoform alpha | <i>CSNK1A1</i> |
| 20.6 | 20.3 | 20.1 | 15.0 | 20.4 | 19.9 | Casein kinase I isoform delta | <i>CSNK1D</i> |
| 23.3 | 23.1 | 22.8 | 22.2 | 23.3 | 22.8 | Casein kinase I isoform epsilon | <i>CSNK1E</i> |
| 20.5 | 20.8 | 19.4 | 15.0 | 20.8 | 20.2 | Casein kinase II subunit beta | <i>CSNK2B</i> |
| 18.5 | 18.5 | 18.5 | 19.1 | 18.7 | 18.5 | Caseinolytic peptidase B protein homolog | <i>CLPB</i> |
| 18.6 | 19.0 | 18.9 | 15.0 | 18.8 | 18.6 | Catenin delta-1 | <i>CTNND1</i> |
| 20.2 | 19.7 | 19.6 | 15.0 | 20.0 | 19.6 | CCAAT/enhancer-binding protein zeta | <i>CEBPZ</i> |
| 19.8 | 19.9 | 20.1 | 21.5 | 20.0 | 19.8 | CD2 antigen cytoplasmic tail-binding protein 2 | <i>CD2BP2</i> |
| 20.2 | 20.5 | 20.6 | 19.7 | 20.0 | 21.0 | Cdc42 effector protein 1 | <i>CDC42EP1</i> |
| 19.6 | 19.7 | 19.3 | 18.0 | 19.4 | 19.8 | CDK5 regulatory subunit-associated protein 1 | <i>CDK5RAP1</i> |
| 19.5 | 19.5 | 19.6 | 19.7 | 19.4 | 19.3 | CDKN2A-interacting protein | <i>CDKN2AIP</i> |
| 23.8 | 23.7 | 23.7 | 23.3 | 23.8 | 23.5 | Cell division cycle 5-like protein | <i>CDC5L</i> |
| 20.9 | 20.8 | 21.0 | 20.2 | 20.6 | 21.0 | Cell division cycle 7-related protein kinase | <i>CDC7</i> |
| 21.3 | 21.4 | 21.6 | 21.2 | 21.3 | 21.5 | Cell division cycle protein 20 homolog | <i>CDC20</i> |
| 15.0 | 18.9 | 18.4 | 15.0 | 19.2 | 18.8 | Cell division cycle protein 23 homolog | <i>CDC23</i> |
| 17.1 | 17.5 | 17.5 | 17.8 | 17.4 | 17.1 | Cell division cycle protein 27 homolog | <i>CDC27</i> |
| 18.1 | 15.0 | 18.2 | 15.0 | 18.1 | 19.2 | Cell division cycle-associated protein 2 | <i>CDCA2</i> |
| 22.9 | 22.9 | 23.0 | 23.0 | 22.9 | 22.7 | Cell growth-regulating nucleolar protein | <i>LYAR</i> |
| 21.3 | 21.0 | 21.7 | 24.1 | 20.9 | 21.1 | Cellular nucleic acid-binding protein | <i>CNBP</i> |
| 23.9 | 24.1 | 23.5 | 22.5 | 23.7 | 24.0 | Cellular tumor antigen p53 | <i>TP53</i> |
| 20.2 | 20.3 | 20.4 | 15.0 | 20.0 | 20.6 | Centriolar coiled-coil protein of 110 kDa | <i>CCP110</i> |
| 21.2 | 21.3 | 21.3 | 21.9 | 21.6 | 21.2 | Centromere protein F | <i>CENPF</i> |
| 22.1 | 22.3 | 21.5 | 18.1 | 22.1 | 23.1 | Centromere protein J | <i>CENPJ</i> |
| 19.4 | 19.8 | 19.7 | 15.0 | 20.2 | 19.7 | Centromere protein V | <i>CENPV</i> |
| 23.6 | 23.6 | 23.4 | 22.7 | 23.3 | 23.6 | Centrosomal protein of 170 kDa | <i>CEP170</i> |
| 17.1 | 17.8 | 17.6 | 18.4 | 17.5 | 17.4 | Centrosomal protein of 170 kDa protein B | <i>CEP170B</i> |
| 15.0 | 18.6 | 18.6 | 15.0 | 15.0 | 18.4 | Centrosomal protein of 78 kDa | <i>CEP78</i> |
| 20.7 | 20.7 | 20.5 | 15.0 | 20.5 | 21.0 | Centrosomal protein of 97 kDa | <i>CEP97</i> |
| 15.0 | 15.0 | 15.0 | 15.0 | 15.0 | 22.0 | Centrosome and spindle pole-associated protein 1 | <i>CSPP1</i> |
| 18.7 | 19.0 | 18.9 | 15.0 | 19.0 | 19.2 | Centrosome-associated protein 350 | <i>CEP350</i> |
| 21.9 | 21.7 | 21.8 | 22.1 | 22.1 | 21.6 | CGG triplet repeat-binding protein 1 | <i>CGGBP1</i> |
| 15.0 | 18.6 | 19.0 | 20.7 | 18.8 | 15.0 | Charged multivesicular body protein 1a | <i>CHMP1A</i> |
| 15.0 | 15.0 | 15.0 | 15.0 | 15.0 | 15.0 | Charged multivesicular body protein 2b | <i>CHMP2B</i> |
| 19.4 | 19.0 | 18.6 | 19.6 | 19.3 | 18.9 | Chromatin accessibility complex protein 1 | <i>CHRAC1</i> |
| 18.6 | 18.7 | 18.8 | 19.2 | 19.0 | 18.5 | Chromatin assembly factor 1 subunit B | <i>CHAF1B</i> |
| 19.3 | 19.6 | 19.5 | 19.3 | 19.8 | 19.6 | Chromatin complexes subunit BAP18 | <i>BAP18</i> |
| 22.2 | 22.1 | 21.9 | 22.4 | 22.6 | 21.6 | Chromatin target of PRMT1 protein | <i>CHTOP</i> |
| 21.5 | 21.2 | 21.7 | 22.0 | 21.1 | 21.3 | Chromobox protein homolog 3 | <i>CBX3</i> |
| 19.7 | 19.3 | 19.6 | 15.0 | 19.6 | 19.4 | Chromodomain-helicase-DNA-binding protein 3 | <i>CHD3</i> |
| 22.4 | 22.4 | 22.4 | 22.5 | 22.5 | 22.2 | Chromodomain-helicase-DNA-binding protein 4 | <i>CHD4</i> |
| 19.4 | 19.4 | 18.9 | 15.0 | 20.0 | 19.2 | Chromodomain-helicase-DNA-binding protein 8 | <i>CHD8</i> |
| 24.2 | 24.3 | 24.6 | 24.7 | 24.1 | 24.1 | Chromosome-associated kinesin KIF4A | <i>KIF4A</i> |
| 19.7 | 19.5 | 19.2 | 17.7 | 19.7 | 19.0 | Cirhin | <i>CIRH1A</i> |

| | | | | | | | |
|------|------|------|------|------|------|---|----------------|
| 20.7 | 20.5 | 20.0 | 16.7 | 20.8 | 21.6 | Claspin | <i>CLSPN</i> |
| 19.1 | 17.8 | 19.2 | 21.6 | 19.0 | 18.7 | Clathrin heavy chain | <i>CLTC</i> |
| 15.0 | 15.0 | 15.0 | 15.0 | 15.0 | 15.0 | Clathrin light chain A | <i>CLTA</i> |
| 19.9 | 19.8 | 20.3 | 20.0 | 20.5 | 20.0 | Cleavage and polyadenylation specificity factor subunit 1 | <i>CPSF1</i> |
| 22.0 | 21.6 | 21.2 | 21.0 | 22.1 | 21.5 | Cleavage and polyadenylation specificity factor subunit 2 | <i>CPSF2</i> |
| 19.9 | 20.3 | 20.2 | 20.9 | 20.4 | 19.9 | Cleavage and polyadenylation specificity factor subunit 3 | <i>CPSF3</i> |
| 21.1 | 20.8 | 20.8 | 20.5 | 21.0 | 20.7 | Cleavage and polyadenylation specificity factor subunit 4 | <i>CPSF4</i> |
| 23.4 | 23.2 | 23.4 | 23.8 | 23.4 | 23.1 | Cleavage and polyadenylation specificity factor subunit 5 | <i>NUDT21</i> |
| 19.5 | 19.7 | 19.4 | 20.7 | 19.5 | 19.5 | Cleavage and polyadenylation specificity factor subunit 6 | <i>CPSF6</i> |
| 22.0 | 21.9 | 21.7 | 22.0 | 21.9 | 21.7 | Cleavage and polyadenylation specificity factor subunit 7 | <i>CPSF7</i> |
| 20.8 | 20.8 | 20.6 | 21.3 | 20.8 | 20.5 | Cleavage stimulation factor subunit 2 | <i>CSTF2</i> |
| 15.0 | 19.4 | 19.4 | 15.0 | 19.4 | 19.5 | Cleavage stimulation factor subunit 3 | <i>CSTF3</i> |
| 22.8 | 22.8 | 22.9 | 22.6 | 22.8 | 22.6 | CLIP-associating protein 2 | <i>CLASP2</i> |
| 19.8 | 19.8 | 19.5 | 20.2 | 19.9 | 19.7 | Coatomer subunit alpha | <i>COPA</i> |
| 15.0 | 15.0 | 17.6 | 15.0 | 15.0 | 17.3 | COBW domain-containing protein 2 | <i>CBWD2</i> |
| 21.7 | 21.1 | 21.7 | 23.3 | 21.2 | 21.5 | Cofilin-1 | <i>CFL1</i> |
| 19.1 | 19.4 | 19.6 | 20.1 | 19.3 | 19.5 | Coiled-coil domain-containing protein 12 | <i>CCDC12</i> |
| 23.0 | 23.1 | 23.6 | 25.5 | 23.1 | 23.1 | Coiled-coil domain-containing protein 124 | <i>CCDC124</i> |
| 19.9 | 19.0 | 19.7 | 18.9 | 19.1 | 19.1 | Coiled-coil domain-containing protein 137 | <i>CCDC137</i> |
| 20.4 | 20.5 | 20.4 | 20.7 | 20.3 | 20.7 | Coiled-coil domain-containing protein 47 | <i>CCDC47</i> |
| 20.3 | 20.4 | 20.4 | 15.0 | 20.7 | 20.1 | Coiled-coil domain-containing protein 86 | <i>CCDC86</i> |
| 22.5 | 22.1 | 22.0 | 22.3 | 22.4 | 22.0 | Cold shock domain-containing protein E1 | <i>CSDE1</i> |
| 24.0 | 23.7 | 23.7 | 23.3 | 23.9 | 23.2 | Cold-inducible RNA-binding protein | <i>CIRBP</i> |
| 19.6 | 19.5 | 19.7 | 20.3 | 19.3 | 19.7 | Condensin complex subunit 1 | <i>NCAPD2</i> |
| 20.0 | 20.4 | 20.2 | 20.9 | 20.2 | 20.1 | Condensin complex subunit 2 | <i>NCAPH</i> |
| 20.5 | 20.5 | 21.0 | 20.1 | 20.3 | 20.5 | Condensin-2 complex subunit D3 | <i>NCAPD3</i> |
| 19.1 | 19.3 | 19.0 | 19.0 | 19.2 | 19.0 | Condensin-2 complex subunit H2 | <i>NCAPH2</i> |
| 21.5 | 21.3 | 21.2 | 21.0 | 21.3 | 20.9 | Constitutive coactivator of PPAR-gamma-like protein 1 | <i>FAM120A</i> |
| 17.6 | 17.7 | 17.8 | 19.0 | 17.5 | 17.8 | COP9 signalosome complex subunit 3 | <i>COPS3</i> |
| 15.0 | 15.0 | 18.5 | 20.6 | 20.6 | 18.7 | Core histone macro-H2A.1 | <i>H2AFY</i> |
| 15.0 | 15.0 | 16.6 | 18.2 | 15.0 | 16.9 | Corepressor interacting with RBPJ 1 | <i>CIR1</i> |
| 19.5 | 19.2 | 19.8 | 20.4 | 15.0 | 19.2 | Coronin-1C | <i>CORO1C</i> |
| 19.9 | 20.0 | 20.4 | 19.9 | 19.9 | 19.8 | Mitochondrial import inner membrane translocase subunit TIM16 | <i>PAM16</i> |
| 21.7 | 20.4 | 21.6 | 23.4 | 20.9 | 21.7 | Creatine kinase B-type | <i>CKB</i> |
| 21.1 | 20.8 | 21.2 | 22.3 | 20.8 | 20.8 | Creatine kinase U-type, mitochondrial | <i>CKMT1A</i> |
| 19.3 | 19.3 | 19.3 | 19.5 | 15.0 | 19.3 | CREB-binding protein | <i>CREBBP</i> |
| 19.1 | 19.2 | 19.5 | 21.3 | 15.0 | 19.5 | CTP synthase 1 | <i>CTPS1</i> |
| 19.2 | 20.0 | 20.1 | 15.0 | 20.0 | 19.4 | CUGBP Elav-like family member 1 | <i>CELF1</i> |
| 21.2 | 20.6 | 21.4 | 15.0 | 20.6 | 20.3 | Cyclic AMP-dependent transcription factor ATF-4 | <i>ATF4</i> |
| 18.1 | 17.9 | 18.5 | 18.4 | 18.0 | 18.3 | Cyclin-dependent kinase 1 | <i>CDK1</i> |
| 20.1 | 19.9 | 20.0 | 20.8 | 20.0 | 19.8 | Cyclin-dependent kinase 12 | <i>CDK12</i> |
| 19.2 | 19.2 | 19.1 | 19.3 | 18.9 | 18.7 | Cyclin-dependent kinase 13 | <i>CDK13</i> |
| 19.3 | 19.0 | 19.0 | 19.4 | 19.1 | 18.9 | Cyclin-dependent kinase 2 | <i>CDK2</i> |
| 18.3 | 18.1 | 18.2 | 15.0 | 15.0 | 18.1 | Cyclin-dependent kinase 2-associated protein 1 | <i>CDK2AP1</i> |
| 19.0 | 19.0 | 18.9 | 20.5 | 18.8 | 19.4 | Cyclin-dependent kinase 4 | <i>CDK4</i> |
| 19.1 | 19.2 | 18.8 | 19.6 | 19.2 | 19.1 | Cyclin-dependent kinase 9 | <i>CDK9</i> |

| | | | | | | | |
|------|------|------|------|------|------|--|-----------------|
| 19.5 | 19.1 | 19.3 | 20.0 | 19.2 | 19.0 | Cyclin-dependent kinase inhibitor 2A | <i>CDKN2A</i> |
| 19.4 | 19.4 | 19.2 | 15.0 | 19.5 | 19.0 | Cyclin-T1 | <i>CCNT1</i> |
| 18.3 | 15.0 | 18.8 | 21.3 | 15.0 | 18.7 | Cystathionine beta-synthase | <i>CBS</i> |
| 18.8 | 18.8 | 19.9 | 23.0 | 19.0 | 19.2 | Cysteine and glycine-rich protein 2 | <i>CSRP2</i> |
| 18.3 | 18.3 | 18.3 | 20.2 | 18.5 | 18.2 | Cysteine-rich PDZ-binding protein | <i>CRIP1</i> |
| 15.0 | 19.3 | 19.5 | 20.2 | 15.0 | 19.7 | Cytochrome c oxidase assembly factor 3 homolog, mitochondrial | <i>COA3</i> |
| 19.8 | 20.1 | 19.4 | 20.3 | 20.0 | 19.9 | Cytochrome c oxidase subunit 5A, mitochondrial | <i>COX5A</i> |
| 19.4 | 19.7 | 19.7 | 20.9 | 19.4 | 20.0 | Cytoplasmic dynein 1 heavy chain 1 | <i>DYNC1H1</i> |
| 20.0 | 20.0 | 20.2 | 22.3 | 19.8 | 20.1 | Cytoplasmic dynein 1 intermediate chain 2 | <i>DYNC1I2</i> |
| 21.6 | 21.6 | 21.9 | 21.7 | 21.6 | 21.7 | Cytoskeleton-associated protein 2 | <i>CKAP2</i> |
| 24.3 | 24.2 | 24.5 | 24.5 | 24.2 | 24.5 | Cytoskeleton-associated protein 4 | <i>CKAP4</i> |
| 23.9 | 23.9 | 24.1 | 23.6 | 23.7 | 24.2 | Cytoskeleton-associated protein 5 | <i>CKAP5</i> |
| 20.0 | 20.2 | 20.1 | 15.0 | 20.0 | 19.7 | Cytosolic carboxypeptidase 1 | <i>AGTPBP1</i> |
| 18.7 | 19.2 | 19.1 | 15.0 | 15.0 | 19.6 | Cytosolic Fe-S cluster assembly factor NUBP2 | <i>NUBP2</i> |
| 22.7 | 22.4 | 22.7 | 24.5 | 22.7 | 22.5 | D-3-phosphoglycerate dehydrogenase | <i>PHGDH</i> |
| 22.6 | 22.4 | 22.3 | 22.8 | 22.6 | 22.1 | DAZ-associated protein 1 | <i>DAZAP1</i> |
| 21.7 | 21.2 | 21.2 | 21.2 | 21.9 | 21.2 | DBIRD complex subunit ZNF326 | <i>ZNF326</i> |
| 18.5 | 19.0 | 18.3 | 15.0 | 18.8 | 18.5 | DDB1- and CUL4-associated factor 16 | <i>DCAF16</i> |
| 15.0 | 18.8 | 18.8 | 18.7 | 18.4 | 19.4 | DDB1- and CUL4-associated factor 8 | <i>DCAF8</i> |
| 19.2 | 18.8 | 18.9 | 18.6 | 19.7 | 18.6 | Death domain-associated protein 6 | <i>DAXX</i> |
| 20.5 | 20.5 | 20.5 | 20.5 | 20.3 | 20.3 | Death-inducer obliterator 1 | <i>DIDO1</i> |
| 20.9 | 21.6 | 21.7 | 21.2 | 21.2 | 21.5 | Dedicator of cytokinesis protein 7 | <i>DOCK7</i> |
| 18.4 | 18.7 | 18.7 | 19.7 | 18.3 | 18.5 | Delta-1-pyrroline-5-carboxylate synthase | <i>ALDH18A1</i> |
| 19.5 | 19.6 | 19.5 | 20.3 | 19.4 | 19.4 | DENN domain-containing protein 4C | <i>DENND4C</i> |
| 15.0 | 21.0 | 21.3 | 23.5 | 21.4 | 21.3 | Density-regulated protein | <i>DENR</i> |
| 17.3 | 17.0 | 17.1 | 15.0 | 17.1 | 16.7 | Denticleless protein homolog | <i>DTL</i> |
| 15.0 | 19.0 | 19.3 | 15.0 | 15.0 | 19.0 | Deoxynucleoside triphosphate triphosphohydrolase SAMHD1 | <i>SAMHD1</i> |
| 19.9 | 19.0 | 20.8 | 20.8 | 15.0 | 18.8 | Deoxyuridine 5-triphosphate nucleotidohydrolase, mitochondrial | <i>DUT</i> |
| 18.3 | 18.9 | 18.9 | 18.7 | 18.7 | 19.0 | Desmoglein-2 | <i>DSG2</i> |
| 21.0 | 21.3 | 21.1 | 22.3 | 21.2 | 21.2 | Desmoplakin | <i>DSP</i> |
| 15.0 | 15.0 | 15.0 | 21.0 | 15.0 | 15.0 | Destrin | <i>DSTN</i> |
| 21.6 | 21.9 | 22.0 | 20.4 | 21.9 | 21.2 | DET1 homolog | <i>DET1</i> |
| 22.0 | 21.9 | 22.3 | 20.7 | 22.1 | 21.7 | DET1- and DDB1-associated protein 1 | <i>DDA1</i> |
| 21.7 | 21.5 | 21.6 | 21.7 | 21.3 | 21.5 | Developmentally-regulated GTP-binding protein 1 | <i>DRG1</i> |
| 19.0 | 18.4 | 18.6 | 17.8 | 19.1 | 18.5 | Dimethyladenosine transferase 1, mitochondrial | <i>TFB1M</i> |
| 21.0 | 20.9 | 21.0 | 21.0 | 20.9 | 20.9 | DNA (cytosine-5)-methyltransferase 1 | <i>DNMT1</i> |
| 21.3 | 21.3 | 21.7 | 18.8 | 21.6 | 21.2 | DNA damage-binding protein 1 | <i>DDB1</i> |
| 21.7 | 21.7 | 21.1 | 15.0 | 21.1 | 21.9 | DNA endonuclease RBBP8 | <i>RBBP8</i> |
| 20.9 | 20.6 | 20.9 | 21.2 | 20.8 | 20.6 | DNA ligase 3 | <i>LIG3</i> |
| 20.3 | 19.9 | 20.1 | 19.7 | 20.0 | 20.0 | DNA methyltransferase 1-associated protein 1 | <i>DMAP1</i> |
| 19.1 | 15.0 | 19.3 | 21.0 | 19.5 | 19.1 | DNA mismatch repair protein Msh6 | <i>MSH6</i> |
| 20.1 | 20.0 | 19.9 | 20.4 | 20.0 | 19.9 | DNA polymerase epsilon subunit 3 | <i>POLE3</i> |
| 20.5 | 20.2 | 20.0 | 20.0 | 20.1 | 19.9 | DNA polymerase | <i>POLD1</i> |
| 21.5 | 22.1 | 21.6 | 21.7 | 21.3 | 21.8 | DNA repair protein RAD50 | <i>RAD50</i> |
| 21.1 | 20.6 | 20.8 | 21.4 | 20.8 | 20.6 | DNA repair protein XRCC1 | <i>XRCC1</i> |
| 20.1 | 20.1 | 19.9 | 21.4 | 19.6 | 20.5 | DNA replication licensing factor MCM3 | <i>MCM3</i> |
| 15.0 | 15.0 | 15.0 | 19.5 | 15.0 | 15.0 | DNA replication licensing factor MCM6 | <i>MCM6</i> |

| | | | | | | | |
|------|------|------|------|------|------|--|----------------|
| 24.4 | 24.4 | 24.5 | 24.2 | 24.5 | 24.2 | DNA topoisomerase 1 | <i>TOP1</i> |
| 18.3 | 18.3 | 18.9 | 18.6 | 18.5 | 18.1 | DNA topoisomerase 2-alpha | <i>TOP2A</i> |
| 15.0 | 19.9 | 19.8 | 20.4 | 19.9 | 19.4 | DNA-(apurinic or apyrimidinic site) lyase | <i>APEX1</i> |
| 21.2 | 21.0 | 21.0 | 20.8 | 21.2 | 20.9 | DNA-3-methyladenine glycosylase | <i>MPG</i> |
| 19.4 | 19.5 | 19.4 | 15.0 | 19.5 | 19.0 | DNA-binding protein RFX5 | <i>RFX5</i> |
| 25.6 | 25.8 | 26.0 | 25.6 | 25.6 | 25.9 | DNA-dependent protein kinase catalytic subunit | <i>PRKDC</i> |
| 19.5 | 20.0 | 19.7 | 19.3 | 19.7 | 19.6 | DNA-directed RNA polymerase I subunit RPA1 | <i>POLR1A</i> |
| 18.1 | 18.7 | 18.6 | 15.0 | 18.4 | 18.8 | DNA-directed RNA polymerase I subunit RPA2 | <i>POLR1B</i> |
| 21.6 | 21.7 | 21.8 | 21.8 | 21.7 | 21.5 | DNA-directed RNA polymerase I subunit RPA34 | <i>CD3EAP</i> |
| 20.7 | 20.8 | 20.8 | 20.7 | 20.8 | 20.7 | DNA-directed RNA polymerase I subunit RPA49 | <i>POLR1E</i> |
| 20.2 | 20.2 | 19.8 | 15.0 | 20.5 | 19.8 | DNA-directed RNA polymerase II subunit RPB1 | <i>POLR2A</i> |
| 18.4 | 18.3 | 15.0 | 15.0 | 19.0 | 18.4 | DNA-directed RNA polymerase II subunit RPB3 | <i>POLR2C</i> |
| 19.7 | 19.5 | 19.8 | 19.4 | 19.6 | 19.7 | DNA-directed RNA polymerase III subunit RPC1 | <i>POLR3A</i> |
| 15.0 | 18.0 | 18.0 | 15.0 | 15.0 | 18.0 | DNA-directed RNA polymerase III subunit RPC2 | <i>POLR3B</i> |
| 18.9 | 19.0 | 18.9 | 15.0 | 19.1 | 18.9 | DNA-directed RNA polymerase III subunit RPC4 | <i>POLR3D</i> |
| 17.5 | 15.0 | 18.7 | 15.0 | 18.2 | 18.4 | DNA-directed RNA polymerase III subunit RPC5 | <i>POLR3E</i> |
| 19.8 | 19.9 | 20.0 | 15.0 | 19.9 | 19.9 | DNA-directed RNA polymerase, mitochondrial | <i>POLRMT</i> |
| 21.3 | 20.7 | 21.1 | 19.8 | 21.5 | 21.0 | DNA-directed RNA polymerase | <i>POLR2B</i> |
| 21.4 | 21.6 | 21.6 | 21.1 | 21.9 | 21.8 | DNA-directed RNA polymerases I and III subunit RPAC1 | <i>POLR1C</i> |
| 21.1 | 21.2 | 21.1 | 22.0 | 21.3 | 20.9 | DNA-directed RNA polymerases I, II, and III subunit RPABC1 | <i>POLR2E</i> |
| 19.0 | 19.4 | 19.1 | 15.0 | 19.6 | 19.4 | DNA-directed RNA polymerases I, II, and III subunit RPABC5 | <i>POLR2L</i> |
| 24.1 | 24.8 | 24.6 | 23.5 | 24.0 | 25.3 | DnaJ homolog subfamily A member 1 | <i>DNAJA1</i> |
| 23.3 | 24.1 | 24.1 | 23.2 | 23.5 | 24.7 | DnaJ homolog subfamily A member 2 | <i>DNAJA2</i> |
| 23.0 | 23.1 | 23.1 | 22.2 | 22.6 | 23.8 | DnaJ homolog subfamily A member 3, mitochondrial | <i>DNAJA3</i> |
| 19.6 | 20.0 | 19.8 | 20.6 | 19.7 | 20.1 | DnaJ homolog subfamily B member 1 | <i>DNAJB1</i> |
| 18.2 | 18.8 | 19.1 | 18.8 | 18.3 | 18.9 | DnaJ homolog subfamily B member 12 | <i>DNAJB12</i> |
| 18.9 | 19.3 | 19.4 | 19.5 | 18.8 | 19.0 | DnaJ homolog subfamily C member 1 | <i>DNAJC1</i> |
| 20.2 | 21.1 | 21.1 | 20.0 | 20.2 | 21.4 | DnaJ homolog subfamily C member 10 | <i>DNAJC10</i> |
| 19.8 | 19.7 | 19.8 | 21.5 | 19.9 | 19.5 | DnaJ homolog subfamily C member 2 | <i>DNAJC2</i> |
| 15.0 | 17.1 | 17.8 | 15.0 | 16.6 | 17.1 | DnaJ homolog subfamily C member 21 | <i>DNAJC21</i> |
| 21.2 | 21.9 | 21.9 | 21.8 | 20.8 | 22.8 | DnaJ homolog subfamily C member 7 | <i>DNAJC7</i> |
| 20.9 | 21.2 | 21.6 | 23.6 | 21.0 | 21.0 | DnaJ homolog subfamily C member 8 | <i>DNAJC8</i> |
| 19.4 | 19.9 | 19.5 | 20.6 | 19.7 | 19.8 | DnaJ homolog subfamily C member 9 | <i>DNAJC9</i> |
| 23.4 | 23.8 | 24.0 | 23.3 | 23.7 | 23.9 | Dolichyl-diphosphooligosaccharide--protein glycosyltransferase subunit 1 | <i>RPN1</i> |
| 19.6 | 19.7 | 19.4 | 15.0 | 19.7 | 19.5 | Dolichyl-diphosphooligosaccharide--protein glycosyltransferase subunit 2 | <i>RPN2</i> |
| 20.7 | 21.0 | 20.5 | 20.6 | 20.6 | 20.6 | Double-strand break repair protein MRE11A | <i>MRE11A</i> |
| 20.0 | 19.9 | 20.0 | 20.4 | 20.2 | 19.8 | Double-strand-break repair protein rad21 homolog | <i>RAD21</i> |
| 23.2 | 23.3 | 23.3 | 22.5 | 23.3 | 23.2 | Double-stranded RNA-binding protein Staufen homolog 1 | <i>STAU1</i> |
| 20.6 | 20.6 | 20.3 | 20.0 | 20.5 | 20.5 | Double-stranded RNA-binding protein Staufen homolog 2 | <i>STAU2</i> |
| 22.6 | 23.0 | 22.9 | 22.4 | 23.3 | 22.7 | Double-stranded RNA-specific adenosine deaminase | <i>ADAR</i> |
| 15.0 | 18.4 | 18.4 | 19.0 | 19.0 | 18.2 | Dr1-associated corepressor | <i>DRAP1</i> |
| 20.0 | 20.1 | 20.3 | 15.0 | 19.8 | 20.5 | Dual specificity protein kinase TTK | <i>TTK</i> |

| | | | | | | | |
|------|------|------|------|------|------|---|-------------------|
| 17.8 | 18.1 | 18.2 | 15.0 | 18.1 | 18.4 | Dual specificity tyrosine-phosphorylation-regulated kinase 1A | <i>DYRK1A</i> |
| 18.7 | 18.3 | 18.0 | 15.0 | 18.3 | 18.3 | Dynactin subunit 4 | <i>DCTN4</i> |
| 19.5 | 19.2 | 19.7 | 19.8 | 19.3 | 19.1 | Dynein light chain roadblock-type 1 | <i>DYNLRB1</i> |
| 19.0 | 19.1 | 19.4 | 20.6 | 19.0 | 19.2 | E1A-binding protein p400 | <i>EP400</i> |
| 18.5 | 18.7 | 18.4 | 18.1 | 18.9 | 18.4 | E3 ISG15--protein ligase HERC5 | <i>HERC5</i> |
| 21.0 | 21.1 | 20.8 | 20.9 | 21.0 | 20.9 | E3 SUMO-protein ligase RanBP2 | <i>RANBP2</i> |
| 21.1 | 21.0 | 21.0 | 21.7 | 20.8 | 21.1 | E3 ubiquitin-protein ligase BRE1B | <i>RNF40</i> |
| 22.6 | 23.6 | 23.6 | 21.6 | 22.0 | 24.7 | E3 ubiquitin-protein ligase CHIP | <i>STUB1</i> |
| 15.0 | 20.4 | 19.7 | 15.0 | 20.3 | 20.3 | E3 ubiquitin-protein ligase HERC2 | <i>HERC2</i> |
| 22.2 | 22.7 | 22.6 | 20.1 | 22.2 | 23.2 | E3 ubiquitin-protein ligase HUWE1 | <i>HUWE1</i> |
| 21.9 | 22.1 | 21.7 | 20.1 | 21.4 | 21.7 | E3 ubiquitin-protein ligase KCMF1 | <i>KCMF1</i> |
| 18.4 | 18.6 | 18.1 | 15.0 | 15.0 | 19.2 | E3 ubiquitin-protein ligase MARCH7 | <i>Mar-07</i> |
| 20.7 | 20.7 | 20.8 | 20.9 | 20.8 | 20.6 | E3 ubiquitin-protein ligase MYCBP2 | <i>MYCBP2</i> |
| 19.5 | 19.7 | 19.9 | 15.0 | 19.6 | 20.3 | E3 ubiquitin-protein ligase Praja-1 | <i>PJA1</i> |
| 20.9 | 20.9 | 20.8 | 15.0 | 20.8 | 21.6 | E3 ubiquitin-protein ligase Praja-2 | <i>PJA2</i> |
| 20.7 | 20.4 | 20.6 | 20.7 | 20.6 | 20.5 | E3 ubiquitin-protein ligase RBBP6 | <i>RBBP6</i> |
| 25.2 | 25.1 | 25.4 | 24.0 | 25.3 | 24.9 | E3 ubiquitin-protein ligase RFWD2 | <i>RFWD2</i> |
| 17.8 | 18.1 | 18.3 | 18.4 | 18.0 | 18.0 | E3 ubiquitin-protein ligase RING1 | <i>RING1</i> |
| 20.1 | 20.2 | 20.1 | 19.9 | 20.1 | 20.0 | E3 ubiquitin-protein ligase RING2 | <i>RNF2</i> |
| 15.0 | 15.0 | 18.5 | 15.0 | 15.0 | 18.8 | E3 ubiquitin-protein ligase RNF126 | <i>RNF126</i> |
| 19.1 | 18.9 | 18.9 | 18.9 | 19.1 | 19.2 | E3 ubiquitin-protein ligase RNF138 | <i>RNF138</i> |
| 17.6 | 17.7 | 17.5 | 15.0 | 17.4 | 18.1 | E3 ubiquitin-protein ligase RNF169 | <i>RNF169</i> |
| 22.0 | 22.1 | 21.3 | 15.0 | 22.6 | 21.4 | E3 ubiquitin-protein ligase RNF220 | <i>RNF220</i> |
| 18.7 | 18.7 | 18.9 | 15.0 | 18.6 | 18.8 | E3 ubiquitin-protein ligase TRIM37 | <i>TRIM37</i> |
| 17.8 | 17.7 | 17.7 | 15.0 | 17.6 | 17.7 | E3 ubiquitin-protein ligase TRIM56 | <i>TRIM56</i> |
| 19.7 | 19.7 | 19.3 | 15.0 | 20.5 | 19.5 | E3 ubiquitin-protein ligase UBR2 | <i>UBR2</i> |
| 23.4 | 23.6 | 23.2 | 18.4 | 23.1 | 23.2 | E3 ubiquitin-protein ligase UBR4 | <i>UBR4</i> |
| 23.6 | 23.8 | 23.2 | 18.9 | 23.3 | 24.0 | E3 ubiquitin-protein ligase UBR5 | <i>UBR5</i> |
| 21.6 | 21.4 | 21.6 | 21.3 | 21.6 | 21.3 | E3 ubiquitin-protein ligase UHRF1 | <i>UHRF1</i> |
| 20.7 | 20.2 | 20.9 | 19.7 | 20.6 | 21.1 | E3 ubiquitin-protein ligase ZFP91 | <i>ZFP91-CNTF</i> |
| 21.9 | 21.8 | 21.8 | 21.1 | 21.7 | 21.8 | E3 ubiquitin/ISG15 ligase TRIM25 | <i>TRIM25</i> |
| 20.4 | 20.4 | 20.2 | 20.9 | 20.5 | 20.4 | Echinoderm microtubule-associated protein-like 4 | <i>EML4</i> |
| 22.6 | 22.4 | 22.5 | 22.2 | 22.8 | 22.3 | ELAV-like protein 1 | <i>ELAVL1</i> |
| 18.5 | 18.5 | 15.0 | 15.0 | 18.1 | 19.4 | Electron transfer flavoprotein subunit alpha, mitochondrial | <i>ETFA</i> |
| 27.3 | 28.0 | 28.3 | 27.3 | 27.5 | 28.1 | Elongation factor 1-alpha 1 | <i>EEF1A1</i> |
| 22.5 | 22.5 | 22.7 | 24.3 | 22.3 | 22.6 | Elongation factor 1-beta | <i>EEF1B2</i> |
| 22.7 | 22.8 | 23.2 | 25.2 | 22.5 | 22.6 | Elongation factor 1-delta | <i>EEF1D</i> |
| 21.6 | 21.3 | 21.8 | 23.7 | 21.3 | 21.3 | Elongation factor 1-gamma | <i>EEF1G</i> |
| 23.4 | 23.1 | 23.5 | 25.0 | 23.2 | 23.4 | Elongation factor 2 | <i>EEF2</i> |
| 22.5 | 23.2 | 23.3 | 24.2 | 22.3 | 23.4 | Elongation factor Tu, mitochondrial | <i>TUFM</i> |
| 22.8 | 23.0 | 23.1 | 22.8 | 22.6 | 23.2 | Emerin | <i>EMD</i> |
| 18.2 | 15.0 | 15.0 | 19.6 | 15.0 | 18.9 | Endophilin-A2 | <i>SH3GL1</i> |
| 15.0 | 15.0 | 15.0 | 20.3 | 15.0 | 15.0 | Endoplasmic reticulum resident protein 29 | <i>ERP29</i> |
| 19.9 | 20.1 | 19.7 | 21.3 | 20.3 | 20.6 | Endoplasmin | <i>HSP90B1</i> |
| 20.7 | 21.0 | 20.7 | 19.3 | 20.8 | 20.6 | Endoribonuclease Dicer | <i>DICER1</i> |
| 20.4 | 20.3 | 21.1 | 23.3 | 20.8 | 20.6 | Endothelial differentiation-related factor 1 | <i>EDF1</i> |
| 21.2 | 20.8 | 20.8 | 21.2 | 20.8 | 20.8 | Enhancer of mRNA-decapping protein 4 | <i>EDC4</i> |
| 24.5 | 24.3 | 24.4 | 25.1 | 24.7 | 23.9 | Enhancer of rudimentary homolog | <i>ERH</i> |

| | | | | | | | |
|------|------|------|------|------|------|--|------------------|
| 21.0 | 20.8 | 20.7 | 19.7 | 20.6 | 20.5 | Ensconsin | <i>MAP7</i> |
| 18.9 | 18.7 | 18.4 | 15.0 | 18.8 | 18.8 | Epidermal growth factor-like protein 7 | <i>EGFL7</i> |
| 18.8 | 18.9 | 18.9 | 19.4 | 19.3 | 18.8 | ER membrane protein complex subunit 2 | <i>EMC2</i> |
| 20.7 | 20.9 | 20.7 | 20.8 | 20.7 | 20.4 | ESF1 homolog | <i>ESF1</i> |
| 19.8 | 20.1 | 19.6 | 19.4 | 19.9 | 20.0 | Etoposide-induced protein 2.4 homolog | <i>EI24</i> |
| 20.0 | 19.8 | 20.1 | 21.6 | 20.0 | 20.1 | Eukaryotic initiation factor 4A-I | <i>EIF4A1</i> |
| 22.5 | 22.0 | 22.3 | 23.6 | 22.2 | 22.1 | Eukaryotic initiation factor 4A-III | <i>EIF4A3</i> |
| 21.0 | 21.1 | 21.3 | 21.7 | 21.0 | 21.0 | Eukaryotic translation elongation factor 1 epsilon-1 | <i>EEF1E1</i> |
| 21.2 | 21.4 | 21.8 | 23.7 | 21.7 | 21.5 | Eukaryotic translation initiation factor 1A, X-chromosomal | <i>EIF1AX</i> |
| 23.2 | 22.9 | 22.9 | 22.2 | 23.0 | 23.0 | Eukaryotic translation initiation factor 2 subunit 1 | <i>EIF2S1</i> |
| 23.6 | 23.6 | 23.6 | 23.6 | 23.7 | 23.5 | Eukaryotic translation initiation factor 2 subunit 2 | <i>EIF2S2</i> |
| 23.7 | 23.8 | 23.8 | 23.4 | 23.8 | 23.8 | Eukaryotic translation initiation factor 2 subunit 3 | <i>EIF2S3</i> |
| 22.3 | 22.1 | 22.1 | 21.4 | 22.1 | 22.1 | Eukaryotic translation initiation factor 2A | <i>EIF2A</i> |
| 20.0 | 19.5 | 20.1 | 20.8 | 19.2 | 19.3 | Eukaryotic translation initiation factor 3 subunit A | <i>EIF3A</i> |
| 18.6 | 18.2 | 18.3 | 19.7 | 18.5 | 17.9 | Eukaryotic translation initiation factor 3 subunit C | <i>EIF3C</i> |
| 21.1 | 20.8 | 20.7 | 21.8 | 21.0 | 20.7 | Eukaryotic translation initiation factor 3 subunit D | <i>EIF3D</i> |
| 19.9 | 20.4 | 20.7 | 21.5 | 20.4 | 20.1 | Eukaryotic translation initiation factor 3 subunit I | <i>EIF3I</i> |
| 23.5 | 23.6 | 23.6 | 23.2 | 23.7 | 23.4 | Eukaryotic translation initiation factor 4 gamma 1 | <i>EIF4G1</i> |
| 19.3 | 19.2 | 19.2 | 19.2 | 19.0 | 19.4 | Eukaryotic translation initiation factor 4 gamma 2 | <i>EIF4G2</i> |
| 18.9 | 18.6 | 18.6 | 19.2 | 18.9 | 18.6 | Eukaryotic translation initiation factor 4 gamma 3 | <i>EIF4G3</i> |
| 17.8 | 18.0 | 18.0 | 19.4 | 18.0 | 17.9 | Eukaryotic translation initiation factor 4B | <i>EIF4B</i> |
| 19.0 | 19.1 | 18.9 | 19.1 | 19.1 | 18.5 | Eukaryotic translation initiation factor 4E | <i>EIF4E</i> |
| 20.1 | 20.1 | 20.1 | 19.9 | 20.1 | 20.3 | Eukaryotic translation initiation factor 4E transporter | <i>EIF4ENIF1</i> |
| 17.8 | 17.4 | 19.0 | 22.2 | 18.4 | 18.1 | Eukaryotic translation initiation factor 5 | <i>EIF5</i> |
| 18.7 | 19.2 | 19.7 | 20.7 | 18.6 | 19.3 | Eukaryotic translation initiation factor 5A | <i>EIF5A</i> |
| 22.1 | 22.0 | 22.3 | 22.9 | 21.9 | 21.8 | Eukaryotic translation initiation factor 5B | <i>EIF5B</i> |
| 19.7 | 20.1 | 20.4 | 20.6 | 20.5 | 20.4 | Eukaryotic translation initiation factor 6 | <i>EIF6</i> |
| 18.9 | 18.8 | 18.9 | 15.0 | 18.6 | 18.4 | Exocyst complex component 4 | <i>EXOC4</i> |
| 20.5 | 20.5 | 20.5 | 20.9 | 20.5 | 20.5 | Exonuclease 1 | <i>EXO1</i> |
| 22.2 | 22.1 | 22.2 | 21.9 | 22.3 | 22.1 | Exosome complex component CSL4 | <i>EXOSC1</i> |
| 22.0 | 21.7 | 21.9 | 22.0 | 21.8 | 21.8 | Exosome complex component MTR3 | <i>EXOSC6</i> |
| 21.5 | 21.6 | 21.4 | 20.2 | 21.5 | 21.3 | Exosome complex component RRP4 | <i>EXOSC2</i> |
| 23.0 | 23.1 | 23.2 | 22.6 | 23.0 | 22.9 | Exosome complex component RRP40 | <i>EXOSC3</i> |
| 22.6 | 22.5 | 22.4 | 21.9 | 22.6 | 22.3 | Exosome complex component RRP41 | <i>EXOSC4</i> |
| 19.6 | 19.5 | 19.6 | 15.0 | 19.7 | 15.0 | Exosome complex component RRP42 | <i>EXOSC7</i> |
| 22.1 | 22.0 | 22.1 | 21.6 | 22.2 | 21.8 | Exosome complex component RRP43 | <i>EXOSC8</i> |
| 20.2 | 20.2 | 20.5 | 19.9 | 20.4 | 20.2 | Exosome complex component RRP45 | <i>EXOSC9</i> |
| 15.0 | 19.5 | 19.8 | 15.0 | 19.4 | 19.6 | Exosome complex component RRP46 | <i>EXOSC5</i> |
| 21.0 | 21.7 | 22.1 | 21.2 | 21.4 | 21.4 | Exosome complex exonuclease RRP44 | <i>DIS3</i> |
| 23.4 | 23.3 | 23.5 | 22.7 | 23.6 | 23.1 | Exosome component 10 | <i>EXOSC10</i> |
| 15.0 | 19.6 | 19.5 | 15.0 | 19.5 | 19.7 | Exportin-1 | <i>XPO1</i> |
| 18.6 | 18.7 | 18.7 | 15.0 | 18.9 | 19.0 | Extended synaptotagmin-2 | <i>ESYT2</i> |
| 17.7 | 17.5 | 17.8 | 20.2 | 17.6 | 17.8 | Ezrin | <i>EZR</i> |
| 20.2 | 20.2 | 20.3 | 21.6 | 20.3 | 20.6 | F-actin-capping protein subunit alpha-1 | <i>CAPZA1</i> |
| 20.1 | 20.0 | 19.9 | 15.0 | 19.9 | 19.9 | F-box only protein 5 | <i>FBXO5</i> |
| 19.2 | 19.1 | 19.8 | 22.0 | 19.8 | 19.4 | FACT complex subunit SPT16 | <i>SUPT16H</i> |

| | | | | | | | |
|------|------|------|------|------|------|---|----------------|
| 15.0 | 19.1 | 19.2 | 15.0 | 15.0 | 19.2 | Fanconi anemia group I protein | <i>FANCI</i> |
| 21.7 | 21.7 | 21.8 | 23.0 | 21.8 | 21.7 | Far upstream element-binding protein 1 | <i>FUBP1</i> |
| 24.6 | 24.6 | 24.7 | 25.9 | 24.7 | 24.3 | Far upstream element-binding protein 2 | <i>KHSRP</i> |
| 24.0 | 23.9 | 23.7 | 23.8 | 24.0 | 23.5 | Far upstream element-binding protein 3 | <i>FUBP3</i> |
| 20.5 | 20.6 | 20.8 | 21.6 | 20.6 | 20.8 | Acyl-carrier-protein S-acetyltransferase | <i>FASN</i> |
| 15.0 | 18.4 | 18.9 | 15.0 | 18.1 | 18.6 | Fatty acyl-CoA reductase 1 | <i>FAR1</i> |
| 21.2 | 21.3 | 21.4 | 21.5 | 21.2 | 21.4 | FH1/FH2 domain-containing protein 1 | <i>FHOD1</i> |
| 22.3 | 22.3 | 21.9 | 19.6 | 21.8 | 22.4 | Fibrillin-2 | <i>FBN2</i> |
| 19.2 | 18.5 | 18.9 | 21.3 | 18.9 | 19.3 | Filamin-A | <i>FLNA</i> |
| 20.3 | 19.9 | 20.4 | 22.4 | 20.0 | 20.0 | Flap endonuclease 1 | <i>FEN1</i> |
| 22.2 | 23.0 | 22.3 | 20.0 | 22.2 | 22.6 | Flap endonuclease GEN homolog 1 | <i>GEN1</i> |
| 20.0 | 19.7 | 19.6 | 20.1 | 19.5 | 19.9 | Forkhead box protein C1 | <i>FOXC1</i> |
| 21.0 | 21.1 | 21.1 | 19.7 | 21.0 | 21.1 | Forkhead box protein K1 | <i>FO XK1</i> |
| 19.1 | 19.2 | 19.0 | 15.0 | 19.2 | 19.0 | Forkhead box protein K2 | <i>FO XK2</i> |
| 17.8 | 17.0 | 17.6 | 17.6 | 17.1 | 17.4 | Four and a half LIM domains protein 1 | <i>FHL1</i> |
| 22.2 | 21.4 | 21.5 | 20.9 | 21.9 | 21.5 | Fragile X mental retardation syndrome-related protein 1 | <i>FXR1</i> |
| 22.6 | 22.6 | 22.5 | 21.9 | 22.8 | 22.4 | Fragile X mental retardation syndrome-related protein 2 | <i>FXR2</i> |
| 22.3 | 21.2 | 22.0 | 24.5 | 21.4 | 22.1 | Fructose-bisphosphate aldolase | <i>ALDOA</i> |
| 21.2 | 21.2 | 20.9 | 20.4 | 21.0 | 21.0 | G patch domain-containing protein 4 | <i>GPATCH4</i> |
| 19.5 | 18.5 | 18.1 | 15.0 | 18.7 | 18.8 | G patch domain-containing protein 8 | <i>GPATCH8</i> |
| 22.0 | 22.3 | 22.0 | 20.8 | 21.8 | 22.2 | G-protein coupled receptor-associated sorting protein 2 | <i>GPRASP2</i> |
| 21.0 | 21.4 | 21.1 | 20.1 | 21.3 | 21.2 | G2 and S phase-expressed protein 1 | <i>GTSE1</i> |
| 20.4 | 20.7 | 20.8 | 22.0 | 20.6 | 20.6 | Gamma-taxilin | <i>TXLNG</i> |
| 18.2 | 18.9 | 15.0 | 15.0 | 18.5 | 18.8 | Gamma-tubulin complex component 2 | <i>TUBGCP2</i> |
| 20.5 | 20.7 | 20.5 | 20.1 | 20.3 | 20.7 | Gamma-tubulin complex component 3 | <i>TUBGCP3</i> |
| 18.7 | 19.6 | 19.4 | 15.0 | 15.0 | 19.7 | Gamma-tubulin complex component 6 | <i>TUBGCP6</i> |
| 21.4 | 21.4 | 21.4 | 20.5 | 21.3 | 21.8 | Gem-associated protein 2 | <i>GEMIN2</i> |
| 15.0 | 17.6 | 17.3 | 15.0 | 16.7 | 17.5 | Gem-associated protein 4 | <i>GEMIN4</i> |
| 20.2 | 19.8 | 20.2 | 19.7 | 19.6 | 20.0 | Gem-associated protein 5 | <i>GEMIN5</i> |
| 19.9 | 19.8 | 19.9 | 15.0 | 20.0 | 20.2 | Gem-associated protein 6 | <i>GEMIN6</i> |
| 20.9 | 21.0 | 20.7 | 20.6 | 20.7 | 21.4 | Gem-associated protein 7 | <i>GEMIN7</i> |
| 19.9 | 20.0 | 20.1 | 20.0 | 19.9 | 20.1 | Gem-associated protein 8 | <i>GEMIN8</i> |
| 22.5 | 22.3 | 22.6 | 20.9 | 22.4 | 22.5 | General transcription factor 3C polypeptide 1 | <i>GTF3C1</i> |
| 15.0 | 19.2 | 19.1 | 15.0 | 19.2 | 19.3 | General transcription factor 3C polypeptide 2 | <i>GTF3C2</i> |
| 22.0 | 21.8 | 21.7 | 20.3 | 21.7 | 21.7 | General transcription factor 3C polypeptide 4 | <i>GTF3C4</i> |
| 22.0 | 21.8 | 21.8 | 20.6 | 21.8 | 21.8 | General transcription factor 3C polypeptide 5 | <i>GTF3C5</i> |
| 22.5 | 22.1 | 22.2 | 20.9 | 22.3 | 22.2 | General transcription factor II-I | <i>GTF2I</i> |
| 15.0 | 18.8 | 19.0 | 21.7 | 19.0 | 18.8 | General transcription factor IIF subunit 1 | <i>GTF2F1</i> |
| 18.9 | 18.9 | 18.7 | 21.3 | 19.2 | 19.0 | General transcription factor IIF subunit 2 | <i>GTF2F2</i> |
| 18.7 | 15.0 | 18.4 | 18.9 | 15.0 | 18.4 | General transcription factor IIH subunit 2-like protein | <i>GTF2H2C</i> |
| 18.0 | 18.4 | 18.4 | 15.0 | 17.7 | 19.0 | Germinal-center associated nuclear protein | <i>MCM3AP</i> |
| 20.6 | 20.4 | 20.1 | 19.8 | 20.7 | 20.3 | Glioma tumor suppressor candidate region gene 2 protein | <i>GLTSCR2</i> |
| 15.0 | 15.0 | 15.0 | 21.9 | 15.0 | 15.0 | Glucose-6-phosphate isomerase | <i>GPI</i> |
| 15.0 | 15.0 | 18.5 | 15.0 | 15.0 | 18.9 | Glucosidase 2 subunit beta | <i>PRKCSH</i> |
| 19.3 | 19.3 | 19.5 | 20.2 | 19.5 | 19.9 | Glutamate dehydrogenase 1, mitochondrial | <i>GLUD1</i> |
| 23.0 | 22.5 | 22.6 | 21.5 | 22.7 | 22.5 | Glutamate-rich WD repeat-containing protein 1 | <i>GRWD1</i> |

| | | | | | | | |
|------|------|------|------|------|------|---|-------------------|
| 15.0 | 18.3 | 18.1 | 15.0 | 18.1 | 18.4 | Glutamine and serine-rich protein 1 | <i>QSER1</i> |
| 21.5 | 21.4 | 21.3 | 22.0 | 21.3 | 21.3 | Glutamine--tRNA ligase | <i>QARS</i> |
| 19.3 | 15.0 | 19.8 | 21.9 | 15.0 | 19.5 | Glutathione S-transferase P | <i>GSTP1</i> |
| 23.7 | 23.4 | 23.9 | 24.8 | 23.7 | 23.8 | Glyceraldehyde-3-phosphate dehydrogenase | <i>GAPDH</i> |
| 21.0 | 20.4 | 20.4 | 20.8 | 20.1 | 20.5 | Glycylpeptide N-tetradecanoyltransferase 1 | <i>NMT1</i> |
| 15.0 | 15.0 | 15.0 | 19.4 | 15.0 | 15.0 | GMP synthase [glutamine-hydrolyzing] | <i>GMPS</i> |
| 18.7 | 18.7 | 18.7 | 15.0 | 18.7 | 18.6 | Golgi apparatus protein 1 | <i>GLG1</i> |
| 20.3 | 20.7 | 20.5 | 19.9 | 20.2 | 20.5 | Golgin subfamily A member 2 | <i>GOLGA2</i> |
| 17.9 | 18.7 | 18.9 | 23.8 | 17.9 | 18.7 | Golgin subfamily A member 4 | <i>GOLGA4</i> |
| 20.1 | 20.1 | 20.1 | 20.3 | 20.3 | 19.9 | Granulins | <i>GRN</i> |
| 21.8 | 21.9 | 21.1 | 21.0 | 22.1 | 21.4 | Growth arrest and DNA damage-inducible proteins-interacting protein 1 | <i>GADD45GIP1</i> |
| 21.8 | 21.6 | 22.2 | 24.1 | 21.9 | 21.8 | GTP-binding nuclear protein Ran | <i>RAN</i> |
| 22.6 | 22.4 | 22.7 | 22.2 | 22.4 | 22.4 | GTP-binding protein 1 | <i>GTPBP1</i> |
| 20.6 | 20.5 | 20.3 | 19.7 | 20.6 | 20.6 | GTPase Era, mitochondrial | <i>ERAL1</i> |
| 19.8 | 20.3 | 20.4 | 20.7 | 19.8 | 19.7 | Guanine nucleotide-binding protein subunit beta-2-like 1 | <i>GNB2L1</i> |
| 15.0 | 15.0 | 18.5 | 19.4 | 15.0 | 18.0 | Guanine nucleotide-binding protein subunit beta-like protein 1 | <i>GNB1L</i> |
| 15.0 | 15.0 | 15.0 | 19.5 | 17.2 | 18.1 | Guanine nucleotide-binding protein-like 1 | <i>GNL1</i> |
| 23.8 | 23.7 | 23.8 | 22.7 | 23.9 | 23.7 | Guanine nucleotide-binding protein-like 3 | <i>GNL3</i> |
| 21.6 | 21.5 | 21.6 | 20.9 | 21.6 | 21.6 | Guanine nucleotide-binding protein-like 3-like protein | <i>GNL3L</i> |
| 22.0 | 21.3 | 21.3 | 19.9 | 21.5 | 21.0 | H/ACA ribonucleoprotein complex subunit 1 | <i>GAR1</i> |
| 21.8 | 21.6 | 21.3 | 21.2 | 21.8 | 21.2 | H/ACA ribonucleoprotein complex subunit 2 | <i>NHP2</i> |
| 22.9 | 22.9 | 22.6 | 21.5 | 23.2 | 22.7 | H/ACA ribonucleoprotein complex subunit 3 | <i>NOP10</i> |
| 23.1 | 22.9 | 22.9 | 21.5 | 23.0 | 22.8 | H/ACA ribonucleoprotein complex subunit 4 | <i>DKC1</i> |
| 20.1 | 20.2 | 19.9 | 20.0 | 19.8 | 20.1 | HAUS augmin-like complex subunit 6 | <i>HAUS6</i> |
| 20.2 | 20.2 | 20.5 | 20.4 | 20.2 | 20.5 | HAUS augmin-like complex subunit 8 | <i>HAUS8</i> |
| 20.3 | 20.1 | 20.1 | 20.2 | 20.4 | 19.8 | HBS1-like protein | <i>HBS1L</i> |
| 20.5 | 20.7 | 20.6 | 20.4 | 20.3 | 21.3 | HCLS1-associated protein X-1 | <i>HAX1</i> |
| 19.1 | 19.0 | 19.1 | 18.7 | 15.0 | 19.2 | Heat shock 70 kDa protein 14 | <i>HSPA14</i> |
| 29.6 | 29.9 | 29.7 | 27.6 | 29.5 | 30.4 | Heat shock 70 kDa protein 1B | <i>HSPA1B</i> |
| 24.1 | 24.2 | 23.8 | 21.8 | 23.7 | 24.5 | Heat shock 70 kDa protein 4 | <i>HSPA4</i> |
| 24.3 | 24.3 | 24.1 | 22.1 | 24.1 | 24.6 | Heat shock 70 kDa protein 4L | <i>HSPA4L</i> |
| 24.0 | 24.7 | 24.7 | 23.2 | 24.2 | 24.8 | Heat shock 70 kDa protein 6 | <i>HSPA6</i> |
| 29.9 | 30.3 | 30.0 | 28.2 | 29.9 | 30.6 | Heat shock cognate 71 kDa protein | <i>HSPA8</i> |
| 24.0 | 24.5 | 23.9 | 21.9 | 24.0 | 24.7 | Heat shock protein 105 kDa | <i>HSPH1</i> |
| 23.2 | 23.9 | 24.0 | 23.9 | 22.7 | 25.0 | Heat shock protein HSP 90-alpha | <i>HSP90AA1</i> |
| 24.6 | 25.3 | 25.5 | 24.7 | 24.1 | 26.4 | Heat shock protein HSP 90-beta | <i>HSP90AB1</i> |
| 19.2 | 19.2 | 19.6 | 19.7 | 19.6 | 18.9 | Helicase SRCAP | <i>SRCAP</i> |
| 20.5 | 20.6 | 20.7 | 19.0 | 20.4 | 20.7 | Helicase-like transcription factor | <i>HLTF</i> |
| 18.6 | 18.7 | 18.8 | 21.1 | 18.7 | 18.2 | Hematological and neurological expressed 1-like protein | <i>HN1L</i> |
| 18.6 | 18.5 | 19.8 | 21.0 | 19.3 | 19.0 | Hepatoma-derived growth factor | <i>HDGF</i> |
| 15.0 | 15.0 | 15.0 | 21.3 | 15.0 | 15.0 | Hepatoma-derived growth factor-related protein 2 | <i>HDGFRP2</i> |
| 24.0 | 24.1 | 23.9 | 23.6 | 24.0 | 23.8 | Heterochromatin protein 1-binding protein 3 | <i>HP1BP3</i> |
| 25.5 | 25.3 | 25.4 | 24.5 | 25.6 | 25.1 | Heterogeneous nuclear ribonucleoprotein A/B | <i>HNRNPAB</i> |
| 24.8 | 24.8 | 24.7 | 23.7 | 24.9 | 24.5 | Heterogeneous nuclear ribonucleoprotein A0 | <i>HNRNPA0</i> |
| 28.0 | 27.8 | 27.9 | 27.3 | 28.1 | 27.7 | Heterogeneous nuclear ribonucleoprotein A1 | <i>HNRNPA1</i> |

| | | | | | | | |
|------|------|------|------|------|------|--|-------------------|
| 25.8 | 25.5 | 25.7 | 25.4 | 26.0 | 25.6 | Heterogeneous nuclear ribonucleoprotein A3 | <i>HNRNPA3</i> |
| 24.7 | 24.3 | 24.2 | 23.5 | 25.1 | 24.1 | Heterogeneous nuclear ribonucleoprotein D-like | <i>HNRNPDL</i> |
| 25.8 | 25.7 | 25.7 | 24.9 | 25.9 | 25.6 | Heterogeneous nuclear ribonucleoprotein D0 | <i>HNRNPD</i> |
| 23.5 | 23.4 | 23.3 | 23.4 | 23.7 | 23.4 | Heterogeneous nuclear ribonucleoprotein F | <i>HNRNPF</i> |
| 25.7 | 25.5 | 25.5 | 25.2 | 25.9 | 25.3 | Heterogeneous nuclear ribonucleoprotein H | <i>HNRNPH1</i> |
| 23.3 | 22.9 | 22.5 | 21.9 | 23.3 | 22.8 | Heterogeneous nuclear ribonucleoprotein H2 | <i>HNRNPH2</i> |
| 21.4 | 21.1 | 21.3 | 21.9 | 21.9 | 21.0 | Heterogeneous nuclear ribonucleoprotein H3 | <i>HNRNPH3</i> |
| 25.7 | 25.3 | 25.2 | 25.4 | 25.7 | 25.2 | Heterogeneous nuclear ribonucleoprotein K | <i>HNRNPK</i> |
| 25.7 | 25.1 | 25.1 | 24.7 | 25.8 | 24.9 | Heterogeneous nuclear ribonucleoprotein L | <i>HNRNPL</i> |
| 15.0 | 19.1 | 19.0 | 15.0 | 19.6 | 18.7 | Heterogeneous nuclear ribonucleoprotein L-like | <i>HNRNPLL</i> |
| 27.1 | 27.3 | 27.2 | 27.1 | 27.2 | 27.0 | Heterogeneous nuclear ribonucleoprotein M | <i>HNRNPM</i> |
| 26.1 | 25.9 | 25.9 | 25.1 | 26.0 | 25.8 | Heterogeneous nuclear ribonucleoprotein Q | <i>SYNCRIP</i> |
| 24.8 | 24.4 | 24.5 | 23.4 | 24.9 | 24.3 | Heterogeneous nuclear ribonucleoprotein R | <i>HNRNPR</i> |
| 27.5 | 27.4 | 27.3 | 26.3 | 27.6 | 27.3 | Heterogeneous nuclear ribonucleoprotein U | <i>HNRNPU</i> |
| 23.9 | 23.7 | 23.8 | 22.4 | 24.1 | 23.6 | Heterogeneous nuclear ribonucleoprotein U-like protein 1 | <i>HNRNPUL1</i> |
| 23.0 | 22.9 | 22.9 | 21.9 | 23.4 | 22.7 | Heterogeneous nuclear ribonucleoprotein U-like protein 2 | <i>HNRNPUL2</i> |
| 27.2 | 27.0 | 27.1 | 26.6 | 27.5 | 26.8 | Heterogeneous nuclear ribonucleoproteins A2/B1 | <i>HNRNPA2B1</i> |
| 24.6 | 25.1 | 25.6 | 28.2 | 25.1 | 25.1 | High mobility group protein B1 | <i>HMGB1</i> |
| 23.2 | 23.5 | 24.2 | 26.9 | 23.5 | 23.8 | High mobility group protein B2 | <i>HMGB2</i> |
| 22.9 | 22.6 | 23.0 | 24.7 | 22.8 | 22.4 | High mobility group protein B3 | <i>HMGB3</i> |
| 21.1 | 20.9 | 21.4 | 24.1 | 21.3 | 21.1 | High mobility group protein HMG-I/HMG-Y | <i>HMGA1</i> |
| 15.0 | 15.0 | 20.0 | 21.6 | 18.4 | 18.9 | Histidine triad nucleotide-binding protein 1 | <i>HINT1</i> |
| 20.6 | 20.7 | 20.7 | 20.1 | 20.3 | 20.8 | Histone acetyltransferase p300 | <i>EP300</i> |
| 20.0 | 19.6 | 19.2 | 22.1 | 20.4 | 19.9 | Histone deacetylase 1 | <i>HDAC1</i> |
| 21.5 | 21.3 | 21.3 | 24.4 | 21.2 | 21.2 | Histone deacetylase 10 | <i>HDAC10</i> |
| 25.5 | 25.6 | 26.1 | 28.8 | 25.6 | 25.6 | Histone deacetylase 6 | <i>HDAC6</i> |
| 19.2 | 19.2 | 19.4 | 15.0 | 19.4 | 19.1 | Histone deacetylase complex subunit SAP130 | <i>SAP130</i> |
| 18.2 | 18.3 | 18.9 | 19.7 | 18.7 | 18.4 | Histone deacetylase complex subunit SAP18 | <i>SAP18</i> |
| 23.3 | 23.5 | 23.6 | 23.5 | 23.2 | 23.2 | Histone H1.0 | <i>H1F0</i> |
| 26.2 | 26.2 | 26.2 | 26.5 | 26.2 | 26.2 | Histone H1.2 | <i>HIST1H1C</i> |
| 23.2 | 22.9 | 23.1 | 22.7 | 23.2 | 22.9 | Histone H1.3 | <i>HIST1H1D</i> |
| 29.3 | 29.3 | 29.3 | 29.3 | 29.4 | 29.2 | Histone H1.4 | <i>HIST1H1E</i> |
| 24.4 | 24.5 | 24.5 | 24.2 | 24.4 | 24.2 | Histone H1x | <i>H1FX</i> |
| 21.7 | 21.2 | 22.5 | 21.9 | 21.8 | 22.1 | Histone H2A type 1-C | <i>HIST1H2AC</i> |
| 25.8 | 25.5 | 26.1 | 26.1 | 26.0 | 25.9 | Histone H2A type 1-J | <i>HIST1H2AJ</i> |
| 20.9 | 20.7 | 20.6 | 24.0 | 22.4 | 21.5 | Histone H2A.V | <i>H2AFV</i> |
| 15.0 | 15.0 | 15.6 | 15.0 | 15.0 | 15.0 | Histone H2AX | <i>H2AFX</i> |
| 26.4 | 26.2 | 26.6 | 27.0 | 26.5 | 26.2 | Histone H2B type 1-H | <i>HIST1H2BH</i> |
| 23.1 | 23.0 | 23.0 | 23.8 | 23.7 | 23.3 | Histone H2B type 1-K | <i>HIST1H2BK</i> |
| 22.6 | 22.7 | 23.0 | 24.1 | 23.1 | 23.3 | Histone H2B type 1-O | <i>HIST1H2BO</i> |
| 18.5 | 19.3 | 19.1 | 20.1 | 19.9 | 19.3 | Histone H2B type 3-B | <i>HIST3H2BB</i> |
| 21.5 | 21.2 | 21.7 | 22.5 | 21.8 | 21.7 | Histone H3 | <i>HIST2H3PS2</i> |
| 25.0 | 24.7 | 25.7 | 26.4 | 25.3 | 25.2 | Histone H3.1 | <i>HIST1H3A</i> |

| | | | | | | | |
|------|------|------|------|------|------|---|-----------------|
| 25.6 | 25.4 | 26.5 | 26.9 | 26.0 | 25.8 | Histone H4 | <i>HIST1H4A</i> |
| 21.0 | 21.3 | 21.1 | 20.8 | 20.9 | 21.5 | Histone lysine demethylase PHF8 | <i>PHF8</i> |
| 15.0 | 19.6 | 19.5 | 19.0 | 19.4 | 19.5 | Histone RNA hairpin-binding protein | <i>SLBP</i> |
| 20.9 | 21.2 | 21.3 | 21.7 | 21.0 | 21.5 | Histone-binding protein RBBP4 | <i>RBBP4</i> |
| 22.2 | 22.3 | 22.6 | 23.1 | 22.1 | 22.4 | Histone-binding protein RBBP7 | <i>RBBP7</i> |
| 19.7 | 15.0 | 18.9 | 15.0 | 21.1 | 15.0 | Histone-lysine N-methyltransferase 2A | <i>KMT2A</i> |
| 15.0 | 19.9 | 19.4 | 21.2 | 19.6 | 15.0 | Histone-lysine N-methyltransferase 2C | <i>KMT2C</i> |
| 18.8 | 18.7 | 18.9 | 19.1 | 18.8 | 18.7 | Histone-lysine N-methyltransferase 2D | <i>KMT2D</i> |
| 18.9 | 19.3 | 19.1 | 15.0 | 19.1 | 18.9 | Histone-lysine N-methyltransferase EHMT1 | <i>EHMT1</i> |
| 17.7 | 17.8 | 18.4 | 18.6 | 15.0 | 17.6 | Histone-lysine N-methyltransferase NSD3 | <i>WHSC1L1</i> |
| 19.5 | 19.9 | 19.6 | 19.3 | 19.5 | 19.9 | Histone-lysine N-methyltransferase SETD2 | <i>SETD2</i> |
| 21.4 | 20.2 | 19.2 | 19.7 | 21.7 | 19.2 | HIV Tat-specific factor 1 | <i>HTATSF1</i> |
| 18.9 | 18.9 | 19.1 | 15.0 | 18.2 | 20.0 | HLA class I histocompatibility antigen, Cw-7 alpha chain | <i>HLA-C</i> |
| 19.8 | 20.2 | 20.0 | 18.9 | 19.8 | 20.1 | HMG box transcription factor BBX | <i>BBX</i> |
| 19.6 | 19.5 | 19.3 | 18.8 | 19.6 | 19.5 | Holliday junction recognition protein | <i>HJURP</i> |
| 18.7 | 18.8 | 19.0 | 15.0 | 18.9 | 18.8 | Homeobox protein SIX1 | <i>SIX1</i> |
| 20.2 | 19.9 | 20.3 | 22.5 | 18.3 | 19.5 | Hsc70-interacting protein | <i>ST13</i> |
| 21.6 | 21.3 | 21.3 | 21.4 | 21.4 | 21.0 | Hyaluronan mediated motility receptor | <i>HMMR</i> |
| 20.2 | 20.5 | 21.1 | 23.5 | 20.1 | 20.0 | Hydroxyacylglutathione hydrolase, mitochondrial | <i>HAGH</i> |
| 21.4 | 21.0 | 20.7 | 15.0 | 20.9 | 20.9 | Hypermethylated in cancer 2 protein | <i>HIC2</i> |
| 22.8 | 22.5 | 22.2 | 21.1 | 23.0 | 22.5 | Importin subunit alpha-1 | <i>KPNA2</i> |
| 20.7 | 20.5 | 20.2 | 19.6 | 20.9 | 20.2 | Importin subunit alpha-4 | <i>KPNA3</i> |
| 21.0 | 20.2 | 19.7 | 20.2 | 21.0 | 19.7 | Importin subunit alpha-5 | <i>KPNA1</i> |
| 23.4 | 23.3 | 23.0 | 22.4 | 23.4 | 23.2 | Importin subunit beta-1 | <i>KPNB1</i> |
| 20.6 | 20.5 | 20.4 | 15.0 | 20.4 | 21.3 | Inactive ubiquitin carboxyl-terminal hydrolase 54 | <i>USP54</i> |
| 19.3 | 19.3 | 19.3 | 15.0 | 19.4 | 19.4 | Inner nuclear membrane protein Man1 | <i>LEM3</i> |
| 20.0 | 19.7 | 19.7 | 21.7 | 19.8 | 19.4 | Inorganic pyrophosphatase | <i>PPA1</i> |
| 22.0 | 21.4 | 21.8 | 23.1 | 21.6 | 21.6 | Inosine-5-monophosphate dehydrogenase 2 | <i>IMPDH2</i> |
| 19.5 | 18.9 | 19.1 | 15.0 | 19.3 | 19.5 | Insulin receptor substrate 2 | <i>IRS2</i> |
| 25.3 | 25.5 | 25.6 | 24.4 | 25.3 | 26.1 | Insulin receptor substrate 4 | <i>IRS4</i> |
| 26.5 | 26.5 | 26.4 | 26.0 | 26.4 | 26.3 | Insulin-like growth factor 2 mRNA-binding protein 1 | <i>IGF2BP1</i> |
| 22.0 | 22.1 | 22.0 | 21.4 | 22.1 | 21.9 | Insulin-like growth factor 2 mRNA-binding protein 2 | <i>IGF2BP2</i> |
| 23.1 | 23.2 | 23.3 | 23.4 | 23.3 | 23.1 | Insulin-like growth factor 2 mRNA-binding protein 3 | <i>IGF2BP3</i> |
| 15.0 | 18.0 | 18.1 | 15.0 | 15.0 | 18.0 | Integrator complex subunit 12 | <i>INTS12</i> |
| 18.4 | 18.1 | 18.2 | 15.0 | 18.4 | 18.5 | Integrator complex subunit 3 | <i>INTS3</i> |
| 17.9 | 17.6 | 18.0 | 17.7 | 15.0 | 18.1 | Integrin-linked protein kinase | <i>ILK</i> |
| 20.3 | 20.2 | 19.9 | 20.1 | 20.6 | 20.2 | Interferon-induced, double-stranded RNA-activated protein kinase | <i>EIF2AK2</i> |
| 19.7 | 20.0 | 20.2 | 15.0 | 19.9 | 19.6 | Interferon-inducible double-stranded RNA-dependent protein kinase activator A | <i>PRKRA</i> |
| 23.0 | 22.8 | 22.7 | 22.0 | 23.4 | 22.7 | Interleukin enhancer-binding factor 2 | <i>ILF2</i> |
| 25.0 | 25.0 | 24.9 | 24.4 | 25.0 | 24.8 | Interleukin enhancer-binding factor 3 | <i>ILF3</i> |
| 19.2 | 19.2 | 19.0 | 15.0 | 18.8 | 19.4 | Interleukin-1 receptor-associated kinase 1 | <i>IRAK1</i> |
| 17.7 | 17.6 | 17.5 | 15.0 | 17.7 | 17.6 | Intraflagellar transport protein 172 homolog | <i>IFT172</i> |
| 20.8 | 20.3 | 20.4 | 21.3 | 20.9 | 20.3 | Intraflagellar transport protein 74 homolog | <i>IFT74</i> |
| 19.8 | 20.0 | 19.8 | 19.6 | 19.6 | 19.9 | IQ motif and SEC7 domain-containing protein 1 | <i>IQSEC1</i> |

| | | | | | | | |
|------|------|------|------|------|------|---|----------------|
| 20.2 | 20.1 | 20.1 | 20.5 | 20.0 | 19.9 | Isoleucine--tRNA ligase, cytoplasmic | <i>IARS</i> |
| 18.8 | 18.9 | 18.7 | 15.0 | 18.8 | 18.9 | Junctophilin-1 | <i>JPH1</i> |
| 15.0 | 17.4 | 17.6 | 15.0 | 17.8 | 17.5 | KAT8 regulatory NSL complex subunit 2 | <i>KANSL2</i> |
| 20.0 | 20.1 | 15.0 | 21.6 | 15.0 | 18.8 | Keratinocyte proline-rich protein | <i>KPRP</i> |
| 20.9 | 20.7 | 20.4 | 23.0 | 21.1 | 20.5 | Ketosamine-3-kinase | <i>FN3KRP</i> |
| 26.0 | 25.7 | 25.4 | 25.4 | 26.0 | 25.2 | KH domain-containing, RNA-binding, signal transduction-associated protein 1 | <i>KHDRBS1</i> |
| 18.0 | 18.1 | 17.9 | 15.0 | 17.7 | 17.9 | Kinase suppressor of Ras 1 | <i>KSR1</i> |
| 21.9 | 22.0 | 22.3 | 22.9 | 21.8 | 22.0 | Kinectin | <i>KTN1</i> |
| 18.3 | 18.1 | 18.2 | 18.6 | 18.1 | 18.1 | Kinesin-1 heavy chain | <i>KIF5B</i> |
| 23.0 | 22.9 | 23.2 | 24.4 | 23.2 | 23.4 | Kinesin-like protein KIF14 | <i>KIF14</i> |
| 17.5 | 17.6 | 17.5 | 15.0 | 17.6 | 17.6 | Kinesin-like protein KIF18A | <i>KIF18A</i> |
| 24.2 | 24.2 | 23.9 | 15.0 | 24.0 | 24.1 | Kinesin-like protein KIF20B | <i>KIF20B</i> |
| 19.4 | 19.3 | 19.1 | 15.0 | 18.8 | 19.1 | Kinesin-like protein KIF21A | <i>KIF21A</i> |
| 19.7 | 19.6 | 19.8 | 19.5 | 19.8 | 19.6 | Kinesin-like protein KIF22 | <i>KIF22</i> |
| 21.1 | 21.2 | 21.2 | 21.5 | 21.1 | 20.9 | Kinesin-like protein KIF23 | <i>KIF23</i> |
| 21.5 | 21.4 | 21.4 | 21.6 | 21.3 | 21.3 | Kinesin-like protein KIF2A | <i>KIF2A</i> |
| 21.0 | 20.7 | 21.0 | 20.9 | 21.2 | 20.4 | Kinesin-like protein KIF2C | <i>KIF2C</i> |
| 18.3 | 19.2 | 18.5 | 15.0 | 19.9 | 21.0 | Kinesin-like protein KIF3B | <i>KIF3B</i> |
| 19.5 | 19.3 | 19.3 | 19.8 | 19.1 | 19.3 | Kinesin-like protein KIF7 | <i>KIF7</i> |
| 21.2 | 21.4 | 21.3 | 21.0 | 21.0 | 21.2 | Kinesin-like protein KIFC1 | <i>KIFC1</i> |
| 19.8 | 19.3 | 20.0 | 15.0 | 19.6 | 19.4 | Centromere-associated protein E | <i>CENPE</i> |
| 19.8 | 20.0 | 20.1 | 20.3 | 19.9 | 20.1 | Kinesin-like protein KIF1B | <i>KIF1B</i> |
| 15.0 | 18.6 | 18.6 | 15.0 | 18.6 | 20.7 | Kinesin-like protein KIF3A | <i>KIF3A</i> |
| 15.0 | 15.7 | 15.0 | 15.0 | 15.0 | 16.8 | Kinesin-like protein KIF3C | <i>KIF3C</i> |
| 15.0 | 18.0 | 17.9 | 17.6 | 17.8 | 18.0 | KN motif and ankyrin repeat domain-containing protein 1 | <i>KANK1</i> |
| 19.4 | 19.2 | 19.0 | 15.0 | 19.1 | 19.2 | KN motif and ankyrin repeat domain-containing protein 2 | <i>KANK2</i> |
| 22.1 | 22.6 | 22.3 | 20.8 | 22.4 | 22.5 | KRR1 small subunit processome component homolog | <i>KRR1</i> |
| 15.0 | 15.0 | 15.0 | 19.5 | 15.0 | 15.0 | L-lactate dehydrogenase A chain | <i>LDHA</i> |
| 20.8 | 20.3 | 20.9 | 22.3 | 20.3 | 20.8 | L-lactate dehydrogenase B chain | <i>LDHB</i> |
| 24.0 | 24.1 | 24.0 | 22.7 | 24.2 | 23.9 | La-related protein 1 | <i>LARP1</i> |
| 21.3 | 21.3 | 21.1 | 15.0 | 21.5 | 21.2 | La-related protein 4 | <i>LARP4</i> |
| 20.0 | 20.1 | 19.8 | 19.6 | 19.8 | 20.1 | La-related protein 4B | <i>LARP4B</i> |
| 22.1 | 22.1 | 21.7 | 20.5 | 22.4 | 21.6 | La-related protein 7 | <i>LARP7</i> |
| 19.7 | 18.1 | 19.1 | 20.8 | 15.0 | 15.0 | Lactoylglutathione lyase | <i>GLO1</i> |
| 17.3 | 18.0 | 18.5 | 18.2 | 17.7 | 17.8 | Lamin-B receptor | <i>LBR</i> |
| 21.4 | 21.2 | 21.6 | 22.4 | 21.8 | 21.6 | Lamin-B1 | <i>LMNB1</i> |
| 18.5 | 18.1 | 17.9 | 19.2 | 19.2 | 18.8 | Lamin-B2 | <i>LMNB2</i> |
| 20.7 | 20.6 | 21.1 | 20.3 | 20.7 | 20.8 | Thymopoietin | <i>TMPO</i> |
| 23.4 | 23.5 | 23.8 | 23.5 | 23.5 | 23.6 | Thymopoietin | <i>TMPO</i> |
| 15.0 | 15.0 | 19.3 | 15.0 | 15.0 | 15.0 | Laminin subunit beta-2 | <i>LAMB2</i> |
| 18.9 | 18.8 | 18.5 | 18.4 | 18.9 | 18.7 | Large subunit GTPase 1 homolog | <i>LSG1</i> |
| 19.4 | 19.4 | 19.1 | 15.0 | 19.6 | 19.0 | Latent-transforming growth factor beta-binding protein 4 | <i>LTBP4</i> |
| 20.3 | 20.3 | 20.6 | 20.1 | 20.2 | 20.3 | LETM1 and EF-hand domain-containing protein 1, mitochondrial | <i>LETM1</i> |
| 19.8 | 19.5 | 19.5 | 15.0 | 19.5 | 19.4 | Leucine zipper protein 1 | <i>LUZP1</i> |
| 20.7 | 20.8 | 21.0 | 19.2 | 20.3 | 21.9 | Leucine zipper putative tumor suppressor 2 | <i>LZTS2</i> |
| 21.1 | 21.2 | 20.7 | 20.8 | 20.7 | 21.0 | Leucine--tRNA ligase, cytoplasmic | <i>LARS</i> |
| 21.4 | 21.7 | 21.8 | 19.7 | 21.6 | 21.3 | Leucine-rich PPR motif-containing protein, mitochondrial | <i>LRPPRC</i> |

| | | | | | | | |
|------|------|------|------|------|------|--|-----------------|
| 15.0 | 19.0 | 19.6 | 18.3 | 18.9 | 19.5 | Leucine-rich repeat and WD repeat-containing protein 1 | <i>LRWD1</i> |
| 20.1 | 20.0 | 20.1 | 21.0 | 20.1 | 19.8 | Leucine-rich repeat flightless-interacting protein 1 | <i>LRRFIP1</i> |
| 21.1 | 21.0 | 21.4 | 23.2 | 20.9 | 21.1 | Leucine-rich repeat-containing protein 47 | <i>LRRC47</i> |
| 25.7 | 26.0 | 26.1 | 26.0 | 26.0 | 25.9 | Leucine-rich repeat-containing protein 59 | <i>LRRC59</i> |
| 20.1 | 19.6 | 20.6 | 21.7 | 19.3 | 19.7 | Leydig cell tumor 10 kDa protein homolog | <i>C19orf53</i> |
| 15.0 | 17.0 | 17.2 | 15.0 | 15.0 | 17.1 | Lipoamide acyltransferase component of branched-chain alpha-keto acid dehydrogenase complex, mitochondrial | <i>DBT</i> |
| 20.2 | 20.4 | 20.3 | 20.8 | 20.2 | 20.4 | Liprin-alpha-1 | <i>PPFIA1</i> |
| 19.7 | 19.9 | 20.0 | 15.0 | 19.6 | 19.8 | Liprin-beta-1 | <i>PPFIBP1</i> |
| 20.2 | 20.9 | 21.0 | 20.4 | 20.0 | 21.0 | Lon protease homolog, mitochondrial | <i>LONP1</i> |
| 19.4 | 19.7 | 19.8 | 18.5 | 19.5 | 19.6 | Long-chain fatty acid transport protein 4 | <i>SLC27A4</i> |
| 15.0 | 19.4 | 20.1 | 19.4 | 19.1 | 19.9 | Long-chain-fatty-acid--CoA ligase 3 | <i>ACSL3</i> |
| 23.2 | 23.3 | 23.2 | 24.4 | 23.4 | 23.4 | Luc7-like protein 3 | <i>LUC7L3</i> |
| 24.6 | 24.6 | 24.9 | 24.0 | 24.6 | 24.7 | Lupus La protein | <i>SSB</i> |
| 19.7 | 20.4 | 19.9 | 15.0 | 20.0 | 20.3 | Lymphoid-specific helicase | <i>HELLS</i> |
| 20.9 | 20.7 | 20.8 | 21.5 | 20.5 | 20.5 | Lysine--tRNA ligase | <i>KARS</i> |
| 20.9 | 21.0 | 20.9 | 20.5 | 21.0 | 20.7 | Lysine-rich nucleolar protein 1 | <i>KNOP1</i> |
| 15.0 | 19.4 | 19.4 | 19.6 | 19.0 | 19.2 | Lysine-specific demethylase 3B | <i>KDM3B</i> |
| 19.0 | 19.7 | 19.7 | 19.0 | 19.8 | 19.7 | Lysine-specific histone demethylase 1A | <i>KDM1A</i> |
| 20.3 | 19.8 | 19.8 | 20.0 | 20.2 | 19.9 | M-phase phosphoprotein 6 | <i>MPHOSPH6</i> |
| 23.7 | 22.7 | 23.1 | 25.4 | 23.1 | 22.6 | Macrophage migration inhibitory factor | <i>MIF</i> |
| 15.0 | 15.0 | 15.0 | 20.3 | 15.0 | 15.0 | Malate dehydrogenase, cytoplasmic | <i>MDH1</i> |
| 15.0 | 23.5 | 23.3 | 15.0 | 23.8 | 23.3 | Malonyl-CoA-acyl carrier protein transacylase, mitochondrial | <i>MCAT</i> |
| 20.3 | 20.3 | 20.7 | 19.7 | 20.5 | 20.6 | Mannosyl-oligosaccharide glucosidase | <i>MOGS</i> |
| 18.9 | 18.6 | 18.6 | 15.0 | 18.6 | 15.0 | MAP kinase-interacting serine/threonine-protein kinase 2 | <i>MKNK2</i> |
| 17.7 | 17.9 | 17.5 | 15.0 | 17.6 | 17.1 | MAP/microtubule affinity-regulating kinase 3 | <i>MARK3</i> |
| 21.5 | 21.6 | 21.8 | 21.1 | 21.5 | 21.6 | MAP7 domain-containing protein 1 | <i>MAP7D1</i> |
| 19.3 | 19.4 | 19.3 | 15.0 | 19.3 | 19.4 | MAP7 domain-containing protein 2 | <i>MAP7D2</i> |
| 21.8 | 22.5 | 22.4 | 20.1 | 22.1 | 22.2 | MAP7 domain-containing protein 3 | <i>MAP7D3</i> |
| 17.6 | 18.1 | 18.8 | 20.9 | 17.4 | 17.6 | MARCKS-related protein | <i>MARCKSL1</i> |
| 20.1 | 20.2 | 20.2 | 15.0 | 20.1 | 20.2 | Maternal embryonic leucine zipper kinase | <i>MELK</i> |
| 25.5 | 25.7 | 25.4 | 24.7 | 25.6 | 26.4 | Matrin-3 | <i>MATR3</i> |
| 19.5 | 19.6 | 19.5 | 19.7 | 19.5 | 19.6 | MAX gene-associated protein | <i>MGA</i> |
| 22.2 | 21.8 | 21.9 | 22.4 | 22.1 | 21.8 | Mediator of DNA damage checkpoint protein 1 | <i>MDC1</i> |
| 18.1 | 17.8 | 18.1 | 18.7 | 18.5 | 17.7 | Mediator of RNA polymerase II transcription subunit 1 | <i>MED1</i> |
| 15.0 | 20.2 | 19.8 | 15.0 | 20.0 | 19.8 | Mediator of RNA polymerase II transcription subunit 12 | <i>MED12</i> |
| 18.5 | 19.1 | 19.4 | 20.0 | 19.1 | 19.0 | Mediator of RNA polymerase II transcription subunit 15 | <i>MED15</i> |
| 15.0 | 15.0 | 18.1 | 19.4 | 18.8 | 18.5 | Mediator of RNA polymerase II transcription subunit 22 | <i>MED22</i> |
| 18.6 | 18.5 | 18.5 | 15.0 | 18.5 | 18.5 | Meiosis arrest female protein 1 | <i>KIAA0430</i> |
| 24.2 | 24.4 | 24.5 | 24.6 | 24.3 | 25.3 | Melanoma-associated antigen D1 | <i>MAGED1</i> |
| 20.5 | 21.0 | 21.3 | 21.5 | 20.5 | 21.3 | Melanoma-associated antigen D2 | <i>MAGED2</i> |
| 18.8 | 18.9 | 18.7 | 15.0 | 18.7 | 19.3 | Melanoma-associated antigen D4 | <i>MAGED4</i> |
| 20.3 | 20.8 | 20.5 | 21.1 | 20.1 | 20.8 | Membrane-associated progesterone receptor component 1 | <i>PGRMC1</i> |
| 21.4 | 20.8 | 21.0 | 21.5 | 21.0 | 21.2 | Metastasis-associated protein MTA2 | <i>MTA2</i> |
| 19.9 | 19.6 | 19.4 | 20.2 | 19.7 | 19.5 | Methionine aminopeptidase 1 | <i>METAP1</i> |
| 19.4 | 19.4 | 19.6 | 20.6 | 19.1 | 19.7 | Methionine aminopeptidase 2 | <i>METAP2</i> |

| | | | | | | | |
|------|------|------|------|------|------|--|-----------------|
| 22.3 | 22.2 | 22.3 | 21.9 | 21.9 | 22.1 | Methionine--tRNA ligase, cytoplasmic | <i>MARS</i> |
| 20.3 | 20.2 | 20.0 | 19.7 | 20.4 | 19.9 | Methyl-CpG-binding domain protein 3 | <i>MBD3</i> |
| 19.4 | 18.7 | 18.6 | 15.0 | 19.0 | 18.9 | Methyltransferase-like protein 17, mitochondrial | <i>METTL17</i> |
| 19.2 | 19.1 | 19.5 | 15.0 | 19.1 | 19.1 | MICOS complex subunit MIC19 | <i>CHCHD3</i> |
| 19.6 | 19.7 | 20.3 | 20.5 | 20.2 | 19.7 | MICOS complex subunit MIC60 | <i>IMMT</i> |
| 20.5 | 20.4 | 20.5 | 20.1 | 20.4 | 20.3 | Microfibrillar-associated protein 1 | <i>MFAP1</i> |
| 20.0 | 20.5 | 20.2 | 15.0 | 19.5 | 20.2 | Microtubule cross-linking factor 1 | <i>MTCL1</i> |
| 17.2 | 17.5 | 18.1 | 15.0 | 17.1 | 17.5 | Microtubule-associated protein 1A | <i>MAP1A</i> |
| 21.7 | 21.4 | 21.7 | 22.1 | 21.4 | 21.8 | Microtubule-associated protein 1B | <i>MAP1B</i> |
| 24.2 | 24.2 | 24.3 | 24.6 | 24.0 | 24.2 | Microtubule-associated protein | <i>MAP4</i> |
| 20.3 | 20.9 | 20.9 | 20.4 | 20.5 | 21.0 | Midasin | <i>MDN1</i> |
| 19.1 | 18.9 | 19.1 | 15.0 | 19.0 | 18.9 | Midkine | <i>MDK</i> |
| 20.4 | 20.6 | 20.5 | 15.0 | 20.2 | 20.4 | Mitochondrial 2-oxoglutarate/malate carrier protein | <i>SLC25A11</i> |
| 21.3 | 21.1 | 21.2 | 19.5 | 20.9 | 21.8 | Mitochondrial fission regulator 1-like | <i>MTRF1L</i> |
| 19.6 | 19.8 | 20.1 | 15.0 | 19.8 | 20.2 | Mitochondrial glutamate carrier 1 | <i>SLC25A22</i> |
| 25.3 | 25.6 | 25.8 | 24.1 | 25.2 | 26.0 | Mitochondrial import inner membrane translocase subunit Tim13 | <i>TIMM13</i> |
| 21.1 | 21.7 | 21.7 | 21.8 | 21.5 | 21.5 | Mitochondrial import inner membrane translocase subunit TIM14 | <i>DNAJC19</i> |
| 20.2 | 20.7 | 20.7 | 20.1 | 20.2 | 21.2 | Mitochondrial import inner membrane translocase subunit TIM50 | <i>TIMM50</i> |
| 26.1 | 26.6 | 27.5 | 24.7 | 26.4 | 27.7 | Mitochondrial import inner membrane translocase subunit Tim8 A | <i>TIMM8A</i> |
| 25.2 | 25.6 | 26.3 | 24.9 | 24.8 | 26.5 | Mitochondrial import inner membrane translocase subunit Tim8 B | <i>TIMM8B</i> |
| 18.9 | 19.6 | 19.7 | 15.0 | 18.9 | 19.6 | Mitochondrial import inner membrane translocase subunit Tim9 | <i>TIMM9</i> |
| 19.7 | 19.4 | 19.7 | 21.3 | 19.4 | 19.8 | Mitochondrial import receptor subunit TOM34 | <i>TOMM34</i> |
| 19.8 | 20.6 | 20.9 | 20.7 | 19.7 | 20.8 | Mitochondrial import receptor subunit TOM70 | <i>TOMM70A</i> |
| 15.0 | 18.8 | 18.5 | 15.0 | 15.0 | 19.1 | Mitochondrial Rho GTPase 2 | <i>RHOT2</i> |
| 18.4 | 18.2 | 18.7 | 18.6 | 18.3 | 18.1 | Mitogen-activated protein kinase kinase kinase 4 | <i>MAP4K4</i> |
| 20.9 | 20.9 | 21.1 | 21.9 | 20.9 | 20.8 | Mitotic checkpoint protein BUB3 | <i>BUB3</i> |
| 18.6 | 18.6 | 18.2 | 18.7 | 18.3 | 18.4 | Mitotic checkpoint serine/threonine-protein kinase BUB1 beta | <i>BUB1B</i> |
| 20.2 | 20.1 | 15.0 | 19.9 | 15.0 | 20.6 | Mitotic-spindle organizing protein 1 | <i>MZT1</i> |
| 19.5 | 19.8 | 19.7 | 19.8 | 19.2 | 19.8 | Mitotic-spindle organizing protein 2B | <i>MZT2B</i> |
| 20.9 | 21.3 | 21.8 | 19.3 | 21.5 | 20.8 | MKI67 FHA domain-interacting nucleolar phosphoprotein | <i>NIFK</i> |
| 15.0 | 15.0 | 15.0 | 19.8 | 15.0 | 15.0 | Moesin | <i>MSN</i> |
| 20.1 | 20.1 | 20.2 | 19.8 | 20.1 | 20.1 | Monofunctional C1-tetrahydrofolate synthase, mitochondrial | <i>MTHFD1L</i> |
| 18.9 | 18.6 | 18.9 | 18.7 | 18.8 | 18.7 | MORC family CW-type zinc finger protein 2 | <i>MORC2</i> |
| 19.8 | 19.5 | 19.8 | 20.4 | 19.4 | 19.3 | Mortality factor 4-like protein 1 | <i>MORF4L1</i> |
| 19.8 | 19.6 | 20.1 | 20.5 | 19.9 | 19.7 | Mortality factor 4-like protein 2 | <i>MORF4L2</i> |
| 20.8 | 20.8 | 20.8 | 21.1 | 20.6 | 20.7 | mRNA export factor | <i>RAE1</i> |
| 20.8 | 20.6 | 21.0 | 20.4 | 20.9 | 20.8 | mRNA turnover protein 4 homolog | <i>MRTO4</i> |
| 20.9 | 21.7 | 20.7 | 19.8 | 21.1 | 21.4 | Msx2-interacting protein | <i>SPEN</i> |
| 22.2 | 21.7 | 21.4 | 21.1 | 21.9 | 21.4 | Multifunctional methyltransferase subunit TRM112-like protein | <i>TRMT112</i> |
| 19.4 | 19.4 | 19.5 | 22.0 | 15.0 | 19.5 | Multifunctional protein ADE2 | <i>PAICS</i> |
| 21.0 | 20.6 | 20.7 | 22.0 | 21.0 | 20.8 | Multiple myeloma tumor-associated protein 2 | <i>MMTAG2</i> |
| 19.1 | 18.9 | 19.0 | 19.3 | 19.1 | 18.8 | Multivesicular body subunit 12A | <i>MVB12A</i> |
| 20.3 | 20.3 | 20.1 | 19.2 | 19.8 | 19.9 | Muscleblind-like protein 1 | <i>MBNL1</i> |
| 22.3 | 22.4 | 22.7 | 22.0 | 22.3 | 22.4 | Myb-binding protein 1A | <i>MYBBP1A</i> |
| 15.0 | 18.8 | 18.4 | 18.0 | 15.0 | 18.7 | Myb-related protein B | <i>MYBL2</i> |

| | | | | | | | |
|------|------|------|------|------|------|--|----------------|
| 19.4 | 19.6 | 19.3 | 15.0 | 19.1 | 20.0 | Myc proto-oncogene protein | <i>MYC</i> |
| 24.1 | 23.9 | 24.0 | 23.5 | 24.1 | 23.8 | Myc-associated zinc finger protein | <i>MAZ</i> |
| 21.3 | 21.1 | 21.1 | 20.5 | 21.6 | 20.9 | Myelin expression factor 2 | <i>MYEF2</i> |
| 20.3 | 20.7 | 20.9 | 15.0 | 20.1 | 20.9 | Myeloid leukemia factor 2 | <i>MLF2</i> |
| 15.0 | 16.5 | 16.5 | 15.0 | 16.2 | 16.4 | Myosin light chain 6B | <i>MYL6B</i> |
| 21.4 | 21.0 | 21.1 | 22.3 | 21.0 | 21.2 | Myosin light polypeptide 6 | <i>MYL6</i> |
| 18.7 | 18.6 | 18.9 | 20.3 | 15.0 | 18.8 | Myosin-10 | <i>MYH10</i> |
| 19.4 | 17.8 | 19.3 | 20.7 | 18.0 | 19.1 | Myosin-9 | <i>MYH9</i> |
| 20.7 | 20.3 | 20.2 | 20.2 | 20.4 | 20.4 | Myotubularin-related protein 5 | <i>SBF1</i> |
| 20.7 | 21.2 | 20.8 | 19.9 | 21.2 | 21.0 | N-acetyltransferase 10 | <i>NAT10</i> |
| 23.0 | 22.9 | 23.2 | 23.6 | 23.0 | 23.0 | N-acylneuraminate cytidyltransferase | <i>CMAS</i> |
| 20.2 | 20.0 | 19.3 | 15.0 | 20.2 | 19.6 | SirtT1 75 kDa fragment | <i>SIRT1</i> |
| 19.1 | 20.4 | 21.2 | 23.7 | 20.8 | 20.6 | NAD-dependent protein deacylase sirtuin-5, mitochondrial | <i>SIRT5</i> |
| 15.0 | 18.0 | 18.2 | 15.0 | 17.5 | 18.8 | NADH dehydrogenase [ubiquinone] 1 alpha subcomplex subunit 10, mitochondrial | <i>NDUFA10</i> |
| 19.7 | 19.3 | 19.3 | 19.5 | 19.8 | 19.5 | NADH dehydrogenase [ubiquinone] 1 alpha subcomplex subunit 2 | <i>NDUFA2</i> |
| 19.7 | 19.8 | 19.8 | 20.3 | 19.7 | 19.9 | NADH dehydrogenase [ubiquinone] 1 alpha subcomplex subunit 5 | <i>NDUFA5</i> |
| 19.8 | 20.0 | 19.9 | 20.4 | 20.2 | 20.4 | NADH dehydrogenase [ubiquinone] 1 alpha subcomplex subunit 8 | <i>NDUFA8</i> |
| 19.7 | 19.5 | 19.7 | 20.1 | 19.3 | 19.8 | NADH dehydrogenase [ubiquinone] 1 beta subcomplex subunit 10 | <i>NDUFB10</i> |
| 19.3 | 19.2 | 19.2 | 15.0 | 19.6 | 19.5 | NADH dehydrogenase [ubiquinone] iron-sulfur protein 6, mitochondrial | <i>NDUFS6</i> |
| 18.2 | 18.4 | 18.5 | 15.0 | 18.1 | 18.6 | NADH dehydrogenase [ubiquinone] iron-sulfur protein 7, mitochondrial | <i>NDUFS7</i> |
| 19.6 | 19.8 | 19.6 | 19.1 | 19.6 | 20.2 | NADH dehydrogenase [ubiquinone] iron-sulfur protein 8, mitochondrial | <i>NDUFS8</i> |
| 20.1 | 19.3 | 19.3 | 20.2 | 19.4 | 19.3 | NADH-ubiquinone oxidoreductase 75 kDa subunit, mitochondrial | <i>NDUFS1</i> |
| 19.7 | 20.0 | 20.0 | 23.2 | 19.8 | 20.7 | Nascent polypeptide-associated complex subunit alpha | <i>NACA</i> |
| 19.7 | 19.5 | 19.4 | 19.9 | 19.4 | 19.4 | Negative elongation factor A | <i>NELFA</i> |
| 20.7 | 20.2 | 20.0 | 20.6 | 20.4 | 20.0 | Negative elongation factor E | <i>NELFE</i> |
| 15.0 | 19.0 | 18.9 | 19.7 | 19.0 | 19.3 | Neuroblast differentiation-associated protein AHNAK | <i>AHNAK</i> |
| 18.2 | 18.5 | 18.5 | 15.0 | 18.5 | 19.4 | Neurogenic locus notch homolog protein 2 | <i>NOTCH2</i> |
| 15.0 | 18.2 | 17.8 | 15.0 | 17.2 | 19.0 | Neurogenic locus notch homolog protein 3 | <i>NOTCH3</i> |
| 19.4 | 19.4 | 19.6 | 19.4 | 19.2 | 19.7 | Neuron navigator 1 | <i>NAV1</i> |
| 20.8 | 20.7 | 20.5 | 20.9 | 20.4 | 21.3 | Neutral alpha-glucosidase AB | <i>GANAB</i> |
| 23.5 | 23.3 | 23.6 | 21.0 | 23.7 | 23.3 | NF-kappa-B-repressing factor | <i>NKRF</i> |
| 22.3 | 22.5 | 22.6 | 22.2 | 22.1 | 22.3 | NF-X1-type zinc finger protein NFXL1 | <i>NFXL1</i> |
| 23.3 | 23.2 | 22.9 | 22.8 | 23.6 | 22.9 | NHP2-like protein 1 | <i>NHP2L1</i> |
| 15.0 | 16.9 | 17.0 | 18.7 | 16.7 | 17.8 | Nitric oxide synthase-interacting protein | <i>NOSIP</i> |
| 20.8 | 20.5 | 20.4 | 15.0 | 20.5 | 20.3 | Nitric oxide-associated protein 1 | <i>NOA1</i> |
| 15.0 | 16.6 | 15.0 | 18.1 | 17.0 | 16.5 | Non-histone chromosomal protein HMG-14 | <i>HMGN1</i> |
| 28.0 | 28.1 | 28.3 | 29.0 | 28.3 | 28.0 | Non-POU domain-containing octamer-binding protein | <i>NONO</i> |
| 15.0 | 17.3 | 16.9 | 18.7 | 16.6 | 17.3 | Non-structural maintenance of chromosomes element 4 homolog A | <i>NSMCE4A</i> |
| 18.9 | 20.4 | 20.2 | 21.6 | 20.2 | 20.3 | Nuclear autoantigenic sperm protein | <i>NASP</i> |
| 19.7 | 19.3 | 18.9 | 15.0 | 19.6 | 18.9 | Nuclear cap-binding protein subunit 1 | <i>NCBP1</i> |
| 19.8 | 19.3 | 19.0 | 15.0 | 19.7 | 19.2 | Nuclear cap-binding protein subunit 2 | <i>NCBP2</i> |
| 19.1 | 18.7 | 18.4 | 15.0 | 18.6 | 19.1 | Nuclear distribution protein nudeE homolog 1 | <i>NDE1</i> |
| 19.6 | 19.8 | 19.6 | 15.0 | 19.8 | 19.8 | Nuclear factor of activated T-cells, cytoplasmic 3 | <i>NFATC3</i> |

| | | | | | | | |
|------|------|------|------|------|------|---|------------------|
| 20.4 | 20.1 | 20.4 | 20.5 | 20.6 | 20.3 | Nuclear fragile X mental retardation-interacting protein 2 | <i>NUFIP2</i> |
| 19.3 | 18.9 | 19.4 | 21.7 | 18.1 | 19.4 | Nuclear migration protein nudC | <i>NUDC</i> |
| 19.1 | 18.7 | 19.1 | 19.8 | 19.4 | 18.9 | Nuclear mitotic apparatus protein 1 | <i>NUMA1</i> |
| 22.5 | 22.6 | 21.9 | 20.4 | 22.3 | 22.2 | Nuclear pore complex protein Nup153 | <i>NUP153</i> |
| 19.1 | 18.5 | 18.7 | 15.0 | 18.9 | 18.8 | Nuclear receptor coactivator 5 | <i>NCOA5</i> |
| 20.4 | 20.7 | 20.3 | 20.4 | 20.3 | 20.9 | Nuclear receptor corepressor 1 | <i>NCOR1</i> |
| 18.5 | 18.4 | 18.3 | 15.0 | 18.6 | 18.3 | Nuclear RNA export factor 1 | <i>NXF1</i> |
| 18.9 | 18.7 | 18.7 | 15.0 | 18.7 | 18.6 | Nuclear speckle splicing regulatory protein 1 | <i>NSRP1</i> |
| 20.6 | 21.1 | 21.2 | 24.6 | 20.8 | 20.8 | Nuclear ubiquitous casein and cyclin-dependent kinase substrate 1 | <i>NUCKS1</i> |
| 19.8 | 20.3 | 20.2 | 19.9 | 20.0 | 20.1 | Nuclear valosin-containing protein-like | <i>NVL</i> |
| 25.3 | 25.2 | 25.0 | 24.1 | 25.3 | 25.1 | Nuclease-sensitive element-binding protein 1 | <i>YBX1</i> |
| 21.4 | 21.0 | 20.8 | 22.2 | 21.5 | 20.7 | Nucleolar and coiled-body phosphoprotein 1 | <i>NOLC1</i> |
| 19.2 | 19.0 | 18.6 | 15.0 | 15.0 | 18.5 | Nucleolar and spindle-associated protein 1 | <i>NUSAP1</i> |
| 15.0 | 18.4 | 18.0 | 18.8 | 18.3 | 18.3 | Nucleolar complex protein 2 homolog | <i>NOC2L</i> |
| 20.7 | 20.3 | 20.5 | 20.3 | 20.7 | 20.2 | Nucleolar complex protein 3 homolog | <i>NOC3L</i> |
| 22.3 | 22.2 | 21.4 | 19.8 | 22.3 | 21.5 | Nucleolar complex protein 4 homolog | <i>NOC4L</i> |
| 22.1 | 22.1 | 22.5 | 21.8 | 22.3 | 21.8 | Nucleolar GTP-binding protein 1 | <i>GTPBP4</i> |
| 20.9 | 20.9 | 21.3 | 19.9 | 21.0 | 20.7 | Nucleolar GTP-binding protein 2 | <i>GNL2</i> |
| 19.5 | 19.7 | 19.6 | 15.0 | 19.3 | 19.3 | Nucleolar MIF4G domain-containing protein 1 | <i>NOM1</i> |
| 24.4 | 24.4 | 23.6 | 19.7 | 24.5 | 23.6 | Nucleolar protein 14 | <i>NOP14</i> |
| 19.3 | 19.0 | 19.3 | 18.9 | 19.0 | 19.2 | Nucleolar protein 16 | <i>NOP16</i> |
| 21.4 | 21.9 | 21.5 | 20.9 | 21.8 | 21.6 | Nucleolar protein 56 | <i>NOP56</i> |
| 20.8 | 20.8 | 20.7 | 20.5 | 21.3 | 20.7 | Nucleolar protein 58 | <i>NOP58</i> |
| 19.2 | 19.3 | 19.2 | 15.0 | 19.6 | 19.1 | Nucleolar protein 7 | <i>NOL7</i> |
| 18.8 | 19.0 | 18.8 | 15.0 | 18.9 | 18.8 | Nucleolar protein 9 | <i>NOP9</i> |
| 26.1 | 26.0 | 26.1 | 25.1 | 26.2 | 26.0 | Nucleolar RNA helicase 2 | <i>DDX21</i> |
| 19.7 | 20.7 | 20.0 | 21.7 | 21.3 | 20.3 | Nucleolar transcription factor 1 | <i>UBTF</i> |
| 26.6 | 26.6 | 26.8 | 26.3 | 26.6 | 26.5 | Nucleolin | <i>NCL</i> |
| 27.7 | 27.6 | 27.5 | 27.7 | 27.8 | 27.3 | Nucleophosmin | <i>NPM1</i> |
| 23.1 | 22.7 | 22.7 | 22.4 | 23.0 | 23.0 | Nucleoplasmin-3 | <i>NPM3</i> |
| 20.0 | 19.0 | 19.9 | 21.7 | 20.2 | 19.4 | Nucleoprotein TPR | <i>TPR</i> |
| 21.0 | 21.0 | 21.5 | 23.1 | 20.3 | 21.8 | Nucleoside diphosphate kinase | <i>NME1-NME2</i> |
| 20.8 | 20.8 | 20.8 | 21.1 | 21.0 | 20.9 | Nucleoside diphosphate kinase, mitochondrial | <i>NME4</i> |
| 22.0 | 22.6 | 22.5 | 23.1 | 22.0 | 22.6 | Nucleosome assembly protein 1-like 1 | <i>NAP1L1</i> |
| 20.4 | 20.4 | 20.0 | 21.5 | 20.0 | 20.7 | Nucleosome assembly protein 1-like 4 | <i>NAP1L4</i> |
| 19.0 | 18.6 | 18.6 | 15.0 | 18.6 | 18.6 | Nucleosome-remodeling factor subunit BPTF | <i>BPTF</i> |
| 20.0 | 20.6 | 19.8 | 15.0 | 19.6 | 20.5 | Nucleus accumbens-associated protein 1 | <i>NACC1</i> |
| 18.5 | 18.2 | 18.3 | 15.0 | 18.6 | 18.3 | Numb-like protein | <i>NUMBL</i> |
| 19.6 | 19.7 | 20.0 | 15.0 | 20.0 | 19.5 | Obscurin-like protein 1 | <i>OBSL1</i> |
| 17.5 | 15.0 | 18.2 | 19.0 | 18.3 | 18.2 | Origin recognition complex subunit 2 | <i>ORC2</i> |
| 15.0 | 18.0 | 18.0 | 15.0 | 17.8 | 18.0 | Origin recognition complex subunit 6 | <i>ORC6</i> |
| 19.0 | 19.2 | 19.0 | 18.7 | 19.2 | 18.9 | OTU domain-containing protein 4 | <i>OTUD4</i> |
| 17.5 | 17.5 | 17.4 | 15.0 | 17.9 | 17.8 | p53 and DNA damage-regulated protein 1 | <i>PDRG1</i> |
| 19.9 | 19.4 | 19.4 | 15.0 | 19.4 | 19.6 | Paired amphipathic helix protein Sin3a | <i>SIN3A</i> |
| 22.7 | 22.4 | 22.2 | 22.4 | 22.8 | 22.3 | Parafibromin | <i>CDC73</i> |
| 23.3 | 23.0 | 23.4 | 24.1 | 23.2 | 23.0 | Paraspeckle component 1 | <i>PSPC1</i> |

| | | | | | | | |
|------|------|------|------|------|------|---|----------------|
| 15.0 | 17.9 | 18.3 | 19.3 | 17.9 | 18.0 | Parathyrosin | <i>PTMS</i> |
| 23.0 | 23.2 | 23.2 | 19.8 | 22.6 | 22.3 | Parkinson disease 7 domain-containing protein 1 | <i>PDDC1</i> |
| 23.8 | 24.0 | 23.8 | 23.2 | 24.0 | 23.9 | Partner of Y14 and mago | <i>WIBG</i> |
| 22.4 | 23.0 | 22.6 | 19.5 | 22.0 | 23.2 | PAS domain-containing serine/threonine-protein kinase | <i>PASK</i> |
| 23.0 | 22.7 | 22.8 | 23.4 | 23.0 | 22.8 | PC4 and SFRS1-interacting protein | <i>PSIP1</i> |
| 19.1 | 19.9 | 19.6 | 20.1 | 19.5 | 19.8 | PDZ and LIM domain protein 7 | <i>PDLIM7</i> |
| 18.9 | 18.6 | 18.8 | 15.0 | 18.6 | 20.1 | PDZ domain-containing protein 11 | <i>PDZD11</i> |
| 21.4 | 21.0 | 20.8 | 15.0 | 21.6 | 20.8 | Pentatricopeptide repeat domain-containing protein 3, mitochondrial | <i>PTCD3</i> |
| 18.4 | 18.4 | 19.2 | 18.3 | 18.6 | 18.4 | Pentatricopeptide repeat-containing protein 1, mitochondrial | <i>PTCD1</i> |
| 20.0 | 19.9 | 19.9 | 15.0 | 19.9 | 20.0 | Peptide deformylase, mitochondrial | <i>PDF</i> |
| 24.1 | 23.0 | 23.9 | 26.3 | 23.4 | 23.9 | Peptidyl-prolyl cis-trans isomerase A | <i>PPIA</i> |
| 21.2 | 21.4 | 22.1 | 23.5 | 21.4 | 21.7 | Peptidyl-prolyl cis-trans isomerase B | <i>PPIB</i> |
| 15.0 | 15.0 | 19.1 | 20.1 | 15.0 | 15.0 | Peptidyl-prolyl cis-trans isomerase F | <i>PPIF</i> |
| 21.9 | 21.9 | 22.5 | 23.8 | 22.2 | 22.1 | Peptidyl-prolyl cis-trans isomerase FKBP3 | <i>FKBP3</i> |
| 19.6 | 15.0 | 19.8 | 21.5 | 19.5 | 20.3 | Peptidyl-prolyl cis-trans isomerase FKBP4 | <i>FKBP4</i> |
| 19.2 | 19.7 | 19.6 | 19.2 | 19.1 | 19.7 | Peptidyl-prolyl cis-trans isomerase FKBP8 | <i>FKBP8</i> |
| 20.3 | 20.2 | 20.5 | 20.7 | 20.7 | 20.4 | Peptidyl-prolyl cis-trans isomerase G | <i>PPIG</i> |
| 21.6 | 21.5 | 21.9 | 23.3 | 21.6 | 21.3 | Peptidyl-prolyl cis-trans isomerase NIMA-interacting 4 | <i>PIN4</i> |
| 18.9 | 19.5 | 19.5 | 20.3 | 19.0 | 19.2 | Peptidyl-prolyl cis-trans isomerase-like 1 | <i>PPIL1</i> |
| 18.9 | 18.9 | 18.7 | 19.3 | 18.7 | 18.8 | Peptidyl-prolyl cis-trans isomerase-like 2 | <i>PPIL2</i> |
| 19.8 | 19.8 | 20.0 | 19.4 | 19.8 | 20.1 | Peptidyl-tRNA hydrolase 2, mitochondrial | <i>PTRH2</i> |
| 21.5 | 21.5 | 20.7 | 20.3 | 21.6 | 21.0 | Peptidyl-tRNA hydrolase ICT1, mitochondrial | <i>ICT1</i> |
| 18.5 | 18.2 | 18.1 | 15.0 | 18.2 | 18.3 | Pericentriolar material 1 protein | <i>PCM1</i> |
| 25.8 | 25.5 | 25.6 | 27.5 | 25.7 | 25.4 | Peroxiredoxin-1 | <i>PRDX1</i> |
| 23.6 | 23.3 | 23.2 | 24.4 | 23.6 | 23.2 | Peroxiredoxin-2 | <i>PRDX2</i> |
| 21.7 | 20.9 | 21.0 | 15.0 | 21.5 | 21.3 | Peroxiredoxin-4 | <i>PRDX4</i> |
| 22.4 | 21.9 | 21.6 | 21.7 | 22.4 | 21.6 | Peroxiredoxin-5, mitochondrial | <i>PRDX5</i> |
| 15.0 | 15.0 | 15.0 | 21.6 | 15.0 | 15.0 | Peroxiredoxin-6 | <i>PRDX6</i> |
| 20.3 | 20.3 | 20.4 | 21.7 | 20.2 | 20.4 | Peroxisomal multifunctional enzyme type 2 | <i>HSD17B4</i> |
| 22.3 | 22.4 | 22.4 | 21.7 | 22.2 | 22.4 | PERQ amino acid-rich with GYF domain-containing protein 2 | <i>GIGYF2</i> |
| 21.6 | 21.2 | 21.5 | 20.1 | 21.6 | 21.5 | Pescadillo homolog | <i>PES1</i> |
| 20.3 | 20.3 | 20.4 | 22.5 | 20.6 | 20.2 | PEST proteolytic signal-containing nuclear protein | <i>PCNP</i> |
| 19.5 | 19.4 | 19.3 | 18.7 | 19.2 | 19.6 | PHD finger protein 10 | <i>PHF10</i> |
| 20.5 | 20.5 | 20.6 | 20.5 | 20.4 | 20.4 | PHD finger protein 3 | <i>PHF3</i> |
| 24.9 | 24.9 | 25.2 | 26.0 | 24.8 | 24.8 | PHD finger protein 6 | <i>PHF6</i> |
| 22.2 | 21.9 | 21.7 | 22.1 | 22.1 | 21.5 | PHD finger-like domain-containing protein 5A | <i>PHF5A</i> |
| 21.6 | 21.9 | 22.1 | 21.9 | 21.8 | 22.1 | Phenylalanine--tRNA ligase alpha subunit | <i>FARSA</i> |
| 17.5 | 15.0 | 18.0 | 19.8 | 15.0 | 17.8 | Phenylalanine--tRNA ligase beta subunit | <i>FARSB</i> |
| 22.2 | 22.9 | 22.8 | 21.3 | 22.6 | 23.1 | Phosphate carrier protein, mitochondrial | <i>SLC25A3</i> |
| 19.6 | 15.0 | 19.7 | 20.4 | 15.0 | 15.0 | Phosphatidylethanolamine-binding protein 1 | <i>PEBP1</i> |
| 15.0 | 18.8 | 18.7 | 15.0 | 18.4 | 19.1 | Phosphatidylinositol 3-kinase regulatory subunit beta | <i>PIK3R2</i> |
| 19.0 | 18.7 | 19.5 | 22.0 | 18.5 | 19.3 | Phosphoglycerate kinase 1 | <i>PGK1</i> |
| 20.3 | 15.0 | 20.2 | 22.5 | 19.3 | 20.1 | Phosphoglycerate mutase 1 | <i>PGAM1</i> |
| 19.4 | 19.4 | 19.4 | 20.8 | 18.9 | 20.0 | Phosphoribosylformylglycinamide synthase | <i>PFAS</i> |

| | | | | | | | |
|------|------|------|------|------|------|---|----------------|
| 20.2 | 19.5 | 19.2 | 19.8 | 20.8 | 19.5 | Phosphorylated adapter RNA export protein | <i>PHAX</i> |
| 20.0 | 20.3 | 20.5 | 21.6 | 20.6 | 19.4 | Pinin | <i>PNN</i> |
| 20.6 | 20.7 | 20.9 | 20.6 | 20.6 | 21.0 | Plakophilin-2 | <i>PKP2</i> |
| 24.3 | 24.2 | 24.6 | 25.0 | 24.0 | 24.1 | Plasminogen activator inhibitor 1 RNA-binding protein | <i>SERBP1</i> |
| 15.0 | 15.0 | 17.8 | 19.9 | 15.0 | 15.0 | Plastin-3 | <i>PLS3</i> |
| 21.9 | 22.0 | 21.9 | 18.1 | 21.8 | 23.9 | Pleckstrin homology domain-containing family A member 5 | <i>PLEKHA5</i> |
| 17.5 | 17.6 | 17.7 | 15.0 | 15.0 | 17.2 | Pleckstrin homology-like domain family B member 3 | <i>PHLDB3</i> |
| 21.6 | 21.5 | 21.2 | 20.9 | 21.5 | 21.4 | Pleiotropic regulator 1 | <i>PLRG1</i> |
| 27.7 | 27.6 | 27.9 | 28.1 | 27.7 | 27.6 | Poly [ADP-ribose] polymerase 1 | <i>PARP1</i> |
| 27.9 | 27.5 | 27.0 | 19.5 | 28.2 | 26.6 | Poly(A)-specific ribonuclease PARN | <i>PARN</i> |
| 24.4 | 24.3 | 24.4 | 24.7 | 24.3 | 24.2 | Poly(rC)-binding protein 1 | <i>PCBP1</i> |
| 23.3 | 23.4 | 23.4 | 23.4 | 23.4 | 23.3 | Poly(rC)-binding protein 2 | <i>PCBP2</i> |
| 22.3 | 22.0 | 22.3 | 22.4 | 22.0 | 22.1 | Poly(U)-binding-splicing factor PUF60 | <i>PUF60</i> |
| 26.6 | 26.5 | 26.3 | 25.8 | 26.7 | 26.3 | Polyadenylate-binding protein 1 | <i>PABPC1</i> |
| 22.4 | 22.3 | 22.0 | 21.8 | 22.6 | 22.1 | Polyadenylate-binding protein 2 | <i>PABPN1</i> |
| 23.6 | 23.6 | 23.7 | 23.2 | 23.8 | 23.5 | Polyadenylate-binding protein | <i>PABPC4</i> |
| 23.7 | 23.4 | 23.2 | 23.5 | 23.8 | 23.3 | Polymerase delta-interacting protein 3 | <i>POLDIP3</i> |
| 19.7 | 19.6 | 19.2 | 15.0 | 19.6 | 19.3 | Polynucleotide 5-hydroxyl-kinase NOL9 | <i>NOL9</i> |
| 24.0 | 24.0 | 24.1 | 23.7 | 24.0 | 24.0 | Polypyrimidine tract-binding protein 1 | <i>PTBP1</i> |
| 19.4 | 18.8 | 18.9 | 18.6 | 19.7 | 19.4 | Polypyrimidine tract-binding protein 3 | <i>PTBP3</i> |
| 20.1 | 20.0 | 20.2 | 20.1 | 19.8 | 19.6 | POZ-, AT hook-, and zinc finger-containing protein 1 | <i>PATZ1</i> |
| 20.7 | 20.2 | 20.0 | 19.6 | 20.4 | 20.2 | pre-mRNA 3 end processing protein WDR33 | <i>WDR33</i> |
| 22.3 | 22.0 | 22.0 | 21.9 | 22.4 | 22.2 | Pre-mRNA 3-end-processing factor FIP1 | <i>FIP1L1</i> |
| 24.5 | 24.7 | 24.7 | 24.4 | 24.7 | 24.7 | Pre-mRNA-processing factor 19 | <i>PRPF19</i> |
| 20.3 | 20.3 | 20.4 | 21.4 | 20.2 | 20.2 | Pre-mRNA-processing factor 40 homolog A | <i>PRPF40A</i> |
| 22.4 | 22.4 | 22.4 | 23.2 | 22.5 | 22.1 | Pre-mRNA-processing factor 6 | <i>PRPF6</i> |
| 22.5 | 22.2 | 22.4 | 21.8 | 22.2 | 22.3 | Pre-mRNA-processing-splicing factor 8 | <i>PRPF8</i> |
| 18.4 | 18.4 | 18.5 | 19.1 | 18.5 | 18.5 | Pre-mRNA-splicing factor 38B | <i>PRPF38B</i> |
| 23.9 | 23.7 | 23.7 | 22.6 | 23.8 | 23.5 | Pre-mRNA-splicing factor ATP-dependent RNA helicase DHX15 | <i>DHX15</i> |
| 19.3 | 19.7 | 19.3 | 15.0 | 19.5 | 19.4 | Pre-mRNA-splicing factor ISY1 homolog | <i>ISY1</i> |
| 18.9 | 18.3 | 18.5 | 18.7 | 18.8 | 18.3 | Pre-mRNA-splicing factor RBM22 | <i>RBM22</i> |
| 22.7 | 22.7 | 22.5 | 22.1 | 22.7 | 22.4 | Pre-mRNA-splicing factor SPF27 | <i>BCAS2</i> |
| 21.5 | 21.4 | 21.0 | 21.6 | 21.4 | 21.1 | Pre-mRNA-splicing regulator WTAP | <i>WTAP</i> |
| 21.6 | 21.6 | 21.7 | 20.1 | 21.6 | 21.3 | pre-rRNA processing protein FTSJ3 | <i>FTSJ3</i> |
| 23.2 | 23.0 | 22.5 | 21.0 | 23.1 | 22.6 | Pre-rRNA-processing protein TSR1 homolog | <i>TSR1</i> |
| 15.0 | 18.8 | 19.0 | 19.3 | 15.0 | 19.2 | Prefoldin subunit 1 | <i>PFDN1</i> |
| 20.7 | 20.9 | 21.1 | 22.0 | 20.5 | 21.2 | Prefoldin subunit 2 | <i>PFDN2</i> |
| 17.8 | 18.7 | 19.0 | 20.6 | 17.5 | 19.3 | Prefoldin subunit 3 | <i>VBP1</i> |
| 20.1 | 20.0 | 20.1 | 20.5 | 19.7 | 20.4 | Prefoldin subunit 6 | <i>PFDN6</i> |
| 18.8 | 18.7 | 18.6 | 19.9 | 18.5 | 18.5 | Prelamin-A/C | <i>LMNA</i> |
| 19.1 | 18.7 | 18.5 | 15.0 | 18.9 | 18.5 | Probable 18S rRNA (guanine-N(7))-methyltransferase | <i>WBSCR22</i> |
| 20.3 | 20.5 | 20.5 | 19.5 | 20.4 | 20.0 | Probable 28S rRNA (cytosine-C(5))-methyltransferase | <i>NSUN5</i> |
| 22.9 | 22.9 | 23.1 | 22.9 | 23.0 | 22.7 | Probable 28S rRNA (cytosine(4447)-C(5))-methyltransferase | <i>NOP2</i> |
| 19.4 | 19.8 | 19.7 | 19.3 | 19.8 | 19.4 | Probable ATP-dependent RNA helicase DDX10 | <i>DDX10</i> |
| 26.1 | 25.9 | 25.9 | 26.0 | 26.0 | 25.6 | Probable ATP-dependent RNA helicase DDX17 | <i>DDX17</i> |

| | | | | | | | |
|------|------|------|------|------|------|--|-----------------|
| 20.6 | 20.4 | 20.5 | 20.6 | 20.7 | 21.2 | Probable ATP-dependent RNA helicase DDX20 | <i>DDX20</i> |
| 20.6 | 20.6 | 20.9 | 21.2 | 20.6 | 20.3 | Probable ATP-dependent RNA helicase DDX23 | <i>DDX23</i> |
| 20.0 | 20.0 | 20.0 | 15.0 | 20.2 | 19.8 | Probable ATP-dependent RNA helicase DDX27 | <i>DDX27</i> |
| 19.3 | 19.1 | 18.9 | 15.0 | 18.9 | 18.9 | Probable ATP-dependent RNA helicase DDX28 | <i>DDX28</i> |
| 18.8 | 18.9 | 18.8 | 15.0 | 18.4 | 18.8 | Probable ATP-dependent RNA helicase DDX31 | <i>DDX31</i> |
| 19.3 | 19.6 | 19.6 | 20.6 | 19.5 | 19.7 | Probable ATP-dependent RNA helicase DDX41 | <i>DDX41</i> |
| 22.4 | 22.3 | 22.2 | 24.0 | 22.7 | 21.9 | Probable ATP-dependent RNA helicase DDX46 | <i>DDX46</i> |
| 21.2 | 21.2 | 21.5 | 21.7 | 21.3 | 21.3 | Probable ATP-dependent RNA helicase DDX47 | <i>DDX47</i> |
| 26.4 | 26.4 | 26.5 | 25.9 | 26.6 | 26.5 | Probable ATP-dependent RNA helicase DDX5 | <i>DDX5</i> |
| 20.4 | 20.7 | 20.3 | 19.6 | 20.4 | 20.0 | Probable ATP-dependent RNA helicase DDX52 | <i>DDX52</i> |
| 18.8 | 18.8 | 18.7 | 18.4 | 19.1 | 18.7 | Probable ATP-dependent RNA helicase DDX56 | <i>DDX56</i> |
| 19.4 | 19.4 | 19.3 | 19.2 | 19.1 | 19.3 | Probable ATP-dependent RNA helicase DDX6 | <i>DDX6</i> |
| 20.4 | 20.4 | 20.6 | 15.0 | 20.5 | 20.2 | Probable ATP-dependent RNA helicase DHX37 | <i>DHX37</i> |
| 15.0 | 18.7 | 18.6 | 15.0 | 18.4 | 18.4 | Probable ATP-dependent RNA helicase DHX40 | <i>DHX40</i> |
| 22.3 | 22.4 | 22.4 | 20.8 | 22.3 | 22.4 | Probable ATP-dependent RNA helicase YTHDC2 | <i>YTHDC2</i> |
| 18.9 | 18.6 | 18.8 | 15.0 | 18.4 | 18.9 | Probable dimethyladenosine transferase | <i>DIMT1</i> |
| 15.0 | 18.6 | 18.9 | 15.0 | 15.0 | 18.5 | Probable helicase senataxin | <i>SETX</i> |
| 17.3 | 17.7 | 17.8 | 15.0 | 17.7 | 17.7 | Probable ribosome biogenesis protein RLP24 | <i>RSL24D1</i> |
| 15.0 | 15.0 | 19.7 | 20.7 | 15.0 | 19.6 | Probable RNA-binding protein EIF1AD | <i>EIF1AD</i> |
| 20.8 | 20.4 | 20.6 | 21.0 | 20.8 | 20.5 | Probable rRNA-processing protein EBP2 | <i>EBNA1BP2</i> |
| 20.4 | 19.9 | 19.3 | 15.0 | 20.8 | 19.8 | Probable ubiquitin carboxyl-terminal hydrolase FAF-X | <i>USP9X</i> |
| 19.5 | 15.0 | 19.6 | 21.4 | 17.8 | 19.1 | Profilin-1 | <i>PFN1</i> |
| 17.9 | 17.4 | 17.9 | 21.0 | 15.0 | 17.6 | Profilin-2 | <i>PFN2</i> |
| 18.2 | 15.0 | 18.4 | 20.4 | 19.1 | 19.0 | Programmed cell death 6-interacting protein | <i>PDCD6IP</i> |
| 20.2 | 19.9 | 19.6 | 20.8 | 19.4 | 19.3 | Programmed cell death protein 2-like | <i>PDCD2L</i> |
| 19.5 | 19.6 | 20.4 | 20.8 | 19.4 | 19.5 | Programmed cell death protein 5 | <i>PDCD5</i> |
| 23.9 | 24.2 | 24.2 | 24.7 | 24.0 | 23.8 | Prohibitin | <i>PHB</i> |
| 22.7 | 23.3 | 23.4 | 23.8 | 22.9 | 23.2 | Prohibitin-2 | <i>PHB2</i> |
| 20.4 | 20.3 | 20.6 | 15.0 | 20.1 | 20.4 | Prolactin regulatory element-binding protein | <i>PREB</i> |
| 19.6 | 19.6 | 19.6 | 21.2 | 19.3 | 20.2 | Proliferating cell nuclear antigen | <i>PCNA</i> |
| 24.7 | 24.5 | 24.6 | 24.8 | 24.5 | 24.4 | Proliferation-associated protein 2G4 | <i>PA2G4</i> |
| 19.4 | 19.3 | 19.4 | 18.4 | 19.7 | 19.5 | Proline-, glutamic acid- and leucine-rich protein 1 | <i>PELP1</i> |
| 19.9 | 18.0 | 18.1 | 15.0 | 20.2 | 18.3 | Proline-rich AKT1 substrate 1 | <i>AKT1S1</i> |
| 15.0 | 17.7 | 17.7 | 18.2 | 17.6 | 17.5 | Proline-rich protein 12 | <i>PRR12</i> |
| 19.0 | 18.9 | 19.0 | 15.0 | 18.7 | 18.8 | Proline-rich protein 36 | <i>PRR36</i> |
| 15.0 | 15.0 | 17.7 | 19.2 | 15.0 | 15.0 | Proline-rich protein PRCC | <i>PRCC</i> |
| 15.0 | 18.6 | 18.5 | 15.0 | 18.6 | 18.5 | Proline/serine-rich coiled-coil protein 1 | <i>PSRC1</i> |
| 20.4 | 20.8 | 21.3 | 23.2 | 19.8 | 20.7 | Prostaglandin E synthase 3 | <i>PTGES3</i> |
| 21.5 | 22.2 | 21.8 | 20.7 | 21.6 | 22.1 | Proteasomal ubiquitin receptor ADRM1 | <i>ADRM1</i> |
| 20.2 | 20.5 | 20.4 | 19.8 | 19.8 | 20.2 | Proteasome activator complex subunit 3 | <i>PSME3</i> |
| 24.2 | 24.6 | 24.3 | 23.3 | 24.0 | 24.5 | Proteasome subunit alpha type-1 | <i>PSMA1</i> |
| 19.6 | 20.5 | 20.2 | 15.0 | 19.9 | 20.3 | Proteasome subunit alpha type-3 | <i>PSMA3</i> |
| 22.2 | 23.0 | 22.8 | 22.1 | 22.1 | 23.0 | Proteasome subunit alpha type-5 | <i>PSMA5</i> |
| 23.6 | 24.5 | 24.1 | 20.1 | 23.7 | 24.3 | Proteasome subunit alpha type-7 | <i>PSMA7</i> |

| | | | | | | | |
|------|------|------|------|------|------|--|----------------|
| 22.3 | 23.3 | 22.8 | 20.3 | 22.5 | 22.9 | Proteasome subunit alpha type-2 | <i>PSMA2</i> |
| 23.4 | 24.0 | 23.8 | 22.3 | 23.4 | 24.0 | Proteasome subunit alpha type-6 | <i>PSMA6</i> |
| 20.0 | 20.8 | 20.7 | 15.0 | 20.1 | 21.0 | Proteasome subunit beta type-1 | <i>PSMB1</i> |
| 20.7 | 21.5 | 21.5 | 20.2 | 20.9 | 21.5 | Proteasome subunit beta type-2 | <i>PSMB2</i> |
| 19.5 | 20.7 | 20.5 | 15.0 | 20.0 | 20.4 | Proteasome subunit beta type-4 | <i>PSMB4</i> |
| 20.3 | 21.1 | 21.1 | 20.1 | 20.3 | 21.0 | Proteasome subunit beta type-5 | <i>PSMB5</i> |
| 21.7 | 22.8 | 22.7 | 21.4 | 22.1 | 22.8 | Proteasome subunit beta type-6 | <i>PSMB6</i> |
| 20.0 | 20.6 | 20.7 | 20.0 | 20.2 | 20.7 | Proteasome subunit beta type-7 | <i>PSMB7</i> |
| 18.4 | 18.8 | 18.1 | 15.0 | 19.0 | 18.2 | Protein AATF | <i>AATF</i> |
| 20.2 | 20.7 | 20.8 | 15.0 | 20.5 | 21.8 | Protein AF1q | <i>MLLT11</i> |
| 18.9 | 18.7 | 18.9 | 19.2 | 18.6 | 18.6 | Protein arginine N-methyltransferase 5 | <i>PRMT5</i> |
| 18.4 | 18.7 | 18.7 | 15.0 | 18.5 | 18.7 | Protein argonaute-2 | <i>AGO2</i> |
| 19.7 | 19.7 | 20.0 | 20.4 | 20.1 | 19.7 | Protein BUD31 homolog | <i>BUD31</i> |
| 18.4 | 18.3 | 18.5 | 19.1 | 18.3 | 18.1 | Protein CASC3 | <i>CASC3</i> |
| 15.0 | 18.5 | 19.2 | 15.0 | 15.0 | 18.8 | Protein CASC5 | <i>CASC5</i> |
| 19.6 | 19.2 | 19.4 | 15.0 | 19.4 | 19.0 | Protein CASP | <i>CUX1</i> |
| 19.7 | 15.0 | 19.9 | 22.0 | 19.2 | 19.3 | Protein CDV3 homolog | <i>CDV3</i> |
| 19.8 | 19.4 | 19.9 | 15.0 | 19.5 | 20.0 | Protein CMSS1 | <i>CMSS1</i> |
| 18.1 | 18.4 | 18.2 | 17.4 | 18.2 | 18.0 | Protein cordon-bleu | <i>COBL</i> |
| 18.3 | 18.4 | 18.8 | 21.1 | 18.2 | 18.5 | Protein deglycase DJ-1 | <i>PARK7</i> |
| 23.9 | 23.8 | 24.4 | 25.4 | 23.9 | 24.6 | Protein DEK | <i>DEK</i> |
| 18.8 | 18.6 | 18.7 | 18.8 | 19.1 | 18.7 | Protein DGCR14 | <i>DGCR14</i> |
| 19.2 | 19.0 | 19.5 | 21.0 | 18.9 | 19.7 | Protein disulfide-isomerase | <i>P4HB</i> |
| 19.8 | 19.4 | 20.5 | 23.0 | 19.2 | 20.5 | Protein disulfide-isomerase A3 | <i>PDIA3</i> |
| 18.3 | 19.4 | 19.4 | 22.0 | 18.9 | 20.4 | Protein disulfide-isomerase A4 | <i>PDIA4</i> |
| 19.3 | 19.1 | 19.8 | 21.1 | 19.3 | 19.3 | Protein disulfide-isomerase A6 | <i>PDIA6</i> |
| 23.9 | 24.1 | 23.9 | 21.8 | 24.5 | 23.5 | Protein dpy-30 homolog | <i>DPY30</i> |
| 15.0 | 15.0 | 15.0 | 21.7 | 15.0 | 15.0 | Protein Dr1 | <i>DR1</i> |
| 18.6 | 18.4 | 18.4 | 15.0 | 18.3 | 18.2 | Protein ECT2 | <i>ECT2</i> |
| 18.5 | 18.1 | 19.7 | 15.0 | 18.7 | 18.7 | Protein EMSY | <i>EMSY</i> |
| 15.0 | 15.0 | 15.0 | 19.6 | 15.0 | 15.0 | Protein enabled homolog | <i>ENAH</i> |
| 15.0 | 15.0 | 15.0 | 21.2 | 18.7 | 19.0 | Protein FAM133B | <i>FAM133B</i> |
| 22.5 | 22.8 | 22.2 | 15.0 | 22.1 | 22.5 | Protein FAM193A | <i>FAM193A</i> |
| 15.0 | 18.7 | 18.5 | 15.0 | 18.4 | 18.6 | Protein FAM195A | <i>FAM195A</i> |
| 22.2 | 22.0 | 22.0 | 20.2 | 22.4 | 21.8 | Protein FAM199X | <i>FAM199X</i> |
| 24.0 | 23.5 | 22.7 | 19.9 | 23.7 | 23.1 | Protein FAM207A | <i>FAM207A</i> |
| 15.0 | 15.0 | 15.0 | 20.3 | 15.0 | 15.0 | Protein FAM32A | <i>FAM32A</i> |
| 20.1 | 20.1 | 21.1 | 23.5 | 19.8 | 19.7 | Protein FAM50A | <i>FAM50A</i> |
| 19.0 | 19.0 | 18.8 | 15.0 | 18.9 | 18.7 | Protein FAM64A | <i>FAM64A</i> |
| 19.4 | 19.9 | 20.0 | 20.1 | 19.2 | 19.6 | Protein FAM76A | <i>FAM76A</i> |
| 18.2 | 18.0 | 18.6 | 15.0 | 18.3 | 18.2 | Protein FAM76B | <i>FAM76B</i> |
| 18.2 | 18.6 | 18.3 | 18.5 | 18.2 | 18.4 | Protein FAM83D | <i>FAM83D</i> |
| 20.0 | 20.2 | 19.6 | 20.0 | 20.0 | 19.6 | Protein FAM98A | <i>FAM98A</i> |
| 20.4 | 20.1 | 20.2 | 19.6 | 20.2 | 20.1 | Protein FAM98B | <i>FAM98B</i> |
| 20.0 | 20.0 | 20.0 | 20.3 | 19.7 | 20.0 | Protein flightless-1 homolog | <i>FLII</i> |
| 19.1 | 19.4 | 19.7 | 21.1 | 19.2 | 19.0 | Protein FRG1 | <i>FRG1</i> |
| 22.3 | 22.4 | 22.2 | 20.7 | 22.3 | 22.0 | Protein KRI1 homolog | <i>KRI1</i> |
| 21.4 | 21.3 | 21.5 | 21.0 | 21.8 | 21.2 | Protein lin-28 homolog B | <i>LIN28B</i> |
| 19.2 | 19.1 | 19.5 | 19.5 | 19.2 | 19.2 | Protein lin-54 homolog | <i>LIN54</i> |
| 19.4 | 15.0 | 19.5 | 20.3 | 19.7 | 19.3 | Protein lin-7 homolog C | <i>LIN7C</i> |

| | | | | | | | |
|------|------|------|------|------|------|--|-----------------|
| 21.6 | 21.7 | 21.6 | 22.6 | 21.6 | 21.7 | Protein LSM12 homolog | <i>LSM12</i> |
| 19.3 | 19.4 | 19.5 | 15.0 | 19.8 | 19.7 | Protein LSM14 homolog A | <i>LSM14A</i> |
| 20.9 | 20.8 | 20.7 | 20.0 | 20.8 | 20.8 | Protein LSM14 homolog B | <i>LSM14B</i> |
| 22.9 | 22.8 | 22.1 | 20.4 | 22.6 | 22.4 | Protein LTV1 homolog | <i>LTV1</i> |
| 22.4 | 22.4 | 22.6 | 22.2 | 22.3 | 22.4 | Protein LYRIC | <i>MTDH</i> |
| 20.0 | 20.2 | 19.6 | 19.7 | 19.9 | 20.0 | Protein max | <i>MAX</i> |
| 20.4 | 20.3 | 20.2 | 15.0 | 20.7 | 20.3 | Protein MCM10 homolog | <i>MCM10</i> |
| 15.0 | 15.0 | 18.9 | 19.3 | 18.8 | 19.3 | Protein NipSnap homolog 1 | <i>NIPSNAP1</i> |
| 20.6 | 20.4 | 20.3 | 20.5 | 20.4 | 20.2 | Protein numb homolog | <i>NUMB</i> |
| 21.4 | 21.3 | 21.0 | 20.0 | 21.4 | 21.1 | Protein PAT1 homolog 1 | <i>PATL1</i> |
| 19.2 | 19.7 | 20.0 | 19.8 | 18.9 | 19.8 | Protein PBDC1 | <i>PBDC1</i> |
| 20.1 | 19.9 | 19.9 | 21.8 | 19.9 | 20.2 | Protein pelota homolog | <i>PELO</i> |
| 23.7 | 24.4 | 24.2 | 24.6 | 23.6 | 24.3 | Protein phosphatase 1G | <i>PPM1G</i> |
| 23.8 | 24.0 | 23.7 | 23.0 | 24.0 | 23.7 | Protein PRRC2A | <i>PRRC2A</i> |
| 21.7 | 21.7 | 21.6 | 21.2 | 21.9 | 21.8 | Protein PRRC2B | <i>PRRC2B</i> |
| 24.1 | 24.3 | 24.3 | 23.8 | 24.3 | 24.3 | Protein PRRC2C | <i>PRRC2C</i> |
| 22.6 | 22.5 | 22.3 | 21.9 | 22.5 | 22.2 | Protein quaking | <i>QKI</i> |
| 23.1 | 23.4 | 23.7 | 25.3 | 23.2 | 23.3 | Protein RCC2 | <i>RCC2</i> |
| 22.3 | 22.0 | 21.9 | 22.4 | 22.2 | 21.9 | Protein Red | <i>IK</i> |
| 21.7 | 21.5 | 21.8 | 21.0 | 21.7 | 21.5 | Protein regulator of cytokinesis 1 | <i>PRC1</i> |
| 20.8 | 20.8 | 20.9 | 19.6 | 20.7 | 20.5 | Protein RRP5 homolog | <i>PDCD11</i> |
| 19.9 | 22.0 | 15.0 | 20.6 | 20.5 | 19.3 | Protein S100-A9 | <i>S100A9</i> |
| 18.5 | 19.5 | 19.7 | 19.4 | 18.9 | 19.7 | Protein SCO2 homolog, mitochondrial | <i>SCO2</i> |
| 19.2 | 19.4 | 19.2 | 15.0 | 19.2 | 19.2 | Protein SDA1 homolog | <i>SDAD1</i> |
| 21.2 | 21.3 | 20.5 | 15.0 | 20.6 | 21.7 | Protein SEC13 homolog | <i>SEC13</i> |
| 21.6 | 21.3 | 20.9 | 22.9 | 21.9 | 21.0 | Protein SET | <i>SET</i> |
| 15.0 | 18.4 | 18.7 | 15.0 | 15.0 | 18.6 | Protein Smaug homolog 2 | <i>SAMD4B</i> |
| 20.9 | 21.4 | 20.9 | 18.7 | 20.5 | 21.4 | Protein SOGA1 | <i>SOGA1</i> |
| 22.9 | 22.8 | 22.8 | 22.0 | 23.0 | 21.9 | Protein SON | <i>SON</i> |
| 18.7 | 19.2 | 19.4 | 19.3 | 19.4 | 19.0 | Protein SPT2 homolog | <i>SPTY2D1</i> |
| 15.0 | 18.6 | 18.6 | 20.4 | 19.0 | 18.9 | Protein SREK1IP1 | <i>SREK1IP1</i> |
| 21.5 | 21.6 | 20.9 | 15.0 | 21.2 | 21.7 | Protein transport protein Sec16A | <i>SEC16A</i> |
| 21.8 | 22.2 | 22.8 | 22.6 | 21.9 | 22.2 | Protein transport protein Sec61 subunit beta | <i>SEC61B</i> |
| 21.4 | 21.2 | 20.3 | 19.4 | 21.3 | 20.6 | Protein VPRBP | <i>VPRBP</i> |
| 23.5 | 22.9 | 23.4 | 24.1 | 23.4 | 23.0 | Protein-L-isoaspartate O-methyltransferase | <i>PCMT1</i> |
| 20.5 | 21.8 | 21.2 | 24.0 | 20.6 | 20.9 | Prothymosin alpha | <i>PTMA</i> |
| 21.0 | 20.8 | 20.3 | 20.0 | 20.6 | 20.6 | Pumilio homolog 1 | <i>PUM1</i> |
| 23.5 | 23.3 | 23.3 | 22.5 | 23.4 | 23.1 | Putative ATP-dependent RNA helicase DHX30 | <i>DHX30</i> |
| 20.5 | 20.4 | 20.4 | 15.0 | 20.4 | 20.4 | Putative ATP-dependent RNA helicase DHX57 | <i>DHX57</i> |
| 21.1 | 20.5 | 20.5 | 19.9 | 20.7 | 20.7 | Putative helicase MOV-10 | <i>MOV10</i> |
| 15.0 | 18.6 | 18.8 | 15.0 | 18.8 | 18.7 | Putative methyltransferase C9orf114 | <i>C9orf114</i> |
| 20.3 | 20.7 | 20.9 | 19.8 | 20.5 | 20.6 | Putative oxidoreductase GLYR1 | <i>GLYR1</i> |
| 21.2 | 21.3 | 21.6 | 22.5 | 21.5 | 21.2 | Putative RNA-binding protein 15 | <i>RBM15</i> |
| 18.9 | 18.9 | 19.0 | 19.0 | 19.2 | 18.9 | Putative RNA-binding protein 15B | <i>RBM15B</i> |
| 21.3 | 21.4 | 21.4 | 21.4 | 21.2 | 21.2 | Putative RNA-binding protein Luc7-like 1 | <i>LUC7L</i> |
| 24.6 | 24.6 | 24.8 | 26.7 | 24.6 | 24.6 | Putative RNA-binding protein Luc7-like 2 | <i>LUC7L2</i> |
| 20.4 | 20.1 | 20.2 | 21.0 | 20.1 | 20.3 | Pyrroline-5-carboxylate reductase 1, mitochondrial | <i>PYCR1</i> |
| 21.1 | 20.9 | 21.0 | 20.7 | 20.7 | 20.8 | Pyrroline-5-carboxylate reductase 2 | <i>PYCR2</i> |

| | | | | | | | |
|------|------|------|------|------|------|---|-----------------|
| 20.0 | 19.7 | 19.8 | 21.0 | 19.9 | 19.9 | Pyruvate dehydrogenase E1 component subunit beta, mitochondrial | <i>PDHB</i> |
| 22.8 | 22.0 | 23.0 | 25.2 | 22.2 | 22.5 | Pyruvate kinase PKM | <i>PKM</i> |
| 20.2 | 20.2 | 20.1 | 19.7 | 20.2 | 20.2 | R3H domain-containing protein 1 | <i>R3HDM1</i> |
| 20.7 | 21.0 | 21.0 | 21.0 | 20.7 | 20.9 | Rac GTPase-activating protein 1 | <i>RACGAP1</i> |
| 21.3 | 21.6 | 21.5 | 20.9 | 21.2 | 22.1 | RAF proto-oncogene serine/threonine-protein kinase | <i>RAF1</i> |
| 20.6 | 20.5 | 20.2 | 21.1 | 20.5 | 20.2 | Ran GTPase-activating protein 1 | <i>RANGAP1</i> |
| 19.5 | 18.8 | 18.5 | 19.1 | 19.9 | 18.7 | Ran-binding protein 9 | <i>RANBP9</i> |
| 19.8 | 19.4 | 19.9 | 22.6 | 15.0 | 19.8 | Ran-specific GTPase-activating protein | <i>RANBP1</i> |
| 19.3 | 18.9 | 19.4 | 15.0 | 18.8 | 19.3 | Rapamycin-insensitive companion of mTOR | <i>RICTOR</i> |
| 24.7 | 24.6 | 24.5 | 23.6 | 24.6 | 24.4 | Ras GTPase-activating protein-binding protein 1 | <i>G3BP1</i> |
| 23.4 | 23.8 | 23.5 | 23.1 | 23.7 | 23.5 | Ras GTPase-activating protein-binding protein 2 | <i>G3BP2</i> |
| 19.3 | 19.3 | 19.8 | 19.6 | 19.0 | 19.4 | Ras-related protein Rab-13 | <i>RAB13</i> |
| 15.0 | 19.5 | 20.0 | 15.0 | 19.7 | 20.1 | Receptor expression-enhancing protein 4 | <i>REEP4</i> |
| 21.4 | 20.8 | 21.0 | 20.7 | 21.1 | 20.7 | Regulator of chromosome condensation | <i>RCC1</i> |
| 23.9 | 24.2 | 24.0 | 22.5 | 24.2 | 23.8 | Regulator of nonsense transcripts 1 | <i>UPF1</i> |
| 19.6 | 19.3 | 19.2 | 19.0 | 19.0 | 18.9 | Regulator of nonsense transcripts 2 | <i>UPF2</i> |
| 20.3 | 20.0 | 20.4 | 20.5 | 20.0 | 20.0 | Regulator of nonsense transcripts 3B | <i>UPF3B</i> |
| 18.3 | 18.3 | 18.4 | 18.9 | 15.0 | 18.1 | Regulatory factor X-associated protein | <i>RFXAP</i> |
| 22.5 | 22.6 | 22.9 | 21.9 | 22.5 | 22.6 | Replication factor C subunit 1 | <i>RFC1</i> |
| 22.4 | 22.5 | 22.5 | 21.9 | 22.5 | 22.4 | Replication factor C subunit 2 | <i>RFC2</i> |
| 22.0 | 22.2 | 22.3 | 21.5 | 22.0 | 22.0 | Replication factor C subunit 3 | <i>RFC3</i> |
| 23.1 | 23.3 | 23.3 | 22.5 | 23.3 | 23.1 | Replication factor C subunit 4 | <i>RFC4</i> |
| 21.6 | 20.2 | 21.8 | 15.0 | 20.3 | 21.4 | Replication factor C subunit 5 | <i>RFC5</i> |
| 19.8 | 19.4 | 20.0 | 20.0 | 19.8 | 19.3 | Replication protein A 14 kDa subunit | <i>RPA3</i> |
| 20.9 | 21.6 | 21.4 | 20.1 | 20.7 | 22.2 | Reticulocalbin-2 | <i>RCN2</i> |
| 23.4 | 22.8 | 22.3 | 19.5 | 23.7 | 22.3 | Retinoblastoma-binding protein 5 | <i>RBBP5</i> |
| 18.9 | 19.1 | 19.1 | 15.0 | 18.9 | 19.0 | Rho GTPase-activating protein 19 | <i>ARHGAP19</i> |
| 22.1 | 21.9 | 22.0 | 21.1 | 22.3 | 21.8 | Rho guanine nucleotide exchange factor 2 | <i>ARHGEF2</i> |
| 15.0 | 15.0 | 15.0 | 15.0 | 15.0 | 16.8 | Rho guanine nucleotide exchange factor 28 | <i>ARHGEF28</i> |
| 18.9 | 19.4 | 19.0 | 18.8 | 19.2 | 19.3 | Rhotekin | <i>RTKN</i> |
| 15.0 | 18.0 | 18.4 | 18.7 | 18.1 | 18.1 | Ribonuclease inhibitor | <i>RNH1</i> |
| 20.2 | 20.2 | 20.2 | 19.8 | 20.2 | 20.2 | Ribonuclease P protein subunit p20 | <i>POP7</i> |
| 19.1 | 18.8 | 18.8 | 19.1 | 19.0 | 18.5 | Ribonuclease P protein subunit p25 | <i>RPP25</i> |
| 19.5 | 19.6 | 19.8 | 19.7 | 19.6 | 19.4 | Ribonuclease P protein subunit p25-like protein | <i>RPP25L</i> |
| 21.4 | 21.6 | 21.6 | 20.6 | 21.8 | 21.5 | Ribonucleases P/MRP protein subunit POP1 | <i>POP1</i> |
| 20.8 | 21.0 | 21.0 | 20.8 | 20.6 | 20.8 | Ribose-phosphate pyrophosphokinase 1 | <i>PRPS1</i> |
| 24.1 | 24.1 | 23.9 | 22.8 | 24.1 | 23.8 | Ribosomal L1 domain-containing protein 1 | <i>RSL1D1</i> |
| 15.0 | 20.3 | 19.9 | 15.0 | 20.7 | 19.7 | Ribosomal protein 63, mitochondrial | <i>MRPL57</i> |
| 20.0 | 19.9 | 19.6 | 15.0 | 20.1 | 19.6 | Ribosomal protein L34 | <i>MRPL34</i> |
| 19.3 | 19.1 | 19.1 | 19.5 | 19.2 | 19.2 | Ribosomal RNA processing protein 1 homolog A | <i>RRP1</i> |
| 23.7 | 23.6 | 23.6 | 23.7 | 23.7 | 23.6 | Ribosomal RNA processing protein 1 homolog B | <i>RRP1B</i> |
| 21.1 | 20.9 | 20.8 | 15.0 | 20.8 | 20.8 | Ribosomal RNA small subunit methyltransferase NEP1 | <i>EMG1</i> |
| 15.0 | 18.9 | 18.8 | 18.6 | 19.3 | 18.7 | Ribosomal RNA-processing protein 8 | <i>RRP8</i> |
| 19.4 | 19.8 | 19.5 | 15.0 | 19.8 | 19.4 | Ribosome biogenesis protein BMS1 homolog | <i>BMS1</i> |
| 20.2 | 20.1 | 20.3 | 15.0 | 20.3 | 20.2 | Ribosome biogenesis protein BOP1 | <i>BOP1</i> |

| | | | | | | | |
|------|------|------|------|------|------|--|---------------|
| 22.8 | 22.4 | 22.7 | 20.4 | 22.7 | 22.4 | Ribosome biogenesis protein BRX1 homolog | <i>BRIX1</i> |
| 21.6 | 21.3 | 21.8 | 20.6 | 21.5 | 20.7 | Ribosome biogenesis regulatory protein homolog | <i>RRS1</i> |
| 15.0 | 15.0 | 18.1 | 21.3 | 17.4 | 18.7 | Ribosome maturation protein SBDS | <i>SBDS</i> |
| 20.9 | 21.1 | 20.7 | 20.8 | 21.1 | 20.8 | Ribosome production factor 2 homolog | <i>RPF2</i> |
| 22.8 | 22.8 | 23.2 | 23.7 | 23.1 | 23.0 | Ribosome-binding protein 1 | <i>RRBP1</i> |
| 18.5 | 18.6 | 18.9 | 15.0 | 18.7 | 18.3 | RING finger protein 10 | <i>RNF10</i> |
| 22.0 | 22.5 | 22.4 | 20.5 | 22.0 | 22.8 | RING finger protein 219 | <i>RNF219</i> |
| 19.0 | 19.3 | 19.2 | 15.0 | 19.2 | 19.2 | RING finger protein unkempt homolog | <i>UNK</i> |
| 18.7 | 18.7 | 18.8 | 18.8 | 18.8 | 18.7 | RISC-loading complex subunit TARBP2 | <i>TARBP2</i> |
| 22.1 | 22.2 | 21.9 | 19.8 | 22.2 | 21.9 | RNA 3-terminal phosphate cyclase | <i>RTCA</i> |
| 21.3 | 21.3 | 21.4 | 22.5 | 21.3 | 21.0 | RNA demethylase ALKBH5 | <i>ALKBH5</i> |
| 20.5 | 20.4 | 20.5 | 19.8 | 20.7 | 20.2 | RNA exonuclease 4 | <i>REXO4</i> |
| 21.3 | 20.9 | 20.7 | 20.2 | 21.5 | 20.4 | RNA polymerase II-associated factor 1 homolog | <i>PAF1</i> |
| 20.0 | 20.3 | 20.3 | 20.8 | 20.3 | 19.9 | RNA polymerase II-associated protein 3 | <i>RPAP3</i> |
| 20.0 | 19.7 | 18.5 | 19.2 | 20.1 | 18.7 | RNA polymerase-associated protein LEO1 | <i>LEO1</i> |
| 21.4 | 21.2 | 21.2 | 21.0 | 21.3 | 21.4 | RNA pseudouridylate synthase domain-containing protein 3 | <i>RPUSD3</i> |
| 18.4 | 18.2 | 17.9 | 15.0 | 18.4 | 15.0 | RNA-binding E3 ubiquitin-protein ligase MEX3C | <i>MEX3C</i> |
| 23.1 | 23.1 | 23.1 | 23.3 | 23.4 | 22.9 | RNA-binding motif protein, X chromosome | <i>RBMX</i> |
| 19.9 | 20.4 | 20.0 | 15.0 | 20.5 | 20.3 | RNA-binding motif, single-stranded-interacting protein 1 | <i>RBMS1</i> |
| 22.1 | 21.6 | 21.6 | 21.5 | 22.3 | 21.5 | RNA-binding protein 10 | <i>RBM10</i> |
| 25.5 | 25.0 | 25.0 | 24.8 | 25.6 | 24.8 | RNA-binding protein 14 | <i>RBM14</i> |
| 21.7 | 22.0 | 21.8 | 22.9 | 22.0 | 21.6 | RNA-binding protein 25 | <i>RBM25</i> |
| 22.7 | 23.1 | 23.2 | 23.4 | 22.8 | 22.9 | RNA-binding protein 26 | <i>RBM26</i> |
| 22.2 | 22.2 | 22.3 | 21.0 | 22.2 | 22.1 | RNA-binding protein 27 | <i>RBM27</i> |
| 22.1 | 22.0 | 21.9 | 21.8 | 22.2 | 21.8 | RNA-binding protein 28 | <i>RBM28</i> |
| 23.1 | 22.8 | 22.4 | 21.2 | 23.4 | 22.3 | RNA-binding protein 3 | <i>RBM3</i> |
| 22.0 | 22.1 | 21.6 | 21.7 | 22.0 | 21.5 | RNA-binding protein 33 | <i>RBM33</i> |
| 22.9 | 22.4 | 22.8 | 20.7 | 22.7 | 22.5 | RNA-binding protein 34 | <i>RBM34</i> |
| 23.8 | 23.7 | 23.7 | 24.0 | 23.9 | 23.9 | RNA-binding protein 39 | <i>RBM39</i> |
| 23.0 | 23.4 | 23.2 | 22.8 | 23.2 | 23.4 | RNA-binding protein 4 | <i>RBM4</i> |
| 22.0 | 22.1 | 21.8 | 20.8 | 21.7 | 21.7 | RNA-binding protein 42 | <i>RBM42</i> |
| 18.7 | 18.4 | 18.3 | 18.5 | 18.8 | 18.1 | RNA-binding protein 45 | <i>RBM45</i> |
| 19.2 | 19.0 | 18.8 | 15.0 | 19.1 | 19.2 | RNA-binding protein 4B | <i>RBM4B</i> |
| 20.7 | 20.0 | 20.3 | 15.0 | 20.5 | 20.1 | RNA-binding protein 6 | <i>RBM6</i> |
| 19.3 | 18.9 | 18.8 | 15.0 | 19.4 | 19.2 | RNA-binding protein 7 | <i>RBM7</i> |
| 24.0 | 23.7 | 23.7 | 23.0 | 24.0 | 23.7 | RNA-binding protein EWS | <i>EWSR1</i> |
| 24.6 | 24.4 | 24.2 | 21.5 | 24.6 | 24.1 | RNA-binding protein FUS | <i>FUS</i> |
| 19.1 | 19.1 | 19.2 | 15.0 | 19.3 | 19.2 | RNA-binding protein MEX3A | <i>MEX3A</i> |
| 23.9 | 24.5 | 24.0 | 24.4 | 24.1 | 24.2 | RNA-binding protein MEX3D | <i>MEX3D</i> |
| 21.9 | 21.7 | 22.0 | 20.4 | 21.3 | 21.8 | RNA-binding protein Musashi homolog 1 | <i>MSI1</i> |
| 20.8 | 20.9 | 20.6 | 19.0 | 20.4 | 20.8 | RNA-binding protein Musashi homolog 2 | <i>MSI2</i> |
| 21.4 | 21.4 | 21.2 | 20.3 | 21.4 | 21.2 | RNA-binding protein NOB1 | <i>NOB1</i> |
| 21.1 | 20.8 | 20.5 | 20.2 | 20.7 | 20.5 | RNA-binding protein PNO1 | <i>PNO1</i> |
| 20.9 | 20.3 | 20.7 | 20.8 | 21.0 | 20.4 | RNA-binding protein Raly | <i>RALY</i> |
| 21.8 | 22.0 | 21.8 | 22.8 | 22.1 | 21.5 | RNA-binding protein with serine-rich domain 1 | <i>RNPS1</i> |
| 20.2 | 20.1 | 20.2 | 20.5 | 20.3 | 20.1 | Round spermatid basic protein 1 | <i>RSBN1</i> |
| 20.2 | 20.3 | 20.2 | 15.0 | 20.3 | 20.2 | Round spermatid basic protein 1-like protein | <i>RSBN1L</i> |

| | | | | | | | |
|------|------|------|------|------|------|--|----------------|
| 23.5 | 23.7 | 23.7 | 21.8 | 24.0 | 23.6 | rRNA 2-O-methyltransferase fibrillar | <i>FBL</i> |
| 22.3 | 22.1 | 21.9 | 20.6 | 22.2 | 21.9 | rRNA methyltransferase 3, mitochondrial | <i>RNMTL1</i> |
| 24.5 | 24.2 | 23.5 | 21.6 | 24.4 | 23.7 | RRP12-like protein | <i>RRP12</i> |
| 21.1 | 21.1 | 21.4 | 21.1 | 21.0 | 21.0 | RRP15-like protein | <i>RRP15</i> |
| 23.5 | 23.7 | 23.8 | 24.0 | 23.6 | 24.0 | RuvB-like 1 | <i>RUVBL1</i> |
| 23.4 | 23.4 | 23.6 | 24.1 | 23.4 | 23.7 | RuvB-like 2 | <i>RUVBL2</i> |
| 19.2 | 19.2 | 19.1 | 15.0 | 18.8 | 18.8 | S phase cyclin A-associated protein in the endoplasmic reticulum | <i>SCAPER</i> |
| 21.2 | 21.1 | 21.0 | 19.8 | 21.2 | 20.9 | S1 RNA-binding domain-containing protein 1 | <i>SRBD1</i> |
| 20.1 | 20.0 | 20.0 | 15.0 | 20.3 | 19.7 | SAFB-like transcription modulator | <i>SLTM</i> |
| 19.5 | 19.5 | 19.7 | 19.4 | 19.6 | 19.3 | SAGA-associated factor 29 homolog | <i>CCDC101</i> |
| 19.2 | 19.9 | 19.6 | 15.0 | 15.0 | 20.0 | Sal-like protein 2 | <i>SALL2</i> |
| 21.7 | 21.6 | 22.2 | 24.5 | 21.7 | 21.8 | SAP domain-containing ribonucleoprotein | <i>SARNP</i> |
| 15.0 | 15.0 | 15.0 | 19.1 | 15.0 | 15.0 | SAP30-binding protein | <i>SAP30BP</i> |
| 22.8 | 23.7 | 23.6 | 21.3 | 22.6 | 23.7 | Sarcoplasmic/endoplasmic reticulum calcium ATPase 2 | <i>ATP2A2</i> |
| 22.1 | 21.6 | 21.9 | 22.4 | 22.3 | 21.5 | Scaffold attachment factor B1 | <i>SAFB</i> |
| 19.5 | 19.4 | 19.5 | 15.0 | 19.9 | 19.4 | Scaffold attachment factor B2 | <i>SAFB2</i> |
| 15.0 | 18.9 | 19.0 | 15.0 | 15.0 | 19.2 | Sec1 family domain-containing protein 1 | <i>SCFD1</i> |
| 21.5 | 21.8 | 21.8 | 21.0 | 21.9 | 21.6 | Selenocysteine-specific elongation factor | <i>EEFSEC</i> |
| 19.6 | 20.7 | 19.3 | 15.0 | 19.1 | 20.1 | Sentrin-specific protease 1 | <i>SEN1</i> |
| 15.0 | 19.0 | 19.4 | 15.0 | 19.6 | 19.1 | Sentrin-specific protease 3 | <i>SEN3</i> |
| 20.8 | 21.0 | 21.4 | 23.8 | 20.6 | 21.0 | Septin-11 | <i>Sep-11</i> |
| 22.4 | 22.4 | 22.7 | 24.1 | 22.4 | 22.2 | Septin-2 | <i>Sep-02</i> |
| 15.0 | 15.0 | 19.1 | 21.7 | 19.2 | 18.7 | Septin-6 | <i>Sep-06</i> |
| 21.6 | 21.8 | 22.1 | 24.5 | 21.5 | 21.7 | Septin-7 | <i>Sep-07</i> |
| 15.0 | 15.0 | 15.0 | 19.9 | 15.0 | 15.0 | Septin-8 | <i>Sep-08</i> |
| 21.6 | 21.6 | 21.9 | 24.3 | 21.5 | 21.5 | Septin-9 | <i>Sep-09</i> |
| 19.5 | 19.0 | 19.1 | 20.6 | 19.0 | 19.5 | Serine hydroxymethyltransferase, mitochondrial | <i>SHMT2</i> |
| 15.0 | 20.2 | 20.1 | 19.2 | 19.3 | 20.2 | Serine palmitoyltransferase 1 | <i>SPTLC1</i> |
| 20.9 | 20.8 | 20.9 | 20.3 | 20.8 | 20.9 | Serine-threonine kinase receptor-associated protein | <i>STRAP</i> |
| 19.7 | 20.1 | 20.4 | 15.0 | 20.3 | 19.9 | Serine/arginine repetitive matrix protein 1 | <i>SRRM1</i> |
| 23.8 | 23.7 | 23.6 | 24.2 | 24.0 | 23.4 | Serine/arginine repetitive matrix protein 2 | <i>SRRM2</i> |
| 22.1 | 22.3 | 22.6 | 23.7 | 22.5 | 21.9 | Serine/arginine-rich splicing factor 1 | <i>SRSF1</i> |
| 21.9 | 21.7 | 21.5 | 21.6 | 22.6 | 21.6 | Serine/arginine-rich splicing factor 10 | <i>SRSF10</i> |
| 21.2 | 21.3 | 21.2 | 21.6 | 20.8 | 20.9 | Serine/arginine-rich splicing factor 11 | <i>SRSF11</i> |
| 21.9 | 21.8 | 22.4 | 23.4 | 22.1 | 22.0 | Serine/arginine-rich splicing factor 2 | <i>SRSF2</i> |
| 24.6 | 24.5 | 24.5 | 25.8 | 24.5 | 24.3 | Serine/arginine-rich splicing factor 3 | <i>SRSF3</i> |
| 20.2 | 19.6 | 20.4 | 20.8 | 20.3 | 19.7 | Serine/arginine-rich splicing factor 4 | <i>SRSF4</i> |
| 21.5 | 21.5 | 21.0 | 21.0 | 21.9 | 20.8 | Serine/arginine-rich splicing factor 5 | <i>SRSF5</i> |
| 21.9 | 21.9 | 22.1 | 22.7 | 22.4 | 21.6 | Serine/arginine-rich splicing factor 6 | <i>SRSF6</i> |
| 21.7 | 21.1 | 21.6 | 22.0 | 21.7 | 21.2 | Serine/arginine-rich splicing factor 7 | <i>SRSF7</i> |
| 18.8 | 18.9 | 18.6 | 19.2 | 18.6 | 18.5 | Serine/arginine-rich splicing factor 8 | <i>SRSF8</i> |
| 21.7 | 22.4 | 21.8 | 21.2 | 22.5 | 21.9 | Serine/arginine-rich splicing factor 9 | <i>SRSF9</i> |
| 21.7 | 21.7 | 22.1 | 20.5 | 21.8 | 21.5 | Serine/threonine-protein kinase 40 | <i>STK40</i> |
| 18.6 | 19.0 | 18.9 | 15.0 | 18.4 | 19.2 | Serine/threonine-protein kinase A-Raf | <i>ARAF</i> |
| 19.6 | 20.1 | 20.1 | 15.0 | 19.5 | 19.2 | Serine/threonine-protein kinase D2 | <i>PRKD2</i> |
| 20.8 | 21.3 | 21.0 | 19.4 | 20.3 | 21.4 | Serine/threonine-protein kinase greatwall | <i>MASTL</i> |
| 20.5 | 20.6 | 20.9 | 21.2 | 20.6 | 20.6 | Serine/threonine-protein kinase MARK2 | <i>MARK2</i> |
| 22.0 | 20.8 | 20.7 | 18.8 | 22.1 | 19.2 | Serine/threonine-protein kinase N3 | <i>PKN3</i> |

| | | | | | | | |
|------|------|------|------|------|------|---|-----------------|
| 20.0 | 19.8 | 19.7 | 20.1 | 19.6 | 19.6 | Serine/threonine-protein kinase PLK1 | <i>PLK1</i> |
| 21.3 | 21.4 | 21.4 | 20.6 | 21.4 | 21.1 | Serine/threonine-protein kinase PRP4 homolog | <i>PRPF4B</i> |
| 15.0 | 18.0 | 18.6 | 18.0 | 15.0 | 17.8 | Serine/threonine-protein kinase tousled-like 2 | <i>TLK2</i> |
| 19.7 | 19.4 | 19.3 | 19.6 | 19.5 | 19.5 | Serine/threonine-protein phosphatase 1 regulatory subunit 10 | <i>PPP1R10</i> |
| 22.8 | 21.9 | 21.4 | 15.0 | 23.2 | 21.5 | Serine/threonine-protein phosphatase 2A 55 kDa regulatory subunit B alpha isoform | <i>PPP2R2A</i> |
| 25.0 | 24.0 | 23.7 | 22.1 | 25.5 | 23.6 | Serine/threonine-protein phosphatase 2A 65 kDa regulatory subunit A alpha isoform | <i>PPP2R1A</i> |
| 22.6 | 21.7 | 21.1 | 19.1 | 23.1 | 21.4 | Serine/threonine-protein phosphatase 2A catalytic subunit alpha isoform | <i>PPP2CA</i> |
| 20.5 | 20.5 | 20.1 | 19.4 | 20.6 | 20.5 | Serine/threonine-protein phosphatase 6 catalytic subunit | <i>PPP6C</i> |
| 20.2 | 19.7 | 19.4 | 15.0 | 20.1 | 19.5 | Serine/threonine-protein phosphatase 6 regulatory ankyrin repeat subunit A | <i>ANKRD28</i> |
| 21.4 | 21.4 | 21.1 | 15.0 | 21.3 | 21.3 | Serine/threonine-protein phosphatase 6 regulatory subunit 1 | <i>PPP6R1</i> |
| 21.4 | 21.5 | 20.7 | 19.9 | 21.3 | 21.6 | Serine/threonine-protein phosphatase 6 regulatory subunit 3 | <i>PPP6R3</i> |
| 20.6 | 20.6 | 21.3 | 20.4 | 20.8 | 20.8 | Serine/threonine-protein phosphatase PGAM5, mitochondrial | <i>PGAM5</i> |
| 15.0 | 18.6 | 18.6 | 15.0 | 18.6 | 18.6 | Serine/threonine-protein phosphatase PP1-alpha catalytic subunit | <i>PPP1CA</i> |
| 17.3 | 15.0 | 17.6 | 18.5 | 15.0 | 18.2 | Serine/threonine-protein phosphatase 5 | <i>PPP5C</i> |
| 22.0 | 22.0 | 22.3 | 22.0 | 21.8 | 22.0 | Serine/threonine-protein phosphatase PP1-gamma catalytic subunit | <i>PPP1CC</i> |
| 22.8 | 22.9 | 22.2 | 15.0 | 22.7 | 22.7 | Serologically defined colon cancer antigen 3 | <i>SDCCAG3</i> |
| 18.2 | 15.0 | 18.0 | 19.2 | 15.0 | 15.0 | Serpin H1 | <i>SERPINH1</i> |
| 20.8 | 20.4 | 20.3 | 20.9 | 20.7 | 20.1 | Serrate RNA effector molecule homolog | <i>SRRT</i> |
| 20.4 | 20.8 | 20.8 | 15.0 | 20.6 | 20.5 | SET domain-containing protein 5 | <i>SETD5</i> |
| 24.7 | 24.4 | 23.9 | 17.1 | 25.0 | 23.8 | Set1/Ash2 histone methyltransferase complex subunit ASH2 | <i>ASH2L</i> |
| 19.2 | 18.9 | 19.1 | 19.7 | 19.1 | 18.8 | Sex comb on midleg-like protein 2 | <i>SCML2</i> |
| 20.2 | 20.0 | 19.7 | 15.0 | 20.2 | 19.5 | SH2 domain-containing adapter protein B | <i>SHB</i> |
| 15.0 | 18.1 | 18.2 | 15.0 | 15.0 | 15.0 | SH3 and PX domain-containing protein 2A | <i>SH3PXD2A</i> |
| 24.9 | 24.8 | 24.9 | 24.5 | 24.7 | 24.8 | Signal recognition particle 14 kDa protein | <i>SRP14</i> |
| 18.3 | 18.5 | 18.3 | 20.0 | 15.0 | 17.7 | Signal recognition particle 54 kDa protein | <i>SRP54</i> |
| 23.8 | 23.9 | 24.0 | 23.9 | 23.8 | 23.6 | Signal recognition particle 9 kDa protein | <i>SRP9</i> |
| 19.9 | 20.0 | 20.2 | 19.8 | 20.0 | 20.2 | Signal recognition particle receptor subunit alpha | <i>SRPR</i> |
| 21.8 | 22.1 | 22.2 | 21.7 | 21.9 | 22.2 | Signal recognition particle receptor subunit beta | <i>SRPRB</i> |
| 15.0 | 18.2 | 15.0 | 15.0 | 18.6 | 15.0 | Signal recognition particle subunit SRP68 | <i>SRP68</i> |
| 15.0 | 19.3 | 18.7 | 15.0 | 15.0 | 20.3 | Signal-induced proliferation-associated 1-like protein 1 | <i>SIPA1L1</i> |
| 19.3 | 20.2 | 19.7 | 15.0 | 19.0 | 20.9 | Signal-induced proliferation-associated 1-like protein 2 | <i>SIPA1L2</i> |
| 23.4 | 23.0 | 23.1 | 23.0 | 23.0 | 23.0 | Single-stranded DNA-binding protein, mitochondrial | <i>SSBP1</i> |
| 20.2 | 20.7 | 20.9 | 20.8 | 20.3 | 20.3 | Sister chromatid cohesion protein PDS5 homolog A | <i>PDS5A</i> |
| 18.9 | 18.6 | 18.7 | 15.0 | 18.5 | 18.6 | Sister chromatid cohesion protein PDS5 homolog B | <i>PDS5B</i> |
| 20.1 | 19.9 | 19.4 | 20.4 | 20.7 | 19.6 | Sjogren syndrome/scleroderma autoantigen 1 | <i>SSSCA1</i> |
| 22.4 | 22.8 | 22.5 | 22.3 | 22.4 | 23.0 | SLAIN motif-containing protein 1 | <i>SLAIN1</i> |
| 19.2 | 19.2 | 19.4 | 15.0 | 19.4 | 19.3 | SLAIN motif-containing protein 2 | <i>SLAIN2</i> |
| 17.9 | 17.9 | 18.4 | 15.0 | 17.8 | 17.8 | Slit homolog 2 protein | <i>SLIT2</i> |
| 20.4 | 20.3 | 20.2 | 22.2 | 20.0 | 20.2 | Small acidic protein | <i>SMAP</i> |
| 19.9 | 15.0 | 19.2 | 19.8 | 19.3 | 19.1 | Small glutamine-rich tetratricopeptide repeat-containing protein alpha | <i>SGTA</i> |
| 22.9 | 22.7 | 23.0 | 23.2 | 23.1 | 21.7 | Small nuclear ribonucleoprotein E | <i>SNRPE</i> |

| | | | | | | | |
|------|------|------|------|------|------|--|-----------------|
| 19.6 | 19.8 | 19.5 | 19.6 | 19.5 | 19.8 | Small nuclear ribonucleoprotein G | <i>SNRPG</i> |
| 21.4 | 21.3 | 21.1 | 22.2 | 21.6 | 21.3 | Small nuclear ribonucleoprotein Sm D1 | <i>SNRPD1</i> |
| 21.9 | 22.1 | 21.6 | 21.3 | 22.4 | 21.8 | Small nuclear ribonucleoprotein Sm D2 | <i>SNRPD2</i> |
| 23.8 | 23.8 | 23.6 | 23.8 | 24.2 | 23.6 | Small nuclear ribonucleoprotein Sm D3 | <i>SNRPD3</i> |
| 23.2 | 23.0 | 22.9 | 23.4 | 23.1 | 23.0 | Small nuclear ribonucleoprotein-associated protein N | <i>SNRPN</i> |
| 18.0 | 18.2 | 15.0 | 15.0 | 18.6 | 17.8 | Small subunit processome component 20 homolog | <i>UTP20</i> |
| 15.0 | 18.0 | 18.3 | 15.0 | 18.1 | 18.0 | Small ubiquitin-related modifier 1 | <i>SUMO1</i> |
| 22.8 | 22.7 | 22.7 | 22.9 | 22.7 | 22.6 | SNW domain-containing protein 1 | <i>SNW1</i> |
| 19.0 | 18.8 | 16.8 | 15.0 | 15.0 | 19.0 | Sodium channel modifier 1 | <i>SCNM1</i> |
| 23.5 | 24.5 | 24.6 | 23.1 | 23.7 | 24.8 | Sodium/potassium-transporting ATPase subunit alpha-1 | <i>ATP1A1</i> |
| 18.9 | 19.5 | 19.0 | 15.0 | 19.2 | 18.5 | Something about silencing protein 10 | <i>UTP3</i> |
| 18.4 | 15.0 | 15.0 | 19.9 | 15.0 | 15.0 | Sorting nexin-2 | <i>SNX2</i> |
| 15.0 | 15.0 | 15.0 | 19.1 | 15.0 | 15.0 | Sorting nexin-5 | <i>SNX5</i> |
| 18.9 | 18.7 | 18.8 | 19.0 | 18.6 | 18.7 | SPATS2-like protein | <i>SPATS2L</i> |
| 18.4 | 15.0 | 18.8 | 21.8 | 15.0 | 18.3 | Spectrin alpha chain, non-erythrocytic 1 | <i>SPTAN1</i> |
| 15.0 | 15.0 | 15.0 | 21.2 | 15.0 | 15.0 | Spectrin beta chain, non-erythrocytic 1 | <i>SPTBN1</i> |
| 18.8 | 17.9 | 17.2 | 15.0 | 17.7 | 18.2 | Spermatid perinuclear RNA-binding protein | <i>STRBP</i> |
| 18.9 | 18.7 | 19.1 | 15.0 | 18.8 | 19.0 | Spermatogenesis-associated protein 5 | <i>SPATA5</i> |
| 20.4 | 20.5 | 20.5 | 19.9 | 20.4 | 20.5 | Spermatogenesis-associated protein 5-like protein 1 | <i>SPATA5L1</i> |
| 19.9 | 20.1 | 20.0 | 19.7 | 20.0 | 19.9 | Spermatogenesis-associated serine-rich protein 2 | <i>SPATS2</i> |
| 19.4 | 19.4 | 19.4 | 15.0 | 19.2 | 19.1 | Sphingosine-1-phosphate lyase 1 | <i>SGPL1</i> |
| 18.2 | 18.6 | 18.6 | 15.0 | 15.0 | 18.5 | Spindle and kinetochore-associated protein 1 | <i>SKA1</i> |
| 18.2 | 18.7 | 18.4 | 15.0 | 18.2 | 18.2 | Spindle and kinetochore-associated protein 3 | <i>SKA3</i> |
| 19.7 | 19.6 | 19.9 | 20.2 | 15.0 | 19.5 | Spliceosome RNA helicase DDX39B | <i>DDX39B</i> |
| 23.7 | 23.7 | 23.9 | 23.9 | 23.7 | 23.5 | Splicing factor 1 | <i>SF1</i> |
| 20.7 | 20.6 | 20.2 | 20.9 | 21.0 | 20.1 | Splicing factor 3A subunit 1 | <i>SF3A1</i> |
| 19.8 | 19.6 | 19.0 | 20.1 | 19.6 | 19.0 | Splicing factor 3A subunit 2 | <i>SF3A2</i> |
| 21.3 | 20.6 | 20.4 | 21.2 | 21.2 | 20.0 | Splicing factor 3A subunit 3 | <i>SF3A3</i> |
| 23.3 | 23.2 | 22.9 | 23.3 | 23.5 | 22.7 | Splicing factor 3B subunit 1 | <i>SF3B1</i> |
| 24.4 | 24.0 | 23.9 | 23.8 | 24.4 | 23.8 | Splicing factor 3B subunit 2 | <i>SF3B2</i> |
| 21.9 | 21.8 | 22.0 | 20.4 | 22.3 | 21.7 | Splicing factor 3B subunit 3 | <i>SF3B3</i> |
| 22.7 | 22.4 | 22.3 | 23.1 | 22.6 | 22.0 | Splicing factor 3B subunit 5 | <i>SF3B5</i> |
| 21.8 | 21.7 | 21.5 | 21.8 | 21.8 | 21.6 | Splicing factor 45 | <i>RBM17</i> |
| 23.3 | 22.9 | 22.9 | 23.7 | 23.1 | 22.9 | Splicing factor U2AF 35 kDa subunit | <i>U2AF1</i> |
| 23.4 | 23.2 | 23.4 | 24.5 | 23.6 | 23.2 | Splicing factor U2AF 65 kDa subunit | <i>U2AF2</i> |
| 18.9 | 19.1 | 18.8 | 18.2 | 19.0 | 19.0 | Splicing factor, arginine/serine-rich 15 | <i>SCAF4</i> |
| 27.6 | 27.6 | 27.8 | 28.5 | 27.7 | 27.6 | Splicing factor, proline- and glutamine-rich | <i>SFPQ</i> |
| 18.7 | 18.7 | 18.4 | 19.1 | 18.7 | 18.8 | Splicing factor, suppressor of white-apricot homolog | <i>SFSWAP</i> |
| 15.0 | 15.0 | 19.2 | 19.8 | 15.0 | 15.0 | Splicing regulatory glutamine/lysine-rich protein 1 | <i>SREK1</i> |
| 23.3 | 22.7 | 22.1 | 19.9 | 23.3 | 21.9 | Squamous cell carcinoma antigen recognized by T-cells 3 | <i>SART3</i> |
| 22.0 | 21.6 | 21.6 | 21.3 | 21.7 | 21.4 | SRA stem-loop-interacting RNA-binding protein, mitochondrial | <i>SLIRP</i> |
| 15.0 | 15.0 | 18.1 | 20.8 | 15.0 | 19.1 | Src substrate cortactin | <i>CTTN</i> |
| 22.7 | 22.6 | 22.7 | 21.5 | 22.8 | 22.6 | SRSF protein kinase 1 | <i>SRPK1</i> |
| 15.0 | 19.3 | 19.3 | 19.1 | 19.0 | 18.8 | SRSF protein kinase 2 | <i>SRPK2</i> |
| 23.6 | 23.2 | 23.4 | 23.4 | 23.4 | 23.3 | Staphylococcal nuclease domain-containing protein 1 | <i>SND1</i> |

| | | | | | | | |
|------|------|------|------|------|------|---|--------------------|
| 20.7 | 15.0 | 20.0 | 22.0 | 15.0 | 15.0 | Stathmin | <i>STMN1</i> |
| 15.0 | 15.0 | 18.2 | 18.1 | 15.0 | 18.0 | Stomatin-like protein 2, mitochondrial | <i>STOML2</i> |
| 21.0 | 21.2 | 19.8 | 15.0 | 20.6 | 21.3 | Stonin-1 | <i>STON1</i> |
| 27.2 | 27.0 | 26.7 | 26.3 | 27.2 | 27.0 | Stress-70 protein, mitochondrial | <i>HSPA9</i> |
| 24.6 | 25.7 | 25.8 | 23.6 | 23.6 | 27.0 | Stress-induced-phosphoprotein 1 | <i>STIP1</i> |
| 19.8 | 19.7 | 19.8 | 20.7 | 19.7 | 19.6 | Structural maintenance of chromosomes flexible hinge domain-containing protein 1 | <i>SMCHD1</i> |
| 24.1 | 24.2 | 24.4 | 25.1 | 24.1 | 24.0 | Structural maintenance of chromosomes protein 1A | <i>SMC1A</i> |
| 22.9 | 22.9 | 23.1 | 23.2 | 22.6 | 22.7 | Structural maintenance of chromosomes protein 2 | <i>SMC2</i> |
| 23.2 | 23.1 | 23.4 | 23.9 | 23.1 | 23.2 | Structural maintenance of chromosomes protein 3 | <i>SMC3</i> |
| 15.0 | 19.3 | 19.2 | 15.0 | 19.2 | 18.6 | Structural maintenance of chromosomes protein 6 | <i>SMC6</i> |
| 22.6 | 22.7 | 23.0 | 22.8 | 22.5 | 23.0 | Structural maintenance of chromosomes protein | <i>SMC4</i> |
| 21.1 | 21.5 | 21.5 | 22.1 | 21.4 | 21.5 | Succinate dehydrogenase [ubiquinone] flavoprotein subunit, mitochondrial | <i>SDHA</i> |
| 20.3 | 20.3 | 20.4 | 21.1 | 20.5 | 20.5 | Succinate dehydrogenase [ubiquinone] iron-sulfur subunit, mitochondrial | <i>SDHB</i> |
| 15.0 | 15.0 | 15.0 | 19.2 | 15.0 | 15.0 | SUMO-activating enzyme subunit 2 | <i>UBA2</i> |
| 19.1 | 19.1 | 19.0 | 15.0 | 19.1 | 19.0 | SUN domain-containing protein 2 | <i>SUN2</i> |
| 22.4 | 22.2 | 22.1 | 20.9 | 22.6 | 22.1 | Superkiller viralicidic activity 2-like 2 | <i>SKIV2L2</i> |
| 19.1 | 18.3 | 19.3 | 21.7 | 18.9 | 19.0 | Superoxide dismutase [Cu-Zn] | <i>SOD1</i> |
| 21.1 | 21.0 | 21.1 | 20.3 | 21.2 | 20.7 | Suppressor of SWI4 1 homolog | <i>PPAN-P2RY11</i> |
| 21.3 | 21.2 | 21.5 | 20.5 | 21.1 | 20.9 | Surfeit locus protein 6 | <i>SURF6</i> |
| 20.0 | 20.3 | 20.2 | 15.0 | 20.2 | 20.5 | SURP and G-patch domain-containing protein 2 | <i>SUGP2</i> |
| 22.7 | 22.7 | 23.0 | 22.6 | 22.8 | 23.2 | Survival motor neuron protein | <i>SMN1</i> |
| 20.0 | 20.5 | 20.5 | 20.8 | 20.4 | 20.4 | SWI/SNF complex subunit SMARCC1 | <i>SMARCC1</i> |
| 20.4 | 20.3 | 20.2 | 20.1 | 20.3 | 20.2 | SWI/SNF-related matrix-associated actin-dependent regulator of chromatin subfamily A member 5 | <i>SMARCA5</i> |
| 19.0 | 15.0 | 19.1 | 15.0 | 18.6 | 18.9 | Symplekin | <i>SYMPK</i> |
| 24.5 | 25.2 | 25.6 | 23.9 | 24.6 | 25.9 | T-complex protein 1 subunit alpha | <i>TCP1</i> |
| 26.4 | 26.8 | 27.3 | 24.7 | 26.2 | 27.5 | T-complex protein 1 subunit beta | <i>CCT2</i> |
| 24.9 | 25.2 | 25.8 | 24.7 | 24.7 | 26.0 | T-complex protein 1 subunit delta | <i>CCT4</i> |
| 25.4 | 26.0 | 26.7 | 24.8 | 25.4 | 26.9 | T-complex protein 1 subunit epsilon | <i>CCT5</i> |
| 25.6 | 26.2 | 26.5 | 24.4 | 25.5 | 26.9 | T-complex protein 1 subunit eta | <i>CCT7</i> |
| 26.6 | 27.1 | 27.4 | 25.9 | 26.5 | 27.9 | T-complex protein 1 subunit gamma | <i>CCT3</i> |
| 25.7 | 26.3 | 26.6 | 25.2 | 25.7 | 27.0 | T-complex protein 1 subunit theta | <i>CCT8</i> |
| 26.0 | 26.6 | 26.9 | 24.8 | 26.0 | 27.2 | T-complex protein 1 subunit zeta | <i>CCT6A</i> |
| 22.3 | 22.6 | 22.8 | 22.9 | 22.2 | 22.7 | TAR DNA-binding protein 43 | <i>TDP43</i> |
| 22.6 | 22.8 | 22.8 | 22.7 | 23.0 | 22.7 | Targeting protein for Xklp2 | <i>TPX2</i> |
| 18.7 | 18.5 | 18.5 | 15.0 | 18.7 | 18.6 | TATA box-binding protein-associated factor RNA polymerase I subunit C | <i>TAF1C</i> |
| 21.6 | 21.2 | 21.1 | 21.5 | 21.6 | 20.9 | TATA-binding protein-associated factor 2N | <i>TAF15</i> |
| 18.8 | 18.6 | 18.7 | 15.0 | 18.7 | 18.6 | TBC1 domain family member 4 | <i>TBC1D4</i> |
| 21.6 | 21.6 | 21.7 | 21.5 | 21.5 | 21.8 | Telomere-associated protein RIF1 | <i>RIF1</i> |
| 20.1 | 20.0 | 19.9 | 19.0 | 20.2 | 20.2 | Telomeric repeat-binding factor 2 | <i>TERF2</i> |
| 19.3 | 18.9 | 18.8 | 15.0 | 19.1 | 18.8 | Terminal uridylyltransferase 4 | <i>ZCCHC11</i> |
| 19.3 | 19.1 | 18.9 | 15.0 | 19.2 | 18.7 | Terminal uridylyltransferase 7 | <i>ZCCHC6</i> |
| 20.3 | 20.1 | 20.1 | 19.7 | 20.3 | 20.2 | Testis-specific Y-encoded-like protein 1 | <i>TSPYL1</i> |
| 18.6 | 18.6 | 18.7 | 15.0 | 18.5 | 18.4 | TFIIH basal transcription factor complex helicase XPB subunit | <i>ERCC3</i> |
| 15.0 | 15.0 | 17.8 | 15.0 | 15.0 | 17.6 | TFIIH basal transcription factor complex helicase XPD subunit | <i>ERCC2</i> |

| | | | | | | | |
|------|------|------|------|------|------|---|----------------|
| 20.4 | 20.8 | 20.8 | 22.2 | 20.5 | 20.7 | Thioredoxin | <i>TXN</i> |
| 21.0 | 20.9 | 21.0 | 22.0 | 21.4 | 21.0 | Thioredoxin domain-containing protein 5 | <i>TXNDC5</i> |
| 20.2 | 19.8 | 19.7 | 15.0 | 19.9 | 20.1 | Thioredoxin-dependent peroxide reductase, mitochondrial | <i>PRDX3</i> |
| 19.6 | 20.3 | 19.8 | 20.0 | 20.3 | 20.7 | Thioredoxin-like protein 1 | <i>TXNL1</i> |
| 15.0 | 18.9 | 18.8 | 19.0 | 19.3 | 18.9 | THO complex subunit 1 | <i>THOC1</i> |
| 18.7 | 18.9 | 18.5 | 15.0 | 18.9 | 18.8 | THO complex subunit 2 | <i>THOC2</i> |
| 19.5 | 19.4 | 19.8 | 20.2 | 19.5 | 19.6 | THO complex subunit 3 | <i>THOC3</i> |
| 24.6 | 24.3 | 24.1 | 23.0 | 24.8 | 24.3 | THO complex subunit 4 | <i>ALYREF</i> |
| 19.4 | 18.6 | 18.8 | 18.6 | 19.3 | 15.0 | THO complex subunit 7 homolog | <i>THOC7</i> |
| 19.0 | 19.0 | 19.4 | 19.1 | 19.5 | 19.4 | Threonine--tRNA ligase, mitochondrial | <i>TARS2</i> |
| 19.3 | 19.5 | 19.6 | 21.1 | 19.2 | 19.3 | Thymidine kinase | <i>TK1</i> |
| 15.0 | 18.3 | 18.8 | 19.4 | 18.9 | 18.1 | Thymocyte nuclear protein 1 | <i>THYN1</i> |
| 22.9 | 22.5 | 22.8 | 23.7 | 22.9 | 22.2 | Thyroid hormone receptor-associated protein 3 | <i>THRAP3</i> |
| 20.9 | 21.0 | 20.0 | 20.8 | 20.6 | 20.2 | Thyroid receptor-interacting protein 6 | <i>TRIP6</i> |
| 18.2 | 15.0 | 18.5 | 18.7 | 15.0 | 18.2 | Thyroid transcription factor 1-associated protein 26 | <i>CCDC59</i> |
| 19.2 | 19.2 | 18.9 | 19.6 | 19.2 | 19.1 | Tight junction protein ZO-1 | <i>TJP1</i> |
| 20.1 | 20.5 | 20.3 | 20.7 | 20.6 | 20.1 | Tight junction protein ZO-2 | <i>TJP2</i> |
| 20.8 | 20.6 | 20.6 | 19.8 | 20.7 | 20.4 | TOX high mobility group box family member 4 | <i>TOX4</i> |
| 21.0 | 21.5 | 21.4 | 21.0 | 20.7 | 21.7 | TRAF-type zinc finger domain-containing protein 1 | <i>TRAFD1</i> |
| 19.0 | 19.3 | 19.2 | 19.3 | 19.3 | 19.3 | Transcription activator BRG1 | <i>SMARCA4</i> |
| 19.4 | 19.9 | 20.4 | 20.5 | 19.7 | 20.0 | Transcription and mRNA export factor ENY2 | <i>ENY2</i> |
| 22.1 | 22.2 | 22.6 | 24.7 | 22.2 | 22.2 | Transcription elongation factor A protein 1 | <i>TCEA1</i> |
| 15.0 | 18.5 | 17.5 | 18.9 | 15.0 | 15.0 | Transcription elongation factor A protein-like 4 | <i>TCEAL4</i> |
| 21.4 | 21.5 | 21.7 | 22.0 | 21.5 | 21.8 | Transcription elongation factor B polypeptide 1 | <i>TCEB1</i> |
| 19.7 | 19.0 | 18.8 | 18.5 | 19.5 | 19.3 | Transcription elongation factor B polypeptide 2 | <i>TCEB2</i> |
| 21.8 | 21.8 | 21.9 | 21.9 | 21.8 | 21.5 | Transcription elongation factor B polypeptide 3 | <i>TCEB3</i> |
| 19.8 | 19.4 | 19.0 | 20.2 | 20.0 | 19.2 | Transcription elongation factor SPT4 | <i>SUPT4H1</i> |
| 19.6 | 18.4 | 15.0 | 19.1 | 18.9 | 18.2 | Transcription elongation factor SPT5 | <i>SUPT5H</i> |
| 21.7 | 21.6 | 21.6 | 22.5 | 21.3 | 21.5 | Transcription elongation regulator 1 | <i>TCERG1</i> |
| 21.4 | 21.8 | 22.2 | 19.4 | 21.3 | 22.2 | Transcription factor 25 | <i>TCF25</i> |
| 20.9 | 21.1 | 21.2 | 21.1 | 21.1 | 21.1 | Transcription factor A, mitochondrial | <i>TFAM</i> |
| 17.3 | 17.2 | 17.9 | 22.5 | 18.1 | 18.9 | Transcription factor BTF3 | <i>BTF3</i> |
| 21.4 | 20.7 | 20.8 | 22.9 | 21.6 | 21.0 | Transcription factor BTF3 | <i>BTF3</i> |
| 16.5 | 15.0 | 15.0 | 19.7 | 15.0 | 17.2 | Transcription factor BTF3 homolog 4 | <i>BTF3L4</i> |
| 15.0 | 17.9 | 17.9 | 15.0 | 17.7 | 17.8 | Transcription factor E2F7 | <i>E2F7</i> |
| 22.4 | 22.7 | 22.2 | 18.8 | 22.2 | 25.2 | Transcription factor Sp1 | <i>SP1</i> |
| 15.0 | 17.3 | 17.5 | 15.0 | 17.4 | 17.9 | Transcription factor Sp2 | <i>SP2</i> |
| 15.0 | 15.0 | 15.0 | 15.0 | 15.0 | 18.2 | Transcription factor Sp3 | <i>SP3</i> |
| 19.6 | 19.9 | 19.7 | 15.0 | 19.7 | 19.7 | Transcription initiation factor TFIID subunit 10 | <i>TAF10</i> |
| 20.1 | 20.0 | 20.0 | 19.7 | 19.9 | 19.8 | Transcription initiation factor TFIID subunit 4 | <i>TAF4</i> |
| 19.7 | 20.0 | 19.7 | 20.1 | 19.7 | 19.5 | Transcription initiation factor TFIID subunit 8 | <i>TAF8</i> |
| 15.0 | 18.9 | 18.6 | 15.0 | 15.0 | 18.7 | Transcription initiation factor TFIID subunit 9B | <i>TAF9B</i> |
| 24.9 | 24.9 | 24.9 | 24.2 | 24.8 | 25.4 | Transcription intermediary factor 1-beta | <i>TRIM28</i> |
| 18.5 | 18.0 | 18.5 | 15.0 | 18.0 | 18.4 | Transcription termination factor 2 | <i>TTF2</i> |
| 16.4 | 15.0 | 16.3 | 15.0 | 15.0 | 15.9 | Transcriptional activator GLI3 | <i>GLI3</i> |

| | | | | | | | |
|------|------|------|------|------|------|--|----------------|
| 20.7 | 20.4 | 20.6 | 20.5 | 20.7 | 20.6 | Transcriptional activator protein Pur-alpha | <i>PURA</i> |
| 19.6 | 19.6 | 19.7 | 19.1 | 19.6 | 19.4 | Transcriptional activator protein Pur-beta | <i>PURB</i> |
| 15.0 | 18.8 | 18.8 | 18.3 | 18.5 | 18.6 | Transcriptional adapter 2-beta | <i>TADA2B</i> |
| 17.9 | 17.7 | 18.2 | 18.3 | 17.7 | 17.9 | Transcriptional adapter 3 | <i>TADA3</i> |
| 18.0 | 18.3 | 18.5 | 15.0 | 18.5 | 18.6 | Transcriptional regulator Kaiso | <i>ZBTB33</i> |
| 23.4 | 23.2 | 23.4 | 22.6 | 23.3 | 23.3 | Transcriptional repressor CTCF | <i>CTCF</i> |
| 21.0 | 21.1 | 21.1 | 20.9 | 21.2 | 21.0 | Transcriptional repressor NF-X1 | <i>NFX1</i> |
| 20.7 | 20.8 | 20.9 | 22.5 | 20.7 | 20.6 | Transcriptional repressor p66-alpha | <i>GATAD2A</i> |
| 15.0 | 19.9 | 19.8 | 20.3 | 20.0 | 19.8 | Transcriptional repressor p66-beta | <i>GATAD2B</i> |
| 21.9 | 22.0 | 22.3 | 22.7 | 22.2 | 22.0 | Transcriptional repressor protein YY1 | <i>YY1</i> |
| 21.2 | 21.6 | 21.6 | 21.0 | 21.7 | 21.4 | Transducin beta-like protein 2 | <i>TBL2</i> |
| 20.3 | 20.2 | 19.7 | 19.5 | 20.4 | 20.0 | Transducin beta-like protein 3 | <i>TBL3</i> |
| 19.3 | 19.5 | 19.4 | 19.8 | 19.3 | 19.2 | Transformation/transcription domain-associated protein | <i>TRRAP</i> |
| 21.9 | 21.5 | 21.6 | 21.5 | 22.1 | 21.6 | Transformer-2 protein homolog alpha | <i>TRA2A</i> |
| 20.5 | 20.2 | 20.4 | 20.7 | 20.9 | 20.0 | Transformer-2 protein homolog beta | <i>TRA2B</i> |
| 21.2 | 21.1 | 20.9 | 22.6 | 20.6 | 20.9 | Transitional endoplasmic reticulum ATPase | <i>VCP</i> |
| 18.8 | 18.6 | 19.4 | 20.2 | 18.9 | 19.0 | Transketolase | <i>TKT</i> |
| 15.0 | 17.8 | 17.9 | 15.0 | 15.0 | 15.0 | Translation initiation factor eIF-2B subunit gamma | <i>EIF2B3</i> |
| 19.2 | 18.8 | 18.7 | 15.0 | 19.2 | 18.4 | Translation initiation factor IF-3, mitochondrial | <i>MTIF3</i> |
| 22.4 | 22.2 | 22.4 | 23.4 | 22.3 | 22.1 | Translation machinery-associated protein 16 | <i>TMA16</i> |
| 20.7 | 21.0 | 22.4 | 24.9 | 20.8 | 20.9 | Translation machinery-associated protein 7 | <i>TMA7</i> |
| 20.6 | 21.1 | 21.4 | 21.0 | 20.7 | 21.2 | Translational activator GCN1 | <i>GCN1L1</i> |
| 19.4 | 19.5 | 19.8 | 19.9 | 19.1 | 19.4 | Translocation protein SEC62 | <i>SEC62</i> |
| 20.2 | 20.5 | 20.6 | 20.0 | 20.2 | 20.8 | Translocon-associated protein subunit delta | <i>SSR4</i> |
| 17.8 | 18.1 | 18.0 | 17.6 | 18.0 | 18.1 | Transmembrane and TPR repeat-containing protein 3 | <i>TMTC3</i> |
| 18.6 | 18.8 | 19.1 | 15.0 | 18.9 | 19.1 | Transmembrane protein 263 | <i>TMEM263</i> |
| 23.6 | 23.7 | 23.5 | 23.9 | 23.7 | 23.5 | Treacle protein | <i>TCOF1</i> |
| 17.9 | 17.9 | 18.0 | 17.8 | 17.7 | 17.7 | Treslin | <i>TICRR</i> |
| 32.6 | 32.3 | 32.0 | 15.0 | 32.9 | 32.1 | Tribbles homolog 3 | <i>TRIB3</i> |
| 22.6 | 22.6 | 22.4 | 21.9 | 22.6 | 22.5 | Trifunctional enzyme subunit alpha, mitochondrial | <i>HADHA</i> |
| 22.8 | 22.5 | 22.0 | 21.5 | 22.6 | 22.4 | Trifunctional enzyme subunit beta, mitochondrial | <i>HADHB</i> |
| 20.0 | 19.7 | 20.1 | 22.7 | 20.0 | 20.1 | Trifunctional purine biosynthetic protein adenosine-3 | <i>GART</i> |
| 19.7 | 18.4 | 20.5 | 23.3 | 18.6 | 20.3 | Triosephosphate isomerase | <i>TPI1</i> |
| 19.4 | 19.6 | 19.4 | 18.5 | 19.5 | 19.4 | Tripartite motif-containing protein 26 | <i>TRIM26</i> |
| 19.4 | 19.6 | 19.1 | 19.9 | 19.5 | 19.2 | Tripartite motif-containing protein 65 | <i>TRIM65</i> |
| 21.6 | 21.7 | 21.8 | 15.0 | 21.7 | 21.3 | TRMT1-like protein | <i>TRMT1L</i> |
| 24.3 | 24.5 | 24.3 | 24.3 | 24.4 | 24.2 | tRNA-splicing ligase RtcB homolog | <i>RTCB</i> |
| 15.0 | 15.0 | 15.0 | 19.7 | 15.0 | 15.0 | Tryptophan--tRNA ligase, cytoplasmic | <i>WARS</i> |
| 18.5 | 18.4 | 18.4 | 15.0 | 18.0 | 18.8 | Tuberin | <i>TSC2</i> |
| 21.7 | 22.7 | 22.4 | 21.9 | 22.3 | 23.1 | Tubulin alpha-1A chain | <i>TUBA1A</i> |
| 27.4 | 28.0 | 28.0 | 27.6 | 27.4 | 28.5 | Tubulin alpha-1B chain | <i>TUBA1B</i> |
| 22.5 | 22.9 | 22.5 | 21.0 | 22.3 | 23.3 | Tubulin alpha-1C chain | <i>TUBA1C</i> |
| 25.7 | 26.3 | 26.2 | 25.7 | 25.6 | 26.8 | Tubulin beta chain | <i>TUBB</i> |
| 20.8 | 21.3 | 21.3 | 21.6 | 21.0 | 21.8 | Tubulin beta-2A chain | <i>TUBB2A</i> |
| 22.3 | 22.8 | 23.0 | 22.5 | 22.3 | 23.3 | Tubulin beta-2B chain | <i>TUBB2B</i> |
| 19.8 | 21.8 | 21.8 | 21.7 | 21.3 | 22.2 | Tubulin beta-4A chain | <i>TUBB4A</i> |

| | | | | | | | |
|------|------|------|------|------|------|---|------------------|
| 27.7 | 28.4 | 28.2 | 27.9 | 27.7 | 28.8 | Tubulin beta-4B chain | <i>TUBB4B</i> |
| 21.9 | 22.5 | 22.5 | 22.3 | 21.6 | 22.9 | Tubulin beta-6 chain | <i>TUBB6</i> |
| 23.8 | 24.9 | 24.7 | 22.6 | 24.2 | 25.6 | Tubulin beta-8 chain | <i>TUBB8</i> |
| 19.9 | 19.6 | 19.6 | 19.2 | 19.6 | 19.9 | Tubulin gamma-1 chain | <i>TUBG1</i> |
| 19.5 | 15.0 | 19.8 | 22.3 | 19.9 | 19.1 | Tubulin-specific chaperone A | <i>TBCA</i> |
| 19.0 | 19.5 | 19.5 | 15.0 | 18.7 | 20.4 | Tumor suppressor candidate 2 | <i>TUSC2</i> |
| 19.4 | 15.0 | 19.5 | 20.6 | 15.0 | 20.0 | Tyrosine--tRNA ligase, cytoplasmic | <i>YARS</i> |
| 18.8 | 15.0 | 18.8 | 15.0 | 15.0 | 19.3 | Tyrosine-protein phosphatase non-receptor type 13 | <i>PTPN13</i> |
| 21.7 | 21.3 | 21.7 | 22.5 | 21.6 | 21.4 | U1 small nuclear ribonucleoprotein 70 kDa | <i>SNRNP70</i> |
| 20.8 | 20.4 | 20.2 | 20.8 | 20.5 | 20.0 | U1 small nuclear ribonucleoprotein A | <i>SNRPA</i> |
| 23.8 | 23.9 | 24.3 | 26.4 | 24.0 | 23.8 | U2 small nuclear ribonucleoprotein A | <i>SNRPA1</i> |
| 21.3 | 21.1 | 20.8 | 20.5 | 21.5 | 20.9 | U2 small nuclear ribonucleoprotein B | <i>SNRPB2</i> |
| 20.4 | 20.9 | 20.7 | 21.9 | 20.9 | 20.3 | U2 snRNP-associated SURP motif-containing protein | <i>U2SURP</i> |
| 19.1 | 19.1 | 19.0 | 18.5 | 19.3 | 19.1 | U3 small nucleolar ribonucleoprotein protein IMP3 | <i>IMP3</i> |
| 19.4 | 19.6 | 18.6 | 15.0 | 19.2 | 15.0 | U3 small nucleolar ribonucleoprotein protein MPP10 | <i>MPHOSPH10</i> |
| 20.2 | 20.1 | 19.8 | 20.0 | 20.3 | 19.7 | U3 small nucleolar RNA-associated protein 14 homolog A | <i>UTP14A</i> |
| 18.6 | 19.0 | 18.8 | 15.0 | 19.6 | 19.0 | U3 small nucleolar RNA-associated protein 15 homolog | <i>UTP15</i> |
| 20.1 | 20.5 | 20.4 | 20.3 | 20.8 | 20.5 | U3 small nucleolar RNA-associated protein 18 homolog | <i>UTP18</i> |
| 23.0 | 22.9 | 22.8 | 22.4 | 22.8 | 22.5 | U4/U6 small nuclear ribonucleoprotein Prp3 | <i>PRPF3</i> |
| 20.8 | 20.2 | 19.8 | 20.4 | 20.2 | 19.7 | U4/U6 small nuclear ribonucleoprotein Prp31 | <i>PRPF31</i> |
| 22.3 | 22.0 | 21.9 | 22.0 | 22.0 | 21.9 | U4/U6 small nuclear ribonucleoprotein Prp4 | <i>PRPF4</i> |
| 20.7 | 20.2 | 20.4 | 21.0 | 20.7 | 15.0 | U4/U6.U5 small nuclear ribonucleoprotein 27 kDa protein | <i>SNRNP27</i> |
| 22.0 | 21.8 | 21.6 | 21.8 | 21.9 | 21.6 | U4/U6.U5 tri-snRNP-associated protein 1 | <i>SART1</i> |
| 20.2 | 20.2 | 20.2 | 20.6 | 20.2 | 20.1 | U4/U6.U5 tri-snRNP-associated protein 2 | <i>USP39</i> |
| 22.4 | 22.1 | 22.1 | 21.2 | 22.5 | 22.0 | U5 small nuclear ribonucleoprotein 200 kDa helicase | <i>SNRNP200</i> |
| 21.9 | 22.0 | 22.0 | 22.6 | 22.2 | 21.8 | U5 small nuclear ribonucleoprotein 40 kDa protein | <i>SNRNP40</i> |
| 21.4 | 21.4 | 21.4 | 19.4 | 21.2 | 21.1 | U6 snRNA-associated Sm-like protein LSm1 | <i>LSM1</i> |
| 20.6 | 20.6 | 20.1 | 20.1 | 20.7 | 19.9 | U6 snRNA-associated Sm-like protein LSm2 | <i>LSM2</i> |
| 20.7 | 20.6 | 20.3 | 19.9 | 21.4 | 20.4 | U6 snRNA-associated Sm-like protein LSm3 | <i>LSM3</i> |
| 19.4 | 20.0 | 19.9 | 19.4 | 20.6 | 19.6 | U6 snRNA-associated Sm-like protein LSm4 | <i>LSM4</i> |
| 21.5 | 21.5 | 21.5 | 21.0 | 21.7 | 21.8 | Ubiquitin carboxyl-terminal hydrolase 10 | <i>USP10</i> |
| 19.1 | 20.2 | 18.5 | 15.0 | 18.9 | 18.9 | Ubiquitin carboxyl-terminal hydrolase 34 | <i>USP34</i> |
| 19.1 | 19.6 | 19.3 | 19.0 | 19.1 | 19.8 | Ubiquitin carboxyl-terminal hydrolase isozyme L5 | <i>UCHL5</i> |
| 26.3 | 26.0 | 26.2 | 26.0 | 25.9 | 25.7 | Ubiquitin-40S ribosomal protein S27a | <i>RPS27A</i> |
| 23.1 | 23.3 | 23.1 | 23.5 | 23.3 | 23.1 | Ubiquitin-60S ribosomal protein L40 | <i>UBA52</i> |
| 19.6 | 19.4 | 19.5 | 15.0 | 19.2 | 19.4 | Ubiquitin-associated protein 2 | <i>UBAP2</i> |
| 21.7 | 21.6 | 21.9 | 22.2 | 21.8 | 21.9 | Ubiquitin-associated protein 2-like | <i>UBAP2L</i> |
| 19.6 | 18.3 | 19.9 | 21.7 | 18.9 | 19.1 | Ubiquitin-like modifier-activating enzyme 1 | <i>UBA1</i> |
| 15.0 | 18.9 | 18.6 | 15.0 | 18.8 | 19.1 | Uncharacterized protein C15orf39 | <i>C15orf39</i> |
| 17.5 | 18.2 | 17.9 | 19.6 | 17.2 | 17.0 | Uncharacterized protein C19orf43 | <i>C19orf43</i> |
| 18.8 | 19.2 | 19.0 | 18.7 | 19.1 | 19.3 | Uncharacterized protein C7orf50 | <i>C7orf50</i> |
| 15.0 | 18.4 | 17.8 | 15.0 | 15.0 | 18.0 | Uncharacterized protein KIAA0232 | <i>KIAA0232</i> |
| 15.0 | 15.0 | 15.0 | 15.0 | 15.0 | 15.0 | Uncharacterized protein KIAA1143 | <i>KIAA1143</i> |
| 15.0 | 15.0 | 19.8 | 15.0 | 15.0 | 19.7 | Uncharacterized protein KIAA1522 | <i>KIAA1522</i> |

| | | | | | | | |
|------|------|------|------|------|------|--|------------------|
| 20.2 | 20.5 | 20.6 | 19.2 | 20.5 | 21.4 | Uncharacterized protein KIAA1671 | <i>KIAA1671</i> |
| 18.5 | 18.9 | 19.0 | 15.0 | 18.4 | 18.8 | Unconventional myosin-IXb | <i>MYO9B</i> |
| 19.6 | 19.7 | 19.7 | 15.0 | 19.2 | 19.4 | Unconventional prefoldin RPB5 interactor 1 | <i>URI1</i> |
| 18.6 | 18.1 | 18.4 | 19.8 | 18.6 | 19.4 | UPF0428 protein CXorf56 | <i>CXorf56</i> |
| 22.9 | 22.4 | 22.5 | 22.2 | 22.7 | 22.5 | UPF0488 protein C8orf33 | <i>C8orf33</i> |
| 15.0 | 19.2 | 19.1 | 15.0 | 19.2 | 19.3 | UPF0568 protein C14orf166 | <i>C14orf166</i> |
| 19.6 | 19.4 | 19.4 | 15.0 | 19.6 | 19.1 | UPF0711 protein C18orf21 | <i>C18orf21</i> |
| 15.0 | 17.2 | 17.1 | 15.0 | 17.2 | 17.3 | Upstream stimulatory factor 1 | <i>USF1</i> |
| 19.2 | 18.8 | 18.8 | 20.2 | 19.2 | 19.0 | Vacuolar protein sorting-associated protein 28 homolog | <i>VPS28</i> |
| 15.0 | 15.0 | 18.4 | 15.0 | 15.0 | 18.6 | Vacuolar protein sorting-associated protein 4A | <i>VPS4A</i> |
| 20.0 | 19.9 | 20.0 | 20.8 | 19.6 | 20.1 | Vascular endothelial zinc finger 1 | <i>VEZF1</i> |
| 15.0 | 19.1 | 19.2 | 15.0 | 18.6 | 19.1 | Very-long-chain 3-oxoacyl-CoA reductase | <i>HSD17B12</i> |
| 22.5 | 22.6 | 23.1 | 22.1 | 22.4 | 23.0 | Very-long-chain enoyl-CoA reductase | <i>TECR</i> |
| 18.8 | 19.1 | 19.1 | 18.9 | 18.7 | 19.0 | Vesicle-associated membrane protein-associated protein A | <i>VAPA</i> |
| 20.0 | 20.2 | 20.3 | 20.5 | 19.9 | 20.2 | Vesicle-associated membrane protein-associated protein B/C | <i>VAPB</i> |
| 19.5 | 19.8 | 19.9 | 19.7 | 19.7 | 20.1 | Vesicle-trafficking protein SEC22b | <i>SEC22B</i> |
| 24.1 | 24.2 | 24.0 | 22.9 | 23.9 | 23.9 | Vigilin | <i>HDLBP</i> |
| 22.9 | 22.7 | 23.1 | 24.2 | 22.8 | 23.9 | Vimentin | <i>VIM</i> |
| 20.5 | 20.2 | 20.7 | 20.6 | 20.2 | 20.2 | Voltage-dependent anion-selective channel protein 2 | <i>VDAC2</i> |
| 23.7 | 23.7 | 23.2 | 18.5 | 23.6 | 23.9 | WD repeat and coiled-coil-containing protein C2orf44 | <i>C2orf44</i> |
| 19.6 | 19.7 | 19.8 | 20.1 | 19.9 | 19.5 | WD repeat-containing protein 18 | <i>WDR18</i> |
| 15.0 | 15.0 | 17.9 | 15.0 | 18.3 | 18.2 | WD repeat-containing protein 26 | <i>WDR26</i> |
| 20.7 | 20.7 | 20.4 | 19.6 | 20.8 | 20.3 | WD repeat-containing protein 3 | <i>WDR3</i> |
| 21.1 | 20.9 | 20.7 | 19.9 | 21.2 | 20.8 | WD repeat-containing protein 36 | <i>WDR36</i> |
| 19.6 | 19.5 | 19.2 | 15.0 | 19.4 | 19.3 | WD repeat-containing protein 43 | <i>WDR43</i> |
| 17.9 | 15.0 | 17.8 | 15.0 | 17.8 | 18.0 | WD repeat-containing protein 48 | <i>WDR48</i> |
| 23.6 | 23.5 | 23.4 | 21.0 | 23.8 | 23.4 | WD repeat-containing protein 5 | <i>WDR5</i> |
| 18.8 | 18.3 | 18.3 | 18.9 | 18.9 | 18.9 | WD repeat-containing protein 55 | <i>WDR55</i> |
| 18.4 | 18.2 | 18.2 | 15.0 | 15.0 | 18.8 | WD repeat-containing protein 59 | <i>WDR59</i> |
| 20.5 | 20.6 | 20.6 | 19.3 | 20.4 | 20.9 | WD repeat-containing protein 6 | <i>WDR6</i> |
| 19.4 | 19.3 | 19.7 | 19.2 | 19.2 | 19.2 | WD repeat-containing protein 92 | <i>WDR92</i> |
| 18.3 | 18.5 | 18.4 | 18.7 | 18.5 | 18.5 | WD repeat-containing protein mio | <i>MIOS</i> |
| 21.3 | 21.3 | 21.0 | 21.0 | 21.1 | 21.1 | WD40 repeat-containing protein SMU1 | <i>SMU1</i> |
| 18.4 | 18.4 | 18.1 | 15.0 | 18.5 | 18.1 | Williams-Beuren syndrome chromosomal region 16 protein | <i>WBSCR16</i> |
| 21.9 | 21.9 | 20.9 | 20.8 | 21.5 | 21.9 | Wings apart-like protein homolog | <i>WAPAL</i> |
| 25.3 | 25.3 | 25.3 | 24.0 | 25.5 | 25.3 | X-ray repair cross-complementing protein 5 | <i>XRCC5</i> |
| 26.7 | 26.7 | 26.7 | 25.6 | 26.7 | 26.6 | X-ray repair cross-complementing protein 6 | <i>XRCC6</i> |
| 22.6 | 22.5 | 22.4 | 21.4 | 22.6 | 22.5 | Y-box-binding protein 3 | <i>YBX3</i> |
| 20.1 | 19.9 | 20.0 | 19.9 | 19.8 | 20.0 | YEATS domain-containing protein 2 | <i>YEATS2</i> |
| 21.5 | 21.3 | 21.5 | 22.0 | 21.5 | 21.2 | YLP motif-containing protein 1 | <i>YLPM1</i> |
| 19.3 | 19.7 | 19.5 | 15.0 | 19.4 | 19.4 | YTH domain-containing family protein 1 | <i>YTHDF1</i> |
| 20.6 | 20.6 | 20.7 | 15.0 | 20.2 | 20.6 | YTH domain-containing family protein 2 | <i>YTHDF2</i> |
| 18.0 | 18.0 | 18.2 | 19.3 | 18.6 | 17.9 | YTH domain-containing protein 1 | <i>YTHDC1</i> |
| 19.1 | 19.1 | 19.1 | 15.0 | 19.2 | 19.3 | Zinc finger and BTB domain-containing protein 1 | <i>ZBTB1</i> |
| 19.6 | 19.1 | 18.3 | 15.0 | 19.5 | 19.3 | Zinc finger and BTB domain-containing protein 10 | <i>ZBTB10</i> |

| | | | | | | | |
|------|------|------|------|------|------|--|----------|
| 19.3 | 19.5 | 19.6 | 15.0 | 19.1 | 19.3 | Zinc finger and BTB domain-containing protein 11 | ZBTB11 |
| 21.1 | 20.6 | 20.7 | 20.0 | 20.7 | 20.9 | Zinc finger and BTB domain-containing protein 21 | ZBTB21 |
| 18.3 | 19.0 | 19.1 | 15.0 | 18.6 | 18.5 | Zinc finger and BTB domain-containing protein 24 | ZBTB24 |
| 20.0 | 20.1 | 20.5 | 15.0 | 20.1 | 20.8 | Zinc finger and BTB domain-containing protein 34 | ZBTB34 |
| 18.8 | 17.4 | 17.7 | 15.0 | 18.5 | 18.0 | Zinc finger and BTB domain-containing protein 43 | ZBTB43 |
| 15.0 | 15.0 | 15.0 | 15.0 | 15.0 | 20.3 | Zinc finger and BTB domain-containing protein 46 | ZBTB46 |
| 19.5 | 18.9 | 18.2 | 15.0 | 17.9 | 22.3 | Zinc finger and BTB domain-containing protein 5 | ZBTB5 |
| 15.0 | 17.2 | 17.4 | 15.0 | 17.2 | 17.3 | Zinc finger and BTB domain-containing protein 7A | ZBTB7A |
| 17.6 | 17.6 | 18.0 | 15.0 | 17.5 | 17.7 | Zinc finger and SCAN domain-containing protein 21 | ZSCAN21 |
| 15.0 | 15.0 | 15.0 | 15.0 | 15.0 | 18.0 | Zinc finger and SCAN domain-containing protein 26 | ZSCAN26 |
| 18.9 | 18.7 | 18.8 | 15.0 | 18.9 | 18.6 | Zinc finger C2HC domain-containing protein 1A | ZC2HC1A |
| 19.3 | 19.4 | 19.2 | 19.1 | 19.2 | 19.2 | Zinc finger C3H1 domain-containing protein | ZFC3H1 |
| 20.9 | 20.8 | 20.5 | 18.6 | 20.9 | 20.5 | Zinc finger C4H2 domain-containing protein | ZC4H2 |
| 21.9 | 21.7 | 21.8 | 21.9 | 22.1 | 21.5 | Zinc finger CCCH domain-containing protein 11A | ZC3H11A |
| 21.9 | 22.1 | 21.9 | 25.3 | 21.4 | 22.2 | Zinc finger CCCH domain-containing protein 13 | ZC3H13 |
| 19.4 | 19.4 | 19.4 | 19.5 | 19.8 | 19.3 | Zinc finger CCCH domain-containing protein 14 | ZC3H14 |
| 21.6 | 21.5 | 21.7 | 21.7 | 21.3 | 21.3 | Zinc finger CCCH domain-containing protein 15 | ZC3H15 |
| 18.8 | 18.9 | 19.0 | 19.7 | 19.1 | 18.8 | Zinc finger CCCH domain-containing protein 18 | ZC3H18 |
| 22.9 | 22.7 | 22.4 | 20.8 | 23.4 | 22.4 | Zinc finger CCCH domain-containing protein 4 | ZC3H4 |
| 18.3 | 17.7 | 17.3 | 15.0 | 18.0 | 17.5 | Zinc finger CCCH domain-containing protein 7B | ZC3H7B |
| 23.6 | 23.7 | 23.6 | 23.6 | 23.7 | 23.6 | Zinc finger CCCH-type antiviral protein 1 | ZC3HAV1 |
| 18.2 | 18.6 | 18.4 | 21.3 | 18.5 | 18.2 | Zinc finger CCCH-type antiviral protein 1-like | ZC3HAV1L |
| 15.0 | 17.9 | 18.2 | 15.0 | 18.2 | 18.1 | Zinc finger CCCH-type with G patch domain-containing protein | ZGPAT |
| 19.3 | 19.3 | 19.7 | 15.0 | 19.4 | 19.3 | Zinc finger CCHC domain-containing protein 3 | ZCCHC3 |
| 20.1 | 19.9 | 19.7 | 15.0 | 19.9 | 19.5 | Zinc finger CCHC domain-containing protein 8 | ZCCHC8 |
| 20.4 | 20.5 | 20.0 | 18.6 | 20.9 | 19.8 | Zinc finger CCHC domain-containing protein 9 | ZCCHC9 |
| 19.7 | 19.7 | 19.5 | 15.0 | 19.6 | 19.3 | Zinc finger CCHC-type and RNA-binding motif-containing protein 1 | ZCRB1 |
| 17.2 | 17.0 | 17.0 | 17.0 | 16.6 | 16.9 | Zinc finger E-box-binding homeobox 2 | ZEB2 |
| 17.1 | 17.2 | 17.8 | 19.7 | 17.7 | 17.0 | Zinc finger matrin-type protein 2 | ZMAT2 |
| 18.3 | 18.6 | 18.6 | 15.0 | 18.3 | 18.8 | Zinc finger MYM-type protein 2 | ZMYM2 |
| 20.2 | 20.6 | 20.9 | 19.7 | 20.3 | 20.8 | Zinc finger MYM-type protein 3 | ZMYM3 |
| 19.6 | 20.2 | 20.2 | 20.7 | 19.8 | 20.1 | Zinc finger MYM-type protein 4 | ZMYM4 |
| 19.4 | 19.4 | 19.6 | 19.7 | 19.2 | 19.2 | Zinc finger protein 121 | ZNF121 |
| 17.2 | 16.9 | 17.2 | 15.0 | 16.9 | 17.0 | Zinc finger protein 143 | ZNF143 |
| 18.2 | 17.9 | 18.0 | 17.8 | 18.1 | 18.4 | Zinc finger protein 184 | ZNF184 |
| 16.7 | 17.1 | 16.9 | 15.0 | 16.9 | 17.5 | Zinc finger protein 195 | ZNF195 |
| 17.7 | 17.7 | 17.7 | 15.0 | 17.5 | 18.7 | Zinc finger protein 213 | ZNF213 |
| 19.7 | 19.9 | 19.9 | 19.6 | 19.6 | 19.6 | Zinc finger protein 22 | ZNF22 |
| 25.4 | 24.9 | 25.1 | 22.7 | 25.1 | 26.9 | Zinc finger protein 24 | ZNF24 |
| 15.0 | 15.0 | 18.5 | 15.0 | 15.0 | 18.3 | Zinc finger protein 28 homolog | ZFP28 |
| 21.4 | 21.6 | 21.5 | 19.9 | 21.1 | 22.3 | Zinc finger protein 281 | ZNF281 |
| 18.5 | 18.5 | 18.4 | 15.0 | 18.4 | 20.6 | Zinc finger protein 282 | ZNF282 |

| | | | | | | | |
|------|------|------|------|------|------|---|---------|
| 15.0 | 16.8 | 16.8 | 15.0 | 16.3 | 16.7 | Zinc finger protein 3 | ZNF3 |
| 22.3 | 22.7 | 22.4 | 19.3 | 22.0 | 23.0 | Zinc finger protein 318 | ZNF318 |
| 21.1 | 21.4 | 21.4 | 21.1 | 21.3 | 21.1 | Zinc finger protein 346 | ZNF346 |
| 18.7 | 19.3 | 18.7 | 18.6 | 18.5 | 19.7 | Zinc finger protein 391 | ZNF391 |
| 15.0 | 15.0 | 16.9 | 15.0 | 15.0 | 17.3 | Zinc finger protein 420 | ZNF420 |
| 18.5 | 18.0 | 18.2 | 20.1 | 18.4 | 17.9 | Zinc finger protein 428 | ZNF428 |
| 16.0 | 16.3 | 16.6 | 15.0 | 15.6 | 21.0 | Zinc finger protein 436 | ZNF436 |
| 18.9 | 15.0 | 18.9 | 15.0 | 19.0 | 20.2 | Zinc finger protein 444 | ZNF444 |
| 19.8 | 19.6 | 19.8 | 19.2 | 19.4 | 20.9 | Zinc finger protein 460 | ZNF460 |
| 15.0 | 17.5 | 18.0 | 17.7 | 17.4 | 17.8 | Zinc finger protein 461 | ZNF461 |
| 20.3 | 20.4 | 20.2 | 19.8 | 20.3 | 20.0 | Zinc finger protein 48 | ZNF48 |
| 15.0 | 17.9 | 18.1 | 15.0 | 17.2 | 18.6 | Zinc finger protein 507 | ZNF507 |
| 20.8 | 20.7 | 20.9 | 20.5 | 21.0 | 20.6 | Zinc finger protein 512 | ZNF512 |
| 20.3 | 20.1 | 20.0 | 19.6 | 19.8 | 19.9 | Zinc finger protein 574 | ZNF574 |
| 15.0 | 18.0 | 18.4 | 15.0 | 15.0 | 18.6 | Zinc finger protein 589 | ZNF589 |
| 15.0 | 19.0 | 18.8 | 15.0 | 19.2 | 18.7 | Zinc finger protein 593 | ZNF593 |
| 22.1 | 22.0 | 22.4 | 20.8 | 21.9 | 21.9 | Zinc finger protein 598 | ZNF598 |
| 19.3 | 19.3 | 19.5 | 19.2 | 18.9 | 19.5 | Zinc finger protein 62 homolog | ZFP62 |
| 16.7 | 16.9 | 16.8 | 15.0 | 15.0 | 17.5 | Zinc finger protein 627 | ZNF627 |
| 21.6 | 21.5 | 21.6 | 19.8 | 21.6 | 21.4 | Zinc finger protein 629 | ZNF629 |
| 22.8 | 22.8 | 22.9 | 22.4 | 22.9 | 22.8 | Zinc finger protein 638 | ZNF638 |
| 19.2 | 19.2 | 19.0 | 19.0 | 19.0 | 18.8 | Zinc finger protein 64 homolog, isoforms 1 and 2 | ZFP64 |
| 19.6 | 19.4 | 19.5 | 15.0 | 19.3 | 19.3 | Zinc finger protein 64 homolog, isoforms 3 and 4 | ZFP64 |
| 19.1 | 19.1 | 19.1 | 15.0 | 19.0 | 19.3 | Zinc finger protein 644 | ZNF644 |
| 18.7 | 18.8 | 18.9 | 15.0 | 18.6 | 18.8 | Zinc finger protein 655 | ZNF655 |
| 19.1 | 20.0 | 19.8 | 19.7 | 19.7 | 20.2 | Zinc finger protein 664 | ZNF664 |
| 19.1 | 18.7 | 19.0 | 15.0 | 18.5 | 18.6 | Zinc finger protein 668 | ZNF668 |
| 16.9 | 16.2 | 16.5 | 15.0 | 16.2 | 18.3 | Zinc finger protein 670 | ZNF670 |
| 17.8 | 17.7 | 17.7 | 15.0 | 17.5 | 18.1 | Zinc finger protein 687 | ZNF687 |
| 18.1 | 18.3 | 18.0 | 15.0 | 18.3 | 17.7 | Zinc finger protein 689 | ZNF689 |
| 21.5 | 21.8 | 21.8 | 22.7 | 21.4 | 21.5 | Zinc finger protein 706 | ZNF706 |
| 17.8 | 18.0 | 17.9 | 17.2 | 18.3 | 17.7 | Zinc finger protein 740 | ZNF740 |
| 18.2 | 18.3 | 18.4 | 15.0 | 17.9 | 18.4 | Zinc finger protein 746 | ZNF746 |
| 23.0 | 22.9 | 22.7 | 21.8 | 23.1 | 22.6 | Zinc finger protein 768 | ZNF768 |
| 18.0 | 17.7 | 17.7 | 15.0 | 18.1 | 17.7 | Zinc finger protein 770 | ZNF770 |
| 19.0 | 19.6 | 19.5 | 19.4 | 19.5 | 19.2 | Zinc finger protein 771 | ZNF771 |
| 22.2 | 22.2 | 21.9 | 20.4 | 22.1 | 21.7 | Zinc finger protein 787 | ZNF787 |
| 17.6 | 18.0 | 18.1 | 18.3 | 17.8 | 18.6 | Zinc finger protein 845 | ZNF845 |
| 19.6 | 20.0 | 20.2 | 19.8 | 19.6 | 20.0 | Zinc finger protein OZF | ZNF146 |
| 19.6 | 19.7 | 19.3 | 19.2 | 20.1 | 19.3 | Zinc finger protein ubi-d4 | DPF2 |
| 19.4 | 19.8 | 19.6 | 19.7 | 19.0 | 19.9 | Zinc finger protein with KRAB and SCAN domains 1 | ZKSCAN1 |
| 20.7 | 20.5 | 20.1 | 15.0 | 20.3 | 20.8 | Zinc finger protein with KRAB and SCAN domains 4 | ZKSCAN4 |
| 16.8 | 16.3 | 17.0 | 15.0 | 15.4 | 16.5 | Zinc finger protein with KRAB and SCAN domains 7 | ZKSCAN7 |
| 21.5 | 21.6 | 21.2 | 19.0 | 21.1 | 22.7 | Zinc finger protein with KRAB and SCAN domains 8 | ZKSCAN8 |
| 18.1 | 18.2 | 18.2 | 15.0 | 15.0 | 18.5 | Zinc finger protein ZXDC | ZXDC |
| 21.9 | 21.4 | 21.5 | 24.0 | 22.0 | 21.5 | Zinc finger Ran-binding domain-containing protein 2 | ZRANB2 |
| 23.1 | 22.8 | 22.9 | 20.6 | 22.9 | 22.7 | Zinc finger RNA-binding protein | ZFR |

| | | | | | | | |
|------|------|------|------|------|------|---|-----------------|
| 15.0 | 28.4 | 27.3 | 28.2 | 22.5 | 22.3 | Mitochondrial import inner membrane translocase subunit Tim17-B | <i>TIMM17B</i> |
| 15.0 | 19.1 | 22.8 | 22.8 | 19.0 | 21.9 | Heat shock cognate 71 kDa protein | <i>HSPA8</i> |
| 16.5 | 17.2 | 18.9 | 23.9 | 18.8 | 18.9 | Heterogeneous nuclear ribonucleoprotein D0 | <i>HNRNPD</i> |
| 22.6 | 22.9 | 22.2 | 23.2 | 17.1 | 18.7 | Host cell factor 1 | <i>HCFC1</i> |
| 18.3 | 18.6 | 17.1 | 20.8 | 18.9 | 18.1 | Protein SON | <i>SON</i> |
| 19.2 | 19.5 | 22.9 | 24.0 | 25.3 | 22.0 | Serine/threonine-protein phosphatase 6 regulatory subunit 2 | <i>PPP6R2</i> |
| 21.3 | 21.5 | 21.8 | 16.9 | 21.7 | 21.9 | ATPase family AAA domain-containing protein 3A (Fragment) | <i>ATAD3A</i> |
| 20.9 | 21.1 | 18.4 | 21.6 | 23.9 | 16.7 | Chromosome 11 open reading frame 48, isoform CRA_c | <i>C11orf98</i> |
| 24.8 | 24.9 | 23.6 | 15.0 | 22.8 | 23.8 | Protein transport protein sec16 | <i>SEC16A</i> |
| 15.0 | 15.0 | 20.9 | 15.0 | 21.6 | 25.0 | 60S ribosomal protein L10 | <i>RPL10</i> |
| 15.0 | 15.0 | 15.0 | 15.0 | 19.4 | 19.4 | La-related protein 1B | <i>LARP1B</i> |
| 21.6 | 21.6 | 20.4 | 24.7 | 20.6 | 22.6 | Protein Wiz | <i>WIZ</i> |
| 23.6 | 23.5 | 19.2 | 20.7 | 21.0 | 20.5 | CLIP-associating protein 1 | <i>CLASP1</i> |
| 21.4 | 21.3 | 22.0 | 21.6 | 23.4 | 20.8 | Synaptic functional regulator FMR1 | <i>FMR1</i> |
| 21.0 | 20.9 | 20.8 | 20.0 | 22.8 | 22.6 | Periphilin-1 | <i>PPHLN1</i> |
| 19.2 | 19.1 | 23.0 | 15.0 | 21.7 | 20.8 | Tribbles homolog 3 (Fragment) | <i>TRIB3</i> |
| 20.6 | 20.5 | 22.5 | 21.8 | 15.0 | 20.2 | Protein POLR1D, isoform 2 | <i>POLR1D</i> |
| 20.4 | 20.3 | 21.1 | 20.1 | 15.0 | 21.2 | Heterogeneous nuclear ribonucleoprotein K (Fragment) | <i>HNRNPK</i> |
| 20.3 | 20.1 | 24.5 | 20.3 | 20.3 | 20.1 | Splicing factor 1 (Fragment) | <i>SF1</i> |
| 22.7 | 22.5 | 20.1 | 23.2 | 20.9 | 21.9 | MYC-associated zinc finger protein (Purine-binding transcription factor), isoform CRA_e | <i>MAZ</i> |
| 22.2 | 21.9 | 20.1 | 15.0 | 24.7 | 18.9 | Ribonucleoprotein PTB-binding 1 | <i>RAVER1</i> |
| 24.7 | 24.4 | 20.3 | 15.0 | 22.0 | 20.0 | Heterogeneous nuclear ribonucleoproteins C1/C2 | <i>HNRNPC</i> |
| 23.2 | 22.8 | 16.9 | 15.0 | 20.2 | 17.8 | Bcl-2-associated transcription factor 1 | <i>BCLAF1</i> |
| 20.3 | 19.4 | 18.7 | 15.0 | 18.7 | 22.7 | Tropomyosin alpha-3 chain | <i>TPM3</i> |
| 17.3 | 15.0 | 24.2 | 15.0 | 19.8 | 24.1 | PC4 and SFRS1-interacting protein (Fragment) | <i>PSIP1</i> |

Bibliography

- Adam, F., Guillin, M. C. & Jandrot-Perrus, M. (2003) Glycoprotein Ib-mediated platelet activation - A signalling pathway triggered by thrombin. *European Journal of Biochemistry*, 270(14), 2959-2970.
- Ahluwalia, M., Butcher, L., Donovan, H., Killick-Cole, C., Jones, P. M. & Erusalimsky, J. D. (2015) The gene expression signature of anagrelide provides an insight into its mechanism of action and uncovers new regulators of megakaryopoiesis. *Journal of Thrombosis and Haemostasis*, 13(6), 1103-1112.
- Aime, P., Karuppagounder, S. S., Rao, A., Chen, Y. X., Burke, R. E., Ratan, R. R. & Greene, L. A. (2020) The drug adaptaquin blocks ATF4/CHOP-dependent pro-death Trib3 induction and protects in cellular and mouse models of Parkinson's disease. *Neurobiology of Disease*, 136.
- Aime, P., Sun, X. T., Zareen, N., Rao, A., Berman, Z., Volpicelli-Daley, L., Bernd, P., Crary, J. F., Levy, O. A. & Greene, L. A. (2015) Trib3 Is Elevated in Parkinson's Disease and Mediates Death in Parkinson's Disease Models. *Journal of Neuroscience*, 35(30), 10731-10749.
- Almazni, I., Stapley, R. & Morgan, N. V. (2019) Inherited Thrombocytopenia: Update on Genes and Genetic Variants Which may be Associated With Bleeding. *Frontiers in Cardiovascular Medicine*, 6.
- Andreozzi, F., Formoso, G., Prudente, S., Hribal, M. L., Pandolfi, A., Bellacchio, E., Di Silvestre, S., Trischitta, V., Consoli, A. & Sesti, G. (2008) TRIB3 r84 variant is associated with impaired insulin-mediated nitric oxide production in human endothelial cells. *Arteriosclerosis Thrombosis and Vascular Biology*, 28(7), 1355-1360.
- Arciuch, V. G. A., Galli, S., Franco, M. C., Lam, P. Y., Cadenas, E., Carreras, M. C. & Poderoso, J. J. (2009) Akt1 Intramitochondrial Cycling Is a Crucial Step in the Redox Modulation of Cell Cycle Progression. *Plos One*, 4(10).
- Avila, C., Huang, R. J., Stevens, M. V., Aponte, A. M., Tripodi, D., Kim, K. Y. & Sack, M. N. (2012) Platelet Mitochondrial Dysfunction is Evident in Type 2 Diabetes in Association with Modifications of Mitochondrial Anti-Oxidant Stress Proteins. *Experimental and Clinical Endocrinology & Diabetes*, 120(4), 248-251.
- Baaten, C., Moenen, F., Henskens, Y. M. C., Swieringa, F., Wetzels, R. J. H., van Oerle, R., Heijnen, H. F. G., ten Cate, H., Holloway, G. P., Beckers, E. A. M., Heemskerk, J. W. M. & van der Meijden, P. E. J. (2018) Impaired mitochondrial activity explains platelet dysfunction in thrombocytopenic cancer patients undergoing chemotherapy. *Haematologica*, 103(9), 1557-1567.
- Bauer, M. F., Gempel, K., Reichert, A. S., Rappold, G. A., Lichtner, P., Gerbitz, K. D., Neupert, W., Brunner, M. & Hofmann, S. (1999) Genetic and structural characterization of the human mitochondrial inner membrane translocase. *Journal of Molecular Biology*, 289(1), 69-82.
- Bianchi, E., Norfo, R., Pennucci, V., Zini, R. & Manfredini, R. (2016) Genomic landscape of megakaryopoiesis and platelet function defects. *Blood*, 127(10), 1249-1259.
- Bijur, G. N. & Jope, R. S. (2003) Rapid accumulation of Akt in mitochondria following phosphatidylinositol 3-kinase activation. *Journal of Neurochemistry*, 87(6), 1427-1435.
- Borgatti, P., Martelli, A. M., Bellacosa, A., Casto, R., Massari, L., Capitani, S. & Neri, L. M. (2000) Translocation of Akt/PKB to the nucleus of osteoblast-like MC3T3-E1 cells exposed to proliferative growth factors. *Febs Letters*, 477(1-2), 27-32.

- Bos, J. L. (1995) A Target For Phosphoinositide 3-Kinase - AKT/PKB. *Trends in Biochemical Sciences*, 20(11), 441-442.
- Boulbes, D. R., Shaiken, T. & Sarbassov, D. D. (2011) Endoplasmic reticulum is a main localization site of mTORC2. *Biochemical and Biophysical Research Communications*, 413(1), 46-52.
- Bryan, M. M., Tolman, N. J., Simon, K. L., Huizing, M., Hufnagel, R. B., Brooks, B. P., Speransky, V., Mullikin, J. C., Gahl, W. A., Malicdan, M. C. V. & Gochuico, B. R. (2017) Clinical and molecular phenotyping of a child with Hermansky-Pudlak syndrome-7, an uncommon genetic type of HPS. *Molecular genetics and metabolism*, 120(4), 378-383.
- Bugert, P., Dugrillon, A., Gunayclin, A., Eichler, H. & Kluter, H. (2003) Messenger RNA profiling of human platelets by microarray hybridization. *Thrombosis and Haemostasis*, 90(4), 738-748.
- Bukhari, A. (2016) Investigation of the role of TRIB3 in platelets. MSc dissertation: The University of Sheffield.
- Bunimov, N., Fuller, N. & Hayward, C. P. M. (2013) Genetic Loci Associated with Platelet Traits and Platelet Disorders. *Seminars in Thrombosis and Hemostasis*, 39(3), 291-305.
- Burkhardt, R., Toh, S. A., Lagor, W. R., Birkeland, A., Levin, M., Li, X. Y., Robblee, M., Fedorov, V. D., Yamamoto, M., Satoh, T., Akira, S., Kathiresan, S., Breslow, J. L. & Rader, D. J. (2010) Trib1 is a lipid- and myocardial infarction-associated gene that regulates hepatic lipogenesis and VLDL production in mice. *Journal of Clinical Investigation*, 120(12), 4410-4414.
- Butcher, L., Ahluwalia, M., Ord, T., Johnston, J., Morris, R. H., Kiss-Toth, E. & Erusalimsky, J. D. (2017) Evidence for a role of TRIB3 in the regulation of megakaryocytopoiesis. *Scientific Reports*, 7, 9.
- Calleja, V., Alcor, D., Laguerre, M., Park, J., Vojnovic, B., Hemmings, B. A., Downward, J., Parker, P. J. & Larijani, B. (2007) Intramolecular and intermolecular interactions of protein kinase B define its activation in vivo. *Plos Biology*, 5(4), 780-791.
- Cattaneo, M., Cerletti, C., Harrison, P., Hayward, C. P. M., Kenny, D., Nugent, D., Nurden, P., Rao, A. K., Schmaier, A. H., Watson, S. P., Lussana, F., Pugliano, M. T. & Michelson, A. D. (2013) Recommendations for the standardization of light transmission aggregometry: a consensus of the working party from the platelet physiology subcommittee of SSC/ISTH. *Journal of Thrombosis and Haemostasis*, 11(6), 1183-1189.
- Chen, J. H., De, S., Damron, D. S., Chen, W. S., Hay, N. & Byzova, T. V. (2004) Impaired platelet responses to thrombin and collagen in AKT-1-deficient mice. *Blood*, 104(6), 1703-1710.
- Chen, Z. B., Chen, J. J., Wa, Q. B., He, M., Wang, X., Zhou, J. W. & Cen, Y. (2020) Knockdown of circ_0084043 suppresses the development of human melanoma cells through miR-429/tribbles homolog 2 axis and Wnt/beta-catenin pathway. *Life Sciences*, 243.
- Chen, Z. S., Li, T. L., Kareem, K., Tran, D., Griffith, B. P. & Wu, Z. J. J. (2019) The role of PI3K/Akt signaling pathway in non-physiological shear stress-induced platelet activation. *Artificial Organs*, 43(9), 897-908.
- Curtis, B. R. & McFarland, J. G. (2014) Human platelet antigens-2013. *Vox Sanguinis*, 106(2), 93-102.

- Daly, M. E., Leo, V. C., Lowe, G. C., Watson, S. P. & Morgan, N. V. (2014) What is the role of genetic testing in the investigation of patients with suspected platelet function disorders? *British Journal of Haematology*, 165(2), 193-203.
- Dawood, B. B., Lowe, G. C., Lordkipanidze, M., Bem, D., Daly, M. E., Makris, M., Mumford, A., Wilde, J. T. & Watson, S. P. (2012) Evaluation of participants with suspected heritable platelet function disorders including recommendation and validation of a streamlined agonist panel. *Blood*, 120(25), 5041-5049.
- de Graaf, C. A., Kauppi, M., Baldwin, T., Hyland, C. D., Metcalf, D., Willson, T. A., Carpinelli, M. R., Smyth, G. K., Alexander, W. S. & Hilton, D. J. (2010) Regulation of hematopoietic stem cells by their mature progeny. *Proceedings of the National Academy of Sciences of the United States of America*, 107(50), 21689-21694.
- de la Pena, N. C., Gutierrez-Aguilar, M., Hernandez-Resendiz, I., Marin-Hernandez, A. & Rodriguez-Enriquez, S. (2017) Glycoprotein Ib activation by thrombin stimulates the energy metabolism in human platelets. *Plos One*, 12(8).
- Dedhia, P. H., Keeshan, K., Uljon, S., Xu, L. W., Vega, M. E., Shestova, O., Zaks-Zilberman, M., Romany, C., Blacklow, S. C. & Pear, W. S. (2010) Differential ability of Tribbles family members to promote degradation of C/EBP alpha and induce acute myelogenous leukemia. *Blood*, 116(8), 1321-1328.
- Defronzo, R. A. & Ferrannini, E. (1991) Insulin Resistance - A Multifaceted Syndrome Responsible For NIDDM, Obesity, Hypertension, Dyslipidemia, And Atherosclerotic Cardiovascular-Disease. *Diabetes Care*, 14(3), 173-194.
- Deutsch, V. R. & Tomer, A. (2013) Advances in megakaryocytopoiesis and thrombopoiesis: from bench to bedside. *British Journal of Haematology*, 161(6), 778-793.
- Dixon, A. S., Schwinn, M. K., Hall, M. P., Zimmerman, K., Otto, P., Lubben, T. H., Butler, B. L., Binkowski, B. F., Machleidt, T., Kirkland, T. A., Wood, M. G., Eggers, C. T., Encell, L. P. & Wood, K. V. (2016) NanoLuc Complementation Reporter Optimized for Accurate Measurement of Protein Interactions in Cells. *Acs Chemical Biology*, 11(2), 400-408.
- Douvris, A., Soubeyrand, S., Naing, T., Martinuk, A., Nikpay, M., Williams, A., Buick, J., Yauk, C. & McPherson, R. (2014) Functional Analysis of the TRIB1 Associated Locus Linked to Plasma Triglycerides and Coronary Artery Disease. *Journal of the American Heart Association*, 3(3), 17.
- Downes, K., Megy, K., Duarte, D., Vries, M., Gebhart, J., Hofer, S., Shamardina, O., Deevi, S. V. V., Stephens, J., Mapeta, R., Tuna, S., Al Hasso, N., Besser, M. W., Cooper, N., Daugherty, L., Gleadall, N., Greene, D., Haimel, M., Martin, H., Papadia, S., Revel-Vilk, S., Sivapalaratnam, S., Symington, E., Thomas, W., Thys, C., Tolios, A., Penkett, C. J., Ouwehand, W. H., Abbs, S., Laffan, M. A., Turro, E., Simeoni, I., Mumford, A. D., Henskens, Y. M. C., Pabinger, I., Gomez, K., Freson, K. & Nahr, B. (2019) Diagnostic high-throughput sequencing of 2396 patients with bleeding, thrombotic, and platelet disorders. *Blood*, 134(23), 2082-2091.
- Du, K. Y., Herzig, S., Kulkarni, R. N. & Montminy, M. (2003) TRB3: A tribbles homolog that inhibits Akt/PKB activation by insulin in liver. *Science*, 300(5625), 1574-1577.
- Dunn, K. W., Kamocka, M. M. & McDonald, J. H. (2011) A practical guide to evaluating colocalization in biological microscopy. *American Journal of Physiology-Cell Physiology*, 300(4), C723-C742.

- Eckly, A., Heijnen, H., Pertuy, F., Geerts, W., Proamer, F., Rinckel, J. Y., Leon, C., Lanza, F. & Gachet, C. (2014) Biogenesis of the demarcation membrane system (DMS) in megakaryocytes. *Blood*, 123(6), 921-930.
- Eden, E., Navon, R., Steinfeld, I., Lipson, D. & Yakhini, Z. (2009) GOrilla: a tool for discovery and visualization of enriched GO terms in ranked gene lists. *Bmc Bioinformatics*, 10.
- Emami, Z., Namin, A. M., Kojuri, J., Jalali, F. M. & Rasti, M. (2019) Expression and Activity of Platelet Endothelial Nitric Oxide Synthase Are Decreased in Patients with Coronary Thrombosis and Stenosis. *Avicenna Journal of Medical Biotechnology*, 11(1), 88-93.
- Erazo, T., Lorente, M., Lopez-Plana, A., Munoz-Guardiola, P., Fernandez-Nogueira, P., Garcia-Martinez, J. A., Bragado, P., Fuster, G., Salazar, M., Espadaler, J., Hernandez-Losa, J., Bayascas, J. R., Cortal, M., Vidal, L., Gascon, P., Gomez-Ferrera, M., Alfon, J., Velasco, G., Domenech, C. & Lizcano, J. M. (2016) The New Antitumor Drug ABTL0812 Inhibits the Akt/mTORC1 Axis by Upregulating Tribbles-3 Pseudokinase. *Clinical Cancer Research*, 22(10), 2508-2519.
- Eyers, P. A., Keeshan, K. & Kannan, N. (2016) Tribbles in the 21st Century: The Evolving Roles of Tribbles Pseudokinases in Biology and Disease. *Trends in cell biology*.
- Fabregat, A., Jupe, S., Matthews, L., Sidiropoulos, K., Gillespie, M., Garapati, P., Haw, R., Jassal, B., K€orninger, F., May, B., Milacic, M., Roca, C. D., Rothfels, K., Sevilla, C., Shamovsky, V., Shorsler, S., Varusai, T., Viteri, G., Weiser, J., Wu, G. M., Stein, L., Hermjakob, H. & D'Eustachio, P. (2018) The Reactome Pathway Knowledgebase. *Nucleic Acids Research*, 46(D1), D649-D655.
- Falati, S., Edmead, C. E. & Poole, A. W. (1999) Glycoprotein Ib-V-IX, a receptor for von Willebrand factor, couples physically and functionally to the Fc receptor gamma-chain, Fyn, and Lyn to activate human platelets. *Blood*, 94(5), 1648-1656.
- Feng, Y. F., Liu, Y., Wang, L., Cai, X. Q., Wang, D. X., Wu, K. M., Chen, H. L., Li, J. & Lei, W. (2013) Sustained Oxidative Stress Causes Late Acute Renal Failure via Duplex Regulation on p38 MAPK and Akt Phosphorylation in Severely Burned Rats. *Plos One*, 8(1).
- Fletcher, S. J., Johnson, B., Lowe, G. C., Bem, D., Drake, S., Lordkipanidze, M., Guiu, I. S., Dawood, B., Rivera, J., Simpson, M. A., Daly, M. E., Motwani, J., Collins, P. W., Watson, S. P., Morgan, N. V., Genotyping, U. K. & Phenotyping, P. (2015) SLFN14 mutations underlie thrombocytopenia with excessive bleeding and platelet secretion defects. *Journal of Clinical Investigation*, 125(9), 3600-3605.
- Formoso, G., Di Tomo, P., Andreozzi, F., Succurro, E., Di Silvestre, S., Prudente, S., Perticone, F., Trischitta, V., Sesti, G., Pandolfi, A. & Consoli, A. (2011) The TRIB3 R84 variant is associated with increased carotid intima-media thickness in vivo and with enhanced MAPK signalling in human endothelial cells. *Cardiovascular Research*, 89(1), 184-192.
- Fox, J. E. B., Reynolds, C. C., Morrow, J. S. & Phillips, D. R. (1987) SPECTRIN IS ASSOCIATED WITH MEMBRANE-BOUND ACTIN-FILAMENTS IN PLATELETS AND IS HYDROLYZED BY THE CA-2+-DEPENDENT PROTEASE DURING PLATELET ACTIVATION. *Blood*, 69(2), 537-545.
- Frey, T. G. & Mannella, C. A. (2000) The internal structure of mitochondria. *Trends in Biochemical Sciences*, 25(7), 319-324.

- Fuentes, E., Araya-Maturana, R. & Urra, F. A. (2019) Regulation of mitochondrial function as a promising target in platelet activation-related diseases. *Free Radical Biology and Medicine*, 136, 172-182.
- Galarneau, A., Primeau, M., Trudeau, L. E. & Michnick, S. W. (2002) beta-Lactamase protein fragment complementation assays as in vivo and in vitro sensors of protein-protein interactions. *Nature Biotechnology*, 20(6), 619-622.
- Gardiner, E. E. & Andrews, R. K. (2014) Structure and Function of Platelet Receptors Initiating Blood Clotting, in Corey, S. J., Kimmel, M. & Leonard, J. N. (eds), *Systems Biology Approach to Blood*. Advances in Experimental Medicine and Biology. Berlin: Springer-Verlag Berlin, 263-275.
- Gerrard, J. M., White, J. G. & Peterson, D. A. (1978) PLATELET DENSE TUBULAR SYSTEM - ITS RELATIONSHIP TO PROSTAGLANDIN SYNTHESIS AND CALCIUM FLUX. *Thrombosis and Haemostasis*, 40(2), 224-231.
- Giles, C. (1981) THE PLATELET COUNT AND MEAN PLATELET VOLUME. *British Journal of Haematology*, 48(1), 31-37.
- Grandinetti, K. B., Stevens, T. A., Ha, S., Salamone, R. J., Walker, J. R., Zhang, J., Agarwalla, S., Tenen, D. G., Peters, E. C. & Reddy, V. A. (2011) Overexpression of TRIB2 in human lung cancers contributes to tumorigenesis through downregulation of C/EBP alpha. *Oncogene*, 30(30), 3328-3335.
- Gresele, P. (2015) On behalf of the subcommittee on platelet physiology. Diagnosis of inherited platelet function disorders: guidance from the SSC of the ISTH. *Journal of Thrombosis and Haemostasis*, 13(2), 314-322.
- Gresele, P., Harrison, P., Bury, L., Falcinelli, E., Gachet, C., Hayward, C. P., Kenny, D., Mezzano, D., Mumford, A. D., Nugent, D., Nurden, A. T., Orsini, S. & Cattaneo, M. (2014) Diagnosis of suspected inherited platelet function disorders: results of a worldwide survey. *Journal of Thrombosis and Haemostasis*, 12(9), 1562-1569.
- Grosshans, J. & Wieschaus, E. (2000) A genetic link between morphogenesis and cell division during formation of the ventral furrow in *Drosophila*. *Cell*, 101(5), 523-531.
- Guo, X. M., Wu, J. J., Du, J. J., Ran, J. M. & Xu, J. (2010) Platelets of type 2 diabetic patients are characterized by high ATP content and low mitochondrial membrane potential (vol 20, pg 588, 2009). *Platelets*, 21(1), 84-84.
- Hartley, J. L., Temple, G. F. & Brasch, M. A. (2000) DNA cloning using in vitro site-specific recombination. *Genome Research*, 10(11), 1788-1795.
- Hegedus, Z., Czibula, A. & Kiss-Toth, E. (2007) Tribbles: A family of kinase-like proteins with potent signalling regulatory function. *Cellular Signalling*, 19(2), 238-250.
- Heijnen, H. & van der Sluijs, P. (2015) Platelet secretory behaviour: as diverse as the granules ... or not? *Journal of Thrombosis and Haemostasis*, 13(12), 2141-2151.
- Hill, R., Madureira, P. A., Ferreira, B., Baptista, I., Machado, S., Colaco, L., dos Santos, M., Liu, N. S., Dopazo, A., Ugurel, S., Adrienn, A., Kiss-Toth, E., Isbilen, M., Gure, A. O. & Link, W. (2017) TRIB2 confers resistance to anti-cancer therapy by activating the serine/threonine protein kinase AKT. *Nature Communications*, 8.
- Holinstat, M. (2017) Normal platelet function. *Cancer and Metastasis Reviews*, 36(2), 195-198.
- Hou, Z. L., Guo, K. X., Sun, X. L., Hu, F. Q., Chen, Q. Z., Luo, X. L., Wang, G. H., Hu, J. B. & Sun, L. (2018) TRIB2 functions as novel oncogene in colorectal cancer by blocking cellular senescence through AP4/p21 signaling. *Molecular Cancer*, 17.

- Hughes, C. E. (2018) How to perform aggregometry and lumi-aggregometry in mouse platelets. *Platelets*, 29(7), 638-643.
- Iancu-Rubin, C., Tripodi, J., Gajzer, D., Najfeld, V., Hoffman, R. & Atweh, G. F. (2010) Stathmin-Mediated Dysregulation of Microtubules Impairs Megakaryocyte Maturation and Platelet Production. *Blood*, 116(21), 243-244.
- Ise, R., Han, D. H., Takahashi, Y., Terasaka, S., Inoue, A., Tanji, M. & Kiyama, R. (2005) Expression profiling of the estrogen responsive genes in response to phytoestrogens using a customized DNA microarray. *Febs Letters*, 579(7), 1732-1740.
- Italiano, J. E., Bergmeier, W., Tiwari, S., Falet, H., Hartwig, J. H., Hoffmeister, K. M., Andre, P., Wagner, D. D. & Shivdasani, R. A. (2003) Mechanisms and implications of platelet discoid shape. *Blood*, 101(12), 4789-4796.
- Jin, G. A., Yamazaki, Y., Takuwa, M., Takahara, T., Kaneko, K., Kuwata, T., Miyata, S. & Nakamura, T. (2007) Trib1 and Evi1 cooperate with Hoxa and Meis1 in myeloid leukemogenesis. *Blood*, 109(9), 3998-4005.
- Jirouskova, M., Shet, A. S. & Johnson, G. J. (2007) A guide to murine platelet structure, function, assays, and genetic alterations. *Journal of Thrombosis and Haemostasis*, 5(4), 661-669.
- Johnson, B., Lowe, G. C., Futterer, J., Lordkipanidze, M., MacDonald, D., Simpson, M. A., Sanchez-Guiu, I., Drake, S., Bem, D., Leo, V., Fletcher, S. J., Dawood, B., Rivera, J., Allsup, D., Biss, T., Bolton-Maggs, P. H. B., Collins, P., Curry, N., Grimley, C., James, B., Makris, M., Motwani, J., Pavord, S., Talks, K., Thachil, J., Wilde, J., Williams, M., Harrison, P., Gissen, P., Mundell, S., Mumford, A., Daly, M. E., Watson, S. P., Morgan, N. V. & Grp, U. G. S. (2016) Whole exome sequencing identifies genetic variants in inherited thrombocytopenia with secondary qualitative function defects. *Haematologica*, 101(10), 1170-1179.
- Johnston, J., Angyal, A., Bauer, R., Rader, D., Shoulders, C., Francis, S. & Kiss-Toth, E. (2018) MYELOID TRIB1 CONTROLS EXPERIMENTAL ATHEROSCLEROSIS. *Heart*, 104, A93-A93.
- Kashiwagi, H., Schwartz, M. A., Eigenthaler, M., Davis, K. A., Ginsberg, M. H. & Shattil, S. J. (1997) Affinity modulation of platelet integrin alpha(IIb)beta(3) by beta(3)-endonexin, a selective binding partner of the beta(3) integrin cytoplasmic tail. *Journal of Cell Biology*, 137(6), 1433-1443.
- Kaushansky, K. (2006) Lineage-specific hematopoietic growth factors - Reply. *New England Journal of Medicine*, 355(5), 527-527.
- Kaushansky, K. (2008) Historical review: megakaryopoiesis and thrombopoiesis. *Blood*, 111(3), 981-986.
- Kim, S., Jin, J. G. & Kunapuli, S. P. (2004) Akt activation in platelets depends on G(i) signaling pathways. *Journal of Biological Chemistry*, 279(6), 4186-4195.
- Kircher, M., Witten, D. M., Jain, P., O'Roak, B. J., Cooper, G. M. & Shendure, J. (2014) A general framework for estimating the relative pathogenicity of human genetic variants. *Nature Genetics*, 46(3), 310-+.
- Kiss-Toth, E., Bagstaff, S. M., Sung, H. Y., Jozsa, V., Dempsey, C., Caunt, J. C., Oxley, K. M., Wyllie, D. H., Polgar, T., Harte, M., O'Neill, L. A. J., Qwarnstrom, E. E. & Dower, S. K. (2004) Human tribbles, a protein family controlling mitogen-activated protein kinase cascades. *Journal of Biological Chemistry*, 279(41), 42703-42708.

- Korolchuk, V. I., Saiki, S., Lichtenberg, M., Siddiqi, F. H., Roberts, E. A., Imarisio, S., Jahreiss, L., Sarkar, S., Futter, M., Menzies, F. M., O'Kane, C. J., Deretic, V. & Rubinsztein, D. C. (2011) Lysosomal positioning coordinates cellular nutrient responses. *Nature Cell Biology*, 13(4), 453-U242.
- Kroner, C., Eybrechts, K. & Akkerman, J. W. N. (2000) Dual regulation of platelet protein kinase B. *Journal of Biological Chemistry*, 275(36), 27790-27798.
- Kwon, M., Eom, J., Kim, D., Kim, J., Heredia, J., Kang, S. W. & Song, Y. (2018) Skeletal Muscle Tissue Trib3 Links Obesity with Insulin Resistance by Autophagic Degradation of AKT2. *Cellular Physiology and Biochemistry*, 48(4), 1543-1555.
- Lefrançois, E., Ortiz-Muñoz, G., Caudrillier, A. & al, e. (2017) The lung is a site of platelet biogenesis and a reservoir for haematopoietic progenitors.
- Leng, X. H., Hong, S. Y., Larrucea, S., Zhang, W., Li, T. T., Lopez, J. A. & Bray, P. F. (2004) Platelets of female mice are intrinsically more sensitive to agonists than are platelets of males. *Arteriosclerosis Thrombosis and Vascular Biology*, 24(2), 376-381.
- Leo, V. C., Morgan, N. V., Bem, D., Jones, M. L., Lowe, G. C., Lordkipanidze, M., Drake, S., Simpson, M. A., Gissen, P., Mumford, A., Watson, S. P., Daly, M. E. & Grp, U. G. S. (2015) Use of next-generation sequencing and candidate gene analysis to identify underlying defects in patients with inherited platelet function disorders. *Journal of Thrombosis and Haemostasis*, 13(4), 643-650.
- Lepur, A. & Vugrek, O. (2018) Bimolecular Fluorescence Complementation to Visualize Protein-Protein Interactions in Human Cells Based on Gateway Cloning Technology. *Two-Hybrid Systems: Methods and Protocols*, 1794, 259-267.
- Levin, C., Koren, A., Pretorius, E., Rosenberg, N., Shenkman, B., Hauschner, H., Zalman, L., Khayat, M., Salama, I., Elpeleg, O. & Shalev, S. (2015) Deleterious mutation in the FYB gene is associated with congenital autosomal recessive small-platelet thrombocytopenia. *Journal of Thrombosis and Haemostasis*, 13(7), 1285-1292.
- Li, K., Wang, F., Cao, W. B., Lv, X. X., Hua, F., Cui, B., Yu, J. J., Zhang, X. W., Shang, S., Liu, S. S., Yu, J. M., Han, M. Z., Huang, B., Zhang, T. T., Li, X., Jiang, J. D. & Hu, Z. W. (2017) TRIB3 Promotes APL Progression through Stabilization of the Oncoprotein PML-RAR alpha and Inhibition of p53-Mediated Senescence. *Cancer Cell*, 31(5), 697-+.
- Li, Z. Y., Delaney, M. K., O'Brien, K. A. & Du, X. P. (2010) Signaling During Platelet Adhesion and Activation. *Arteriosclerosis Thrombosis and Vascular Biology*, 30(12), 2341-2349.
- Liang, Y. X., Yu, D., Perez-Soler, R., Klostergaard, J. & Zou, Y. Y. (2017) TRIB2 contributes to cisplatin resistance in small cell lung cancer. *Oncotarget*, 8(65), 109596-109608.
- Luo, X., Zhong, L., Yu, L. H., Xiong, L., Dan, W. R., Li, J., Ye, J., Chu, X., Liu, C. & Liu, B. (2020) TRIB3 destabilizes tumor suppressor PPAR alpha expression through ubiquitin-mediated proteasome degradation in acute myeloid leukemia. *Life Sciences*, 257.
- Machlus, K. R. & Italiano, J. E. (2013) The incredible journey: From megakaryocyte development to platelet formation. *Journal of Cell Biology*, 201(6), 785-796.
- Makhoul, S., Walter, E., Pagel, O., Walter, U., Sickmann, A., Gambaryan, S., Smolenski, A., Zahedi, R. P. & Jurk, K. (2018) Effects of the NO/soluble guanylate cyclase/cGMP system on the functions of human platelets. *Nitric Oxide-Biology and Chemistry*, 76, 71-80.

- Margraf, A., Nussbaum, C. & Sperandio, M. (2019) Ontogeny of platelet function. *Blood Advances*, 3(4), 692-703.
- Marianayagam, N. J., Sunde, M. & Matthews, J. M. (2004) The power of two: protein dimerization in biology. *Trends in Biochemical Sciences*, 29(11), 618-625.
- Marjanovic, J. A., Stojanovic, A., Brovkovich, V. M., Skidgel, R. A. & Du, X. P. (2008) Signaling-mediated Functional Activation of Inducible Nitric-oxide Synthase and Its Role in Stimulating Platelet Activation. *Journal of Biological Chemistry*, 283(43), 28827-28834.
- Mata, J., Curado, S., Ephrussi, A. & Rorth, P. (2000) Tribbles coordinates mitosis and morphogenesis in *Drosophila* by regulating string/CDC25 proteolysis. *Cell*, 101(5), 511-522.
- Maynard, D. M., Heijnen, H. F. G., Horne, M. K., White, J. G. & Gahl, W. A. (2007) Proteomic analysis of platelet alpha-granules using mass spectrometry. *Journal of Thrombosis and Haemostasis*, 5(9), 1945-1955.
- McCarty, J. M., Sprugel, K. H., Fox, N. E., Sabath, D. E. & Kaushansky, K. (1995) Murine Thrombopoietin Messenger-Rna Levels Are Modulated By Platelet Count. *Blood*, 86(10), 3668-3675.
- Melchinger, H., Jain, K., Tyagi, T. & Hwa, J. (2019) Role of Platelet Mitochondria: Life in a Nucleus-Free Zone. *Frontiers in Cardiovascular Medicine*, 6.
- Mondal, D., Mathur, A. & Chandra, P. K. (2016) Tripping on TRIB3 at the junction of health, metabolic dysfunction and cancer. *Biochimie*, 124, 34-52.
- Noetzli, L., Lo, R. W., Lee-Sherick, A. B., Callaghan, M., Noris, P., Savoia, A., Rajpurkar, M., Jones, K., Gowan, K., Balduini, C. L., Pecci, A., Gnan, C., De Rocco, D., Doubek, M., Li, L., Lu, L., Leung, R., Landolt-Marticorena, C., Hunger, S., Heller, P., Gutierrez-Hartmann, A., Liang, X. Y., Pluthero, F. G., Rowley, J. W., Weyrich, A. S., Kahr, W. H. A., Porter, C. C. & Di Paola, J. (2015) Germline mutations in ETV6 are associated with thrombocytopenia, red cell macrocytosis and predisposition to lymphoblastic leukemia. *Nature Genetics*, 47(5), 535-U143.
- Nurden, A. T. (2011) Platelets, inflammation and tissue regeneration. *Thrombosis and Haemostasis*, 105, S13-S33.
- O'Connor, C., Lohan, F., Campos, J., Ohlsson, E., Salome, M., Forde, C., Artschwager, R., Liskamp, R. M., Cahill, M. R., Kiely, P. A., Porse, B. & Keeshan, K. (2016) The presence of C/EBP alpha and its degradation are both required for TRIB2-mediated leukaemia. *Oncogene*, 35(40), 5272-5281.
- Oberkofler, H., Pfeifenberger, A., Soyal, S., Felder, T., Hahne, P., Miller, K., Krempler, F. & Patsch, W. (2010) Aberrant hepatic TRIB3 gene expression in insulin-resistant obese humans. *Diabetologia*, 53(9), 1971-1975.
- Offermanns, S. (2006) Activation of platelet function through G protein-coupled receptors. *Circulation Research*, 99(12), 1293-1304.
- Ohoka, N., Sakai, S., Onozaki, K., Nakanishi, M. & Hayashi, H. (2010) Anaphase-promoting complex/cyclosome-cdh1 mediates the ubiquitination and degradation of TRB3. *Biochemical and Biophysical Research Communications*, 392(3), 289-294.
- Ord, T., Innos, J., Lillevali, K., Tekko, T., Sutt, S., Ord, D., Koks, S. & Vasar, E. (2014) Trib3 Is Developmentally and Nutritionally Regulated in the Brain but Is Dispensable for Spatial Memory, Fear Conditioning and Sensing of Amino Acid-Imbalanced Diet. *Plos One*, 9(4).

- Patel-Hett, S., Wang, H. B., Begonja, A. J., Thon, J. N., Alden, E. C., Wandersee, N. J., An, X. L., Mohandas, N., Hartwig, J. H. & Italiano, J. E. (2011) The spectrin-based membrane skeleton stabilizes mouse megakaryocyte membrane systems and is essential for proplatelet and platelet formation. *Blood*, 118(6), 1641-1652.
- Paulus, J. M. (1975) PLATELET SIZE IN MAN. *Blood*, 46(3), 321-336.
- Prudente, S., Bailetti, D., Mendonca, C., Mannino, G. C., Fontana, A., Andreozzi, F., Hastings, T., Mercuri, L., Alberico, F., Basile, G., Copetti, M., Sesti, G., Doria, A. & Trischitta, V. (2015) Infrequent TRIB3 coding variants and coronary artery disease in type 2 diabetes. *Atherosclerosis*, 242(1), 334-339.
- Prudente, S., Hribal, M. L., Flex, E., Turchi, F., Morini, E., De Cosmo, S., Bacci, S., Tassi, V., Cardellini, M., Lauro, R., Sesti, G., Dallapiccola, B. & Trischitta, V. (2005) The functional Q84R polymorphism of mammalian tribbles homolog TRB3 is associated with insulin resistance and related cardiovascular risk in Caucasians from Italy. *Diabetes*, 54(9), 2807-2811.
- Prudente, S., Scarpelli, D., Chandalia, M., Zhang, Y. Y., Morini, E., Del Guerra, S., Perticone, F., Li, R., Powers, C., Andreozzi, F., Marchetti, P., Dallapiccola, B., Abate, N., Doria, A., Sesti, G. & Trischitta, V. (2009) The TRIB3 Q84R Polymorphism and Risk of Early-Onset Type 2 Diabetes. *Journal of Clinical Endocrinology & Metabolism*, 94(1), 190-196.
- Prudente, S. & Trischitta, V. (2015) The TRIB3 Q84R polymorphism, insulin resistance and related metabolic alterations. *Biochemical Society Transactions*, 43, 1108-1111.
- Radley, J. M. & Hartshorn, M. A. (1987) Megakaryocyte Fragments And The Microtubule Coil. *Blood Cells*, 12(3), 603-610.
- Rand, M. D., Lock, J. B., vantVeer, C., Gaffney, D. P. & Mann, K. G. (1996) Blood clotting in minimally altered whole blood. *Blood*, 88(9), 3432-3445.
- Rehling, P., Wiedemann, N., Pfanner, N. & Truscott, K. N. (2001) The mitochondrial import machinery for preproteins. *Critical Reviews in Biochemistry and Molecular Biology*, 36(3), 291-336.
- Remy, I. & Michnick, S. W. (2004) A cDNA library functional screening strategy based on fluorescent protein complementation assays to identify novel components of signaling pathways. *Methods*, 32(4), 381-388.
- Remy, I. & Michnick, S. W. (2007) Application of protein-fragment complementation assays in cell biology. *Biotechniques*, 42(2), 137-+.
- Rentzsch, P., Witten, D., Cooper, G. M., Shendure, J. & Kircher, M. (2019) CADD: predicting the deleteriousness of variants throughout the human genome. *Nucleic Acids Research*, 47(D1), D886-D894.
- Rishi, L., Hannon, M., Salome, M., Hasemann, M., Frank, A. K., Campos, J., Timoney, J., O'Connor, C., Cahill, M. R., Porse, B. & Keeshan, K. (2014) Regulation of Trib2 by an E2F1-C/EBP alpha feedback loop in AML cell proliferation. *Blood*, 123(15), 2389-2400.
- Rivera, J., Lozano, M. L., Navarro-Nunez, L. & Vicente, V. (2009) Platelet receptors and signaling in the dynamics of thrombus formation. *Haematologica-the Hematology Journal*, 94(5), 700-711.
- Rojas, R., Kametaka, S., Haft, C. R. & Bonifacino, J. S. (2007) Interchangeable but essential functions of SNX1 and SNX2 in the association of retromer with endosomes

- and the tracking of mannose 6-phosphate receptors. *Molecular and Cellular Biology*, 27(3), 1112-1124.
- Rowley, J. W., Schwertz, H. & Weyrich, A. S. (2012) Platelet mRNA: the meaning behind the message. *Current Opinion in Hematology*, 19(5), 385-391.
- Rubin, C. I., French, D. L. & Atweh, G. F. (2003) Stathmin expression and megakaryocyte differentiation: A potential role in polyploidy. *Experimental Hematology*, 31(5), 389-397.
- Saji, M., Vasko, V., Kada, F., Allbritton, E. H., Burman, K. D. & Ringel, M. D. (2005) Akt1 contains a functional leucine-rich nuclear export sequence. *Biochemical and Biophysical Research Communications*, 332(1), 167-173.
- Salazar, M., Lorente, M., Garcia-Taboada, E., Gomez, E. P., Davila, D., Zuniga-Garcia, P., Flores, J. M., Rodriguez, A., Hegedus, Z., Mosen-Ansorena, D., Aransay, A. M., Hernandez-Tiedra, S., Lopez-Valero, I., Quintanilla, M., Sanchez, C., Iovanna, J. L., Dusetti, N., Guzman, M., Francis, S. E., Carracedo, A., Kiss-Toth, E. & Velasco, G. (2015) Loss of Tribbles pseudokinase-3 promotes Akt-driven tumorigenesis via FOXO inactivation. *Cell Death and Differentiation*, 22(1), 131-144.
- Salazar, M., Lorente, M., Garcia-Taboada, E., Hernandez-Tiedra, S., Davila, D., Francis, S. E., Guzman, M., Kiss-Toth, E. & Velasco, G. (2013) The pseudokinase tribbles homologue-3 plays a crucial role in cannabinoid anticancer action. *Biochimica Et Biophysica Acta-Molecular and Cell Biology of Lipids*, 1831(10), 1573-1578.
- Saleem, S. & Biswas, S. C. (2017) Tribbles Pseudokinase 3 Induces Both Apoptosis and Autophagy in Amyloid-beta-induced Neuronal Death. *Journal of Biological Chemistry*, 292(7), 2571-2585.
- Sasaki, Y., Sone, T., Yoshida, S., Yahata, K., Hotta, J., Chesnut, J. D., Honda, T. & Imamoto, F. (2004) Evidence for high specificity and efficiency of multiple recombination signals in mixed DNA cloning by the Multisite Gateway system. *Journal of Biotechnology*, 107(3), 233-243.
- Seher, T. C. & Leptin, M. (2000) Tribbles, a cell-cycle brake that coordinates proliferation and morphogenesis during Drosophila gastrulation. *Current Biology*, 10(11), 623-629.
- Sepulveda, C., Hernandez, B., Burgos, C. F., Fuentes, E., Palomo, I. & Alarcon, M. (2019) The cAMP/PKA Pathway Inhibits Beta-amyloid Peptide Release from Human Platelets. *Neuroscience*, 397, 159-171.
- Shahrouzi, P., Astobiza, I., Cortazar, A. R., Torrano, V., Macchia, A., Flores, J. M., Niespolo, C., Mendizabal, I., Caloto, R., Ercilla, A., Camacho, L., Arreal, L., Bizkarguenaga, M., Martinez-Chantar, M. L., Bustelo, X. R., Berra, E., Kiss-Toth, E., Velasco, G., Zabala-Letona, A. & Carracedo, A. (2020) Genomic and Functional Regulation of TRIB1 Contributes to Prostate Cancer Pathogenesis. *Cancers*, 12(9).
- Shekhawat, S. S. & Ghosh, I. (2011) Split-protein systems: beyond binary protein-protein interactions. *Current Opinion in Chemical Biology*, 15(6), 789-797.
- Smolenski, A. (2012) Novel roles of cAMP/cGMP-dependent signaling in platelets. *Journal of Thrombosis and Haemostasis*, 10(2), 167-176.
- Soo Kim, B., Auerbach, D. A., Sadhra, H., Godwin, M., Bhandari, R., Ling, F. S., Mohan, A., Yule, D. I., Wagner, L., 2nd, Rich, D. Q., Ture, S., Morrell, C. N., Timpanaro-Perrotta, L., Younis, A., Goldenberg, I. & Cameron, S. J. (2020) Sex-Specific Platelet Activation Through Protease-Activated Receptors Reverses in Myocardial Infarction. *Arteriosclerosis, thrombosis, and vascular biology*, ATVBAHA120315033-ATVBAHA120315033.

- Sugiyama, M. G., Fairn, G. D. & Antonescu, C. N. (2019) Akt-ing Up Just About Everywhere: Compartment-Specific Akt Activation and Function in Receptor Tyrosine Kinase Signaling. *Frontiers in Cell and Developmental Biology*, 7.
- Sun, X. Y., Song, M., Wang, H., Zhou, H. M., Wang, F., Li, Y., Zhang, Y., Zhang, W., Zhong, M. & Ti, Y. (2017) TRB3 gene silencing activates AMPK in adipose tissue with beneficial metabolic effects in obese and diabetic rats. *Biochemical and Biophysical Research Communications*, 488(1), 22-28.
- Szymonowicz, K., Oeck, S., Malewicz, N. M. & Jendrossek, V. (2018) New Insights into Protein Kinase B/Akt Signaling: Role of Localized Akt Activation and Compartment-Specific Target Proteins for the Cellular Radiation Response. *Cancers*, 10(3).
- Takaishi, K., Takeuchi, M., Tsukamoto, S., Takayama, N., Oshima, M., Kimura, K., Isshiki, Y., Kayamori, K., Hino, Y., Oshima-Hasegawa, N., Mitsukawa, S., Takeda, Y., Mimura, N., Ohwada, C., Iseki, T., Nakamura, S., Eto, K., Iwama, A., Yokote, K., Nakaseko, C. & Sakaida, E. (2020) Suppressive effects of anagrelide on cell cycle progression and the maturation of megakaryocyte progenitor cell lines in human induced pluripotent stem cells. *Haematologica*, 105(5), E216-E220.
- Takino, J., Sato, T., Nagamine, K. & Hori, T. (2019) The inhibition of Bax activation-induced apoptosis by RasGRP2 via R-Ras-PI3K-Akt signaling pathway in the endothelial cells. *Scientific Reports*, 9.
- UKHCDO (2019) *National Haemophilia database Bleeding disorder statistics for 2018-2019 published by the United Kingdom Haemophilia Centre Doctors' Organisation*, 2019. Available online: <http://www.ukhcdo.org/home-2/annual-reports/> [Accessed 20-11-2020].
- Varga-Szabo, D., Pleines, I. & Nieswandt, B. (2008) Cell adhesion mechanisms in platelets. *Arteriosclerosis Thrombosis and Vascular Biology*, 28(3), 403-412.
- Wang, J. Y., Park, J. S., Wei, Y. Y., Rajurkar, M., Cotton, J. L., Fan, Q. S., Lewis, B. C., Ji, H. K. & Mao, J. H. (2013) TRIB2 Acts Downstream of Wnt/TCF in Liver Cancer Cells to Regulate YAP and C/EBP alpha Function. *Molecular Cell*, 51(2), 211-225.
- Wang, L., Wu, Q., Fan, Z. J., Xie, R. F., Wang, Z. C. & Lu, Y. (2017) Platelet mitochondrial dysfunction and the correlation with human diseases. *Biochemical Society Transactions*, 45, 1213-1223.
- Wang, Y. J., Zhou, Y. X., Szabo, K., Haft, C. R. & Trejo, J. (2002) Down-regulation of protease-activated receptor-1 is regulated by sorting nexin 1. *Molecular Biology of the Cell*, 13(6), 1965-1976.
- Watson, S. P., Lowe, G. C., Lordkipanidze, M., Morgan, N. V. & Gapp, C. (2013) Genotyping and phenotyping of platelet function disorders. *Journal of Thrombosis and Haemostasis*, 11, 351-363.
- Wennemers, M., Bussink, J., Grebenchtchikov, N., Sweep, F. & Span, P. N. (2011) TRIB3 protein denotes a good prognosis in breast cancer patients and is associated with hypoxia sensitivity. *Radiotherapy and Oncology*, 101(1), 198-202.
- White, J. G. (1979) Current Concepts Of Platelet Structure. *American Journal of Clinical Pathology*, 71(4), 363-378.
- Wiedemann, N. & Pfanner, N. (2017) Mitochondrial Machineries for Protein Import and Assembly. *Annual Review of Biochemistry*, Vol 86, 86, 685-714.

- Woulfe, D., Jiang, H., Morgans, A., Monks, R., Birnbaum, M. & Brass, L. F. (2004) Defects in secretion, aggregation, and thrombus formation in platelets from mice lacking Akt2. *Journal of Clinical Investigation*, 113(3), 441-450.
- Xu, J. M., Lv, S., Qin, Y., Shu, F., Xu, Y. J., Chen, J., Xu, B. E., Sun, X. Q. & Wu, J. (2007) TRB3 interacts with CtlP and is overexpressed in certain cancers. *Biochimica Et Biophysica Acta-General Subjects*, 1770(2), 273-278.
- Yin, H., Stojanovic, A., Hay, N. & Du, X. P. (2008) The role of Akt in the signaling pathway of the, glycoprotein Ib-IX-induced platelet activation. *Blood*, 111(2), 658-665.
- Yokoyama, T., Kanno, Y., Yamazaki, Y., Takahara, T., Miyata, S. & Nakamura, T. (2010) Trib1 links the MEK1/ERK pathway in myeloid leukemogenesis. *Blood*, 116(15), 2768-2775.
- Yokoyama, T. & Nakamura, T. (2011) Tribbles in disease: Signaling pathways important for cellular function and neoplastic transformation. *Cancer Science*, 102(6), 1115-1122.
- Yu, J. M., Sun, W., Wang, Z. H., Liang, X., Hua, F., Li, K., Lv, X. X., Zhang, X. W., Liu, Y. Y., Yu, J. J., Liu, S. S., Shang, S., Wang, F., Yang, Z. N., Zhao, C. X., Hou, X. Y., Li, P. P., Huang, B., Cui, B. & Hu, Z. W. (2019) TRIB3 supports breast cancer stemness by suppressing FOXO1 degradation and enhancing SOX2 transcription. *Nature Communications*, 10.
- Yun, S. H., Sim, E. H., Goh, R. Y., Park, J. I. & Han, J. Y. (2016) Platelet Activation: The Mechanisms and Potential Biomarkers. *Biomed Research International*, 2016.
- Zanella, F., Renner, O., Garcia, B., Callejas, S., Dopazo, A., Peregrina, S., Carnero, A. & Link, W. (2010) Human TRIB2 is a repressor of FOXO that contributes to the malignant phenotype of melanoma cells. *Oncogene*, 29(20), 2973-2982.
- Zhang, G. Y., Xiang, B. G., Dong, A. P., Skoda, R. C., Daugherty, A., Smyth, S. S., Du, X. P. & Li, Z. Y. (2011) Biphasic roles for soluble guanylyl cyclase (sGC) in platelet activation. *Blood*, 118(13), 3670-3679.
- Zhang, L., Joshi, A. K. & Smith, S. (2003) Cloning, expression, characterization, and interaction of two components of a human mitochondrial fatty acid synthase - Malonyltransferase and acyl carrier protein. *Journal of Biological Chemistry*, 278(41), 40067-40074.
- Zhang, Y. Y. & Diamond, S. L. (2020) Src family kinases inhibition by dasatinib blocks initial and subsequent platelet deposition on collagen under flow, but lacks efficacy with thrombin generation. *Thrombosis Research*, 192, 141-151.
- Zhou, Y., Li, L., Liu, Q. M., Xing, G. C., Kuai, X. Z., Sun, J., Yin, X. S., Wang, J., Zhang, L. Q. & He, F. C. (2008) E3 ubiquitin ligase SIAH1 mediates ubiquitination and degradation of TRB3. *Cellular Signalling*, 20(5), 942-948.
- Zucker-Franklin, D. & Philipp, C. S. (2000) Platelet production in the pulmonary capillary bed - New ultrastructural evidence for an old concept. *American Journal of Pathology*, 157(1), 69-74.